R/V Mirai Cruise Report
MR24-06C (MR24-Itoh)

Arctic Ocean, Bering Sea and north Pacific Ocean

26 August - 30 September, 2024

Japan Agency for Marine-Earth Science Technology (JAMSTEC)

Contents

Front cover illustration by Yuki Oishi, Nippon Marine Enterprises, Ltd.
Last updated on 07th February, 2025

1. Cruise Summary

1.1. Cruise Information

I. Cruise ID: MR24-06C (MR24-Itoh)

II. Name of vessel: R/V Mirai

III. Title of project: Arctic Challenge for Sustainability II (ArCSII)

IV. Title of cruise: Observation cruise of ArCSII

V. Chief Scientist: Motoyo Itoh [Japan Agency for Marine-Earth Science and Technology]

VI. Cruise period: Aug 26 (Sekinehama, Aomori, Japan) –Sep 30, 2024 (Dutch Harbor, AK, USA)

VII. Ports of departure: Sekinehama/ call: Hachinohe / arrival: Dutch Harbor

VIII. Research area: North Pacific, Bering Sea, Arctic Ocean

IX. Research map

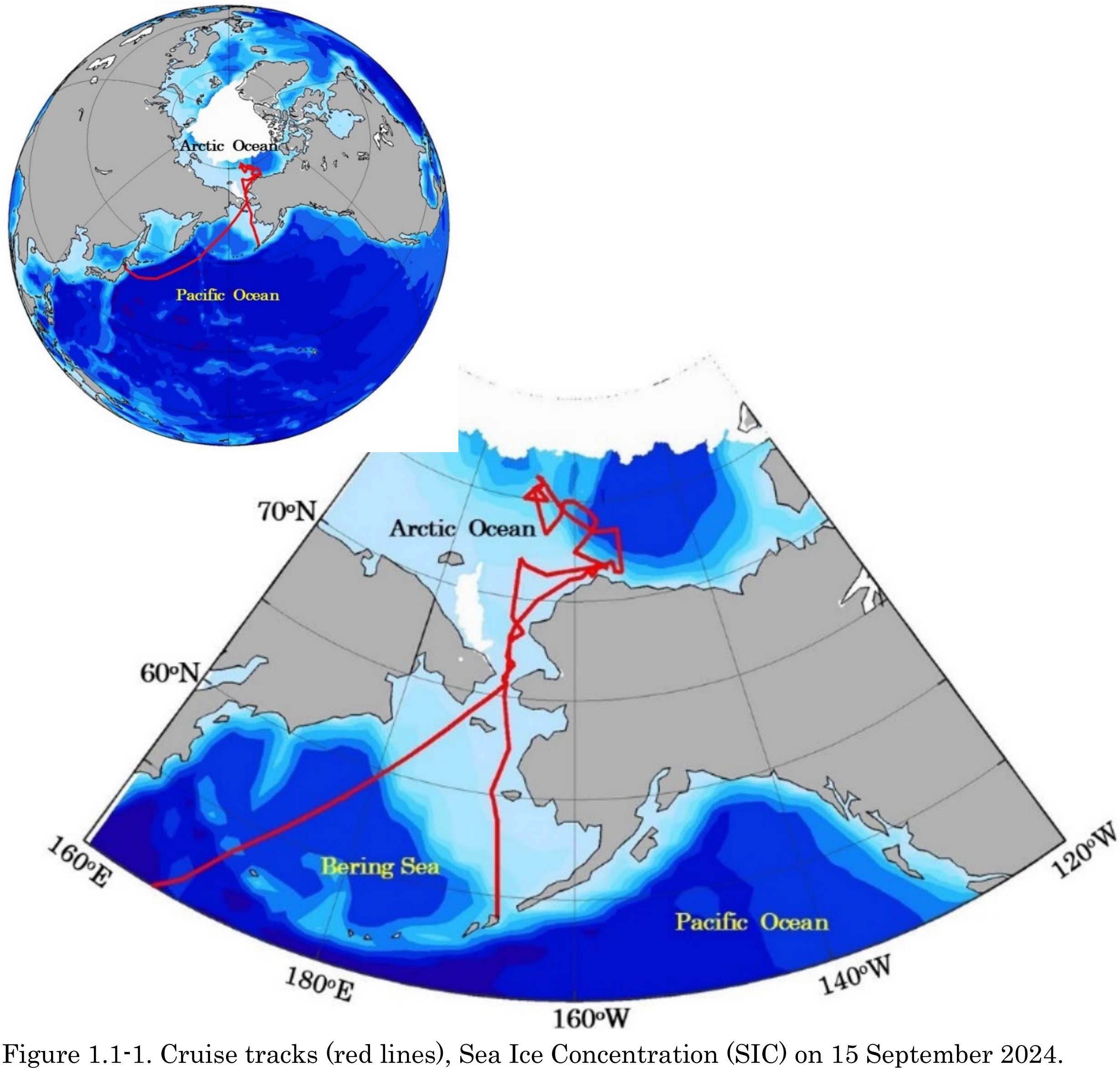

Figure 1.1-1. Cruise tracks (red lines), Sea Ice Concentration (SIC) on 15 September 2024.

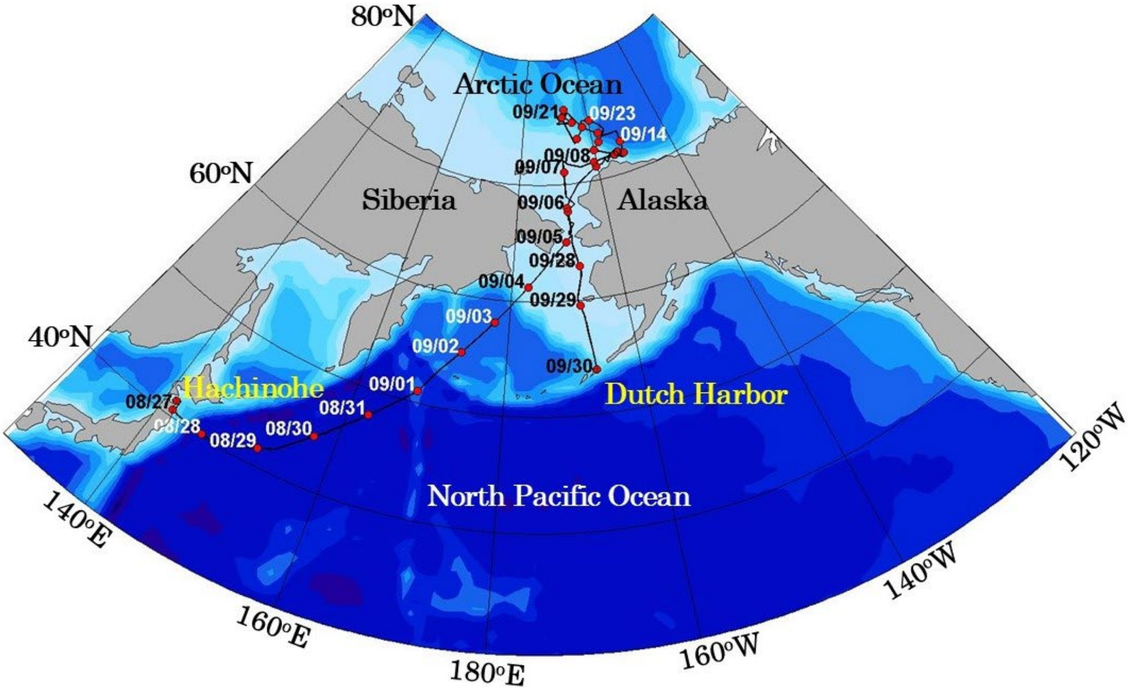

Figure 1.1-2. Map of the entire cruise track. The red dots indicate the noon positions (UTC).

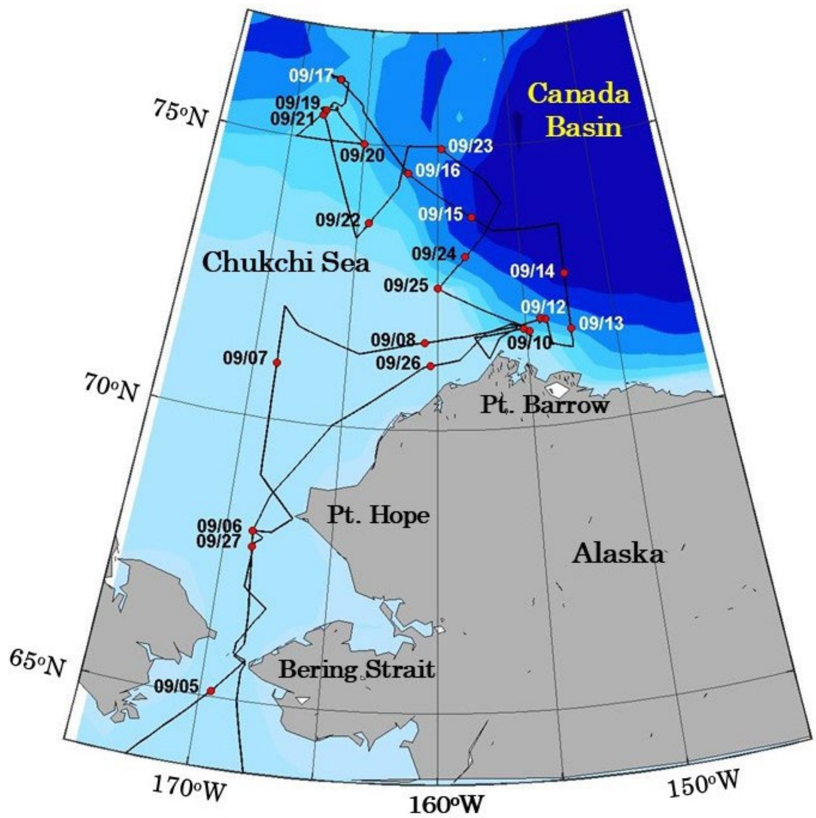

Figure 1.1-3. Detailed cruise tracks for the Chukchi Sea and the Beaufort Sea. The red dots indicate the noon positions (UTC).

1.2. Objectives

The Arctic Ocean is the area with the fastest rate of global oceanic warming in the world. The detailed research of the Research Vessel (R/V) Mirai along with other icebreaking vessels, satellite observation and numerical modeling have documented the impact of inflow of the Pacific origin water. We have observed sea ice decrease and marine ecosystem changes associated with Pacific origin waters bringing heat, nutrients, fresh water into the Arctic. Its impact is getting greater and more widely spread into the entire Arctic. This cruise aimed to develop the dataset that could allow for a synoptic view of the totality of hydrographic and ecosystem changes taking place in the Arctic Ocean and facilitate advancing model development to predict the future state of the Arctic. In addition to observation of present Arctic environments, sediment records were observed to understand differences between the present environmental changes and past warming events in the Arctic Ocean.

Photo 1.2-1 Group photo of the MR24-06C cruise.

1.3. Overview

We conducted the Arctic Ocean cruise from 26 August to 30 September 2024 using the Research Vessel (R/V) Mirai (Figure 1.1-1) under the framework of the project of Arctic Challenge for Sustainability II (ArCS II), which was funded by the Ministry of Education, Culture, Sports, Science and Technology of Japan (MEXT). We left Sekinehama on 26 August and passed through the Bering Strait toward the north on 4 September. We carried out the Arctic Ocean survey for 24 days. On 27 September, we passed through the Bering Strait southward and then arrived at Dutch Harbor on 30 September. According to the report from National Snow and Ice Data Center (NSIDC), the Arctic sea ice appears to have reached its seasonal minimum extent of 4.28 million square kilometers on September 11, 2024. The 2024 minimum is ranked seventh lowest in the 46-year satellite record.

The research areas included the EEZ and the territorial sea of the USA (Figure 1.3-1). We conducted hydrographic, paleoenvironmental and biogeochemical surveys, including plankton and bottom sediment samplings from the Chukchi Sea and the Beaufort Sea to marginal ice zones of the western Canada Basin. The observational activities consisted of CTD/water samplings, XCTD, wave and surface drifting buoy deployments, zooplankton net samplings, sediment samplings, sea ice samplings, ship-board ocean current and surface water monitoring, meteorological measurements and aerosol samplings, trials of an in-water drone, satellite observations, doppler radar, sea ice radar, sea bottom topography, gravity, and magnetic field measurements, and mooring and sediment trap recoveries and deployments.

In this cruise, we had 124 oceanographic stations (46 CTD and 78 XCTD stations) including 39 water sampling sites, 37 NORPAC net sites, 4 clean seawater sampling sites, 36 Asyura sediment sampling sites, 4 sites for drifting buoy launches, 4 sites for recoveries and deployments of hydrographic and sediment trap moorings (see Chapters 3 and 4). We also conducted 2 gravity cores and 1 multiple core samplings at 2 geological stations (see Chapter 6). The trial of an in-water drone, which is designed for oceanographic observation including under sea ice was performed at 6 stations (see Chapter 5). Continuous meteorological and oceanographic observations/samplings were carried out along the cruise tracks. We also carried out intensive oceanographic surveys under an international collaboration (Distributed Biological Observatory) off Pt. Hope (DBO3) and across the Barrow Canyon (DBO5).

These missions were successfully completed thanks to great efforts made by the captain, ice pilot, officers, crews, and all the participants in this cruise. And we would like to express our sincere appreciation to the United States Department of State and the Alaska Fisheries Science Center of the NOAA National Marine Fisheries Service of the Department of Commerce of the United States for allowing us to conduct observations in the areas under their jurisdictions. We would like to express our sincere appreciation to Alaska Eskimo Whaling Commission in USA. Based on the data obtained in this cruise, we will be able to shed light on the Arctic change and its controlling factors and will contribute to the global climate change studies.

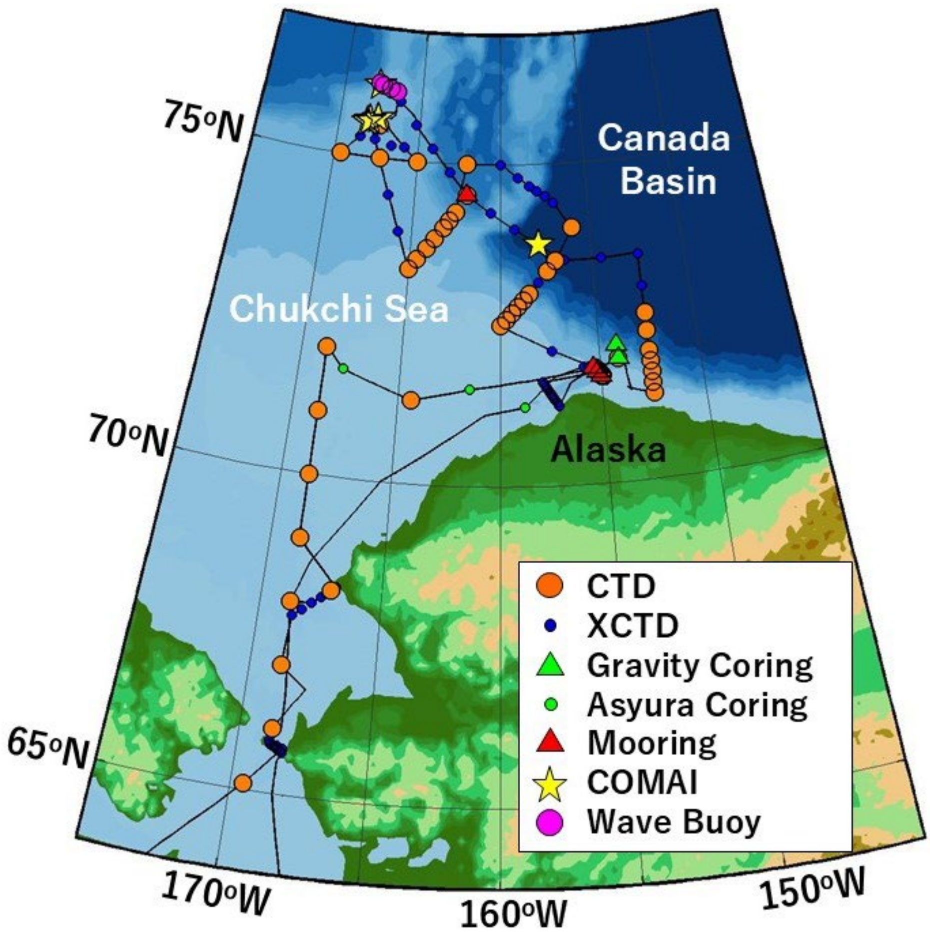

Figure 1.3-1. Close research area for the Chukchi Sea and the Bering Sea. Orange dots indicate stations where we conducted observations using Conductivity-Temperature-Depth (CTD) sensors with water sampling bottles and plankton nets and sediment core sampling (see Chapters 3 and 4). Red triangles (BCC, BCE, BCW and NAP) represent mooring sites (see 3.8 for details). Blue dots reveal where we collected hydrographic data using eXpendable CTD (XCTD) sensor (see 3.2 for the details). Yellow stars are COMAI-under ice drones test survey sites (see Chapter 5). Green triangles and dots represent sediment core sampling sites (see Chapter 6 for the details). Magenta dots indicate wave buoy deployment sites (see 3.4 for the details).

Table 1.3-1. List of stations

Event Num.	Stn	Date	Time	Lat	Lon	Water Depth	CTD/ ROS	CTD	XCTD	Clean	NORPAC / CPICS	Asyura	Flying Drone
001	Stn001	2024 / 09 / 02	19 : 31	58 3.45 N	177 36.20 E	3778	○				○	○	○
002	Stn002	2024 / 09 / 05	00 : 11	65 5.63 N	169 31.11 W	51	○				○	○	
003	XCTD001	2024 / 09 / 05	05 : 38	65 42.41 N	168 16.01 W	46			○				
004	XCTD002	2024 / 09 / 05	06 : 11	65 45.12 N	168 29.88 W	56			○				
005	XCTD003	2024 / 09 / 05	06 : 55	65 49.16 N	168 48.00 W	50			○				
006	Stn003	2024 / 09 / 05	08 : 59	66 0.31 N	168 45.06 W	54	○				○	○	
007	Stn004	2024 / 09 / 05	16 : 20	67 0.12 N	168 44.94 W	46	○				○	○	
008	XCTD004	2024 / 09 / 05	21 : 37	67 47.00 N	168 36.10 W	50			○				
009	XCTD005	2024 / 09 / 05	22 : 34	67 53.88 N	168 14.10 W	58			○				
010	Stn005	2024 / 09 / 06	00 : 13	68 0.03 N	168 45.01 W	59	○					○	
011	XCTD006	2024 / 09 / 06	02 : 20	68 0.80 N	167 52.00 W	52			○				
012	XCTD007	2024 / 09 / 06	03 : 15	68 7.70 N	167 29.70 W	49			○				
013	XCTD008	2024 / 09 / 06	03 : 42	68 11.10 N	167 18.51 W	48			○				
014	Stn006	2024 / 09 / 06	04 : 20	68 14.55 N	167 7.64 W	44	○				○	○	
014	XCTD009	2024 / 09 / 06	05 : 48	68 18.01 N	166 56.12 W	34			○				
015	Stn007	2024 / 09 / 06	11 : 40	68 59.96 N	168 45.36 W	53	○				○	○	
016	Stn008	2024 / 09 / 06	17 : 14	70 0.03 N	168 45.03 W	41	○				○	○	○
017	Stn009	2024 / 09 / 07	00 : 07	70 59.99 N	168 45.17 W	45	○				○	○	
018	Stn010	2024 / 09 / 07	05 : 30	72 0.01 N	168 45.02 W	51	○				○	○	
019	Asyura Core CS-1	2024 / 09 / 07	09 : 01	71 41.02 N	167 48.81 W	50						○	
020	Stn011	2024 / 09 / 07	16 : 47	71 18.01 N	164 20.99 W	46	○						
021	Asyura Core CS-2	2024 / 09 / 07	22 : 02	71 30.52 N	161 29.92 W	48						○	
022	Mooring BCW-22	2024 / 09 / 08	14 : 40	71 47.78 N	155 20.81 W	165							
023	Mooring BCC-22	2024 / 09 / 08	17 : 40	71 44.07 N	155 9.84 W	291							
024	Mooring BCE-22	2024 / 09 / 08	21 : 00	71 40.38 N	154 59.99 W	108							
025	Stn012 BCC	2024 / 09 / 08	22 : 52	71 44.14 N	155 9.55 W	289	○				○	○	
026	XCTD010 DBO-5	2024 / 09 / 09	05 : 02	71 37.20 N	157 55.54 W	62		○					
027	XCTD011 DBO-5	2024 / 09 / 09	05 : 18	71 34.70 N	157 50.43 W	64		○					
028	XCTD012 DBO-5	2024 / 09 / 09	05 : 33	71 32.20 N	157 45.30 W	71		○					
029	XCTD013 DBO-5	2024 / 09 / 09	05 : 49	71 29.80 N	157 40.11 W	83		○					
030	XCTD014 DBO-5	2024 / 09 / 09	06 : 04	71 27.31 N	157 34.91 W	110		○					
031	XCTD015 DBO-5	2024 / 09 / 09	06 : 20	71 24.80 N	157 29.84 W	122		○					
032	XCTD016 DBO-5	2024 / 09 / 09	06 : 35	71 22.31 N	157 24.89 W	112		○					
033	XCTD017 DBO-5	2024 / 09 / 09	06 : 51	71 19.80 N	157 19.92 W	90		○					
034	XCTD018 DBO-5	2024 / 09 / 09	07 : 06	71 17.30 N	157 14.88 W	57		○					
035	XCTD019 DBO-5	2024 / 09 / 09	07 : 23	71 14.80 N	157 9.86 W	47		○					
036	Mooring BCW-24	2024 / 09 / 09	16 : 18	71 47.80 N	155 20.83 W	165							
037	Mooring BCC-24	2024 / 09 / 09	18 : 00	71 44.10 N	155 9.68 W	291							
038	Mooring BCE-24	2024 / 09 / 09	21 : 10	71 40.40 N	154 59.90 W	108							
039	Stn013 BCE	2024 / 09 / 09	22 : 21	71 41.26 N	154 56.49 W	107	○				○	○	
040	XCTD020	2024 / 09 / 10	00 : 39	71 36.00 N	154 48.98 W	42		○					
041	XCTD021	2024 / 09 / 10	00 : 54	71 38.00 N	154 55.31 W	56		○					
042	XCTD022	2024 / 09 / 10	01 : 09	71 40.00 N	155 1.00 W	102		○					
043	XCTD023	2024 / 09 / 10	01 : 23	71 42.00 N	155 6.48 W	179		○					
044	XCTD024	2024 / 09 / 10	01 : 37	71 44.00 N	155 12.01 W	298		○					
045	XCTD025	2024 / 09 / 10	01 : 51	71 46.01 N	155 17.53 W	201		○					
046	XCTD026	2024 / 09 / 10	02 : 05	71 48.00 N	155 22.98 W	148		○					
047	XCTD027	2024 / 09 / 10	02 : 28	71 49.00 N	155 36.91 W	119		○					
048	XCTD028	2024 / 09 / 10	02 : 50	71 50.00 N	155 51.02 W	91		○					
049	Stn014	2024 / 09 / 10	16 : 56	71 55.47 N	154 6.50 W	287	○				○	○	○
050	Gravity Cpre BC2-2	2024 / 09 / 10	19 : 20	71 55.47 N	154 7.25 W	264							○
051	Asyura Core BCT-1	2024 / 09 / 10	21 : 33	71 56.51 N	154 6.02 W	346						○	
052	Asyura Core BCT-2	2024 / 09 / 10	22 : 10	71 55.87 N	154 6.66 W	289						○	
053	Asyura Core BCT-3	2024 / 09 / 10	22 : 44	71 55.31 N	154 7.24 W	260						○	
054	Asyura Core BCT-4	2024 / 09 / 10	23 : 15	71 54.76 N	154 7.89 W	244						○	
055	Asyura Core BCT-5	2024 / 09 / 10	23 : 52	71 53.97 N	154 8.79 W	242						○	
056	Asyura Core BCT-6	2024 / 09 / 11	00 : 37	71 52.62 N	154 10.69 W	196						○	
057	Gravity/Multile Core	2024 / 09 / 11	16 : 54	71 55.15 N	154 4.54 W	279							
058	Towed CTD Dive02	2024 / 09 / 11	20 : 30	71 55.20 N	154 7.20 W	243							
059	XCTD030	2024 / 09 / 11	00 : 02	71 53.92 N	154 8.78 W	237			○				

Event Num.	Stn	Date	Time	Lat	Lon	Water Depth	CTD/ ROS	CTD	XCTD	Clean	NORPAC / CPICS	Asyura	Flying Drone
060	Stn015	2024 / 09 / 12	16 : 13	71 20.01 N	152 29.96 W	63	O				O	O	
061	Stn016	2024 / 09 / 12	20 : 56	71 30.00 N	152 30.15 W	108	O				O	O	O
062	Stn017	2024 / 09 / 13	00 : 12	71 40.02 N	152 29.97 W	318	O				O	O	
063	Stn018	2024 / 09 / 13	05 : 43	71 49.39 N	152 28.81 W	1210	O			O	O		
064	Stn019	2024 / 09 / 13	10 : 33	72 0.02 N	152 29.96 W	1680	O				O		
065	Stn020	2024 / 09 / 13	15 : 48	72 18.02 N	152 30.28 W	2828	X				O		O
066	XCTD031	2024 / 09 / 13	16 : 46	72 18.01 N	152 30.02 W	2626			O				
067	Stn021	2024 / 09 / 13	17 : 30	72 35.04 N	152 29.94 W	3596				O	O		O
068	XCTD032	2024 / 09 / 13	23 : 32	72 34.97 N	152 29.94 W	3596			O				
069	XCTD033	2024 / 09 / 14	01 : 41	72 60.00 N	152 30.01 W	3837			O				
070	XCTD034	2024 / 09 / 14	04 : 06	73 29.99 N	152 30.05 W	3853			O				
071	XCTD035	2024 / 09 / 14	06 : 56	73 29.99 N	154 29.99 W	3858			O				
072	XCTD036	2024 / 09 / 14	09 : 36	73 30.00 N	156 29.98 W	3666			O				
073	COMAI Dive001	2024 / 09 / 14	16 : 00	73 45.04 N	157 51.48 W	3491							
074	COMAI Dive002	2024 / 09 / 14	21 : 00	73 45.00 N	157 51.36 W	3492							
075	XCTD037	2024 / 09 / 15	00 : 28	73 45.36 N	157 52.87 W	3494			O				
076	XCTD038	2024 / 09 / 15	02 : 50	73 60.00 N	159 13.00 W	2940			O				
077	XCTD039	2024 / 09 / 15	05 : 11	74 15.00 N	160 34.41 W	567			O				
078	Mooring NAP-23t	2024 / 09 / 15	15 : 41	74 31.38 N	161 56.54 W	1685							
079	Stn022	2024 / 09 / 15	19 : 37	74 31.13 N	161 48.46 W	1685	O						O
080	Mooring NAP-24t	2024 / 09 / 15	21 : 57	74 31.38 N	161 56.19 W	1680							
081	XCTD040	2024 / 09 / 16	03 : 02	74 52.34 N	163 0.97 W	1678			O				
082	XCTD041	2024 / 09 / 16	05 : 13	75 13.33 N	164 7.00 W	688			O				
083	XCTD042	2024 / 09 / 16	07 : 19	75 33.86 N	165 12.99 W	579			O				
084	XCTD043	2024 / 09 / 16	14 : 26	75 54.11 N	166 19.55 W	342			O				
085	XCTD044	2024 / 09 / 16	16 : 38	76 7.12 N	167 26.18 W	314			O				
086	Buoy001	2024 / 09 / 16	17 : 20	76 7.28 N	167 33.41 W	336							
087	XCTD045	2024 / 09 / 16	17 : 30	76 7.56 N	167 33.37 W	364			O				O
088	Towed CTD Dive02	2024 / 09 / 16	19 : 00	76 7.80 N	167 31.80 W	366							
089	XCTD046	2024 / 09 / 16	22 : 00	76 6.33 N	167 18.24 W	295			O				
090	XCTD047	2024 / 09 / 16	23 : 27	76 5.75 N	167 8.92 W	300			O				
091	Buoy002	2024 / 09 / 17	00 : 39	76 5.13 N	167 3.34 W	286							
092	COMAI Dive003	2024 / 09 / 17	16 : 10	76 6.87 N	167 41.53 W	398							
093	XCTD048	2024 / 09 / 17	16 : 57	76 6.62 N	167 40.56 W	384			O				
094	Sea Ice Sampling	2024 / 09 / 17	21 : 30	76 8.99 N	167 47.71 W	550							
095	Buoy003	2024 / 09 / 17	22 : 45	76 9.10 N	167 46.16 W	432							
096	Buoy004	2024 / 09 / 18	00 : 33	76 3.11 N	166 35.23 W	301							
097	XCTD049	2024 / 09 / 18	16 : 45	75 36.60 N	167 34.45 W	192			O				
098	COMAI Dive004	2024 / 09 / 18	21 : 00	75 36.44 N	167 34.60 W	190							
099	Stn023	2024 / 09 / 18	21 : 22	75 36.38 N	167 32.62 W	191	O				O	O	
100	XCTD050	2024 / 09 / 19	01 : 31	75 18.00 N	168 36.50 W	196			O				
101	Stn024	2024 / 09 / 19	14 : 11	75 0.09 N	169 37.86 W	238	O				O	O	
102	Stn025	2024 / 09 / 19	20 : 12	75 0.05 N	167 14.05 W	254	O				O	O	
103	Stn026	2024 / 09 / 20	00 : 11	74 60.00 N	165 0.00 W	546	O				O		
104	XCTD051	2024 / 09 / 20	03 : 15	75 12.42 N	165 50.01 W	524			O				
105	XCTD052	2024 / 09 / 20	04 : 40	75 24.68 N	166 39.99 W	281			O				
106	COMAI Dive005	2024 / 09 / 20	16 : 00	75 33.50 N	168 5.80 W	174			O				
107	XCTD053	2024 / 09 / 20	17 : 03	75 33.50 N	168 6.22 W	177			O				
108	COMAI Dive006	2024 / 09 / 20	21 : 00	75 32.04 N	168 11.69 W	175			O				
109	XCTD054	2024 / 09 / 20	21 : 49	75 32.12 N	168 11.78 W	173			O				
110	XCTD055	2024 / 09 / 21	00 : 50	75 17.00 N	167 41.52 W	167			O				
111	XCTD056	2024 / 09 / 21	05 : 04	74 27.00 N	166 30.11 W	318			O				
112	XCTD057	2024 / 09 / 21	07 : 53	73 54.00 N	165 44.94 W	150			O				
113	Stn027	2024 / 09 / 21	16 : 09	73 20.00 N	165 0.03 W	72	O				O	O	
114	Stn028	2024 / 09 / 21	20 : 19	73 40.00 N	164 7.35 W	171	O				O	O	
115	Stn029	2024 / 09 / 21	23 : 11	73 29.99 N	164 36.36 W	110		O					
116	Stn030	2024 / 09 / 22	01 : 35	73 49.94 N	163 42.04 W	221		O					
117	Stn031	2024 / 09 / 22	04 : 13	73 59.99 N	163 13.93 W	300	O				O	O	
118	Stn032	2024 / 09 / 22	08 : 15	74 7.50 N	162 54.15 W	400		O					
119	Stn033	2024 / 09 / 22	11 : 26	74 15.02 N	162 33.64 W	1101	O				O		

Event Num.	Stn	Date	Time	Lat	Lon	Water Depth	CTD/ ROS	CTD	XCTD	Clean	NORPAC / CPICS	Asyura	Flying Drone
120	Stn034	2024 / 09 / 22	19 : 29	74 59.94 N	162 0.40 W	1971	○			○	○		
121	XCTD058	2024 / 09 / 22	23 : 34	74 60.00 N	159 59.99 W	1955			○				
122	XCTD059	2024 / 09 / 23	01 : 18	74 48.00 N	158 59.98 W	1204			○				
123	XCTD060	2024 / 09 / 23	02 : 28	74 40.00 N	158 18.50 W	1162			○				
124	XCTD061	2024 / 09 / 23	03 : 09	74 35.00 N	157 54.99 W	1242			○				
125	XCTD062	2024 / 09 / 23	03 : 54	74 29.98 N	157 28.00 W	3855			○				
126	XCTD063	2024 / 09 / 23	04 : 42	74 23.99 N	156 60.00 W	3859			○				
127	Stn035	2024 / 09 / 23	08 : 25	74 0.02 N	155 59.79 W	3858	○				○		
128	Stn036	2024 / 09 / 23	14 : 56	73 30.00 N	157 0.07 W	3261	○						
129	Stn037	2024 / 09 / 23	19 : 55	73 20.00 N	157 28.00 W	2996	○				○		
130	XCTD064	2024 / 09 / 23	23 : 20	73 9.99 N	158 0.05 W	2399			○				
131	Stn038	2024 / 09 / 24	02 : 42	72 59.97 N	158 29.99 W	1268	○			○	○		
132	Stn039	2024 / 09 / 24	08 : 14	72 54.05 N	158 48.01 W	397	○				○	○	
133	Stn040	2024 / 09 / 24	13 : 10	72 48.10 N	159 5.98 W	200	○				○	○	
134	Stn041	2024 / 09 / 24	17 : 47	72 42.01 N	159 23.99 W	84	○				○	○	
135	Stn042	2024 / 09 / 24	21 : 08	72 36.00 N	159 41.97 W	58		○					
136	Stn043	2024 / 09 / 24	23 : 07	72 30.01 N	159 60.00 W	49	○				○	○	
137	XCTD065	2024 / 09 / 25	04 : 15	72 6.00 N	157 23.00 W	78			○				
138	Stn044	2024 / 09 / 25	08 : 09	71 48.85 N	155 20.97 W	164		○					
139	Stn045	2024 / 09 / 25	09 : 38	71 39.98 N	155 3.07 W	111	○						
140	Stn046	2024 / 09 / 25	11 : 14	71 43.51 N	155 7.18 W	235	○				○		
141	XCTD066	2024 / 09 / 25	12 : 49	71 36.51 N	154 46.78 W	44			○				
142	XCTD067	2024 / 09 / 25	13 : 08	71 38.47 N	154 52.08 W	56			○				
143	XCTD068	2024 / 09 / 25	13 : 33	71 42.66 N	155 1.92 W	166			○				
144	XCTD069	2024 / 09 / 25	13 : 47	71 44.75 N	155 7.35 W	286			○				
145	XCTD070	2024 / 09 / 25	13 : 59	71 46.34 N	155 12.31 W	244			○				
146	XCTD071	2024 / 09 / 25	14 : 36	71 49.11 N	155 34.40 W	125			○				
147	XCTD072	2024 / 09 / 25	15 : 03	71 50.00 N	155 50.92 W	91			○				
148	Asyura Core CS-3	2024 / 09 / 25	21 : 07	71 14.07 N	158 48.19 W	39						○	
149	Stn047	2024 / 09 / 26	21 : 14	68 0.02 N	168 45.01 W	59	○				○		
150	XCTD073	2024 / 09 / 27	09 : 38	65 45.84 N	168 44.83 W	51			○				
151	XCTD074	2024 / 09 / 27	09 : 59	65 44.50 N	168 38.94 W	50			○				
152	XCTD075	2024 / 09 / 27	10 : 20	65 42.94 N	168 33.03 W	52			○				
153	XCTD076	2024 / 09 / 27	10 : 40	65 41.74 N	168 27.54 W	53			○				
154	XCTD077	2024 / 09 / 27	11 : 01	65 40.61 N	168 21.35 W	51			○				
155	XCTD078	2024 / 09 / 27	11 : 23	65 38.77 N	168 16.28 W	45			○				

1.4. Research Proposal

This cruise included the following 14 studies

Title of proposal/Representative Personnel

- On board research themes

1. ArCS II: Arctic Challenge for Sustainability II/ WATANABE Eiji [JAMSTEC]
2. Observational study of the Arctic environmental changes: Pacific-Arctic interaction, biogeochemical transport, mixing and marine ecosystem/ ITOH Motoyo [JAMSTEC]
3. Research on sea ice observation technology for the purpose of understanding environmental changes in the Arctic ocean/ YOSHIDA Hiroshi [JAMSTEC]
4. Development of X-band Radar for Detecting Sea Ice and Waves/ WASEDA Takuji [JAMSTEC]
5. Holocene Arctic Palaeoclimatology and Paleoceanography Investigation/ YAMAMOTO Masanobu [Hokkaido University]
6. Spatial and temporal variations in plankton community of the Arctic Ocean: analyzed by imaging systems/ MATSUNO Kohei [Hokkaido University]
7. Effect of freshwater input on pCO2 and CO2 flux in the Arctic Ocean/ NOMURA Daiki[Hokkaido University]
8. Title of proposal: Changes in clouds and aerosols over the ice-free Arctic Ocean/ SATO Kazutoshi [National Institute of Polar Research, Japan]
9. Observation of air-sea-wave-ice interaction in the Marginal Ice Zone/ WASEDA Takuji [The University of Tokyo]
10. Exploring microplankton interactions and their functional roles in a changing Arctic/ Eva Siliva Lopes [Interdisciplinary Centre of Marine and Environmental Research]

- Studies not on board

11. Distribution and abundance of microplastics in the Arctic Ocean/ IKENOUE Takahito [JAMSTEC]
12. Ship-borne observations of trace gases/aerosols over the Arctic/ Fumikazu Taketani [JAMSTEC]
13. Observation of water vapor isotope in the Arctic/ Hotaek Park [JAMSTEC]
14. Ship-board observations of atmospheric greenhouse gases and related species in the Arctic ocean and the western North Pacific/ ISHIDOYA Shigeyuki [National Institute of Advanced Industrial Science and Technology]

1.5. Science Party

Table 1.5-1: List of onboard participants of MR24-06C.

No.	Name	Organization	Position
1	ITOH Motoyo	JAMSTEC	Chief Scientist/ Research Scientist
2	HATTA Mariko	JAMSTEC	2nd chief Scientist/ Research Scientist
3	FUJIWARA Amane	JAMSTEC	3rd chief Scientist/ Research Scientist
4	ONODERA Jonaotaro	JAMSTEC	Senior Scientist
5	KIMURA Satoshi	JAMSTEC	Research Scientist
6	SERVETTAZ, Aymeric Pierre Marie	JAMSTEC	Research Scientist
7	FUKAI Yuri	JAMSTEC	Postdoctoral Researcher
8	HASEGAWA Asahi	JAMSTEC/ The University of Tokyo	Research Assistant
9	KUSAKABE Shota	JAMSTEC/ The University of Tokyo	Research Assistant
10	KAMIYAMA Ikkan	JAMSTEC/ Tokyo University of Marine Science and Technology	Research Assistant
11	UMEMURA Kentaro	JAMSTEC/ Model Art Co., Ltd.	Research Assistant
12	YOSHIDA Hiroshi	JAMSTEC	Principal Researcher
13	TANAKA Kiyotaka	JAMSTEC	Senior Research Technician
14	SUGESAWA Makoto	JAMSTEC	Research Assistant
15	DEI Ryota	Jiji Press, Ltd.	Senior Staff Writer
16	MATSUZAWA Takatoshi	National Maritime Research Institute	Senior Researcher
17	YAMAMOTO Masanobu	Hokkaido University	Professor
18	IWASAKI Shinya	Hokkaido University	Assistant Professor
19	KUMAGAI Shino	Hokkaido University	Graduate Student
20	TOZAWA Manami	Hokkaido University	Graduate Student
21	ARAI Masanori	Hokkaido University	Graduate Student
22	SUZUKI Kenta	Chiba Institute of Technology	Associate Researcher
23	YOSHIDA Kazuho	Nippon Marine Enterprises, Ltd.	Group Leader

24	YAMAMOTO Akane	The University of Tokyo	Graduate Student
25	LOPES, Eva Silva	Interdisciplinary Centre of Marine and Environmental Research	Graduate Student
26	OGAWA Satomi	Nippon Marine Enterprises, Ltd.	Chief Technical Staff
27	SUEYOSHI Soichiro	Nippon Marine Enterprises, Ltd.	Technical Staff
28	OKUMURA Shinya	Nippon Marine Enterprises, Ltd.	Technical Staff
29	YAMANAKA Haruna	Nippon Marine Enterprises, Ltd.	Technical Staff
30	ORUI Masahiro	Marine Works Japan Ltd.	Chief Technical Staff
31	USHIROMURA Hiroki	Marine Works Japan Ltd.	Technical Staff
32	YODA Aine	Marine Works Japan Ltd.	Technical Staff
33	SHINOMIYA Yuta	Marine Works Japan Ltd.	Technical Staff
34	FUJIOKA Riho	Marine Works Japan Ltd.	Technical Staff
35	CHIBA Tomokazu	Marine Works Japan Ltd.	Technical Staff
36	ARIHARA Ko	Marine Works Japan Ltd.	Technical Staff
37	ARII Yasuhiro	Marine Works Japan Ltd.	Technical Staff
38	FUJIKI Nagisa	Marine Works Japan Ltd.	Technical Staff
39	KUWAHARA Misato	Marine Works Japan Ltd.	Technical Staff
40	IZUTSU Takuya	Marine Works Japan Ltd.	Technical Staff
41	MIYOSHI Yuko	Marine Works Japan Ltd.	Technical Staff
42	ODA Yuta	Marine Works Japan Ltd.	Technical Staff
43	ARIGA Shiori	Marine Works Japan Ltd.	Technical Staff
44	SAWADA Ritsuko	Marine Works Japan Ltd.	Technical Staff
45	David Snider	Martech Polar Consulting Ltd.	Ice Pilot

2. Meteorology
2.1. C-band weather radar

(1) Personnel

Jun Inoue	NIPR (National Institute of Polar Research, not on-board)
Kazutoshi Sato	NIPR (not on-board)
Kazuho Yoshida	NME (Nippon Marine Enterprises, Ltd.) -PI
Satomi Ogawa	NME : Technician
Souichiro Sueyoshi	NME : Technician
Shinya Okumura	NME : Technician
Haruna Yamanaka	NME : Technician
Masanori Murakami	MIRAI Crew

(2) Objectives

The objective of weather radar observations is to investigate the structures and evolutions of precipitating systems over the high-latitude region including the Arctic Ocean.

(3) Parameters

Radar variables, which were converted from the power and phase of the backscattered signal at vertically- and horizontally-polarized channels, were as follows:

Radar reflectivity:	Z
Doppler velocity:	Vr
Spectrum width of Doppler velocity:	SW
Differential reflectivity:	Z_{DR}
Differential propagation phase:	Φ_{DP}
Specific differential phase:	K_{DP}
Co-polar correlation coefficients:	ρ_{HV}

(4) Instruments and methods

i) Radar specifications

The C-band weather radar on board the R/V Mirai was used. Basic specifications of the radar are as follows:

Frequency:	5370 MHz (C-band)
Polarimetry:	Horizontal and vertical (simultaneously transmitted and received)
Transmitter:	Solid-state transmitter
Pulse Configuration:	Using pulse-compression
Output Power:	6 kW (H) + 6 kW (V)
Antenna Diameter:	4 meters

Beam Width:	1.0 degrees
Inertial Navigation Unit:	PHINS (IXBLUE S.A.S)

ii) Operation methodology

The antenna was controlled to point the commanded ground-relative direction, by controlling the azimuth and elevation to cancel the ship attitude (roll, pitch and yaw) detected by the laser gyro. The Doppler velocity was also corrected by subtracting the ship movement in beam direction.

For the maintenance, internal signals of the radar were checked and calibrated at the beginning and the end of the cruise. Meanwhile, the following parameters were checked daily; (1) frequency, (2) mean output power, (3) pulse width, and (4) PRF (pulse repetition frequency).

During the cruise, the radar was operated as in Table 2.1-1. A dual PRF mode was used for a volume scan. For RHI and surveillance PPI scans, a single PRF mode was used.

(5) Observation Log

00:00UTC 28 Aug. 2024 to 21:00UTC 29 Sep. 2024

(6) Preliminary results

The C-band weather radar observations were conducted through the cruise, except in the area where the operations were prohibited by Japanese license. The obtained data will be analyzed after the cruise.

(7) Data archive

These data obtained in this cruise will be submitted to the Data Management Group of JAMSTEC, and will be opened to the public via "Data Research System for Whole Cruise Information in JAMSTEC (DARWIN)" in JAMSTEC web site.

<https://www.godac.jamstec.go.jp/darwin/en>

(8) Remarks

i) The following periods, data acquisition was suspended due to UAV operation.

17:43UTC 10 Sep. 2024 - 18:00UTC 10 Sep. 2024
18:29UTC 11 Sep. 2024 - 18:42UTC 11 Sep. 2024
21:30UTC 12 Sep. 2024 - 21:42UTC 12 Sep. 2024
16:31UTC 13 Sep. 2024 - 16:44UTC 13 Sep. 2024
18:46UTC 13 Sep. 2024 - 19:12UTC 13 Sep. 2024
19:10UTC 15 Sep. 2024 - 19:29UTC 15 Sep. 2024
17:54UTC 16 Sep. 2024 - 18:18UTC 16 Sep. 2024

Table 2.1-1: Scan modes of C-band weather radar

<table>
<tr><th></th><th>Survei-
llance
PPI Scan</th><th colspan="6">Volume Scan</th><th>RHI
Scan</th></tr>
<tr><td>Repeated
Cycle (min.)</td><td>30</td><td colspan="6">6</td><td>6</td></tr>
<tr><td>Times in
One Cycle</td><td>1</td><td colspan="6">1</td><td>3</td></tr>
<tr><td rowspan="2">PRF(s) (Hz)</td><td rowspan="2">400</td><td colspan="6">dual PRF (ray alternative)</td><td rowspan="2">1250</td></tr>
<tr><td>667</td><td>833</td><td>938</td><td>1250</td><td>1333</td><td>2000</td></tr>
<tr><td>Azimuth
(deg)</td><td colspan="7">Full Circle</td><td>Option</td></tr>
<tr><td>Bin Spacing
(m)</td><td colspan="8">150</td></tr>
<tr><td>Max. Range
(km)</td><td>300</td><td colspan="2">150</td><td colspan="2">100</td><td colspan="2">60</td><td>100</td></tr>
<tr><td>Elevation
Angle(s)
(deg.)</td><td>0.5</td><td colspan="2">0.5</td><td colspan="2">1.0, 1.8,
2.6, 3.4,
4.2, 5.1,
6.2, 7.6,
9.7, 12.2,
15.2</td><td colspan="2">18.7, 23.0,
27.9, 33.5,
40.0</td><td>0.0 ~
60.0</td></tr>
</table>

2.2. Surface Meteorological Observations

(1) Personnel

Motoyo Itoh	JAMSTEC	-PI
Satomi Ogawa	NME (Nippon Marine Enterprises, Ltd.)	
Souichiro Sueyoshi	NME	
Shinya Okumura	NME	
Haruna Yamanaka	NME	
Masanori Murakami	MIRAI Crew	

(2) Objectives

Surface meteorological parameters are observed as a basic dataset of the meteorology. These parameters provide the temporal variation of the meteorological condition surrounding the ship.

(3) Parameters

i. MIRAI Surface Meteorological (SMet) system measured parameters are listed in Table 2.2-1.

Table 2.2-1: Parameters of MIRAI SMet system

Parameter	Units	Remarks
1 Latitude	degree	
2 Longitude	degree	
3 Ship's speed	knot	MIRAI log
4 Ship's heading	degree	MIRAI gyro
5 Relative wind speed	m/s	6sec./10min. averaged
6 Relative wind direction	degree	6sec./10min. averaged
7 True wind speed	m/s	6sec./10min. averaged
8 True wind direction	degree	6sec./10min. averaged
9 Barometric pressure	hPa	adjusted to sea surface level 6sec. averaged
10 Air temperature (starboard)	degC	6sec. averaged
11 Air temperature (port)	degC	6sec. averaged
12 Dewpoint temperature (starboard)	degC	6sec. averaged
13 Dewpoint temperature (port)	degC	6sec. averaged
14 Relative humidity (starboard)	%	6sec. averaged
15 Relative humidity (port)	%	6sec. averaged
16 Sea surface temperature	degC	6sec. averaged
17 Precipitation intensity (optical rain gauge)	mm/hr	hourly accumulation
18 Precipitation (capacitive rain gauge)	mm/hr	hourly accumulation
19 Downwelling shortwave radiation	W/m^2	6sec. averaged
20 Downwelling infra-red radiation	W/m^2	6sec. averaged

21 Significant wave height (bow)	m	hourly
22 Significant wave height (stern)	m	hourly
23 Significant wave period (bow)	second	hourly
24 Significant wave period (stern)	second	hourly

ii. Shipboard Oceanographic and Atmospheric Radiation (SOAR) system measured parameters are listed in Table 2.2-2.

Table 2.2-2: Parameters of SOAR system (JamMet)

Parameter	Units	Remarks
1 Latitude	degree	
2 Longitude	degree	
3 SOG	knot	
4 COG	degree	
5 Relative wind speed	m/s	
6 Relative wind direction	degree	
7 Barometric pressure	hPa	
8 Air temperature	degC	
9 Relative humidity	%	
10 Precipitation intensity (optical rain gauge)	mm/hr	
11 Precipitation (capacitive rain gauge)	mm/hr	reset at 50 mm
12 Down welling shortwave radiation	W/m^2	
13 Down welling infra-red radiation	W/m^2	
14 Defuse irradiance	W/m^2	
15 PAR	microE/cm^2/sec	
16 UV 305 nm	microW/cm^2/nm	
17 UV 320 nm	microW/cm^2/nm	
18 UV 340 nm	microW/cm^2/nm	
19 UV 380 nm	microW/cm^2/nm	

(4) Instruments and methods

In this cruise, the two systems for the observation were used.

i. *SMet system*

Instruments of SMet system are listed in Table 2.2-3. Data were collected and processed by KOAC-7800 weather data processor made by Koshin-Denki, Japan. The data set consists of 6 seconds averaged data.

Table 2.2-3: Instruments and installation locations of SMet system

Sensors	Type	Manufacturer	Location (altitude from surface)
Anemometer	KS-5900	Koshin Denki, Japan	Foremast (25 m)
Tair/RH	HMP155	Vaisala, Finland	Compass deck (21 m)

with aspirated radiation shield	43408 Gill	R.M. Young, U.S.A.	starboard and port side
Thermometer: SST	RFN2-0	Koshin Denki, Japan	4th deck (-1m, inlet -5m)
Barometer	Model-370	Setra System, U.S.A.	Captain deck (13 m) Weather observation room
Capacitive rain gauge	50202	R. M. Young, U.S.A.	Compass deck (19 m)
Optical rain gauge	ORG-815DS	Osi, USA	Compass deck (19 m)
Radiometer (short wave)	MS-802	Eko Seiki, Japan	Radar mast (28 m)
Radiometer (long wave)	MS-202	Eko Seiki, Japan	Radar mast (28 m)
Wave height meter	WM-2	Tsurumi-seiki, Japan	Bow (10 m) Stern (8m)

ii. SOAR measurement system

SOAR system designed by BNL (Brookhaven National Laboratory, USA) consists of major five parts.

a) Analog meteorological data sampling with CR1000 logger manufactured by Campbell Scientific Inc. Canada – wind, pressure, and rainfall (by a capacitive rain gauge) measurement.
b) Digital meteorological data sampling from individual sensors - air temperature, relative humidity and precipitation (by optical rain gauge (ORG)) measurement.
c) Radiation data sampling with CR1000X logger manufactured by Campbell Inc. and radiometers with ventilation unit manufactured by Hukseflux Thermal Sensors B.V. Netherlands – short and long wave downward radiation measurement.
d) Photosynthetically Available Radiation (PAR) sensor manufactured by Biospherical Instruments Inc. (USA) - PAR measurement.
e) Scientific Computer System (SCS) developed by NOAA (National Oceanic and Atmospheric Administration, USA) - centralized data acquisition and logging of all data sets.

SCS recorded radiation, air temperature, relative humidity, CR1000 and ORG data. SCS composed Event data (JamMet) from these data and ship's navigation data every 6 seconds. Instruments and their locations are listed in Table 2.2-4.

Table 2.2-4: Instruments and installation locations of SOAR system

Sensors (Meteorological)	Type	Manufacturer	Location (altitude from surface)

Anemometer	05106	R.M. Young, USA	Foremast (25 m)
Barometer with pressure port	PTB210 61002 Gill	VAISALA, Finland R.M. Young, USA	Foremast (23 m)
Rain gauge	50202	R.M. Young, USA	Foremast (24 m)
Tair/RH with aspirated radiation shield	HMP155 43408 Gill	VAISALA, Finland R.M. Young, USA	Foremast (23 m)
Optical rain gauge	ORG-815DR	Osi, USA	Foremast (24 m)

Sensors (Radiation)	Type	Manufacturer	Location *
Radiometer (short wave) with ventilation unit	SR20 VU01	Hukseflux Thermal Sensors B.V., Netherlands	Foremast (25 m)
Radiometer (long wave) with ventilation unit	IR20 VU01	Hukseflux Thermal Sensors B.V., Netherlands	Foremast (25 m)

Sensor (PAR&UV)	Type	Manufacturer	Location (altitude from surface)
PAR&UV sensor	PUV-510	Biospherical Instrum ents Inc., USA	Navigation deck (18m)

For the quality control as post processing, we checked the following sensors, before and after the cruise.

i. Young Rain gauge (SMet and SOAR)
   Inspect of the linearity of output value from the rain gauge sensor to change Input value by adding fixed quantity of test water.
ii. Barometer (SMet and SOAR)
   Comparison with the portable barometer value, PTB220, VAISALA
iii. Thermometer (air temperature and relative humidity) (SMet and SOAR)
   Comparison with the portable thermometer value, HM70, VAISALA

(5) Observation log

26 Aug. 2024 - 30 Sep. 2024

(6) Preliminary results

Figure. 2.2-1 shows the time series of the following parameters;

Wind (SOAR)
Air temperature (SMet)
Relative humidity (SMet)
Precipitation (SOAR, ORG)
Short / Long wave radiation (SOAR)
Pressure (SMet)

Sea surface temperature (SMet)
Significant wave height (SMet)

(7) Data archives

These data obtained in this cruise will be submitted to the Data Management Group of JAMSTEC, and will be opened to the public via "Data Research System for Whole Cruise Information in JAMSTEC (DARWIN)" in JAMSTEC web site.
<https://www.godac.jamstec.go.jp/darwin/en>

(8) Remarks

i) The following period, Sea surface temperature of SMet data were available.
08:30UTC 27 Aug. 2024 - 23:56UTC 28 Sep. 2024

ii) The following periods, increasing of SMet capacitive rain gauge data were invalid due to MF/HF radio transmission.
03:26UTC 29 Aug. 2024
22:50UTC 30 Aug. 2024
00:07UTC 31 Aug. 2024
14:51UTC 09 Sep. 2024
23:24UTC 11 Sep. 2024
18:36, 18:59, 19:19, 19:22UTC 29 Sep.2024

iii) The following time, SMet air temp. (starboard side), dewpoint temp. (starboard side) and air pressure data were invalid.
22:43:06UTC 04 Sep. 2024
01:04:36UTC 06 Sep. 2024

iv) The following period, SMet wind speed/direction data were invalid due to system maintenance.
18:04UTC 16 Sep. 2024 - 18:14UTC 16 Sep. 2024

v) The following period, SMet wind speed/direction data were measured by the ultrasonic anemometer on the after mast.
18:14UTC 16 Sep. 2024 - 18:45UTC 16 Sep. 2024

vi) The following period, SMet wind speed/direction were measured by the vane anemometer on the foremast.
18:45UTC 16 Sep. 2024 - 01:52UTC 24 Sep. 2024

vii) The following time, SMet all data were invalid due to system maintenance.
01:42:48UTC 07 Sep. 2024

viii) The following period, wave height and wave period (Bow/Aft) data were invalid.

01:42:48UTC 07 Sep. 2024 - 01:43:18UTC 07 Sep. 2024

ix) The following period, SOAR data intermittently missed and timestamps duplicated.

02:14:33UTC - 02:43:10UTC 18 Sep. 2024

x) The following period, SOAR PAR data acquisition was suspended due to system maintenance.

02:43UTC - 03:07UTC 27 Aug. 2024

20:02:26UTC - 20:08:02UTC 29 Sep. 2024

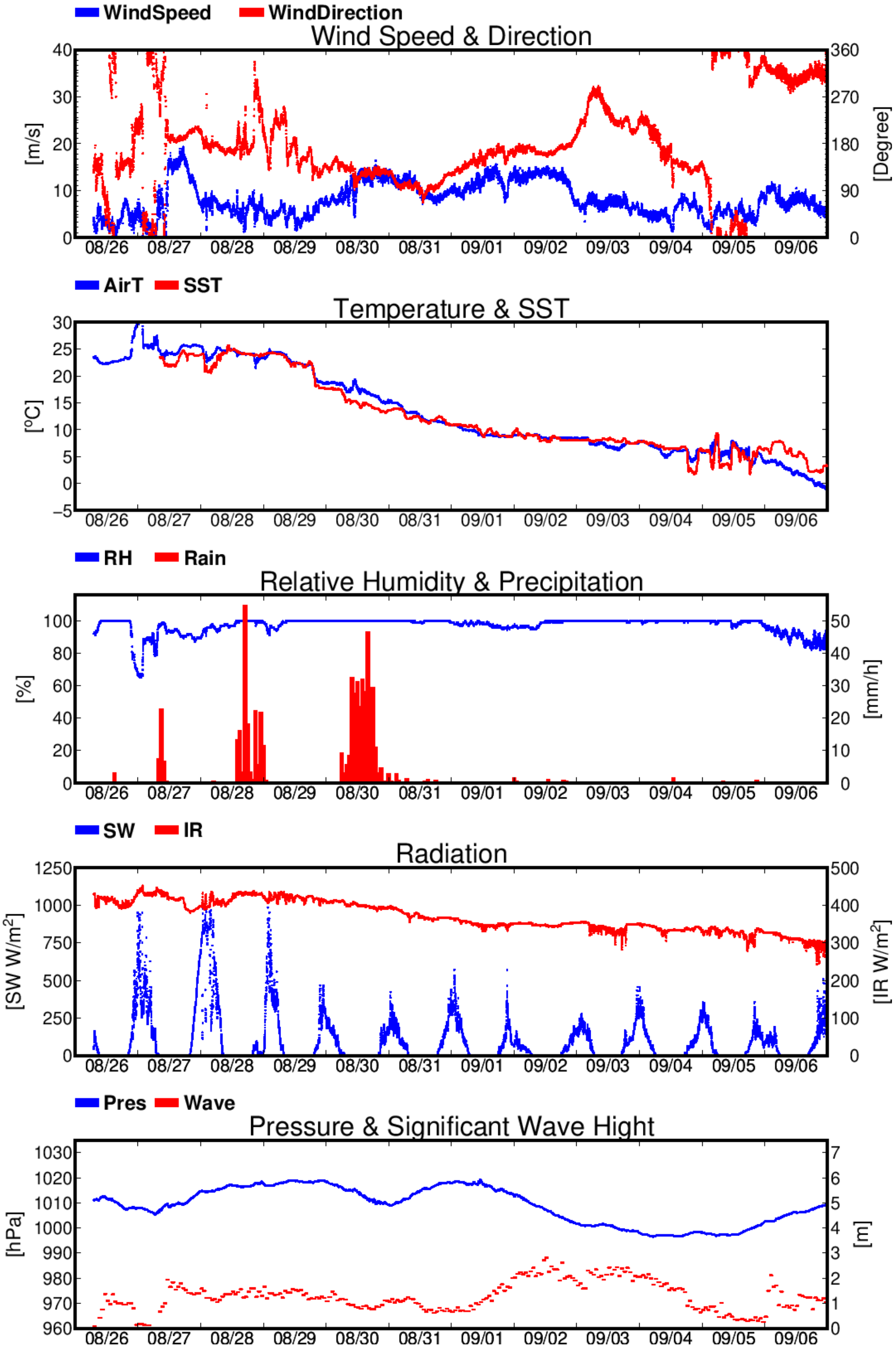

Figure 2.2-1: Time series of surface meteorological parameters during this cruise

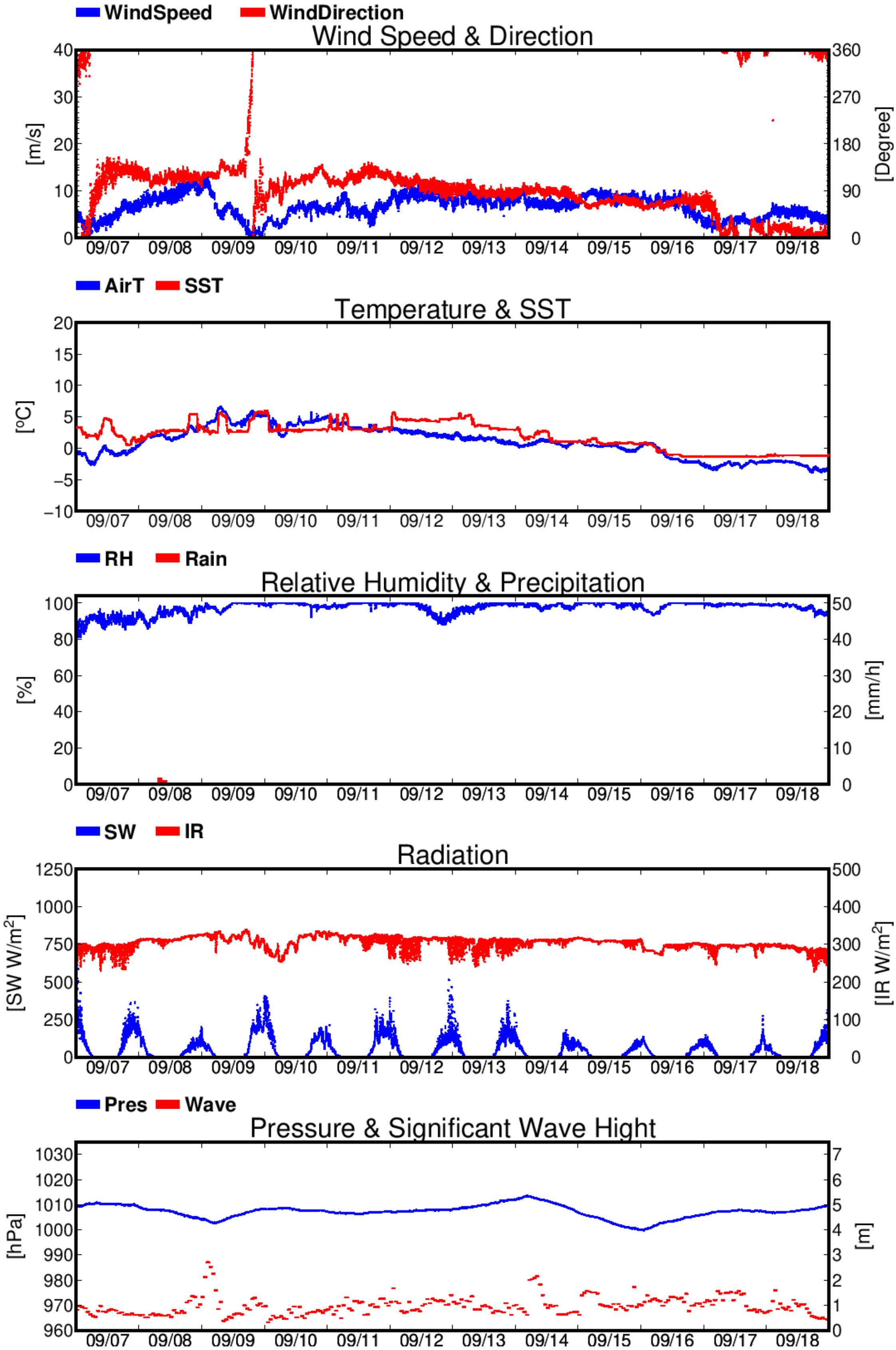

Figure 2.2-1: (Continued)

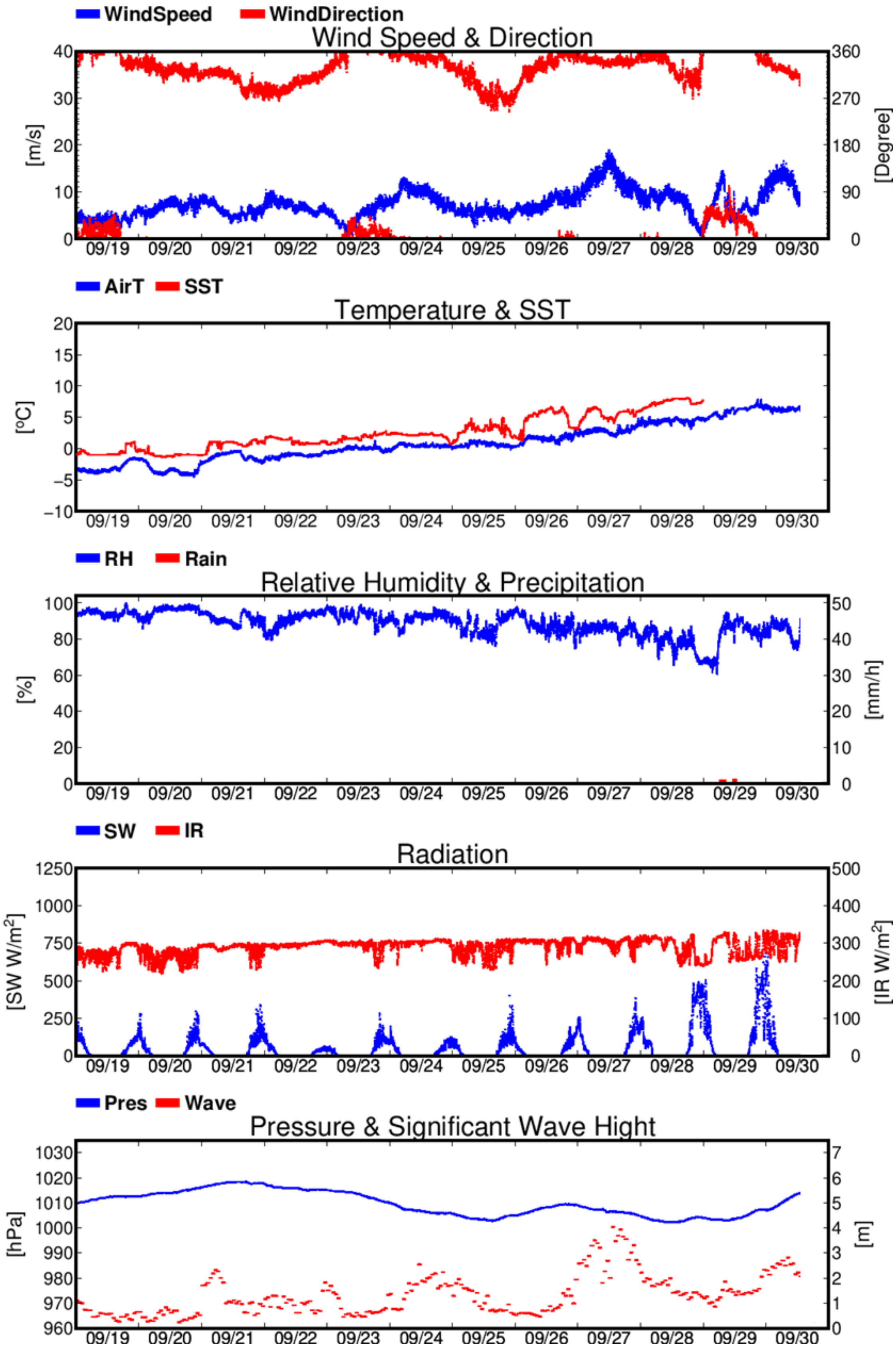

Figure 2.2-1: (Continued)

2.3. Ceilometer

(1) Personnel

Motoyo Itoh	JAMSTEC	-PI
Satomi Ogawa	NME (Nippon Marine Enterprises, Ltd.)	
Souichiro Sueyoshi	NME	
Shinya Okumura	NME	
Haruna Yamanaka	NME	
Masanori Murakami	MIRAI Crew	

(2) Objectives

The information of cloud base height and the liquid water amount around cloud base is important to understand the process on formation of the cloud. As one of the methods to measure them, the ceilometer observation was carried out.

(3) Parameters

Cloud base height [m].

Backscatter profile, sensitivity and range normalized at 10 m resolution.

Estimated cloud amount [oktas] and height [m]; Sky Condition Algorithm.

(4) Instruments and methods

Cloud base height and backscatter profile were observed by ceilometer (CL51, VAISALA, Finland). The measurement configurations are shown in Table 2.3-1. On the archive dataset, cloud base height and backscatter profile are recorded with the resolution of 10 m.

Table 2.3-1: The measurement configurations

Property	Description
Laser source	Indium Gallium Arsenide (InGaAs) Diode
Transmitting center wavelength	910±10 nm at 25 degC
Transmitting average power	19.5 mW
Repetition rate	6.5 kHz
Detector	Silicon avalanche photodiode (APD)
Responsibility at 905 nm	65 A/W
Cloud detection range	0 ~ 13 km
Measurement range	0 ~ 15 km
Resolution	10 m in full range
Sampling rate	36 sec.
Sky Condition	Cloudiness in octas (0 ~ 9) 0 Sky Clear 1 Few 3 Scattered 5-7 Broken 8 Overcast

(5) Observation log

26 Aug. 2024 - 30 Sep. 2024

(6) Preliminary results

Figure 2.3-1 shows the time-series of the lowest, second and third cloud base height during the cruise.

(7) Data archives

These data obtained in this cruise will be submitted to the Data Management Group of JAMSTEC, and will be opened to the public via "Data Research System for Whole Cruise Information in JAMSTEC (DARWIN)" in JAMSTEC web site.
<https://www.godac.jamstec.go.jp/darwin/en>

(8) Remarks

Window cleaning

00:51UTC 05 Sep. 2024
18:50UTC 11 Sep. 2024
17:45UTC 22 Sep. 2024

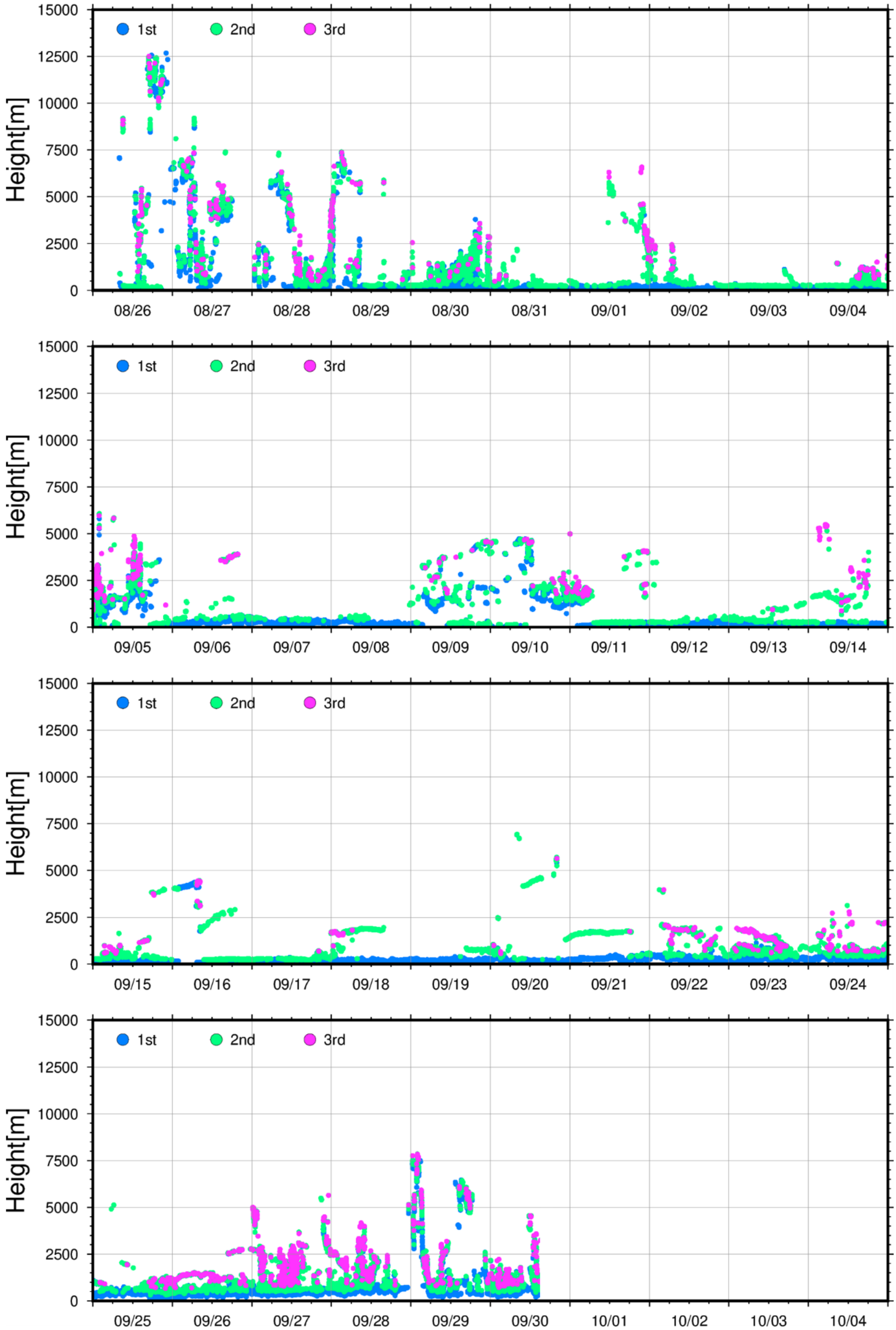

Figure 2.3-1: Time series of cloud base height during this cruise

2.4. Tropospheric gas and particles observation

(1) Personnel

Fumikazu Taketani	JAMSTEC(Principal Investigator)	- not on board
Takeshi Kinase	JAMSTEC	- not on board
Masayuki Takigawa	JAMSTEC	- not on board
Yugo Kanaya	JAMSTEC	- not on board
Takuma Miyakawa	JAMSTEC	- not on board
Hisahiro Takashima	JAMSTEC/Fukuoka Univ.	- not on board
Kazuyo Yamaji	JAMSTEC/Kobe Univ.	- not on board
Zhu Chunmao	JAMSTEC	- not on board

Operation for online instruments was supported by Nippon Marine Enterprises, Ltd

(2) Objectives

- To investigate roles of gas and aerosols in the marine atmosphere in relation to climate change
- To investigate processes of biogeochemical cycles between the atmosphere and the ocean.
- To investigate gas and aerosol transports from anthropogenic activities
- To investigate physical and chemical particle states of aerosols

(3) Parameters

- Particle size distribution
- Fluorescent particles
- Individual particle features of ambient particles
- Surface ozone(O_3), and carbon monoxide(CO) mixing ratios
- Aerosol extinction coefficient (AEC) and trace gases

(4) Instruments and methods

(4-1) Online aerosol observations:

(4-1-1) Particle size distribution

The size distribution of aerosol particles was measured by a handheld optical particle counter (OPC) (KR-12A, Rion).OPC was installed on the compass deck and the sample air was introduced to OPC directly at ambient RH.

(4-1-2) Fluorescent property

Fluorescent properties of aerosol particles were measured by a single particle fluorescence sensor, Waveband Integrated bioaerosol sensor (WIBS-4A, Droplet Measurement Technologies). Two pulsed xenon lamps emitting UV light (280 nm and 370 nm) were used for excitation. Fluorescence emitted from a single particle within 310–400 nm and 420–650 nm wavelength windows was recorded. WIBS-4 was installed on the compass deck and the sample air was introduced to WIBS-4 directly at ambient RH.

(4-2) Ambient aerosol sampling

Aerosol particles were collected on the Cu grid with a Formvar thin film (U1007, EM Japan) to analyze physical and chemical particle features, mixing states, hygroscopicity, and ice nucleation efficiency for individual aerosol particle by a transmission electron microscope (TEM) and an environmental scanning electron microscope (ESEM). These samples were collected by an automated two-stage impactor (AS-24W, Arios) operated at a flow rate of 1.0 L/min. The sampling time length was 40 minutes. AS-24W was usually worked every four hours during the cruise. The samples are going to be analyzed in the laboratory.

(4-3) CO and O_3

Ambient air was continuously sampled on the compass deck and drawn through ~20m long Teflon tubes connected to a nondispersive infrared (NDIR) CO analyzer (Model 48i-TLE, Thermo Fisher Scientific) and a UV photometric ozone analyzer (model 205, 2B Technologies), located in the environmental research room. The data will be used for characterizing air mass origins

(4-4) Aerosol extinction coefficient (AEC) and trace gases

Multi-Axis Differential Optical Absorption Spectroscopy (MAX-DOAS), a passive remote sensing technique measuring spectra of scattered visible and ultraviolet (UV) solar radiation, was used for atmospheric aerosol and gas profile measurements. MAXDOAS were installed at the deck above stabilizer of ship. Our MAX-DOAS instrument consists of two main parts: an outdoor telescope unit and an indoor spectrometer (Acton SP-2358 with Princeton Instruments PIXIS-400B), connected to each other by a 14-m bundle optical fiber cable. The line of sight was in the directions of the portside of the vessel and the scanned elevation angles were 1.5, 3, 5, 10, 20, 30, 90 degrees in the 30-min cycle. The roll motion of the ship was measured to autonomously compensate additional motion of the prism, employed for scanning the elevation angle. For the selected spectra recorded with elevation angles with good accuracy, DOAS spectral fitting was performed to quantify the slant column density (SCD) of NO_2 (and other gases) and O_4 (O_2-O_2, collision complex of oxygen) for each elevation angle. Then, the O_4 SCDs were converted to the aerosol optical depth (AOD) and the vertical profile of aerosol extinction coefficient (AEC) using an optimal estimation inversion method with a radiative transfer model. Using derived aerosol information, retrievals of the tropospheric vertical column/profile of NO_2, IO, and other gases were made.

(5) Data archives

These data obtained in this cruise will be submitted to the Data Management Group

of JAMSTEC, and will be opened to the public via "Data Research System for Whole Cruise Information in JAMSTEC (DARWIN)" in JAMSTEC web site.
<http://www.godac.jamstec.go.jp/darwin/e>

(6) Acknowledgments
We thank the crew of the R/V Mirai, staff of Nippon Marine Enterprises, Ltd., and Dr. Amane FUJIWARA, Dr. Yuri FUKAI, and Dr. Motoyo ITOH for their support with observations throughout the cruise.

2.5. Mie / Raman Lidar

(1) Personnel

Kazutoshi SATO	(NIPR)
Kazuho YOSHIDA	(NME)
Masaki KATSUMATA	(JAMSTEC)
Kyoko TANIGUCHI	(JAMSTEC)

(2) Objective

The objective of this observation is to capture the vertical distribution of clouds, aerosols, and water vapor in high spatio-temporal resolution.

(3) Parameters

355nm Mie scattering signal
532nm Mie scattering signal
1064nm Mie scattering signal
387nm Raman nitrogen scattering signal (nighttime only)
408nm Raman water vapor scattering signal (nighttime only)
607nm Raman nitrogen scattering signal (nighttime only)
660nm Raman water vapor scattering signal (nighttime only)

(4) Instruments and methods

The Mirai Lidar system transmits a 10-Hz pulse laser in three wavelengths: 1064nm, 532nm, 355nm. For cloud and aerosol observation, the system detects Mie scattering at these wavelengths. The separate detections of polarization components at 532 nm and 355 nm obtain additional characteristics of the targets. The system also detects Raman water vapor signals at 660 nm and 408nm, Raman nitrogen signals at 607 nm and 387nm at nighttime. Based on the signal ratio of Raman water vapor to Raman nitrogen, the system offers water vapor mixing ratio profiles.

(5) Preliminary Results

The lidar system observed the lower atmosphere throughout the cruise (26 August to 29 September, 2024). All data will be reviewed after the cruise to maintain data quality.

(6) Data Archive

The obtained data will be submitted to the Data Management Group of JAMSTEC.

2.6. Greenhouse gases observation

(1) Personnel

Shigeyuki Ishidoya	AIST	-PI, not on board
Amane Fujiwara	JAMSTEC	on board
Shinji Morimoto	Tohoku Univ.	-not on board
Daisuke Goto	NIPR	-not on board
Prabir Patra	JAMSTEC	-not on board

(2) Objectives

Discrete flask sampling

In order to clarify spatial variations and air-sea exchanges of the greenhouse gases at northern high latitude, whole air samples were corrected into 8 stainless-steel flasks on-board R/V MIRAI (MR24-06C). The collected air samples will be analyzed for the mixing ratios of CO_2, O_2, Ar, CH_4, CO, N_2O and SF_6 and the stable isotope ratios of CO_2 and CH_4.

Figure 2.6-1 : Flask sampling system during MR24-06C cruise.

(3) Parameters

Mixing ratios of atmospheric CO_2, O_2 (O_2/N_2 ratio), Ar (Ar/N_2 ratio), CH_4, CO, N_2O and SF_6, $\delta^{13}C$ and $\delta^{18}O$ of CO_2, $\delta^{13}C$ and δD of CH_4.

(4) Instruments and methods

The air sampling equipment consisted of an air intake, a diaphragm pump (GAST MOA), a Stirling cooler (Twinbird) with a water trap, solenoid valves (CKD), a flow meter and a back pressure valve. Ambient air was pumped using the diaphragm pump from an air intake, dried cryogenically and filled into a 1 L stainless-steel flask at a pressure of 0.27 MPa.

(5) Station list or Observation log

Sampling logs of the discrete flask sampling are listed in Table 2.6-1.

Table 2.6-1 : List of logs of the discrete flask sampling.

On board ID	Data Collected				
	YYYY	MM	DD	hh:mm	UTC/JST
MR2406-F001	2024	8	28	2:40	UTC
MR2406-F002	2024	8	29	4:11	UTC
MR2406-F003	2024	8	30	2:44	UTC
MR2406-F004	2024	8	31	4:21	UTC
MR2406-F005	2024	9	1	4:00	UTC
MR2406-F006	2024	9	3	5:19	UTC
MR2406-F007	2024	9	4	20:11	UTC
MR2406-F008	2024	9	13	14:04	UTC

(6) Preliminary results

(7) Data archives

These data obtained in this cruise will be submitted to the Data Management Group of JAMSTEC, and will be opened to the public via "Data Research System for Whole Cruise Information in JAMSTEC (DARWIN)" in JAMSTEC web site.
<http://www.godac.jamstec.go.jp/darwin/e>

2.7. Observation of atmospheric water vapor isotopes

(1) Personnel

Hotaek Park (JAMSTEC) Principal investigator

(2) Background and objective

In recent years, the declining Arctic sea-ice caused open sea surface can result in larger evaporation from the surface under the warming climates. The evaporated water vapor likely wets the atmosphere, which is then implicate to the higher water cycle in terrestrial regions as a precipitable water. Observations identified the increase of autumnal precipitation and the increase of winter snow depth in the terrestrial regions, particularly the northeastern Siberia. The increased snow has larger insulation enhancing permafrost warming during the winter season, and the snow meltwater is also correlated to the higher spring peak discharge. The observed Siberian major rivers indicated the increasing trends in the spring river discharge for the recent decades. Furthermore, the snow induced permafrost warming, combined with the warming air temperature, can increase the melting of ground ice within the permafrost, resultantly increasing the connectivity of the melted water to the river discharge. Likewise, these linkages and interactions potentially suggest the impacts of the declining Arctic sea-ice on the terrestrial hydrologic processes.

However, observations have provided little evidence representing the influence of the declined sea-ice on the strengthened terrestrial water cycle. The water vapor evaporated from the sea surface is mixed with other source waters in the atmosphere. Isotope is a useful tool to separate the contribution of the Arctic Ocean sourced water to the terrestrial hydrology, tracking the origins of the terrestrial precipitation. Focused on the advantage of stable water isotope, a precipitation isotope observational network was constructed sampling the precipitation water at the Arctic Ocean and land. As the observational activity using the network, the isotope of the atmospheric water vapor has been monitored at the MIRAI Arctic Ocean cruise from 2019, which was defined as a research topic of the ArCS and ArCS II projects.

The observed data likely provide important information for the spatial and temporal variability of the isotopic ratios along the cruise route over the Arctic sea surface, including the precipitation events. However, the observed records have constraints in identifying the implication of the declined sea ice to the terrestrial water cycle at the spatial and temporal scale. The problems could be reduced by numerical models covering the global scale over longer time period. The observational data need to validate the simulated results. This document reports the isotopic properties of atmospheric water vapor monitored at the R/V MIRAI 2024 Arctic cruise up to the minute.

(3) Parameters

Isotope ratios of oxygen and hydrogen and water vapor concentration

(4) Instrument and method

The isotopic ratios of atmospheric water vapor were monitored by a L2130-*i* Isotope and Gas Concentration Analyzer (Picarro, Fig. 2.7-1), which provides $\delta^{18}O$ and $\delta^{2}H$ values for isotopic H_2O with high-precision measurements 1–2 Hz frequency, including water vapor concentration for the range of 1000 to 50000 ppm. The observed data are archived on the storage of the spectrometer, operated by windows operational system. Two standard liquids, for example with isotopic values of -0.41/-1.59‰ and -31.20/-245.26‰ for $\delta^{18}O/\delta^{2}H$, are individually injected for 15 minutes every 12-hour, in which the derived linear regression equation is used to calibrate the values monitored by the spectrometer.

Fig 2.7-1 Isotope spectrometer system.

(5) Preliminary results

The monitored second resolution of isotopic ratios were averaged to hourly time scales, exhibiting the temporal variability in the Arctic Ocean during the cruse period from September 1 to 27 of 2024, with air and sea surface temperature (Fig. 2.7-2). There were intermittent gaps in the monitoring during the cruise period. The isotopic ratios of $\delta^{18}O/\delta^{2}H$ showed higher values at the initial dates of the cruse, in which the vessel cruised relatively warm regions as identified by air temperature. Then, the ratios gradually decreased and recorded the minimum values (i.e., -28.6‰ for $\delta^{18}O$ and -198.1 for $\delta^{2}H$) on Sep. 22, characterized by the colder air temperature. During the period from Sep. 16 to Sep. 22 as the vessel stayed over the northern Arctic Ocean, the air temperature recorded 0℃ below, and the sea surface temperature was also cold, representing the spatial variability of the sea surface heat condition along the vessel cruising routes.

The isotopic ratios of $\delta^{18}O/\delta^{2}H$ significantly correlated with air temperature. Their variability shows similar patterns in the time series (Fig. 2.7-2), of which the relationship has already identified at the previous cruise years (i.e., 2019–2023). The connectivity of the isotope ratios and air temperature is verified by the d-excess index (= -8×$\delta^{18}O$ + $\delta^{2}H$) that represents humidity and temperature conditions of the evaporated sea surface, exhibiting larger diurnal and daily variability at the range of approximately 40 ‰, relative to the lower variability of $\delta^{18}O$ and $\delta^{2}H$ (Fig. 2.7-2). The d-excess was correlated to the difference between sea surface and air temperature with larger scattering, as certified by the past cruise data. The water vapor recorded relatively lower isotopic ratios at cold temperature, resulting in higher d-excess values (Fig. 2.7-2). The larger difference between air and sea surface temperature represents higher atmospheric demand for evaporation, consequently higher evaporation with higher d-excess values. This suggests that the measurements had captured the impact of water vapor evaporated from the warmer ocean surface on the isotopic ratios.

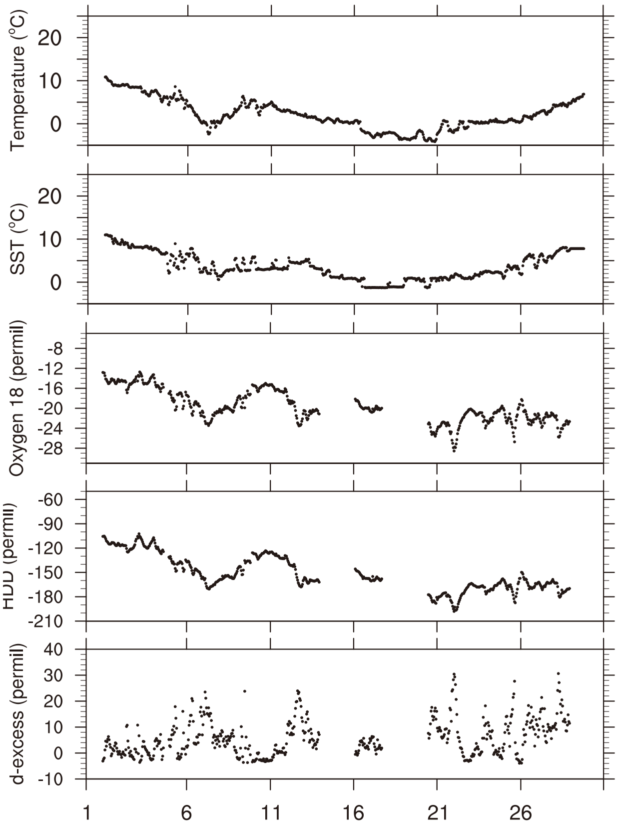

Fig 2.7-2 Time series variability of temperature of air surface and sea surface and water vapor stable isotope variables in September during 2024 MIRAI Arctic Ocean cruise.

The monitored $\delta^{18}O$ and $\delta^{2}H$ ratios indicated significantly higher correlation (Fig. 2.7-3), which yielded the slope of 6.22, ranging medium value compared to the values of 2019–2023. The slope values, including the past cruises distributed within the ranges of 4.8 and 7.6, which was compared with the values (i.e., 5.75 in Tiksi

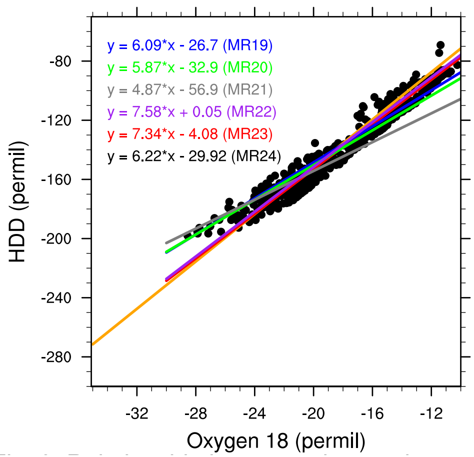

Fig 2.7-3 Relationship between observed oxygen and hydrogen isotopes in individual cruise years from 2019 to 2024, represented by the regression equations.

and 6.0 in Mackenzie delta) obtained at the northernmost terrestrial sites. However, the slopes derived by the six-year cruise is lower than the value 8 of global meteoric water line (GMWL), representing the dependence of isotopic ratios on regional and temporal climatic conditions.

(6) Data archive

The data obtained in this cruise will be submitted to the Data Management Group of JAMSTEC, and will be opened to the public via "Data Research System for Whole Cruise Information in JAMSTEC (DARWIN)" in JAMSTEC web site.
http://www.godac.jamstec.go.jp/darwin/e.

2.8. Mercury observation

(1) Personnel

Osamu NAGAFUCHI Fukuoka Institute of Technology

Masanobu YAMAMOTO Hokkaido University PI

(2) Objective

Mercury from anthropogenic emissions around the world continues to travel to the Arctic environment. However atmospheric levels in the Arctic are generally decreasing. The decreasing trend of atmospheric mercury may be related to a decrease in emissions from regions closer to the Arctic, or to the effects of climate change, or both. However, there are not many observations of long-range transport from East Asia, where mercury emissions are high. Furthermore, observations in the oceanic atmosphere are rare. Measurements of mercury concentrations in the Arctic will make an important contribution to assessments of the effectiveness of the Minamata Convention.

To understand the dynamics of atmospheric mercury on the global scale, gaseous elemental mercury(GEM) was measured on board during the MR24-06C cruise.

(3) Parameters

Gaseous Elemental Mercury (GEM)

(4) Instrument and method

Gaseous elemental mercury (GEM) in the atmosphere was measured using the AM-6F (NIPPON INSTRUMENTS CORPORATION), which is a Fully Automated, Continuous Mercury Monitor designed to measure GEM from ambient air accurately down to the sub nano-gram per cubic-meter level. The technique used is direct Gold Amalgamation Sampling – a cold vapor atomic fluorescence spectrometer (CVAFS).

(5) Observation log

Data from September 19 to September 21 were lost due to equipment trouble.

(6) Preliminary results

Measurements of gaseous elemental mercury (GEM) in the marine boundary layer were performed using a fully automated, continuous mercury monitor AM-6F during this cruse. GEM concentrations varied from 1.06 to 2.67 ng/m3 (n=4207); the average value (1.37±0.16 ng/m3) was lower than the background range of the Northern Hemisphere

(1.5~1.7ng/m3) and corresponded to the background concentrations of the Southern Hemisphere (1.1~1.3 ng/m3). However, each sea area (Sea of Okhotsk, Bering Sea, and Arctic Sea) had its own characteristics. The concentration tended to decrease as one moved northern sea area.

(7) Data archive

These data obtained in this cruise will be submitted to the Data Management Group of JAMSTEC, and will be opened to the public via "Data Research System for Whole Cruise Information in JAMSTEC (DARWIN)" in JAMSTEC web site.

2.9. Drone

(1) Personnel

Jun Inoue	NIPR (not on-board)	- PI
Kazutoshi Sato	NIPR (not on-board)	
Kazuho Yoshida	NME	
Satomi Ogawa	NME	
Souichiro Sueyoshi	NME	
Shinya Okumura	NME	
Haruna Yamanaka	NME	
Masanori Murakami	MIRAI Crew	

(2) Objectives

The objectives of this observation approach were to obtain meteorological profiles.

(3) Parameters

Air Pressure [hPa], Air Temperature [degC], and Relative Humidity [%]

(4) Instruments and methods

The drone that we used was Mavic3 classic, produced by DJI. To monitor the vertical structures of atmosphere, we conducted vertical profiling using a small meteorological sensor onboard drone. The status of the Global Navigation Satellite System (GPS, Galileo & BeiDou), radio waves (2.4 GHz) and gyrocompass were fundamental for stable and safe drone operations.

A meteorological sensor, iMet-XQ2 (hereafter, XQ2) (International Met Systems, Inc.: weight 60 g), was installed on the left front arm of a drone with a radiation shield. The XQ2 can record air temperature, relative humidity, air pressure, and GPS position at 1-s intervals with quality equivalent to that of a radiosonde. The radiation shield reduces the effect of radiation from the sun and that of other infrared radiation from the atmosphere and the body of the drone. Additionally, the shape of the shield also reduces the chance of direct accretion of cloud droplets and precipitation on the probe.

(5) Station list

During the Arctic cruise in 2024, 8 vertical profiles of atmosphere up to a maximum height of 900 m were conducted from 3rd September to 16th September 2024. Table 2.9 presents the flight summary, and Figure 2.9.1 shows the map of flight points.

Table 2.9: Flight summary

No.	m/d	Takeoff (UTC)	Landing (UTC)	Lat (°N)	Lon (°W)	Max Altitude (m)	Purpose of flight, Remarks (station number, other issues)
01	9/3	2:45	2:50	57-57	177-36E	84	St.01 Test flight (No iMet-XQ2 data)
02	9/7	17:17	17:20	71-18	164-21	112	St.08
03	9/10	17:44	17:53	71-55	154-05	508	St.14
04	9/11	18:30	18:37	71-55	154-05	400	BC2-3 (Dripping on drone)
05	9/12	21:32	21:39	71-30	152-30	362	St.16 (Dripping on drone)
06	9/13	16:33	16:39	72-18	152-30	652	St.20 (Dripping on drone)
07	9/13	18:54	19:06	72-36	152-30	900	St.21 (Dripping on drone)
08	9/15	19:18	19:25	74-31	161-49	370	St.22 (Dripping on drone)
09	9/16	17:58	18:12	76-08	167-34	500	Marginal Ice zone (Dripping on drone, Water getting in the aircraft)

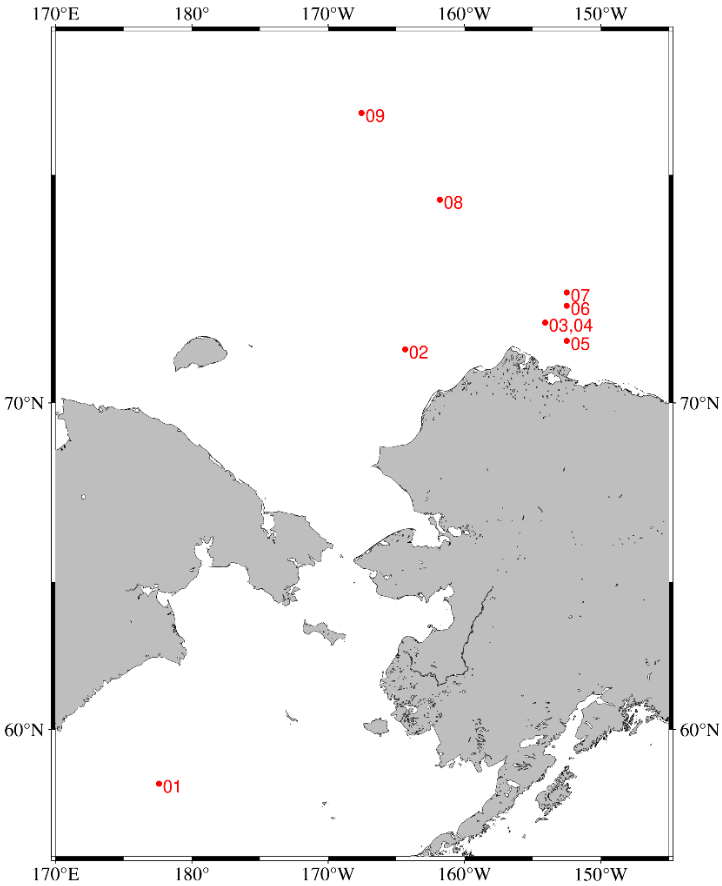

Figure 2.9-1: A map with drone flight points

(6) Preliminary results

Figure 2.9-2 shows the example of vertical profiles up to about 900m of air temperature and relative humidity and air pressure (flight #07).

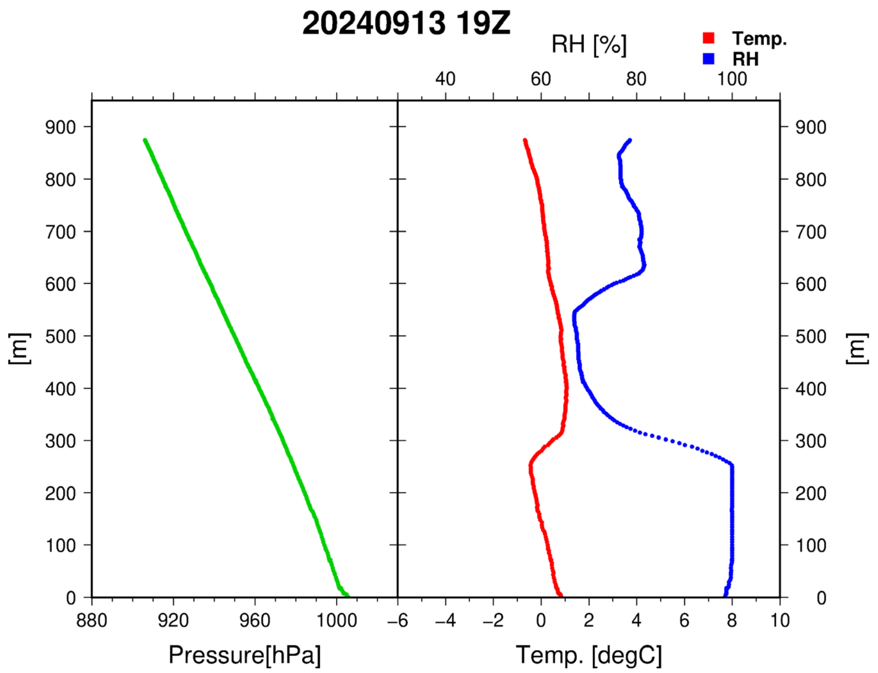

Figure 2.9-2: Vertical profile of air pressure, air temperature and relative humidity in the flight #07.

(7) Data archives

These data obtained in this cruise will be submitted to the Data Management Group of JAMSTEC, and will be opened to the public via "Data Research System for Whole Cruise Information in JAMSTEC (DARWIN)" in JAMSTEC web site.
<https://www.godac.jamstec.go.jp/darwin/en>

2.10. Microwave radiometer

(1) Personnel

Kazutoshi Sato	NIPR (not on board)	- PI
Kazuho Yoshida	NME	
Satomi Ogawa	NME	
Souichiro Sueyoshi	NME	
Shinya Okumura	NME	
Haruna Yamanaka	NME	
Masaki Katsumata	JAMSTEC (not on board)	
Akira Kuwano-Yoshida	Kyoto Univ. (not on board)	
Masahiro Minowa	Furuno Electric Co., Ltd. (not on board)	

(2) Objectives

The objectives of this observation approach were to retrieve the total column integrated water vapor, and the vertical profiles of water vapor and temperature.

(3) Parameters

The total column integrated water vapor, and the vertical profiles of water vapor and temperature.

(4) Instruments and methods

Two microwave radiometers (hereafter MWR; manufactured by Furuno Electric Co., Ltd.) were used. The MWRs received natural microwave within the angle of 20 deg. from zenith. One of the MWRs for the water vapor observed at the frequencies around 22 GHz, to retrieve the column integrated water vapor (or precipitable water), and the vertical profile of the water vapor. The other MWR measured at the frequencies around 55 GHz to retrieve vertical profile of the air temperature.

The observation was made approximately every 20 seconds except when periodic auto-calibration was on-going (once in several minutes). The rain sensor is equipped to identify the period of rainfall.

In addition to the MWRs, the whole sky camera was installed beside the MWR. This is to monitor cloud cover, which also affects the microwave signals. The camera obtained the whole-sky image every 2 minutes.

Both instruments were installed at the top of the roof of aft wheelhouse, as in Figure 2.10. The data were continuously obtained all through the cruise period.

(5) Observation log

26 Aug. 2024 -30 Sep. 2024

(6) Preliminary results

The data have been obtained all through the cruise. The further analyses for the water vapor (column-integrated amount and vertical profile), the air temperature (vertical profile), etc., will be carried out after the cruise.

Figure 2.10: Outlook of the instruments installed at the roof of the aft wheelhouse; the microwave radiometer for the air temperature (right), microwave radiometer for the water vapor (middle), and the whole-sky camera (left).

(7) Data archives

These data obtained in this cruise will be submitted to the Data Management Group of JAMSTEC, and will be opened to the public via “Data Research System for Whole Cruise Information in JAMSTEC (DARWIN)” in JAMSTEC web site.
<https://www.godac.jamstec.go.jp/darwin/en>

2.11. Evaluation of performance of the DFMC SBAS from QZSS

(1) Personnel

Toru Takahashi (ENR, MPATI)

Mitsunori Kitamura (ENRI, MPAT)

(2) Objectives

The aviation and maritime activities in the Arctic are growing with the recession of the Arctic sea ice. A model study suggested that the Global Navigation Satellite System (GNSS), which operates with the augmentation system such as the Satellite-based augmentation systems (SBAS) and Advanced Receiver Autonomous Integrity Monitoring (ARAIM), is effective for the navigation of aviation and maritime in the Arctic because of poor infrastructures (Reid et al., 2016). However, the current L1 SBAS broadcasts augmentation messages from geostationary (GEO) satellites, which are not available practically in the polar region at a latitude of 72 degrees or higher.

The Dual Frequency Multi Constellation Satellite Based Augmentation System (DFMC SBAS) has been standardization by the International Civil Aviation Organization (ICAO). Broadcasting augmentation messages from the Inclined Geosynchronous Orbit (IGSO) satellite is considered to be included in the future updates. The Electronic Navigation Research Institute (ENRI) developed the DFMC SBAS prototype based on the draft standards (Kitamura et al., 2018), and test messages are broadcasted from the Japanese Quasi-Zenith Satellite System (QZSS).

In the polar region, an auroral activity often generates the irregularity ionospheric plasma density and the ionospheric electric filed is intensified simultaneously. The carrier phase of the GNSS signal is fluctuated by the auroral activity. Since the fluctuation sometimes causes the loss of lock on GNSS signals, the impact the auroral activity on the GNSS carrier phase should be investigated.

The main objective of this study is to evaluate the performance DFMC SBAS broadcasted from Japanese QZSS in the Arctic and mid-high latitude regions. To test the DFMC SBAS in the Arctic, we installed the GNSS antenna, GNSS receivers, DFMC SBAS receivers, and Inertial Measurement Unit (IMU) to oceanographic research vessel MIRAI.

(3) Parameters

Signals from GNSS satellites and Dual Frequency and Multi-Constellation (DFMC) Satellite Based Augmentation System (SBAS) messages transmitted from the Quasi-Zenith Satellite System (QZSS) are recorded by GNSS receivers. Performance (accuracy and integrity) of the DFMC SBAS from QZSS is evaluated in the on-board environment at mid to high latitudes.

(4) Instruments and methods

i. GNSS Receiver

A NovAtel OEM6 receiver recorded signals from GPS, Galileo, GLONASS, BeiDou, and QZSS at the frequency of L1, L2, and L5 bands. The receiver recorded the observation message, including the pseudorange and carrier phase, with a sampling rate of 10 Hz. The navigation message, including the satellite obit information were also recorded.

A u-blox F9P also observed the GPS, Galileo, GLONASS, BeiDou, and QZSS signals and provided the antenna position by the NMEA format. A u-blox D9C recorded the MADOCA message broadcasted from QZSS satellite to derive the precise antenna position by a post processing.

ii. DFMC SBAS Message receivers

To obtain DFMC SBAS messages, a Furuno prototype DFMC SBAS receiver and CORE Chronosphere receivers were installed. The DFMC SBAS messages were generated by Electronic Navigation Research Institute (ENRI) and broadcasted from QZS02 and OZS04 satellites with a frequency of 1 Hz.

iii. Scintillation receiver

The GNSS signals are sometimes fluctuated by a combination of the ionospheric irregularity and electric field. The fluctuation is called scintillation and becomes a cause of the loss-of-lock GNSS signal. Since we need to receive the carrier phase with high and precise sampling to observe the scintillation, the Septentrio PolaRx5S, which records the GNSS signals with a sampling rate of 100 Hz.

iv. GNSS Antenna

The GNSS Antenna used was a Trimble GA830 capable of receiving L1, L2, and L5 bands. The antenna was designed for maritime and cold weather specification.

v. Inertial Measurement Unit (IMU)

It is challenging to differentiate GNSS signal fluctuations caused by ionospheric irregularities from those caused by vessel motion. The IMU recorded velocity and acceleration at the antenna's position, which are planned to be used to compensate for the vessel's motion.

(5) Station list or Observation log

This observation continuously conducted from 21 August 2024 to 16 November 2024.

(6) Preliminary Results

We successfully received ranging signals from GPS, Galileo, GLONASS, BeiDou, and QZSS using NovAtel receivers, as well as the DFMC SBAS messages transmitted from QZSS-02, QZSS-04, and QZSS-1R during the cruise. Unfortunately, the Septentrio PolaRx5S stopped the recording the ranging signals on October 7 at 11 UT, and the IMU stopped functioning immediately after leaving shore.

(7) Data archives

These data obtained in this cruise will be submitted to the Data Management Group of JAMSTEC, and will be opened to the public via "Data Research System for Whole Cruise Information in JAMSTEC (DARWIN)" in JAMSTEC web site.
<http://www.godac.jamstec.go.jp/darwin/e>

References

Kitamura, M., Aso, T., & Sakai, T. (2018) Wide Area Augmentation Performance of DFMC SBAS Using Global Monitoring Stations, The 16th IAIN World Congress 2018.

Reid, T., Walter, T., Blanch, J., & Enge, P. (2016) GNSS Integrity in The Arctic. NAVIGATION, 63: 469– 492. doi: 10.1002/navi.169.

3. Physical Oceanography
3.1. CTD cast and water samplings

(1) Personnel

Motoyo ITOH (JAMSTEC) (Principal Investigator)
Aine YODA (MWJ) (Operation Leader)
Riho FUJIOKA(MWJ)
Yuta SHINOMIYA (MWJ)
Ko ARIHARA (MWJ)
Tomokazu CHIBA (MWJ)
Ritsuko SAWADA (MWJ)

(2) Objective

The $CTDO_2$/water sampling measurements were conducted to obtain vertical profiles of seawater properties by sensors and water sampling.

(3) Instruments and method

Instruments used in this cruise are as follows:

Winch and cable

Traction winch system (3.0 ton) (Dynacon, Inc., Bryan, Texas, USA)
Armored cable (φ = 9.53 mm)
Compact underwater slip ring swivel

Frame

592 kg stainless steel frame for 36-position 12-L water sample bottles
Aluminum rectangular fin (54 × 90 cm) to resist frame's rotation

Water sampler and sampling bottle

36-position carousel water sampler, SBE 32 (Sea-Bird Scientific, Washington, USA)
Serial no. 3254451-0826

12-L sample bottle, model OTE 110 (OceanTest Equipment, Inc., Fort Lauderdale, Florida, USA)
(No TEFLON coating, with Viton O-rings)

Deck unit

SBE 11plus (Sea-Bird Scientific, Washington, USA)
Serial no. 11P54451-0872
(Casts Used: 001M001~019M001)
Serial no. 11P39850-0705
(Casts Used: 022M001~047M001)

Underwater unit

Pressure sensor, SBE 9plus (Sea-Bird Scientific, Washington, USA)

Serial no. 09P27443-0677 (79511) (calibration date: June 10, 2022)

Deep standard reference thermometer, SBE 35 (Sea-Bird Scientific, Washington, USA)

Serial no. 53 (calibration date: June 26, 2023)

Temperature sensor, SBE 03Plus (Sea-Bird Scientific, Washington, USA)

Primary, Serial no. 03P2730 (calibration date: January 18, 2024)

Secondary, Serial no. 03P5737 (calibration date: January 17, 2024)

Conductivity sensor, SBE 04C (Sea-Bird Scientific, Washington, USA)

Primary, Serial no. 042854 (calibration date: November 14, 2023)

Secondary, Serial no. 041206 (calibration date: June 06, 2024)

Dissolved oxygen sensor, RINKO III (JFE Advantech Co., Ltd., Hyogo, Japan)

Serial no. 0278 (calibration date: August 05, 2024)

Dissolved oxygen sensor, SBE 43 (Sea-Bird Scientific, Washington, USA)

Serial no. 432471 (calibration date: September 02, 2023)

Chlorophyll fluorometer (Seapoint Sensors Inc., New Hampshire, USA)

Serial no. 3701, Gain: 10X (0-15 ug/L)

Ultraviolet fluorometer (Seapoint Sensors Inc., New Hampshire, USA)

Serial no. 6246, Gain setting: 30X (0-50 QSU)

PAR sensor, PAR-Log ICSW (Sea-Bird Scientific, Washington, USA)

Serial no. 2180 (calibration date: September 14, 2021)

Nitrate sensor (Sea-Bird Scientific, Washington, USA)

Serial no. 1613 (calibration date: September 1, 2024)

Transmissometer, C-Star, (WET Labs, Inc., Philomath, Oregon, USA)

Serial no. 1727DR (calibration date: March 04, 2024)

Pump, SBE 5T (Sea-Bird Scientific, Washington, USA)

Primary, Serial no. 055816

Secondary, Serial no. 054598

Software

Data acquisition software, SEASAVE-Win32, version 7.26.7.121

Data processing software, SBEDataProcessing-Win32, version 7.26.7.129 and some original modules

(4) Data Collection and processing

(4.1) Data collection

The CTD system was powered on at least 15 minutes in advance of the data acquisition to stabilize the pressure sensor. The data was acquired at least two minutes before and after the CTD cast to collect atmospheric pressure data on the ship's deck.

The CTD package was lowered into the water from the starboard side and held 10 m beneath the surface to activate the pump. After the pump was activated, the package was lifted to the surface and lowered at a rate of 1.0 m/s to 200 m (or 300 m when significant wave height was high) then the package was stopped to operate the heave compensator of the crane. The package was lowered again and at 1.0 m/s and after passing the depths where vertical gradient of water properties was large, it was lowered at a rate of 1.2 m/s to the bottom. For the up cast, the package was lifted at a rate of 1.2 m/s except for bottle firing stops. As a rule, the bottle was fired after waiting from the stop for more than 30 seconds and the package was stayed at least 5 seconds for measurement of the SBE 35 at each bottle firing stops. For depths where vertical gradient of water properties was expected to be large, the bottle was fired after waiting from the stop for 60 seconds to enhance changing the water between inside and outside of the bottle. At 200 m (or 300 m) from the surface, the package was stopped to stop the heave compensator of the crane.

(4.2) Data collection problems

There was water ingress in the connector of SUNA battery during cast 001M001.

It wasn't noticed until cast 002M001, after which the connectors were cleaned and the cable was replaced with a spare one.

There was water ingress problem again during cast 012M001. The cable connector was cleaned and the battery case was replaced with a spare one.

During cast 014M001, SUNA data output was abnormal. The battery was checked and found that it was running low. The batteries were replaced with new ones.

At about 600 m depth during cast 020M001, CTD real-time data acquisition was lost. Deck unit was restarted but there was still no data acquisition so the cast was aborted and CTD was retrieved.

After CTD was recovered, it was found that there was an insulation problem in sea cable termination caused by water intrusion.

Also, it was found that the wrong fuse was installed in deck unit's sea-cable line. Because of that, it failed to prevent flow of excess current to the circuit board and caused circuit board failure. The sea-cable was re-terminated and the deck unit was replaced with a spare one.

The definitions of these irregularities are as follows:

(1) noise: not singly but continuously detected outliers.

(2) spike: one-off outlier which is detected after data processing and is

oceanographically impossible.

(3) shift: continuous data trend which is deviated from accurate ones.

(4.3) Data Processing

The following are the data processing software (SBEDataProcessing-Win32) and original software data processing module sequence and specifications used in reduction of CTD data in this cruise.

(The process in order)

DATCNV converted the raw data to engineering unit data. DATCNV also extracts bottle information where scans were marked with the bottle confirm bit during acquisition. The scan duration to be included in bottle file was set to 4.4 seconds, and the offset was set to 0.0 seconds. The hysteresis correction for the SBE 43 data (voltage) was applied for both profile and bottle information data.

TCORP (original module, version 1.1) corrected the pressure sensitivity of the temperature (SBE 03Plus) sensor for both profile and bottle information data.

RINKOCOR (original module, 1.0) corrected the time-dependent, pressure-induced effect (hysteresis) of the RINKOIII profile data.

RINKOCORROS (original module) corrected the time-dependent, pressure-induced effect (hysteresis) of the RINKOIII bottle information data by using the hysteresis-corrected profile data.

BOTTLESUM created a summary of the bottle data. The data were averaged over 4.4 seconds.

ALIGNCTD converted the time-sequence of sensor outputs into the pressure sequence to ensure that all calculations were made using measurements from the same parcel of water. For a SBE 9plus CTD with the ducted temperature and conductivity sensors and a 3000-rpm pump, the typical net advance of the conductivity relative to the temperature is 0.073 seconds. So, the SBE 11plus deck unit was set to advance the primary and the secondary conductivity for 1.73 scans (1.75/24 = 0.073 seconds). Oxygen data are also systematically delayed with respect to depth mainly because of the long-time constant of the oxygen sensor and of an additional delay from the transit time of water in the pumped plumbing line. This delay was compensated by 8 seconds advancing the SBE 43 oxygen sensor output (voltage) relative to the temperature data. Delay of the RINKOIII data was also compensated by 1 second advancing sensor output (voltage) relative to the temperature data. Delay of the transmissometer data was also compensated by 2 seconds advancing sensor output (voltage) relative to the temperature data.

WILDEDIT marked extreme outliers in the data files. The first pass of WILDEDIT obtained the accurate estimate of the true standard deviation of the data. The data were read in blocks of 1000 scans. Data greater than 10 standard deviations were flagged. The second pass computed a standard deviation over the same 1000 scans excluding the flagged values. Values greater than 20 standard deviations were marked bad. This process was applied to pressure, depth, temperature, conductivity, and SBE 43 output.

CELLTM used a recursive filter to remove conductivity cell thermal mass effects from the measured conductivity. Typical values for SBE 9plus with TC duct and 3000 rpm pump which were 0.03 for thermal anomaly amplitude alpha and 7.0 for the time constant 1/beta were used.

FILTER performed a low-pass filter on pressure and depth with a time constant of 0.15 second. In order to produce zero phase lag (no time shift) the filter runs forward first then backward.

WFILTER performed as a median filter to remove spikes in transmissometer data, fluorometer data, and ultraviolet fluorometer data. A median value was determined by 49 scans of the window. The window length is specified as 73 scans for nitrate data.

SECTIONU (original module, version 1.1) selected a time span of data based on scan number in order to reduce a file size. The minimum number was set to be the starting time when the CTD package was beneath the sea-surface after activation of the pump. The maximum number was set to be the end time when the depth of the package was 1-dbar below the surface. The minimum and maximum numbers were automatically calculated in the module.

LOOPEDIT marked scans where the CTD was moving less than the minimum velocity of 0.0 m/s (traveling backwards due to ship roll).

DESPIKE (original module, version 1.0) removed spikes of the data. A median and mean absolute deviation was calculated in 1-dbar pressure bins for both down and up cast, excluding the flagged values. Values greater than 4 mean absolute deviations from the median were marked bad for each bin. This process was performed twice for temperature, conductivity and RINKOIII output.

DERIVE was used to compute dissolved oxygen (SBE 43), salinity, potential temperature, and sigma-theta.

BINAVG averaged the data into 1-dbar pressure bins and 1-second time bins. The center value of the first bin was set equal to the bin size. The bin minimum and maximum values are the center values plus and minus half the bin size. Scans with pressures greater than the minimum and less than or equal to the maximum were averaged. Scans were interpolated so that a data recorded exist every dbar.

BOTTOMCUT (original module, version 0.1) deleted the deepest pressure bin when the averaged scan number of the deepest bin was smaller than the average scan number of the bin just above.

SPLIT was used to split data into down cast and up cast.

(5) Data archive

These data obtained in this cruise will be submitted to the Data Management Group of JAMSTEC, and will be opened to the public via “Data Research System for Whole Cruise Information in JAMSTEC (DARWIN)” in JAMSTEC web site.

3.2. XCTD

(1) Personnel

Motoyo Itoh	JAMSTEC	-PI
Satomi Ogawa	NME (Nippon Marine Enterprises, Ltd.)	
Souichiro Sueyoshi	NME	
Shinya Okumura	NME	
Haruna Yamanaka	NME	
Masanori Murakami	MIRAI Crew	

(2) Objectives

To obtain vertical profiles of sea water temperature and salinity (calculated from temperature, pressure (depth), and conductivity).

(3) Parameters

The ranges and accuracies of parameters measured by the XCTD (eXpendable Conductivity, Temperature & Depth profiler) are as follows; Parameter Range Accuracy Conductivity 0 ~ 60 [mS/cm] +/- 0.03 [mS/cm] Temperature -2 ~ 35 [deg-C] +/- 0.02 [deg-C] Depth 0 ~ 1000 [m] 5 [m] or 2 [%] (either of them is major)

(4) Instruments and methods

We observed vertical profiles of sea water temperature and salinity measured by XCTD-1N probes manufactured by Tsurumi-Seiki Co. (TSK). The electric signal from the probe was converted by MK-150N (TSK), and was recorded by AL-12B software (Ver.1.8.0, TSK). We launched 78 probes by using the automatic launcher. The XCTD observation log is shown in Table 3.2-1.

(5) Observation log

Table 3.2-1: XCT D observation log

No.	Station No.	Date [YYYY/MM/DD]	Time [hh:mm]	Latitude [deg]	Longitude [deg]	Depth [m]	SST [deg-C]	SSS [PSU]	Probe S/N
1	X001	2024/09/05	05:38	65-42.4124N	168-16.0125W	46	9.373	24.666	22072723
2	X002	2024/09/05	06:11	65-45.1233N	168-29.8786W	56	7.924	28.888	22072720
3	X003	2024/09/05	06:55	65-49.1612N	168-47.9978W	50	3.323	31.489	22072719
4	X004	2024/09/05	21:37	67-46.9992N	168-36.0987W	50	6.689	29.117	22072725
5	X005	2024/09/05	22:34	67-53.8832N	168-14.1023W	58	6.571	30.102	22072726
6	X006	2024/09/06	02:20	68-00.8032N	167-51.9985W	52	6.311	30.735	21107534
7	X007	2024/09/06	03:15	68-07.7011N	167-29.7006W	49	7.703	28.564	21107537
8	X008	2024/09/06	03:42	68-11.0978N	167-18.5075W	48	7.781	28.425	22072722
9	X009	2024/09/06	05:48	68-18.0052N	166-56.1239W	34	7.823	27.928	21107531

10	X010	2024/09/09	05:02	71-37.2031N	157-55.5437W	62	2.73	28.516	21107533
11	X011	2024/09/09	05:18	71-34.7010N	157-50.4288W	64	2.686	28.592	21107536
12	X012	2024/09/09	05:33	71-32.2029N	157-45.2962W	71	2.513	29.155	21107539
13	X013	2024/09/09	05:49	71-29.8009N	157-40.1124W	83	2.548	29.796	21107530
14	X014	2024/09/09	06:04	71-27.3053N	157-34.9144W	110	2.543	30.191	21107535
15	X015	2024/09/09	06:20	71-24.8026N	157-29.8395W	122	4.084	30.068	22072667
16	X016	2024/09/09	06:35	71-22.3060N	157-24.8855W	112	5.421	29.498	21107538
17	X017	2024/09/09	06:51	71-19.8015N	157-19.9221W	90	5.535	29.398	22072668
18	X018	2024/09/09	07:06	71-17.3020N	157-14.8810W	57	5.687	29.403	22072669
19	X019	2024/09/09	07:23	71-14.8005N	157-09.8627W	47	5.63	29.407	21107529
20	X020	2024/09/10	00:39	71-35.9964N	154-48.9826W	42	5.752	29.208	22072703
21	X021	2024/09/10	00:54	71-37.9974N	154-55.3082W	56	5.93	28.878	21107532
22	X022	2024/09/10	01:09	71-40.0018N	155-00.9984W	102	5.873	29.029	21107540
23	X023	2024/09/10	01:23	71-42.0009N	155-06.4790W	179	5.441	29.704	22072676
24	X024	2024/09/10	01:37	71-44.0003N	155-12.0122W	298	3.524	28.886	22072677
25	X025	2024/09/10	01:51	71-46.0085N	155-17.5311W	201	2.863	28.948	22072671
26	X026	2024/09/10	02:05	71-48.0015N	155-22.9837W	148	3.058	28.822	22072673
27	X027	2024/09/10	02:28	71-48.9988N	155-36.9051W	119	2.988	26.393	22072670
28	X028	2024/09/10	02:50	71-50.0036N	155-51.0154W	91	2.776	26.185	22072672
29	X029	2024/09/10	21:48	71-56.2508N	154-06.2036W	340	2.943	26.475	22072674
30	X030	2024/09/11	00:02	71-53.9210N	154-08.7776W	237	2.873	28.404	22072675
31	X031	2024/09/13	16:46	72-18.0101N	152-30.0186W	2626	3.249	26.155	22072678
32	X032	2024/09/13	23:32	72-34.9692N	152-29.9426W	3596	3.022	25.474	22072705
33	X033	2024/09/14	01:41	72-59.9965N	152-30.0073W	3837	2.802	25.559	22072714
34	X034	2024/09/14	04:06	73-29.9939N	152-30.0517W	3853	1.805	25.026	22072709
35	X035	2024/09/14	06:56	73-29.9946N	154-29.9862W	3858	1.740	25.050	22072713
36	X036	2024/09/14	09:36	73-30.0016N	156-29.9815W	3666	2.771	25.776	22072712
37	X037	2024/09/15	00:28	73-45.3591N	157-52.8748W	3494	1.125	25.641	22072707
38	X038	2024/09/15	02:50	73-59.9995N	159-13.0012W	2940	0.803	25.492	22072710
39	X039	2024/09/15	05:11	74-14.9972N	160-34.4078W	567	1.529	25.708	22072711
40	X040	2024/09/16	03:02	74-52.3375N	163-00.9722W	1678	0.613	26.518	22072740
41	X041	2024/09/16	05:13	75-13.3345N	164-06.9980W	688	0.301	26.624	22072739
42	X042	2024/09/16	07:19	75-33.8584N	165-12.9909W	579	-0.272	26.340	22072708
43	X043	2024/09/16	14:26	75-54.1082N	166-19.5478W	342	-0.939	26.421	22072706
44	X044	2024/09/16	16:38	76-07.1170N	167-26.1847W	314	-1.286	26.959	22072743
45	X045	2024/09/16	17:30	76-07.5629N	167-33.3741W	364	-1.258	27.181	22072745
46	X046	2024/09/16	22:00	76-06.3319N	167-18.2378W	295	-1.223	27.040	22072742
47	X047	2024/09/16	23:27	76-05.7536N	167-08.9186W	300	-1.301	28.024	22072744
48	X048	2024/09/17	16:57	76-06.6234N	167-40.5560W	384	-1.259	27.345	22072741
49	X049	2024/09/18	16:45	75-36.6039N	167-34.4459W	192	-1.131	26.847	22072704
50	X050	2024/09/19	01:31	75-18.0003N	168-36.4965W	196	-0.748	26.943	22072746
51	X051	2024/09/20	03:15	75-12.4216N	165-50.0053W	524	-0.237	26.534	22072750
52	X052	2024/09/20	04:40	75-24.6807N	166-39.9895W	281	-0.794	26.305	22072748
53	X053	2024/09/20	17:03	75-33.4989N	168-06.2249W	177	-0.917	26.802	22072749

54	X054	2024/09/20	21:49	75-32.1244N	168-11.7841W	173	-0.935	26.807	22072747
55	X055	2024/09/21	00:50	75-16.9993N	167-41.5215W	167	-0.938	26.744	23118184
56	X056	2024/09/21	05:04	74-27.0009N	166-30.1128W	318	1.138	26.646	23118182
57	X057	2024/09/21	07:53	73-54.0031N	165-44.9413W	150	0.883	27.342	23118183
58	X058	2024/09/22	23:34	74-59.9989N	159-59.9858W	1955	1.198	25.608	23118190
59	X059	2024/09/23	01:18	74-47.9953N	158-59.9784W	1204	0.668	25.660	23118193
60	X060	2024/09/23	02:28	74-39.9998N	158-18.5046W	1162	1.012	25.333	23118188
61	X061	2024/09/23	03:09	74-34.9965N	157-54.9886W	1242	0.920	25.404	23118187
62	X062	2024/09/23	03:54	74-29.9761N	157-27.9975W	3855	0.981	25.366	23118191
63	X063	2024/09/23	04:42	74-23.9937N	156-59.9966W	3859	1.422	25.488	23118189
64	X064	2024/09/23	23:20	73-09.9897N	158-00.0509W	2399	2.370	26.348	23118192
65	X065	2024/09/25	04:15	72-06.0014N	157-23.0042W	78	2.717	27.775	23118259
66	X066	2024/09/25	12:49	71-36.5135N	154-46.7839W	44	3.703	28.478	23118186
67	X067	2024/09/25	13:08	71-38.4679N	154-52.0815W	56	3.643	28.454	23118258
68	X068	2024/09/25	13:33	71-42.6636N	155-01.9169W	166	3.072	28.157	23118257
69	X069	2024/09/25	13:47	71-44.7515N	155-07.3545W	286	2.962	28.222	23118255
70	X070	2024/09/25	13:59	71-46.3436N	155-12.3086W	244	3.378	28.450	23118185
71	X071	2024/09/25	14:36	71-49.1086N	155-34.4046W	125	4.638	28.707	23118256
72	X072	2024/09/25	15:03	71-49.9953N	155-50.9209W	91	3.781	29.038	23118254
73	X073	2024/09/27	09:38	65-45.8386N	168-44.8268W	51	5.250	28.774	23118264
74	X074	2024/09/27	09:59	65-44.4962N	168-38.9376W	50	4.868	30.086	23118262
75	X075	2024/09/27	10:20	65-42.9436N	168-33.0332W	52	4.979	30.956	23118260
76	X076	2024/09/27	10:40	65-41.7438N	168-27.5428W	53	4.934	30.889	23118263
77	X077	2024/09/27	11:01	65-40.6095N	168-21.3496W	51	4.950	30.437	23118261
78	X078	2024/09/27	11:01	65-38.7748N	168-16.2832W	45	4.841	30.299	23118265

(6) Data archives

These data obtained in this cruise will be submitted to the Data Management Group of JAMSTEC, and will be opened to the public via "Data Research System for Whole Cruise Information in JAMSTEC (DARWIN)" in JAMSTEC web site.
< https://www.godac.jamstec.go.jp/darwin/en/ >

3.3. Shipboard ADCP

(1) Personnel

Motoyo Itoh	JAMSTEC	-PI
Satomi Ogawa	NME (Nippon Marine Enterprises, Ltd.)	
Souichiro Sueyoshi	NME	
Shinya Okumura	NME	
Haruna Yamanaka	NME	
Masanori Murakami	MIRAI Crew	

(2) Objectives

To obtain continuous measurement data of the current profile along the ship's track.

(3) Parameters

Upper ocean current velocity: horizontal velocity (u), vertical velocity (v) and depth.

(4) Instruments and methods

Upper ocean current measurements were made during this cruise, using the hull-mounted Acoustic Doppler Current Profiler (ADCP) system. For most of its operation, the instrument was configured for water-tracking mode. Bottom-tracking mode, interleaved bottom-ping with water-ping, was made to get the calibration data for evaluating transducer misalignment angle in the shallow water. The system consists of following components;

1. R/V MIRAI has installed the Ocean Surveyor for vessel-mount ADCP (frequency 76.8 kHz; Teledyne RD Instruments, USA). It has a phased-array transducer with single ceramic assembly and creates 4 acoustic beams electronically. We mounted the transducer head rotated to a ship-relative angle of 45 degrees azimuth from the keel.
2. For heading source, we use ship's gyro compass (Tokyo Keiki, Japan), continuously providing heading to the ADCP system directory. Additionally, we have Inertial Navigation Unit (Phins, Ixblue, France) which provide high-precision heading, attitude information, pitch and roll. They are stored in ".N2R" data files with a time stamp.
3. Differential GNSS system (StarPack-D, Fugro, Netherlands) providing precise ship's position.
4. We used VmDas software version 1.50.19(TRDI) for data acquisition.
5. To synchronize time stamp of ping with Computer time, the clock of the logging computer is adjusted to GPS time server by using NTP (Network Time Protocol).

6. Fresh water is charged in the sea chest to prevent bio fouling at transducer face.
7. The sound speed at the transducer does affect the vertical bin mapping and vertical velocity measurement, and that is calculated from temperature, salinity (constant value; 35.0 PSU) and depth (6.5 m; transducer depth) by equation in Medwin (1975).

Data were configured for "8 m" layer intervals starting about 23m below sea surface. Data were recorded every ping as raw ensemble data (.ENR). Additionally, 15 or 60 seconds averaged data were recorded as short-term average (.STA). 300 seconds averaged data were long-term average (.LTA), respectively.

Major acquisition parameters for the measurement, Direct Command, are shown in Table 3.3-1.

Table 3.3-1: Major parameters

Bottom-Track Commands

BP = 001 Pings per Ensemble (almost less than 1,300m depth)

Environmental Sensor Commands

EA = 04500 Heading Alignment (1/100 deg)

ED = 00065 Transducer Depth (0 - 65535 dm)

EF = +001 Pitch/Roll Divisor/Multiplier (pos/neg) [1/99 - 99]

EH = 00000 Heading (1/100 deg)

ES = 35 Salinity (0-40 pp thousand)

EX = 00000 Coordinate Transform (Xform:Type; Tilts; 3Bm; Map)

EZ = 10200010 Sensor Source (C; D; H; P; R; S; T; U)

C (1): Sound velocity calculates using ED, ES, ET (temp.)

D (0): Manual ED

H (2): External synchro

P (0), R (0): Manual EP, ER (0 degree)

S (0): Manual ES

T (1): Internal transducer sensor

U (0): Manual EU

EV = 0 Heading Bias (1/100 deg)

Timing Commands

TE = 00:00:02.00 Time per Ensemble (hrs:min:sec.sec/100)

TP = 00:02.00 Time per Ping (min:sec.sec/100)

Water-Track Commands

WA = 255 False Target Threshold (Max) (0-255 count)

WC = 120 Low Correlation Threshold (0-255)

WD = 111 100 000	Data Out (V; C; A; PG; St; Vsum; Vsum^2; #G; P0)
WE = 1000	Error Velocity Threshold (0-5000 mm/s)
WF = 0800	Blank After Transmit (cm)
WN = 100	Number of depth cells (1-128)
WP = 00001	Pings per Ensemble (0-16384)
WS = 800	Depth Cell Size (cm)
WV = 0390	Radial Ambiguity Velocity (cm/s)

(5) Observation log

26 Aug. 2024 - 30 Sep. 2024

(6) Preliminary results

Figures 3.3-1 and 3.3-2 show the current velocity of Barrow Canyon line.

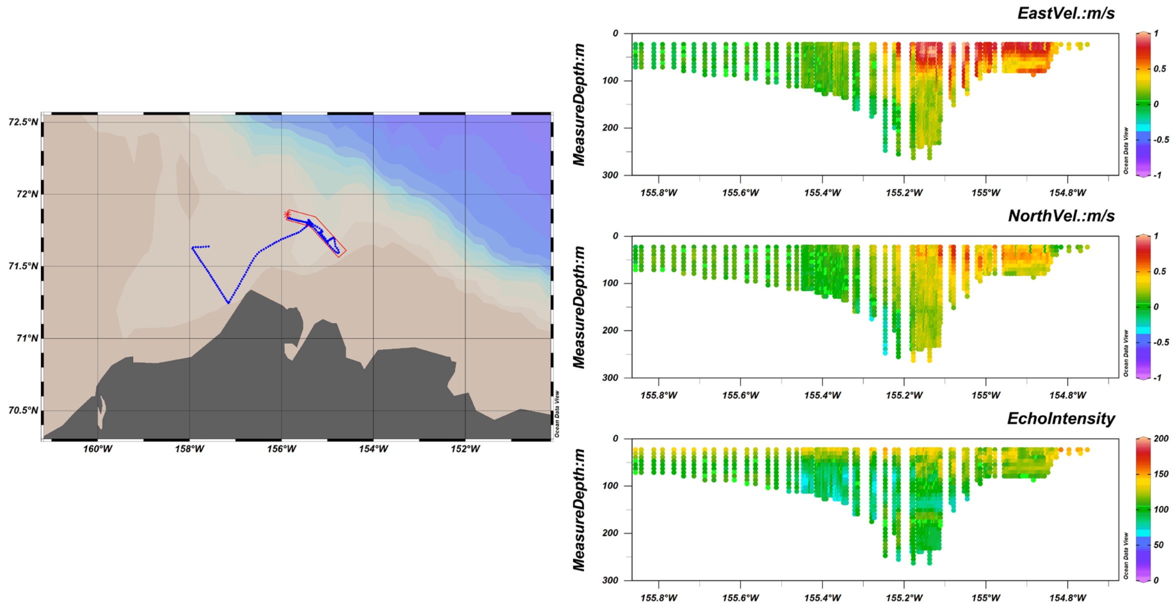

Figure 3.3-1: The current velocity of Barrow Canyon line at 10th September.

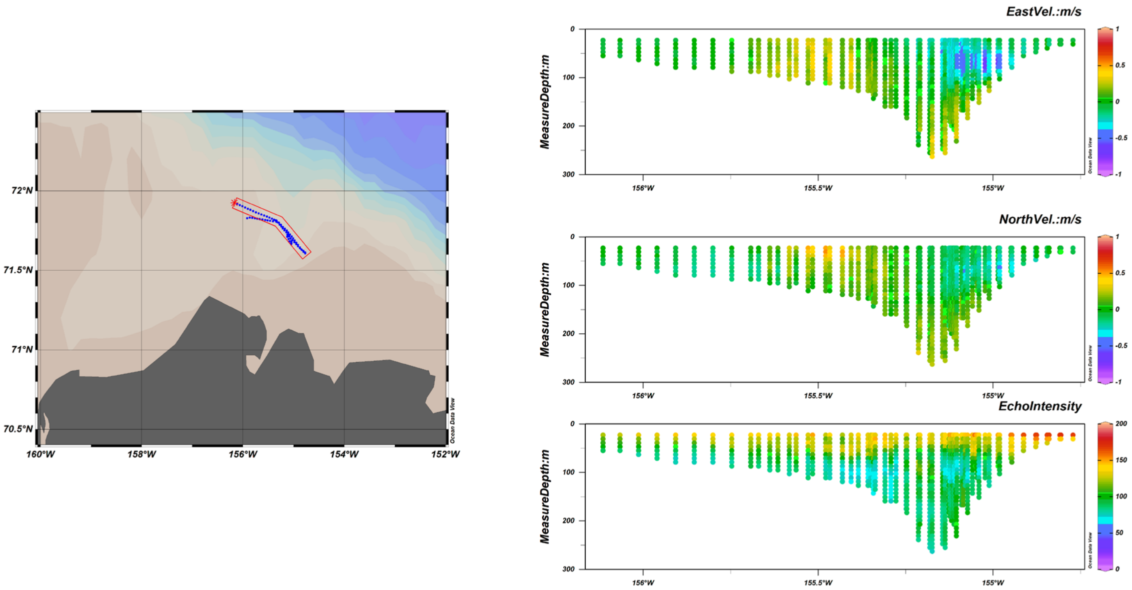

Figure 3.3-2: The current velocity of Barrow Canyon line at 25th September.

(7) Data archives

These data obtained in this cruise will be submitted to the Data Management Group of JAMSTEC, and will be opened to the public via "Data Research System for Whole Cruise Information in JAMSTEC (DARWIN)" in JAMSTEC web site.
< https://www.godac.jamstec.go.jp/darwin/en >

(8) Remarks

i) The following periods, "STA" data was recorded 15 second average.

07:26UTC 26 Aug. 2024 - 15:26UTC 14 Sep. 2024
18:25UTC 20 Sep. 2024 – 14:45UTC 30 Sep. 2024 (End of the Cruise)

ii) The following periods, "STA" data was recorded 60 second average.

15:26UTC 14 Sep. 2024 - 17:14UTC 20 Sep. 2024

iii) The following period, data acquisition was suspended due to operating of the AUV "COMAI"

16:45UTC 14 Sep. 2024 - 19:58UTC 14 Sep. 2024
20:46UTC 14 Sep. 2024 - 22:46UTC 14 Sep. 2024
17:22UTC 17 Sep. 2024 - 18:29UTC 17 Sep. 2024
17:17UTC 18 Sep. 2024 - 18:43UTC 18 Sep. 2024
17:14UTC 20 Sep. 2024 - 18:25UTC 20 Sep. 2024
21:53UTC 20 Sep. 2024 - 22:53UTC 20 Sep. 2024

3.4. Wave Buoy

(1) Personnel
Takuji Waseda (Principal Investigator, The University of Tokyo, not on board)
Tsubasa Kodaira (The University of Tokyo, not on board)
Takehiko Nose (The University of Tokyo, not on board)
Akane Yamamoto (The University of Tokyo)
Takatoshi Matsuzawa (NMRI)
Koya Sato (The University of Tokyo, not on board)
Yukihide Ishiyama (The University of Tokyo, not on board)

(2) Objectives
Interaction processes between ocean waves and sea ice, which are becoming more important in the Arctic Sea, are not fully understood. To deepen their understandings, two types of drifting wave buoys were deployed near the ice edge to measure the waves in the water near the old sea ice and in the freezing season. One type of buoy is commercial product 'Spotter' and the other type of buoy is developed by our research group —'XFZ-V2'.

(3) Parameters
Spotter:
The following statistical parameters are calculated and sent via satellite every hour. Significant wave height, peak wave period, peak wave direction, peak wave directional spread, mean wave period, mean wave direction, mean wave directional spread, sea surface temperature, frequency-directional variance density spectrum, GPS location, wind speed, and wind direction.

XFZ-V2:
The OpenMetBuoy (Rabault et al., 2022) was used as a wave sensor. The following statistical parameters are calculated and sent via satellite: the wave acceleration frequency spectrum, significant wave height estimates, mean wave period, and UTC timestamp. The sampling interval is half an hour.

(4) Instruments and methods
Spotter (see, Figure 3.4-1):
Spotter buoy was manufactured by Sofar Ocean Technologies. The buoy is solar-powered and have a two-way communication function via Iridium satellite communication. We have deployed one Spotter wave buoy into the MIZ of the Canada Basin (see, Figure 3.4-3 and Table 3.4-1).

XFZ-V2 (see, Figure 3.4-2):

The hull of the wave buoy was created by our research group (Kodaira et al., 2023). The OMB sensor was protected by a double waterproof structure. We deployed three XFZ-V2 wave buoys into the MIZ located north of the Chukchi Sea (see, Figure 3.4-3 and Table 3.4-1).

Figure 3.4-1 drifting type wave buoy Spotter

Figure 3.4-2 drifting type wave buoy FZ

(5) Station list or Observation log

Time and locations of wave buoy development are listed in Table 3.4-1.

Table 3.4-1 List of drifting buoy development locations

Deployment time (UTC)	Location		Drifting buoy	
	Latitude	Longitude	Spotter ID	XFZ-V2 ID
2024/09/16 17:20	76.1246N	167.5584W	SPOT-1216	-
2024/09/17 00:39	76.0868N	167.0569W	-	212730
2024/09/17 22:45	76.1530N	167.7685W	-	212735
2024/09/18 00:33	76.0530N	166.5859W	-	212736

(6) Preliminary results

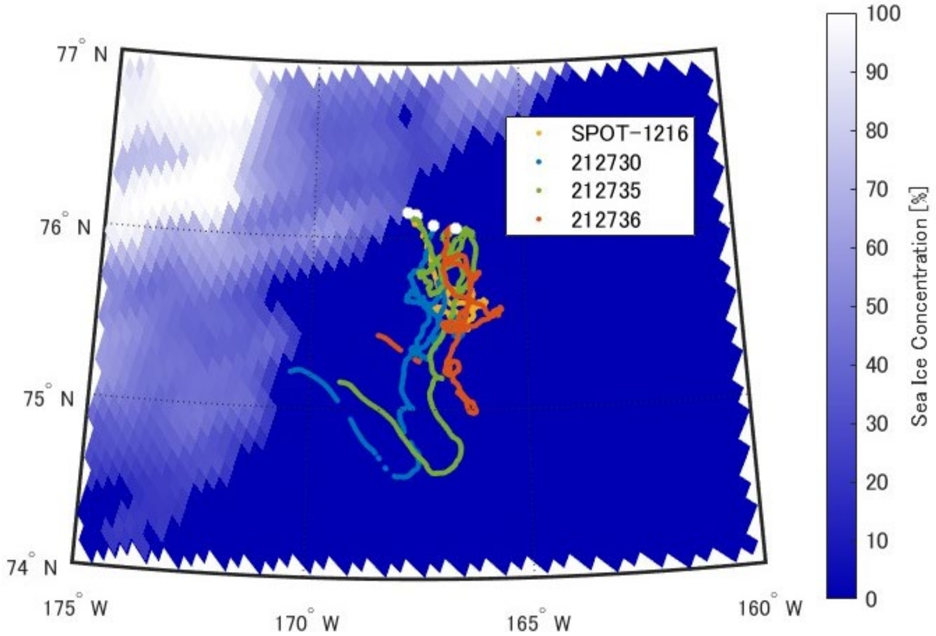

Figure 3.4-3 Map showing trajectories of deployed wave buoys. White dots indicate the locations where the buoys were deployed. Sea ice concentration data from AMSR2 for 09/26/2024

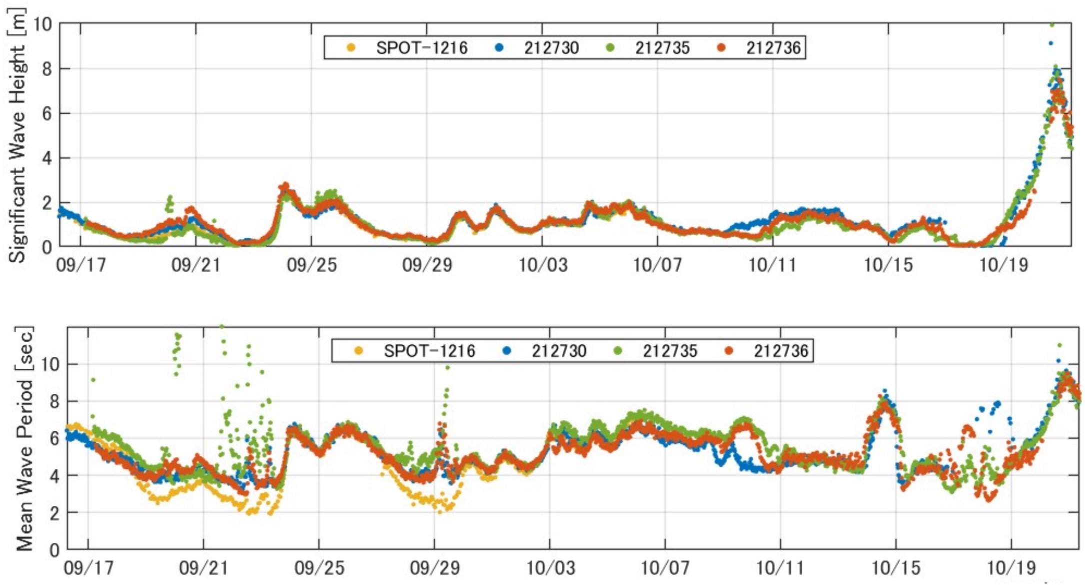

Figure 3.4-4 Time series of significant wave height and mean wave period measured by the deployed wave buoys.

(7) Data archives

These data obtained in this cruise will be submitted to the Data Management Group of JAMSTEC, and will be opened to the public via "Data Research System for Whole Cruise Information in JAMSTEC (DARWIN)" in JAMSTEC web site.
<http://www.godac.jamstec.go.jp/darwin/e>

3.5. Microwave wave gauge

(1) Personnel
Takuji Waseda (Principal Investigator, The University of Tokyo, not on board)
Tsubasa Kodaira (The University of Tokyo, not on board)
Takehiko Nose (The University of Tokyo, not on board)
Akane Yamamoto (The University of Tokyo)
Takatoshi Matsuzawa (NMRI)
Koya Sato (The University of Tokyo, not on board)
Yukihide Ishiyama (The University of Tokyo, not on board)

(2) Objectives
Microwave wave gauge was installed at the bow of R/V Mirai to obtain a continuous and detailed wave data along the ship trajectory.

(3) Parameters
Relative speed of the instrument and the bow to obtain continuous and detailed wave data at the ship location.

(4) Instruments and methods
Microwave wave gauge (SJM-001), produced by Japan Radio Co. Ltd., was installed at the (Figure 3.5-1). It was connected to a computer via ethernet, where the data was continuously recorded.

Figure 3.5-1 Microwave wave gauge installed at the bow.

The sensor radiates microwave signal to the water and measures the Doppler shift frequency of the reflected signal. Doppler shift frequency is converted to the relative speed, and then the accelerometer and the gyro sensor data is used to correct for ship motion to obtain the absolute motion of the water surface.
The data is obtained at 10 Hz frequency, and spectral analysis for noise removal is conducted for every 20 minutes record. Data quality is checked by using the ship heading direction, ship speed, and wind direction.

(5) Station list or Observation log
Data was continuously collected, from 08-26-2024 11:03 to 09-27-2024 16:30 (both in UTC).

(6) Preliminary results

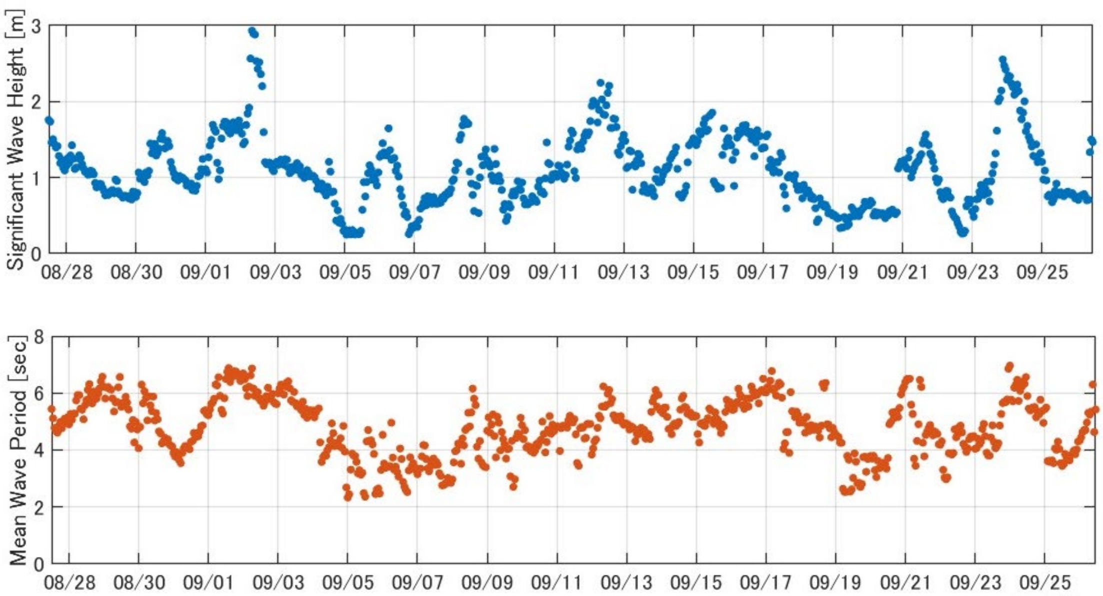

Figure 3.5-2 Time series of the significant wave height, wave period up to 09-27-2024.

(7) Data archives
These data obtained in this cruise will be submitted to the Data Management Group of JAMSTEC, and will be opened to the public via "Data Research System for Whole Cruise Information in JAMSTEC (DARWIN)" in JAMSTEC web site.
<http://www.godac.jamstec.go.jp/darwin/e>

3.6. Stereo and Network cameras

(1) Personnel
Takuji Waseda (Principal Investigator, The University of Tokyo, not on board)
Tsubasa Kodaira (The University of Tokyo, not on board)
Takehiko Nose (The University of Tokyo, not on board)
Akane Yamamoto (The University of Tokyo)
Takatoshi Matsuzawa (NMRI)
Koya Sato (The University of Tokyo, not on board)
Yukihide Ishiyama (The University of Tokyo, not on board)

(2) Objectives
Stereo cameras:
To obtain a spatio-temporal variation of water surface elevation and ice motion

Network-cameras:
To obtain a continuous visual record of waves, sea ice, and sea splay

(3) Parameters
Stereo cameras:
Monochrome images (4064 × 4064 pixels), acceleration (3-axis), gyro(3-axis) and geomagnetism (3-axis).

Network-cameras:
Camera record in MKV format

(4) Instruments and methods
Stereo cameras:
The two cameras, mounted in separate housing on the compass deck of the R/V Mirai, were synchronized to allow stereo reconstruction of the captured images of surface ocean waves (Figure 3.6-1). Both cameras were connected via USB cables to a laptop computer placed in a watertight black plastic box. HDD storage devices whose storage size is 8 TB in total were also installed in the box. The system was directly connected to the environmental research lab with ethernet cables, which enable us to access the system from inside the vessel. A 9-axis inertial unit (ZMP-IMUZ) was also placed in the box to measure the motion of the cameras.

Figure 3.6-1 Installed stereo camera system (left: left camera, right: right camera).

Network cameras:
Three cameras (AXIS M2026-LE Mk II) were installed at the foremast and recorded the whole footage of the cruise. They are connected to a recorder (AXIS S3008, 2TB) placed indoor. The resolution of the recorded movie is 1920×1080 and the frame rate is 15 fps. The location and the directions of the cameras are listed in Table 3.6-1. The installed three cameras are shown in Figure 3.6-2.

Table 3.6-1 List of the installed three cameras.

Camera #	Location	Direction
1	Foremast top	Bow side
2	Foremast top	Port side
3	Foremast top	Starboard side

Figure 3.6-2 Installed network cameras.

(5) Station list or Observation log
Stereo cameras:
Images were collected with 2Hz frequency for 20 minutes of each hour, only in daytime. They started recording in 08-27-2024 and stopped recording in 09-27-2024.

Network cameras:
The three cameras continuously recorded from 08-27-2024 to 09-27-2024.

(6) Preliminary results
Figure 3.6-3 and 3.6-4 shows sample images of the stereo cameras and the network cameras, respectively.

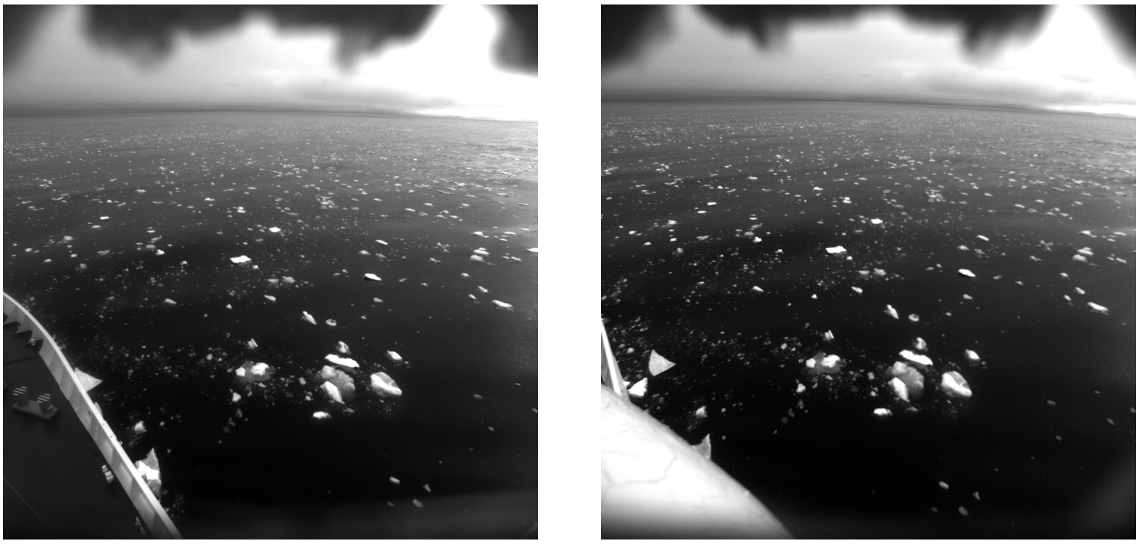

Figure 3.6-3 Sample images of the stereo cameras (left: left camera, right: right camera).

Camera 1

Camera 2

Camera 3

Figure 3.6-4 Sample images of the network cameras.

(7) Data archives

These data obtained in this cruise will be submitted to the Data Management Group of JAMSTEC, and will be opened to the public via "Data Research System for Whole Cruise Information in JAMSTEC (DARWIN)" in JAMSTEC web site.
<http://www.godac.jamstec.go.jp/darwin/e>

3.7. Radar
3.7.1. Ice radar

(1) Personnel

Motoyo Itoh	JAMSTEC	-PI
Satomi Ogawa	NME (Nippon Marine Enterprises, Ltd.)	
Souichiro Sueyoshi	NME	
Shinya Okumura	NME	
Haruna Yamanaka	NME	
Masanori Murakami	MIRAI Crew	

(2) Objectives

In the sea ice areas, marine radar provides an important tool for the detection of sea ice and icebergs. It is importance to monitor the sea ice daily and produce ice forecasts to assist ship traffic and other marine operations. In order to select route optimally, ice condition prediction technology is necessary, and image information of ice-sea radar is used for constructing a route selection algorithm.

(3) Parameters

Capture format: JPEG
Capture interval: 60 seconds
Resolution: 1,024×768 pixel
Color tone: 256 gradations

(4) Instruments and methods

R/V MIRAI is equipped with an Ice Navigation Radar, "sigma S6 Ice Navigator (Rutter Inc.)". The ice navigation radar, the analog signal from the x-band radar is converted by a modular radar interface and displayed as a digital video image (Figure 3.7.1-1). The sea ice radar is equipped with a screen capture function and saves at arbitrary time intervals.

(5) Observation log

04 Sep. 2024 - 27 Sep. 2024

(6) Preliminary results

Figure 3.7-1-1 shows an image of sea ice from Sea ice radar.

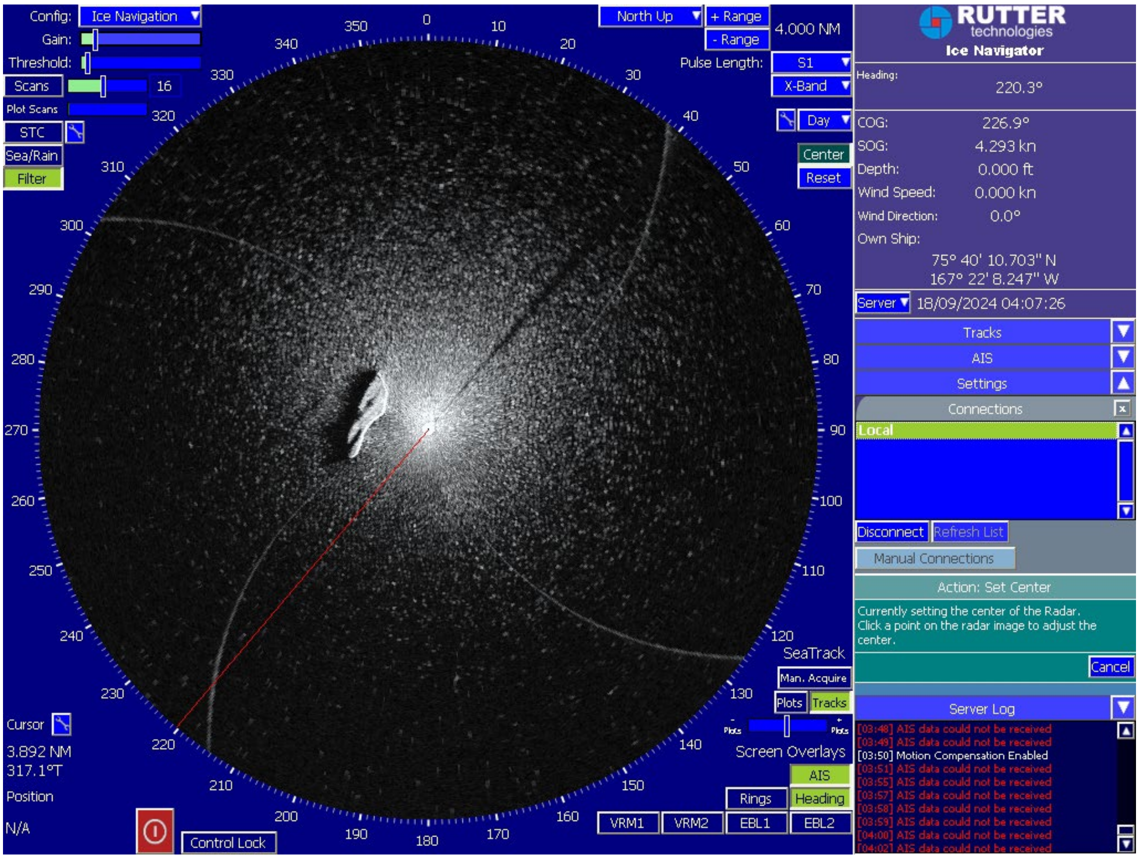

Figure 3.7-1-1: Image of sea ice from Sea ice radar

(7) Data archives

These data obtained in this cruise will be submitted to the Data Management Group of JAMSTEC, and will be opened to the public via "Data Research System for Whole Cruise Information in JAMSTEC (DARWIN)" in JAMSTEC web site.

< https://www.godac.jamstec.go.jp/darwin/en/ >

3.7.2. Wave-ice radar

(1) Personnel
Takuji Waseda (Principal Investigator, JAMSTEC, not on board)
Takatoshi Matsuzawa (National Maritime Research Institute)
Kazutaka Tateyama (Kitami Institute of Technology, not on board)
Masaru Kawaguchi (Japan Radio Co., Ltd., not on board)
Tsubasa Kodaira (The University of Tokyo, not on board)

(2) Objectives
Waves and sea ice are major external resistance factors on a ship's performance navigating in the Arctic Ocean. A joint research project to develop a new X-band radar system for detecting ice and waves with more informative resolution has been conducted by JAMSTEC and other four institutes since 2020. The system consists of two radars, horizontal-polarized (H) and vertical-polarized (V), and the concept will be applied to the ice radar system of the new Arctic research vessel, MIRAI II, to be on duty in 2026. In this cruise, the radar data in various water-surface conditions are recorded to develop a detecting algorithm and visualization method.

(3) Parameters
Radar raw signals from each radar scanner were recorded in a hard disk array and processed to a b-scope data. The visualized image of the b-scope data on the processing PC's screen was recorded. The time-lapse photos of the ice and wave condition in front of the ship were taken by the automated ship-based sea ice condition recording instruments (SSICR) developed by the Kitami Institute of Technology. The SSICR also recorded the ship's GPS positions and the ship motions such as accelerations (xyz) and angular velocities (xyz).

(4) Instruments and methods
The X-band radar base system is JRC JMR-5425-9XR and is customized. We used two sets of systems for H and V, and in addition, a high-resolution processing unit (16bit A/D) was combined with the V system on a trial. The radar scanners of H and V were installed on the radar mast as shown in Figure. 3.7.2-1 (a), while the processing instruments were installed at the Research Information Center on the wheelhouse deck as shown in Figure. 3.7.2-1 (b). The SSICR was installed near the center window in the wheelhouse as shown in Figure 3.7.2-2.

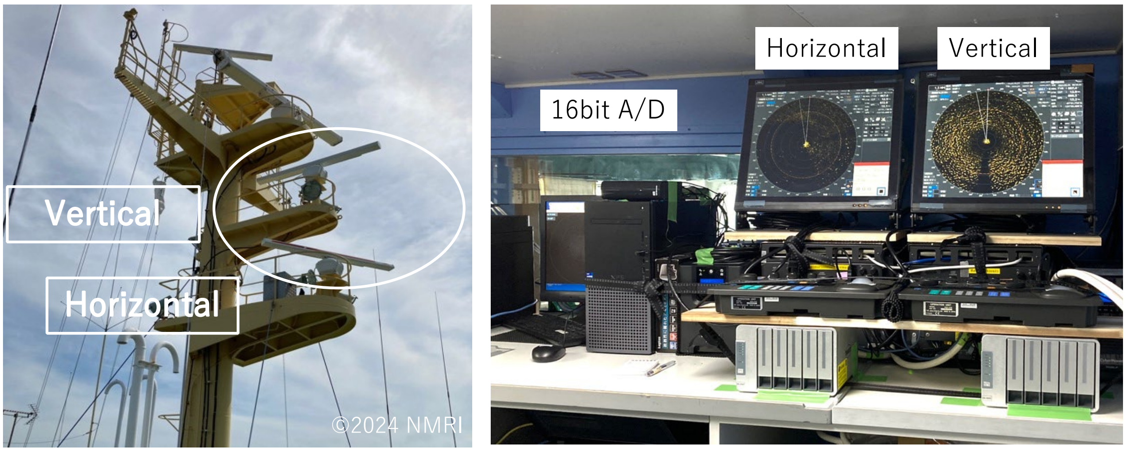

(a) Radar mast (b) Research Information Center

Figure 3.7.2-1: X-band radar system installation on R/V Mirai.

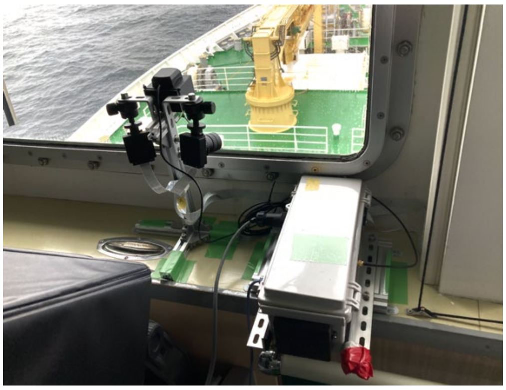

Figure 3.7.2-2: Automated ship-based sea ice condition recording instruments (SSICR) installation in the wheelhouse.

(5) Observation log

The X-band radar system and the SSICR were activated all the time during the Arctic cruise. However, the data collection was not uninterrupted, because the capacity of the hard disk (20TB) was not sufficient for a full-time high-resolution radar data acquisition. We executed a sustained recording only in an area where sea ice was in sight, and for other conditions, 20-minute recordings every 3 hours or so were repeated. Regarding the SSICR, we suffered hardware trouble and failed to record full-time data. Figure. 3.7.2-3 indicates the periods of successful recordings by blue-colored bars for the X-band radar data and time-lapse photos by SSICR.

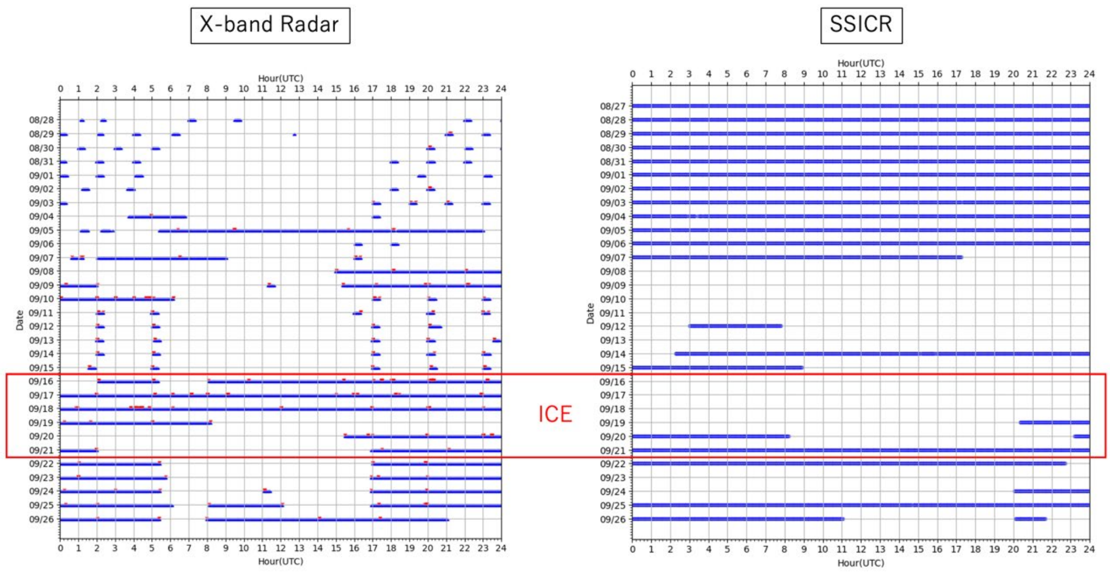

Figure 3.7.2-3: Recording periods of X-band radar data (left) and time-lapse photos by SSICR (right).

(6) Preliminary results

High-resolution radar image processing successfully detected ice and waves from 16 August to 20 August. Figure 3.7.2-4 shows a 3NM range vertical radar image and photos retrieved in small ice floes of 2/10 of concentration. A wave pattern and an ice pattern can be seen in the same radar image. However, ice and waves can be distinguished by the differences not only in the signal's intensity but also in the direction and speed of their movements from a sequence of radar images. Figure 3.7.2-5 shows a radar image and photos of the isolated large multi-year ice floe of 0.9NM wide. Surface roughness and a shadow behind the floe, displayed clearly in the radar image, are good information to estimate the size and the characteristics of the ice floe.

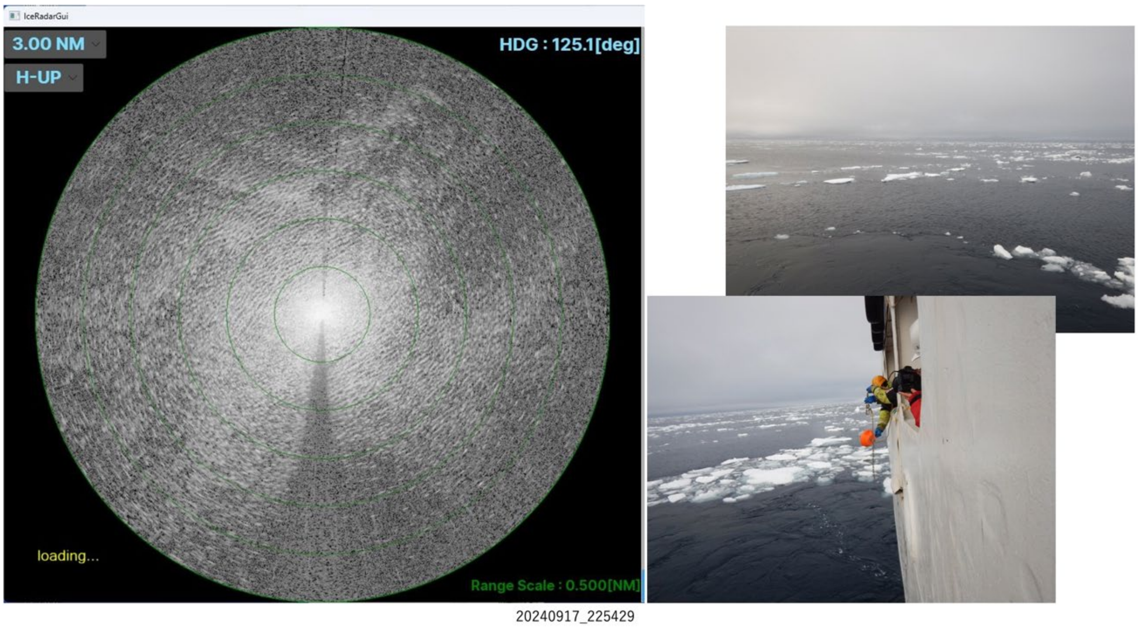

Figure 3.7.2-4: Radar image and photos retrieved in 2/10 concentrated ice on 17 August.

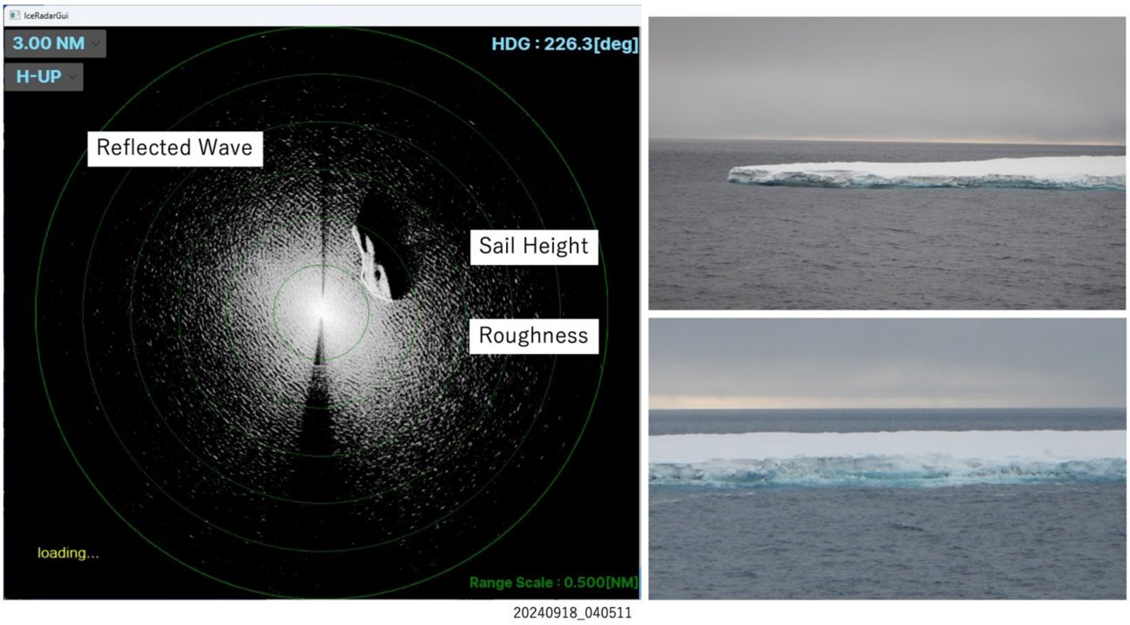

Figure 3.2-2-5: Radar image and photos retrieved near a large ice floe on 18-August.

(7) Data archives

The data obtained in this cruise will be submitted to the Data Management Group of JAMSTEC and will be opened to the public via the "Data Research System for Whole Cruise Information in JAMSTEC (DARWIN)" on the JAMSTEC website.
<http://www.godac.jamstec.go.jp/darwin/e>

3.8. Moorings

Oceanographic moorings continuously measure oceanographic parameters (temperature, salinity, currents, oxygen, chlorophyll, pH, ice thickness) through the year. Three physical oceanographic moorings (BCE-22, BCC-22, BCW-22) in the Barrow Canyon and one sediment trap mooring (NAP-23t) in the Northwind Abyssal Plain are recovered. Three physical oceanographic moorings (BCE-24, BCC-24, BCW-24) are re-deployed in the Barrow Canyon and one sediment trap mooring (NAP-24t) is deployed in the Northwind Abyssal Plain.

3.8.1. Barrow Canyon Moorings

(1) Personnel

Motoyo Itoh (JAMSTEC) Principal Investigator

Hiroki Ushiromura (Marine Works Japan Ltd., MWJ)
as the leader of technical team for mooring operation of MWJ
(Arihara, K)

Satomi Ogawa (Nippon Marine Enterprises, Ltd.; NME)
as the leader for SSBL acoustic survey team of NME
(Sueyoshi, S., Okumura, S, and Yamanaka, H.)

Jonaotaro Onodera (JAMSTEC)

Ikkan Kamiyama (Tokyo University of Marine Science and Technology)

Michiyo Yamamoto-Kawai* (Tokyo University of Marine Science and Technology)

Akane Yamamoto (The University of Tokyo)

Tsubasa Kodaira* (The University of Tokyo)

*: onshore members

(2) Objectives

The objective of mooring measurements in the Barrow Canyon is to monitor the variations of volume, heat and fresh water fluxes of Pacific-origin water through the Barrow Canyon. Barrow Canyon, in the northeast Chukchi Sea, is a major conduit through which the Pacific water enters the Arctic basin. JAMSTEC has conducted subsurface oceanographic mooring observations in the mouth of the Barrow Canyon since 2000.

We recovered three moorings (BCE-22, BCC-22, BCW-22) and re-deployed three similar configuration moorings (BCE-24, BCC-24, BCW-24) in the Barrow Canyon.

(3)Parameters

-Oceanic velocities

-Pressure, Temperature and Conductivity

-Dissolved oxygen

-Chlorophyll-a and turbidity
-Wave height
-Water sampling

(4) Instruments and methods

1) CTD, CT, T, P sensors
SBE37-SM (Sea-Bird Electronics Inc.)
A7CT-USB (JFE Advantech)
DEFI-T (JFE Advantech)
DEFI-D (JFE Advantech)
DEFI-CT (JFE Advantech)

2) Current meters
Workhorse ADCP 300 kHz Sentinel (Teledyne RD Instruments, Inc.)
Aquadopp Current Meter 2MHz (NORTEK AS)

3) Dissolved oxygen sensor
AROW-USB (JFE Advantech)

4) Chlorophyll-a and turbidity sensor
ACLW-USB (JFE Advantech)
MFL50W-USB (JFE Advantech)

5) Acoustic transponder
XT-6000, XT6001 (Teledyne Benthos, Inc.)

6) Acoustic releaser
8242XS (ORE offshore /EdgeTech)
865-A (Teledyne Benthos, Inc.)

7) Water sampler
RAS500 (McLANE)

8) Nitrate sensor
SUNA (Sea-Bird Electronics Inc.)

9) Wave height and current meter
Signature500 (NORTEK AS)

(5) Station list

Table 3.8.1-1: Moorings recovered by MR24-06C

Mooring Name	Recovered Time (UTC)	Latitude	Longitude
BCE-22	2024/09/08	71-40.3849'N	154-59.9879'W
BCC-22	2024/09/08	71-44.0667'N	155-09.8395'W
BCW-22	2024/09/08	71-47.7807'N	155-20.8119'W

Table 3.8.1-2: Moorings deployed by MR24-06C

Mooring Name	Deployed Time (UTC)	Latitude	Longitude	Depth (m)
BCE-24	2024/09/09	71-40.4014'N	154-59.9036'W	108
BCC-24	2024/09/09	71-44.1010'N	155-09.6849'W	291
BCW-24	2024/09/09	71-47.8029'N	155-20.8307'W	165

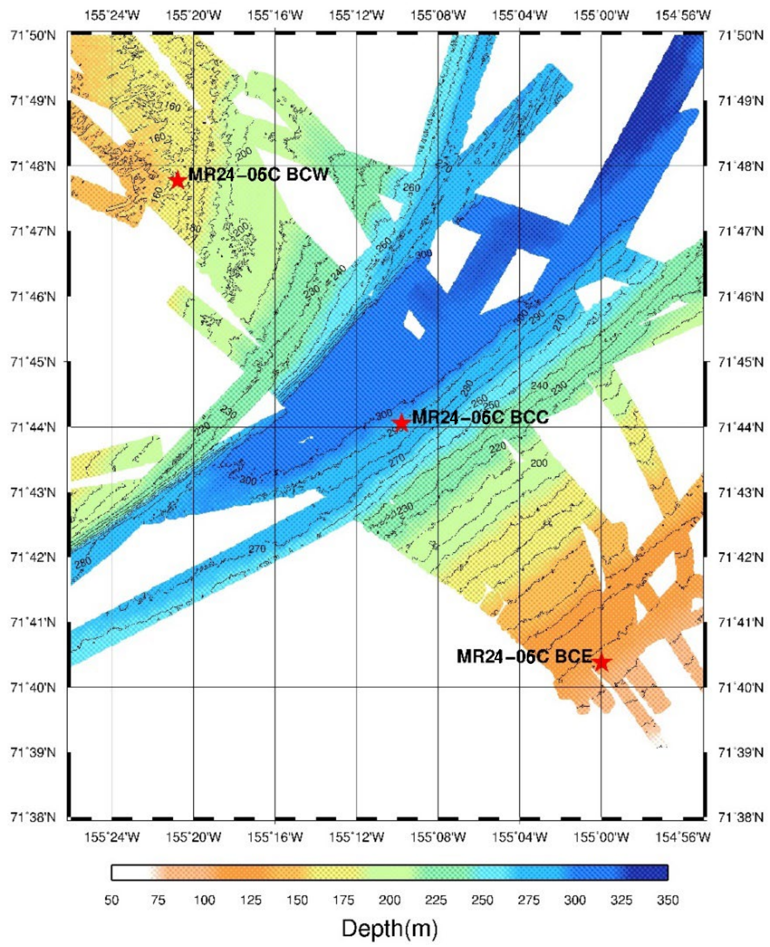

Figure 3.8.1-1: Positions of the moorings (BCE, BCC and BCW).

(7) Data archive

These mooring data will be opened to the public via a web site below.
<http://www.jamstec.go.jp/arctic/data_archive/mooring/mooring_index.html>

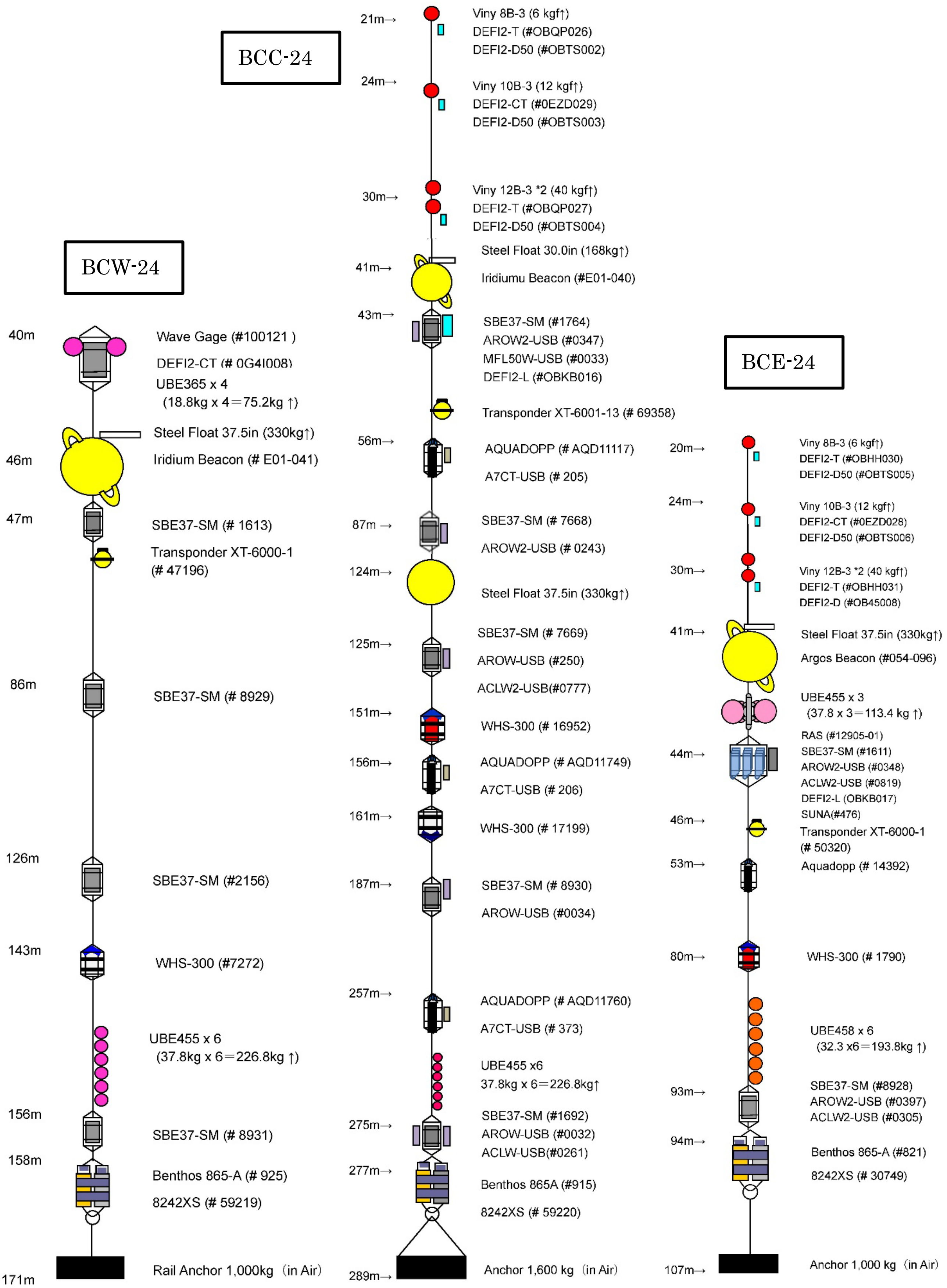

Figure 3.8.1-2: Deployed mooring diagrams.

3.8.2. Sediment Trap

(1) Personnel

Jonaotaro Onodera	JAMSTEC	- Principal Investigator
Motoyo Itoh	JAMSTEC	
Yuichiro Tanaka*	AIST	
Atsushi Suzuki*	AIST	
Katsunori Kimoto*	JAMSTEC	
Eiji Watanabe*	JAMSTEC	
Takuhei Shiozaki*	Tokyo Univ. AORI	

Daiki Ushiromura as the leader of technical team for mooring operation of MWJ
Satomi Ogawa as the leader for SSBL acoustic survey team of NME
(Yoshida, K., Ogawa, S., and Sugimoto, Y.).
*: onshore members

(2) Objectives

- To understand lateral transportation of shelf-origin matter to basin with physical oceanographic condition from northern off Barrow Canyon to the Chukchi Borderland.
- To monitor hydrographic condition regarding to ocean acidification and warming.
- To investigate biodiversity in the study region.

(3) Parameters

Settling particles, water temperature, salinity, current, ice thickness, dissolved oxygen, CO_2, turbidity, chlorophyll-a, PAR, pH

(4) Instruments and methods

<Instruments>

All instruments on recovered and deployed moorings are listed in Tables 3.8.2-1 and -2. The designs of recovered and deployed mooring are shown in Figures 3.8.2-1, -2, and -3.

<Methods>

Acoustic communication of releasers to be deployed were examined with CTD test cast at Station 001 in the Bering Sea (58°03.4'N 177°36.2'W, 3638 m water depth) on Sep. 2, 2024. The releasers were mounted on CTD frame, and it was tested at 1000 m and 300 m depths using ship's acoustic ranging system. The Benthos 865A releaser was successful on the test. The Nichiyu LGCTi releaser might respond to call, but it was uncertain due to the ship's noise. The response of the Nichiyu release was no problem on deck. Therefore, this releaser was applied to the deployment of mooring NAP24t as planned.

For the deployment sensors, log file or photograph of configuration process were taken.

Sample cups of sediment trap were filled-with filtered sea water taken at 500 m depth in the southwestern Canada Basin in previous *Mirai* cruise. The water contains formalin (4v/v%) and sodium hydroborate for pH adjustment (pH ~8.2). The time-series sediment trap was scheduled with 13-days interval from September 19, 2024 to January 1st, 2024 (UTC), from May 7 to September 1st, 2025, and 14-days interval from January 1st to May 7, 2024. The scheduled time to change sample cup is 00:00 (UTC) of the event day. The battery of acoustic releasers is for two-years deployment.

Safety briefing by chief officer was conducted for all related staffs working on stern deck, just before the start of mooring operations. All staffs working on stern deck worn floating jackets, hard hat, safety shoes, and gloves. The "A" frame and capstan winch was applied for the mooring operation on the deck. Just in case, dragging tools, which are composed of hooks, weights, chains, shackles, TRITON wires and ropes, were loaded on the ship for mooring recovery.

Recovery operation for NAP23t started from confirmation of the mooring existence using the water column image, and then acoustic communication between ship's transducer and the transducer of acoustic releaser. The deployed releaser of Benthos 865A was enabled, and release command was transmitted from ~290 m away (horizontal distance). The release was successful, and the ship's zodiac went to the drifting top buoy, and connected a rope from stern to the top buoy. The rope was spooled on deck, and the mooring equipment was recovered on deck from the top buoy to acoustic releasers (Table 3.8.2-1).

For deployment, all serial numbers of deploying equipment and connection of all parts were checked just before the deployment and/or during the deployment operation. Mooring deployment started from the throw-in of top buoy into water (Table 3.8.4-2). The ships go forward with slow speed (~1.0knot). Before the dropping sinker, the slow towing of mooring continued until the ship reaches at the planned target position of the mooring. Deepening and vanish of top buoy from sea surface was confirmed, and then reaching of sinker at ser floor was confirmed by ship's acoustic ranging system. The mooring position was determined using SSBL and transducer of Benthos 865A releaser. The water depth was determined by the depth value of the position in MBES topography map (Figure 3.9.4-4). The position, water depth, top depth, and recovery plan (season and ship) of the NAP24t will be noticed to AOOS and related persons.

The water of 60L taken at 1000m depth of CTD/R Station 22 (St. NAP) is to be used for treatment of recovered samples and waters for next sediment-trap deployment in 2025.

(5) Station list or Observation log

Table 3.8.2-1. Summary on the recovery of NAP23t on September 15, 2024 (UTC).

NAP23t - Coordinates: 74°31.3753’N 161°56.5362’W, Water depth: 1685 m	
Transmitting the enable command of releaser Benthos 865A (~290 m away from NAP23t position)	14:35
Confirmation of response from the releaser	14:35
Transmission of the release command for Benthos 865A (~340 m away from NAP23t position)	15:41
Response of releasing completed	15:41
Finding of the 3rd grass buoy set (~800m) at sea surface	15:55
Finding of the deepest glass buoys with releasers at sea surface	16:02
Weather Condition: cloudy Air Temp. 0.9°C, Atmospheric Press. 1001.9hPa, Wind Direction 77°, Wind Speed 9.4 m/s, SST 0.3°C, Wave 1.86 m (stern), Current 0.1 knot, Curr. Dir. 184.6°	15:30
Zodiac boat on water	16:24
Connection of the ship’s rope to top buoy by the clue on zodiac	16:39

Recovered Mooring Instruments				
Item#	Type	Model	Serial Number	Time
1	Float Ice profiler CT DO Multi-Exciter PAR Iridium Beacon LED Flasher	 IPS-5 A7CT2-USB ARO-USB MFL50W-USB DEFI2-L MMI-513-32000 MMF-523-12000	ASL-SFFC-01 51123 0274 131 19 0F5I016 H01-001 J01-001	16:57
2	Floats	Benthos 17’’ x4	-	16:57
3	CT	SBE37SM	6934	17:04
4	Float	30inch steel	-	17:05
5	CT	SBE37SM	8858	17:12
6	ADCP	WHS-300	15385	17:17
7	CT DO pH	SBE37SM ARO-USB SPS-14Ti +Battery Unit	8860 0135 40306167001	17:17
8	Floats	Benthos 17’’ x5	-	17:24
9	Logger ├ ADCP ├ Pressure ├ DO └ CO2	SeaGuard II DCS4520IW 4117E 4330IW CO2	1958	17:30
10	Sediment trap CT	SMD26S-6000 A7CT-USB	26S032 0626	17:38
12	Floats	Benthos 17’’ x5	-	18:06
13	Sediment Trap	SMD26S-6000	26S033	18:28
14	Floats	Benthos 17’’ x5	-	18:51
15	Releaser Releaser pressure	Benthos 865A Nichiyu LGC DEFI2-D2XHG	867 0021 0F5H001	18:51
End of recovery operation at 74°31.1702’N 161°48.5865’W				18:51

Table 3.8.2-2. Summary on the deployment of NAP24t on September 15-16, 2024 (UTC).

NAP24t Planned Coordinates: 74°31.37’ N 161°55.88’ W, Water Depth: 1685 m	
Start of mooring deployment (74°31.4889’N 162°11.0286’W, 1594 m water depth)	21:57 (UTC)
Weather Condition: cloudy (horizon was usually clear) Air temp. 0.8°C, Atmospheric pressure 1000.5hPa, Wind direction 73°, Wind speed 9.4 m/s, SST -0.2°C, Current direction 193.3°, Current speed 0.2 knot	

Time of instruments and anchor in water				
Item#	Type	Model	Serial Number	Time
1	Float Ice profiler CT DO Multi-Exciter PAR Iridium Beacon LED Flasher	 IPS-5 A7CT2-USB ARO-USB MFL50W-USB DEFI2-L MMI-513-32000 MMF-523-12000	ASL-SFFC-01 51123 0274 131 19 0F5I016 H01-001 J01-055	22:03
2	Floats Transponder	Benthos 17’’ x5 XT-6001	- 75683	22:04
3	CT	SBE37SM	13677	22:05
4	Float	Steel 30’’	-	22:06
5	CT	SBE37SM	13678	22:11
6	ADCP	WH-300 (w/ BT)	24534	22:17
7	CT DO pH	SBE37SM ARO-USB SPS-14Ti +Battery Unit	15456 0136 40306167001	22:18
8	Float	Benthos 17’’ x5	-	22:24
9	ADCP CT	Aquadopp DW A7CT-USB	AQD15193 0799	22:25
10	CT	SBE37SM	1367	22:29
11	Logger ├ ADCP ├ Pressure ├ DO └ CO2 CT	SeaGuard II DCS4520IW 4117E 4330IW CO2 A7CT-USB	1989 0691	22:34
12	Sediment trap CT DO ADCP	SMD26S-6000 A7CT-USB ARO-USB Aquadopp DW	26S034 0613 0219 9944	22:39
13	Floats	Benthos 17’’ x5	-	23:01
14	Sediment trap ADCP	SMD26S-6000 Aquadopp DW	26S035 9948	23:15
15	Floats	Benthos 17’’ x7	-	23:41
16	Releaser Releaser	Benthos 865A Nichiyu LGCTi	1078 005	23:41
17	Anchor (74°31.3597’N 161°55.2551’W, 1692 m)	1000kg in air	-	2016-09-16 00:12

Confirmation of anchor arrival at sea floor		00:27
Communication with releasers (Item#16) , away from ~500m of horizontal distance Benthos 865A slant range: 1666 m Nichiyu LGCTi slant range: 1662 m (only once was successful) Communication with transponder (Item#2): not successful	1078 005 75683	00:31 00:39 00:42
SSBL transponder survey for Benthos 865A Position 74°31.3763'N 161°56.1888'W Water Depth 1680 m (SeaBeam depth of the position) Estimated Top-buoy Depth 28 m		

(6) Preliminary results

The deck works for the recovery and deployment were successful without any injures. On the recovery of the mooring NAP23t, there were some tangled ropes of deeper part in the recovered mooring, which were safely recovered. Two sediment traps unfortunately clogged during the first sampling period in the last September, and thus no time-series samples were retrieved. The hydrographic monitoring of the attached sensors was basically successful. One DO sensor at the top buoy did not work in spite of appropriate configuration. This trouble was not repeated after the recovery, and thus the cause of problem is uncertain at this time. On the pressure sensor attached on the bundled releases, water immersion was found in the sensor housing, although the data was successfully recovered. According to the pressure data taken at 2 sec. interval, the overshoot of releasers and top buoy when sinker reached at seafloor were about 0.6 m and 82 m, respectively (Fig. 3.8.2-4). The deployment work was smoothly operated. The water depth at the position of new mooring NAP24t was 5m shallower than the planned depth (Figure 3.8.2-5). The estimated top buoy depth is 28 m (Table 3.8.2-2).

(7) Data archives

These data obtained in this cruise will be submitted to the Data Management Group of JAMSTEC, and will be opened to the public via “Data Research System for Whole Cruise Information in JAMSTEC (DARWIN)” in JAMSTEC web site.
<http://www.godac.jamstec.go.jp/darwin/e>

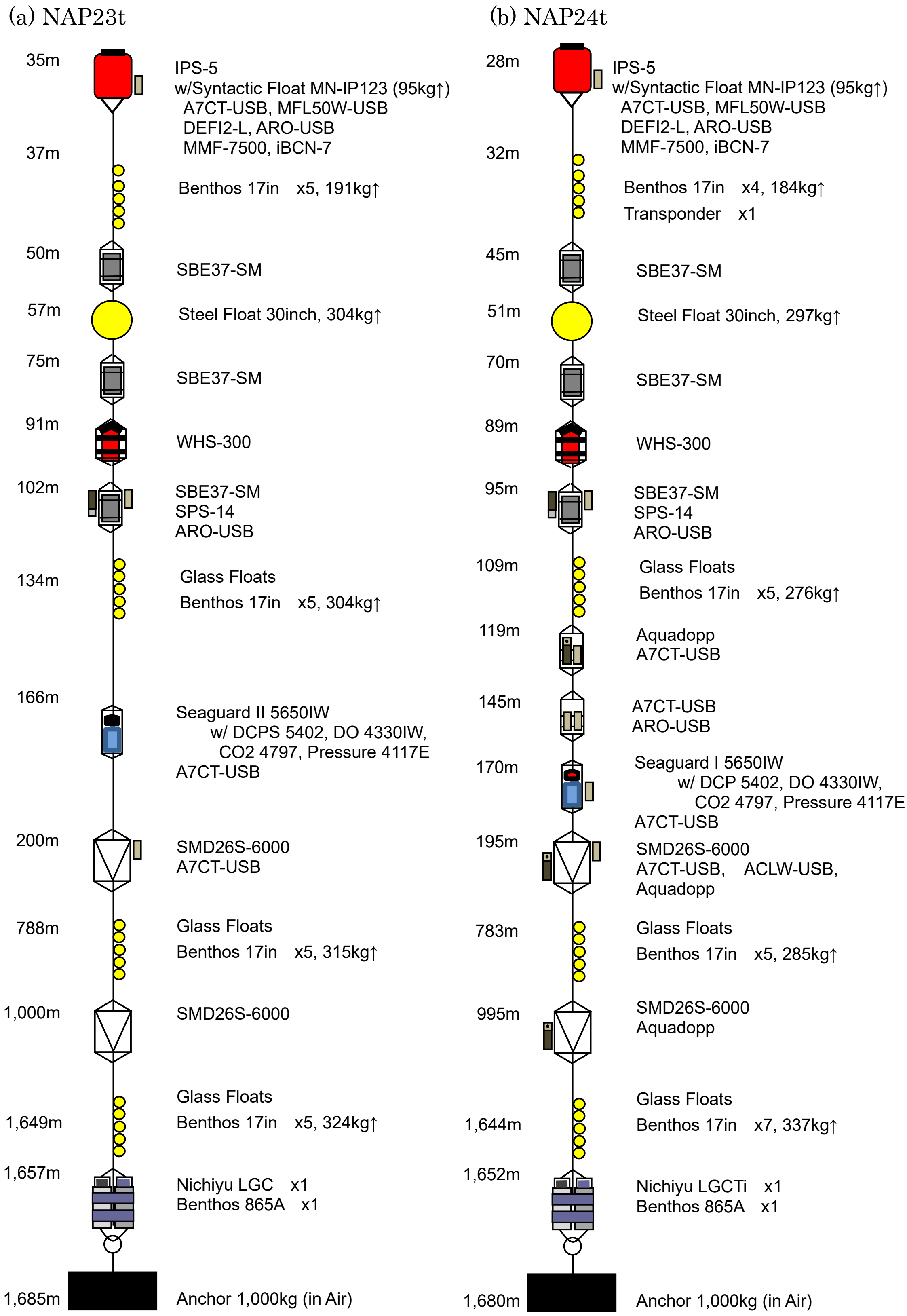

Figure 3.8.2-1. The summary of mooring design for (a) NAP23t and (b) NAP24t.

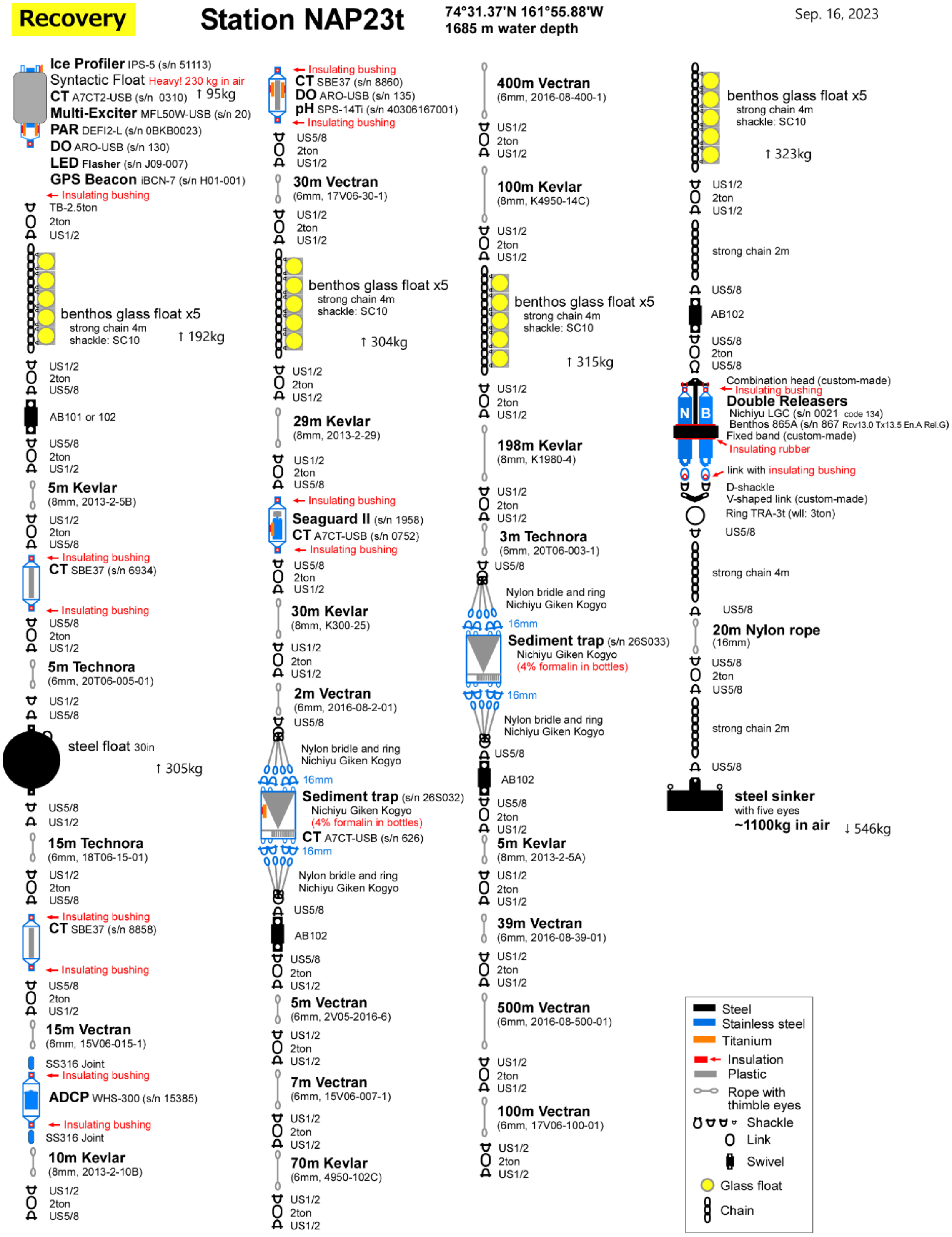

Figure 3.8.2-2. The mooring design of NAP23t for recovery.

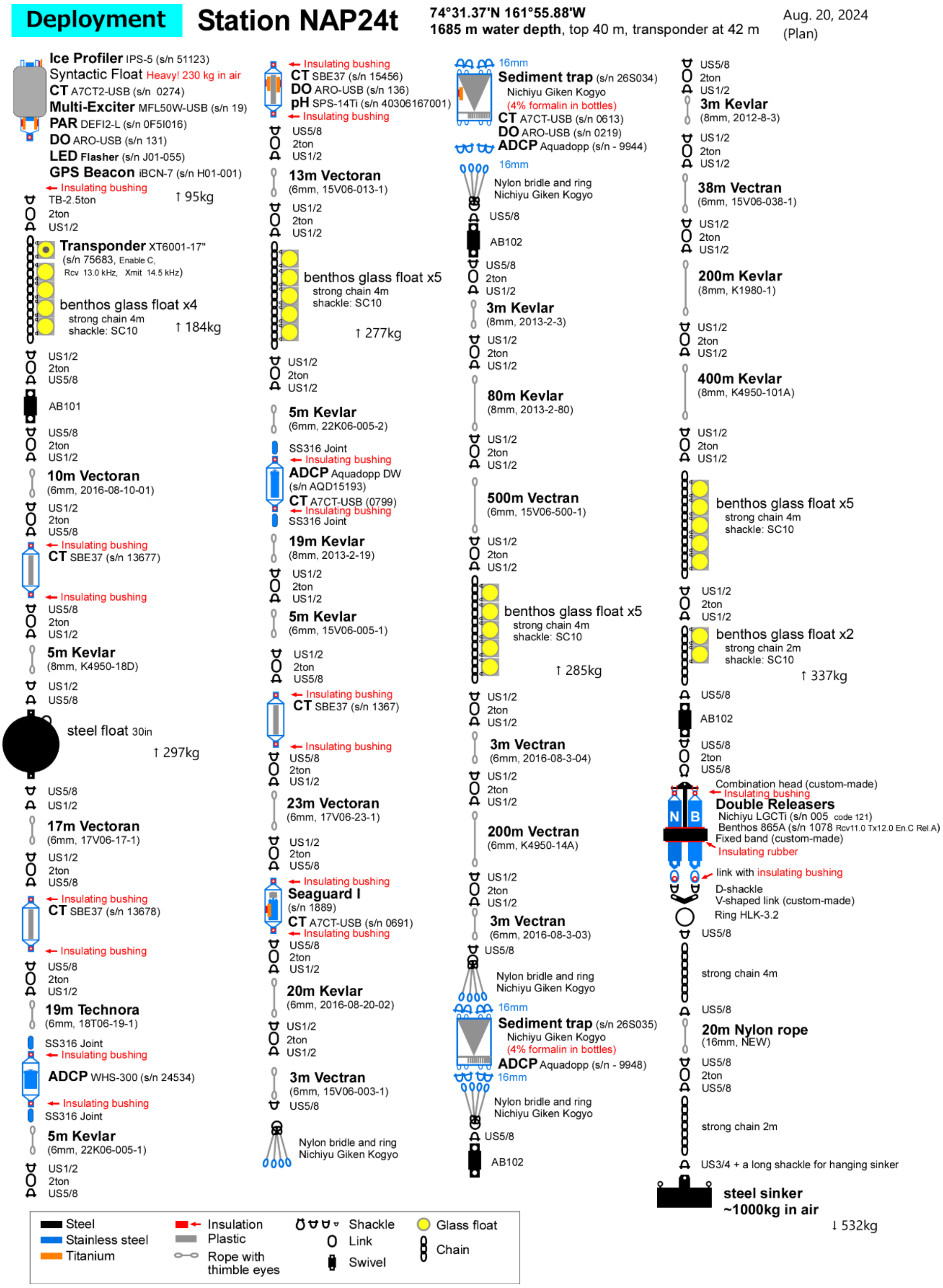

Figure 3.8.2-3. The mooring design of NAP24t for deployment.

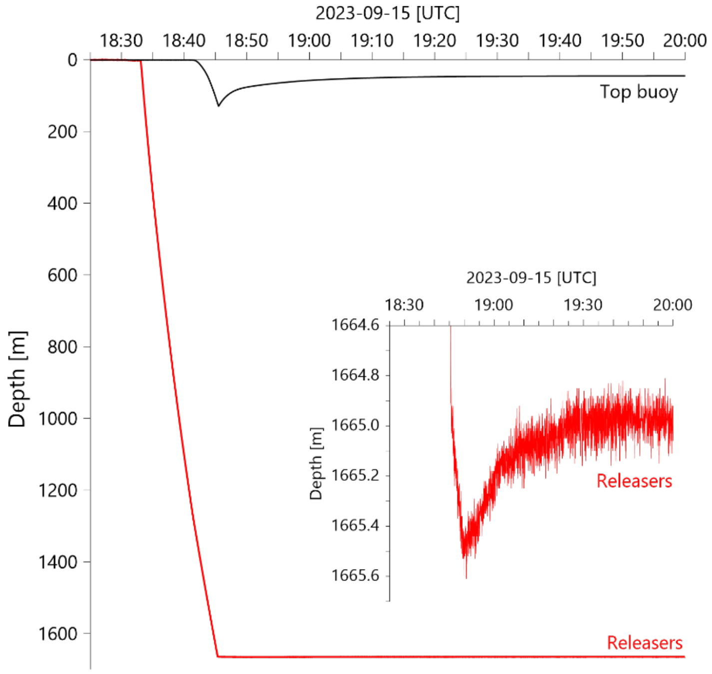

Figure 3.8.2-4.
The depth changes of top buoy and releasers during the deployment of the NAP23t in the last year cruise. The smaller graph is the enlarged part for releasers when the sinker reached sea floor.

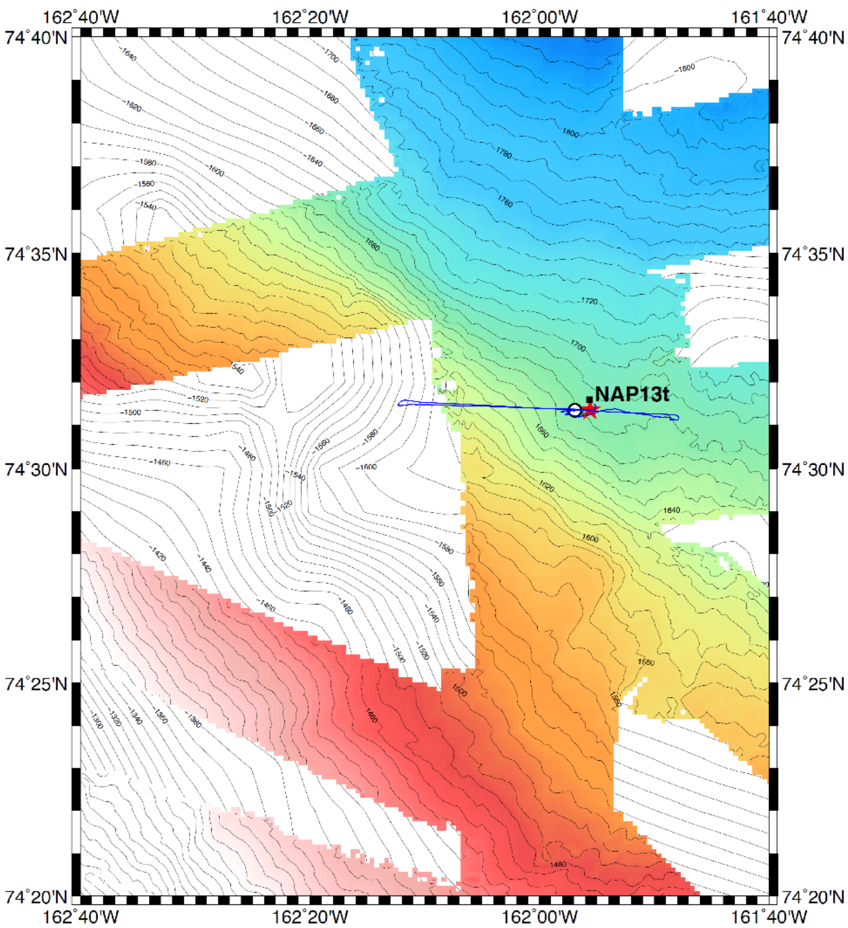

Figure 3.8.2-5.
The MBES topography map showing the mooring positions of NAP23t and 24t (star symbol in red and circular symbol in white, respectively) with vessel's track in blue during the mooring operation.

3.9. A towed CTD chain

(1) Personnel
Satoshi KIMURA (JAMSTEC): Principal Investigator
Motoyo ITOH (JAMSTEC)
Amane FUJIWARA (JAMSTEC)
Yuri FUKAI (JAMSTEC)

(2) Objectives
Although numerous vertical CTD profiles exist, horizontal profiles remain relatively scarce. With increasing interest in submesoscale ocean dynamics, horizontal profiles offer valuable insights into detecting such motions. In this study, horizontal profiles were obtained by towing a chain of CTDs using the A-frame and traction winch aboard the *Mirai* (Figure 3.9-1).

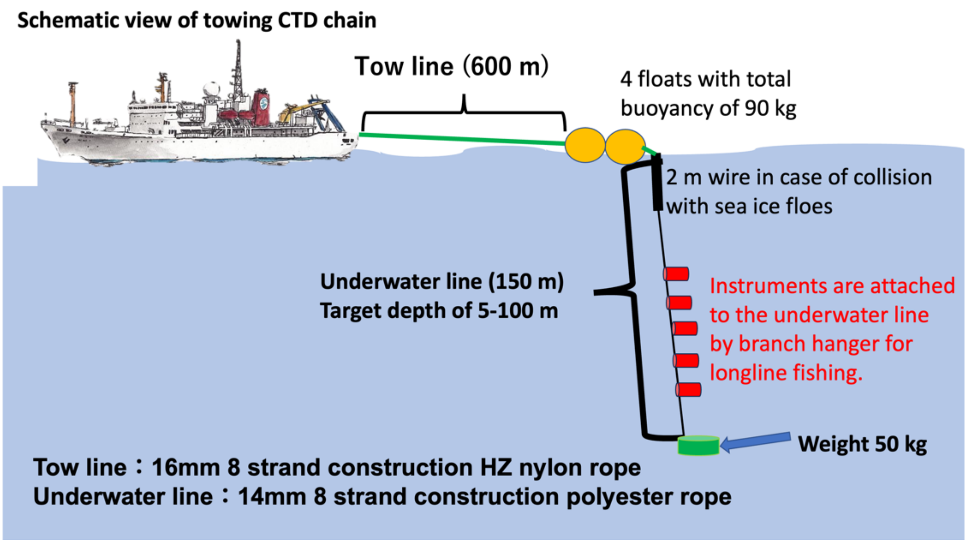

Figure 3.9-1. Schematic view of towing CTD chain using the Mirai.

(3) Parameters
Temperature
Salinity
Pressure

(4) Instruments and methods
We conducted three dives: Dive01, Dive02, and Dive03. Dive01 served as a logistical trial, while complete datasets were obtained during Dive02 and Dive03. This section focuses on the descriptions of Dive02 and Dive03. The time and locations of these dives are summarized in Table 3.9-1 and the locations are shown in Figure 3.9-2.

Dive name	Starting time [UTC]	Starting Longitude [decimal]	Starting Latitude [decimal]	Ending time [UTC]	Ending Longitude [decimal]	Ending Latitude [decimal]
Dive02	9/11/2024 20:30:00	154.12° W	71.92° N	9/12/2024 00:45:00	153.88° W	71.88° N
Dive03	9/16/2024 19:00:00	167.53° W	76.13° N	9/17/2024 00:32:00	167.07° W	76.09° N

Table 3.9-1 Time and locations of Dive02 and Dive03.

In Dive02, we towed 5 instruments, and in Dive03, 18 instruments. Three types of instruments were deployed: JES10mini CTD sensors, DEFI2-T, and DEFI2-P. The JES10mini sensors were designed to measure temperature (T), salinity (S), and pressure (P), while the DEFI2-T and DEFI2-P sensors measured temperature and pressure, respectively. The initial depths and instrument specifications are summarized in Table 3.9-2.

Dive02		
Initial depth [m]	Name of Instrument	Measured variables
5	JES10mini: SN036	S, T, P
10	JES10mini: SN037	S, T, P
15	JES10mini: SN040	S, T, P
20	JES10mini: SN045	S, T, P
25	JES10mini: SN049	S, T, P
50	JES10mini: SN053	S, T, P
Dive03		
Initial depth [m]	Name of Instrument	Measured variables
5	JES10mini: SN036	S, T, P
10	DEFI2-T: OEXY012	T
10	DEFI2-D50: OEL9008	P
15	JES10mini: SN037	S, T, P
20	DEFI2-T: OEXY009	T
20	DEFI2-D50: OBTS013	P
25	JES10mini: SN040	S, T, P
30	DEFI2-T: OEXY006	T
30	DEFI2-D50: OBTS015	P
35	JES10mini: SN045	S, T, P
40	DEFI2-T: OEXY007	T
40	DEFI2-D50: OEL9007	P
60	DEFI2-T: OEXY010	T
60	DEFI2-D50: OCON005	P
80	JES10mini: SN049	S, T, P
90	DEFI2-T: OAAU014	T
90	DEFI2-D50: OCON006	P
100	JES10mini: SN053	S, T, P

Table 3.9-2. Attached instruments in Dive02 and Dive03.

(5) Preliminary results

All instruments successfully recorded data, except for one JES10mini (SN053), for which the issue is currently being addressed with the manufacturer. The two dives traversed a front, as identified from the shipboard surface CTD data (Figure 3.9-2 and Figure 3.9-3a). The ship's velocity was maintained at 1.5 knots relative to the water. The JES10mini CTD data reveal abrupt changes in water properties at the front (Figure 3.9-3b–f). The instrument's depth decreased as the ship accelerated (Figure 3.9-3g). The lift in instruments can be mitigated by adding additional weight, which should be considered for future deployments.

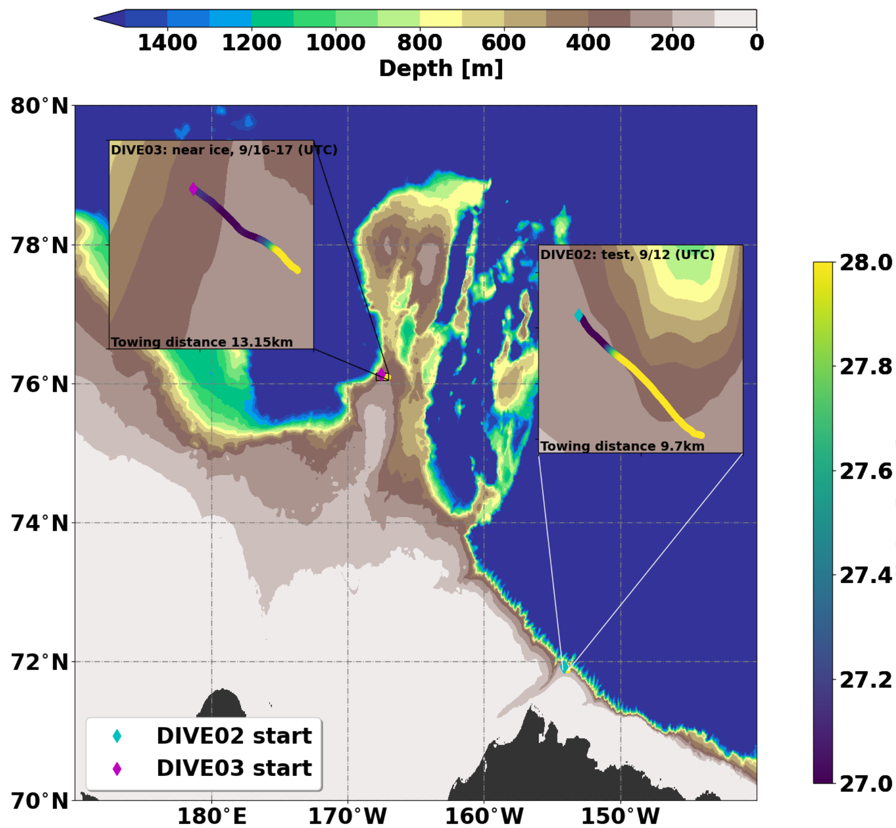

Figure 3.9-2. Locations of Dive02 and Dive03 and bathymetry.

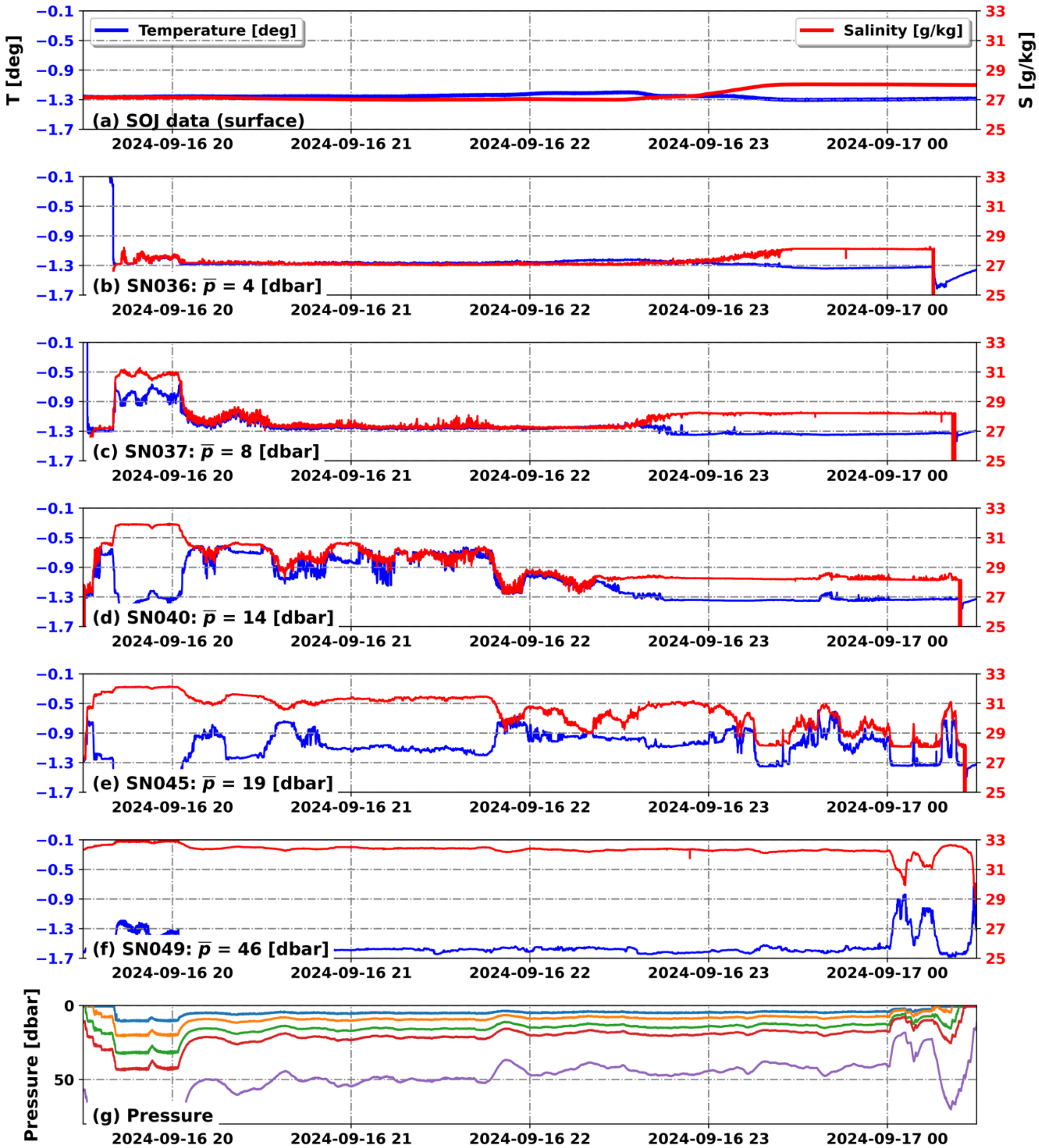

Figure 3.9-3 Temperature, salinity, and pressure from Dive03.

The JES10mini CTD sensors were calibrated against the conductivity measurements obtained from the CTD profile (cast042). Overall, the JES10mini effectively captures variability; however, its mean values may have a systematic offset. To address this, we calibrated the sensor by calculating the cross-correlation between the conductivity measurements from the JES10mini and the onboard seabird CTD sensor, using pressure as the lag variable. The pressure corresponding to the maximum cross-correlation in conductivity was determined, enabling the identification of an offset in the pressure measurements. This pressure offset was subsequently used to correct the conductivity measurements from the JES10mini. The calibrated conductivity data were then utilized to derive temperature and salinity.

(6) Data archives

These data obtained in this cruise will be submitted to the Data Management Group of JAMSTEC, and will be opened to the public via “Data Research System for Whole Cruise Information in JAMSTEC (DARWIN)” in JAMSTEC web site.
<http://www.godac.jamstec.go.jp/darwin/e>

3.10. Salinity

(1) Personnel

Motoyo Itoh	JAMSTEC	- Principal Investigator
Yasuhiro Arii	MWJ	- Operation leader
Nagisa Fujiki	MWJ	

(2) Objectives

To calibrate the measurements of salinity collected from CTD casts, and to provide the data for bucket sampling and clean CTD casts.

(3) Parameters

Salinity

(4) Instruments and methods

a. Sampling

Seawater samples were collected with 12 Liter water sampling bottles and 12 Liter water clean sampling bottles. The salinity sample bottle of the 250 ml brown glass bottle with screw cap was used for collecting the sample water. Each bottle was rinsed 3 times with the sample water, and was filled with sample water to the bottle shoulder. Each bottle was stored for more than 24 hours in the laboratory before the salinity measurement.

The kind and number of samples taken are shown as follows;

Table 3.10-1. Kind and number of samples

Kind of Samples	Number of Samples
Samples for CTD	578
Samples for clean bottle	24
Total	602

b. Instruments and Method

The salinity analysis was carried out on R/V MIRAI during the cruise of MR24-06C using the salinometer (Model 8400B “AUTOSAL”; Guildline Instruments Ltd.: S/N 62556) with an additional peristaltic-type intake pump (Ocean Scientific International, Ltd.). A pair of precision digital thermometers (1502A; FLUKE: S/N B78466 and B81550) were used for monitoring the ambient temperature and the bath temperature of the salinometer.

The specifications of the AUTOSAL salinometer and thermometer are shown as follows;

Salinometer (Model 8400B “AUTOSAL”; Guildline Instruments Ltd.)

Measurement Range : 0.005 to 42 (PSU)

Accuracy : Better than ± 0.002 (PSU) over 24 hours
Maximum Resolution : Better than ± 0.0002 (PSU) at 35 (PSU)

Thermometer (1502A: FLUKE)
Measurement Range : 16 to 30 deg C (Full accuracy)
Resolution : 0.001 deg C
Accuracy : 0.006 deg C (@ 0 deg C)

The measurement system was almost the same as Aoyama *et al.* (2002). The salinometer was operated in the air-conditioned ship's laboratory at a bath temperature of 24 deg C. The ambient temperature varied from approximately 22 deg C to 24 deg C, while the bath temperature was very stable and varied within +/- 0.002 deg C on rare occasion. The measurement for each sample was done with a double conductivity ratio and defined as the median of 34 readings of the salinometer. (Acquisition of the 34 readings took about 11 seconds when the function dial was turned to the 'read' setting) Data were taken after rinsed 5 times with the sample water. The double conductivity ratio of sample was calculated from average value of two measurements. And it was used to calculate the bottle salinity with the algorithm for the practical salinity scale, 1978 (UNESCO, 1981). In the case of the difference between the double conductivity ratio of these two measurements being greater than or equal to 0.00003, continue to be measured up to 3 times. The difference between the double conductivity ratio of these two measurements being smaller than 0.00002 were selected. The measurement was conducted in about 8 hours per day and the cell was cleaned with neutral detergent after the measurement of the day.

(5) Preliminary results

a. Standard Seawater

Standardization control of the salinometer was set to 601. The value of STANDBY was 24+5148 to 24+5149 and that of ZERO was 0.0±0000. The IAPSO Standard Seawater (SSW) batch P168 was used as the standard for salinity. 14 bottles of P168 were measured.

Figure 3.10-1 and 3.10-2 show the time series of the double conductivity ratio of the Standard Seawater batch P168. The average of the double conductivity ratio was 1.99986 and the standard deviation was 0.00001 which is equivalent to 0.0002 in salinity.

The specifications of SSW batch P168 used in this cruise are shown as follows;

Batch : P168
Conductivity ratio : 0.99993
Salinity : 34.997
Expiry : 1st Dec. 2026

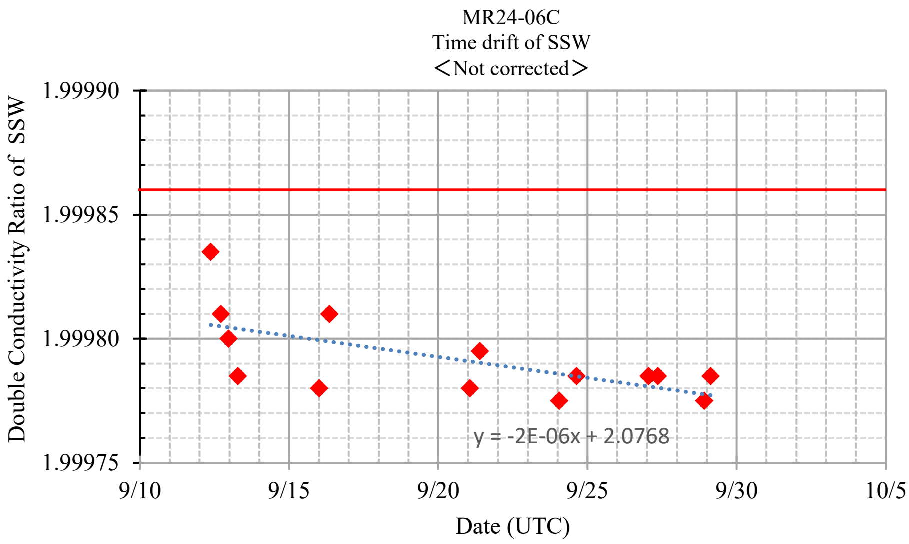

Figure 3.10-1: Time series of double conductivity ratio for the Standard Seawater (before correction)

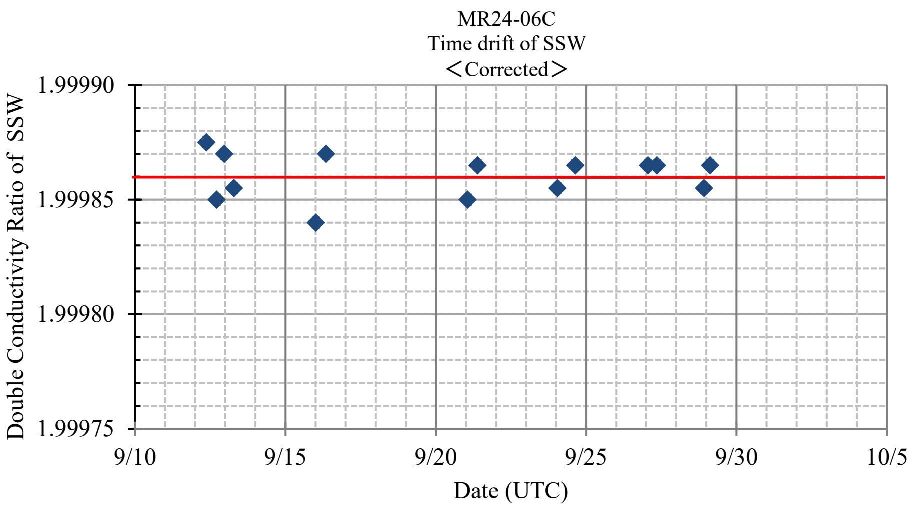

Figure 3.10-2: Time series of double conductivity ratio for the Standard Seawater (after correction)

b. Sub-Standard Seawater

Sub-standard seawater was made from surface sea water filtered by a pore size of 0.45 micrometer and stored in a 20 Liter container made of polyethylene and stirred for at least 24 hours before measuring. It was measured about every 1 hour in order to check for the possible sudden drifts of the salinometer.

c. Replicate Samples

We estimated the precision of this method using 73 pairs of replicate samples taken from the same water sampling bottle. The average and the standard deviation of absolute difference among 73 pairs of replicate samples were 0.0047 and 0.0128 in salinity, respectively.

(6) Data archives

These data obtained in this cruise will be submitted to the Data Management Group of JAMSTEC, and will be opened to the public via “Data Research System for Whole Cruise Information in JAMSTEC (DARWIN)” in JAMSTEC web site.
<http://www.godac.jamstec.go.jp/darwin/e>

(7) References

・Aoyama, M., T. Joyce, T. Kawano and Y. Takatsuki : Standard seawater comparison up to P129. Deep-Sea Research, I, Vol. 49, 1103-1114, 2002.
・UNESCO: Tenth report of the Joint Panel on Oceanographic Tables and Standards. UNESCO Tech. Papers in Mar. Sci., 36, 25 pp., 1981.

4. Biogeochemical Oceanography
4.1. Dissolved Oxygen

(1) Personnel

Mariko HATTA	(JAMSTEC): Principal Investigator
Kentaro UMEMURA	(JAMSTEC)
Ikkan KAMIYAMA	(JAMSTEC)
Shota KUSAKABE	(JAMSTEC)
Misato KUWAHARA	(MWJ): Operation Leader
Takuya IZUTSU	(MWJ)

(2) Objective

To evaluate and monitor dissolved oxygen levels in the Arctic Ocean, with a focus on spatial variability, we determined dissolved oxygen in seawater using the Winkler titration method. The obtained values were also used to calibrate the oxygen sensor attached to the CTD rosette system.

(3) Parameters

Dissolved Oxygen

(4) Instruments and Methods

The following procedure is based on the Winkler method (Dickson, 1996; Culberson, 1991).

a. Instruments

Burette for sodium thiosulfate and potassium iodate;

Automatic piston burette (APB-510 / APB-620) manufactured by Kyoto Electronics Manufacturing Co., Ltd. / 10 cm^3 of titration vessel

Detector;

Automatic photometric titrator (DOT-15X) manufactured by Kimoto Electric Co., Ltd.

Software;

DOT_Terminal Ver. 1.3.1

b. Reagents

Pickling Reagent I: Manganese (II) chloride solution (3 mol dm^{-3})

Pickling Reagent II:

Sodium hydroxide (8 mol dm^{-3}) / Sodium iodide solution (4 mol dm^{-3})

Sulfuric acid solution (5 mol dm^{-3})

Sodium thiosulfate (0.025 mol dm^{-3})

Potassium iodate (0.001667 mol dm^{-3})

c. Sampling

Seawater samples were collected with 12-liter water X-Niskin sampling bottle attached to the CTD/Carousel Water Sampling System (CTD system). For oxygen measurement, seawater was transferred from the bottle to a volume-calibrated glass flask (approximately 100 cm^3), overflowing the flask with double its volume. The temperature was measured simultaneously with a digital thermometer during overflow. After transferring the sample, 1 cm^3 each of two reagent solutions (Reagents I and II) were immediately added, and a stopper was carefully inserted into the flask. The sample flask was then shaken vigorously to mix the contents and evenly disperse the precipitate. Once the precipitate has settled halfway down the flask, it was shaken again vigorously to redistribute the precipitate. The sample flasks containing the preserved samples were stored in the laboratory until titration.

d. Sample measurement

For over two hours after the re-shaking, the preserved samples were measured on board. A 1 cm^3 volume of sulfuric acid solution and a magnetic stirrer bar were added to the sample flask, and then the sample was stirred. The samples were titrated with sodium thiosulfate solution, whose morality was determined using potassium iodate solution. The temperature of the sodium thiosulfate during titration was recorded with a digital thermometer. Dissolved oxygen concentration (μmol kg^{-1}) was calculated using the sample temperature during seawater sampling, the salinity recorded by the CTD system sensor, the flask volume, and the titrated volume of sodium thiosulfate solution, excluding the blank. During this cruise, two sets of titration apparatus were used.

e. Standardization and determination of the blank

The concentration of the sodium thiosulfate titrant was determined using potassium iodate solution. Pure potassium iodate was dried in an oven at 130 °C, and 1.7835 g was dissolved in deionized water and diluted to a final weight of 5 kg in a flask. Using a volume-calibrated dispenser, 10 cm^3 of the standard potassium iodate solution was added to an another flask, followed by 90 cm^3 of deionized water, 1 cm^3 of sulfuric acid solution, and 1 cm^3 each of preserving reagent solution II and I, in that order. The titrated volume of sodium thiosulfate for this diluted potassium iodate standard solution (typically averaged over five times measurements) determined the morality of the sodium thiosulfate titrant.

The oxygen concentration from preserving reagents I (1 cm^3) and II (1 cm^3) was expected to be 7.6×10^{-8} mol (Murray et al., 1968). Every 4 days, the blank correction for factors other than oxygen was determined as follows: 1 cm^3 and 2 cm^3 of the standard potassium iodate solution were added to separate flasks using a calibrated dispenser. To each flask, 100 cm^3 of deionized water, 1 cm^3 of sulfuric acid solution, and 1 cm^3 of each preserving reagent solution (II and I) were added in sequence. The blank was calculated as the difference between the titrated volume of solium thiosulfate for the 1 cm^3 of potassium iodate addition and that for the 2 cm^3 addition. Titrations were conducted in triplicate, and the average value was taken as the blank value.

(5) Observation log

a. Standardization and determination of the blank

Table 4.1-1 shows results of the standardization and the blank determination during this cruise.

Table 4.1-1 Results of the standardization and the blank determinations during cruise

Date (yyyy/mm/dd)	Potassium iodate ID	Sodium thiosulfate ID	DOT-15X (No.9)		DOT-15X (No.10)		Stations ("station number"+M+"cast number")
			End point (cm^3)	Blank (cm^3)	End point (cm^3)	Blank (cm^3)	
2024/08/29	K23D08	T-22I	3.980	0.000	3.975	-0.002	
2024/09/03	K23D03	T-22I	3.977	0.000	3.974	0.000	002M001 003M001 004M001 005M001 006M001 007M001 008M001 009M001
2024/09/07	K23D04	T-22I	3.977	0.001	3.973	0.003	
2024/09/07	K23D05	T-22I	3.978	0.000	3.975	0.001	010M001 011M001 012M001 013M001 014M001
2024/09/12	K23D06	T-22I	3.978	0.000	3.975	0.000	015M001 016M001 017M001 018M001 019M001 022M001
2024/09/18	K23D09	T-22I	3.979	-0.001	3.980	0.001	

2024/09/18	K23D09	T-24A	3.963	0.001	3.962	0.002	023M001 024M001 025M001 026M001 027M001 028M001 031M001 033M001 034M001
2024/09/23	K23D07	T-24A	3.961	0.000	3.959	0.004	
2024/09/23	K23E04	T-24A	3.962	0.002	3.959	0.002	035M001 037M001 038M001 039M001 040M001 041M001 043M001 046M001 047M001
2024/09/27	K23E11	T-24A	*	*	3.963	0.005	

* An unknown issue occurred with the DOT-15X (No. 9) system during the analysis, resulting in data not being obtained during this run.

b. Repeatability of sample measurement

Replicate samples were taken at each CTD cast. Following the protocol of Dickson et al. (2007), the standard deviation of the replicate measurements was 0.20 μmol kg^{-1} (n = 60).

(6) Data archives

These data obtained during this cruise will be submitted to the Data Management Group (DMG) of JAMSTEC, and made publicly available through “Data Research System for Whole Cruise Information in JAMSTEC (DARWIN)” on the JAMSTEC web site.
<http://www.godac.jamstec.go.jp/darwin/e>

(7) References

Culberson, C. H. (1991). *Dissolved Oxygen.* WHPO Publication 91-1.

Dickson, A. G. (1996). Determination of dissolved oxygen in sea water by Winkler titration. In *WOCE Operations Manual*, Part 3.1.3 Operations & Methods, WHP Office

Report WHPO 91-1.

Dickson, A. G., Sabine, C. L., & Christian, J. R.(Eds.), (2007). *Guide to best practices for ocean CO_2 measurements, PICES Special Publication 3*: North Pacific Marine Science Organization.

Murray, C. N., Riley, J. P., & Wilson, T. R. S. (1968). The solubility of oxygen in Winklerreagents used for the determination of dissolved oxygen. *Deep Sea Res.*, 15, 237-238.

4.2. Nutrients

(1) Personnel

Mariko HATTA [1]: Principal Investigator
Shiori ARIGA [2]: Operation Leader
Yuko MIYOSHI [2]
Yuta ODA [2]
1) Japan Agency for Marine-Earth Science and Technology
2) Marine Works Japan Ltd.

(2) Objectives

The objective of this document is to present the current status of nutrient measurements conducted during the R/V MIRAI MR24-06C cruise (EXPOCODE: 49NZ20240827) in the Arctic Ocean.

(3) Parameters

The parameters measured include nitrate, nitrite, silicate, phosphate, and ammonia in seawater.

(4) Instruments and methods

The analytical platform was upgraded from QuAAtro 2-HR to QuAAtro 39 in March 2021. However, following this replacement, several issues were reported with the QuAAtro 39 system (see the cruise report of MR21-05C). In July 2022, to address these issues and improve analytical precision, the following modifications were made: (1) the pumps were replaced with a 14-tube pump (model number: TRA+B014-02, BL TEC K.K.), instead of the original 13-tube pump (model number: 166+B214-01, BL TEC K.K.); (2) the motor brackets were upgraded to a new type that is a stainless model (model number: Motor-Braket-01-Rev-1 and Motor-Braket-02-Rev-1, BL TEC K.K.); and (3) the light source units were secured to reduce vibration. The modified platform, referred to as the "QuAAtro 39-J" was used for this cruise.

The analytical methods for nitrate, nitrite, silicate, and phosphate used in this cruise align with those described in the GO-SHIP repeat hydrography nutrients manual (Hydes et al., 2010; Becker et al., 2019). The method for ammonium follows a vaporization membrane permeability approach (Kimura, 2000).

(4.1) Nitrate + nitrite and nitrite

Nitrate + nitrite and nitrite were analyzed using a methodology modified from Grasshoff (1976). The flow diagrams are shown in Fig. 4.2-1 for nitrate + nitrite and Fig. 4.2-2 for nitrite. In the nitrate + nitrite analysis, samples were mixed with the alkaline imidazole buffer and then pushed through a cadmium coil coated with metallic copper. This step facilitated the reduction of nitrate to nitrite in the sample, allowing for the determination of total nitrate + nitrite in seawater. For the nitrite analysis, the samples were mixed with reagents without undergoing the reduction step. In the flow system, the seawater sample – either with or without the reduction step - was mixed with an acidic sulfanilamide reagent through a mixing coil to produce a diazonium ion. The mixture was then combined with the N-1-naphthylethylenediamine dihydrochloride (NED), producing a red azo dye. This azo dye was subsequently directed to the spectrophotometric detection to monitor the signal at 545 nm. Therefore, for the nitrite analysis, sample bypassed the Cd coil, and nitrate concentrations were calculated by the difference between nitrate + nitrite and nitrite concentrations.

Reagents

a) 50 % Triton solution: 50 mL of Triton® X-100 (CAS No. 9002-93-1) was mixed with 50 mL of ethanol (99.5 %).
b) Imidazole (buffer), 0.06 M (0.4 % w/v): Dissolved 4 g of the imidazole (CAS No. 288-32-4) in 1000 mL ultra-pure water, and then added 2 mL of the hydrogen chloride (CAS No. 7647-01-0). After mixing, 1 mL of the 50 % triton solution was added.
c) Sulfanilamide, 0.06 M (1 % w/v) in 1.2 M HCl: Dissolved 10 g of 4-aminobenzenesulfonamide (CAS No. 63-74-1) in 900 mL of ultra-pure water, and then add 100 mL of the hydrogen chloride (CAS No. 7647-01-0). After mixing, 2 mL of the 50 % triton solution was added.
d) NED, 0.004 M (0.1 % w/v): Dissolved 1 g of N-(1-naphthalenyl)-1,2-ethanediamine dihydrochloride (CAS No. 1465-25-4) in 1000 mL of ultra-pure water and then added 10 mL of hydrogen chloride (CAS No. 7647-01-0). After mixing, 1 mL of the 50 % triton solution was added. This reagent was stored in a dark bottle.

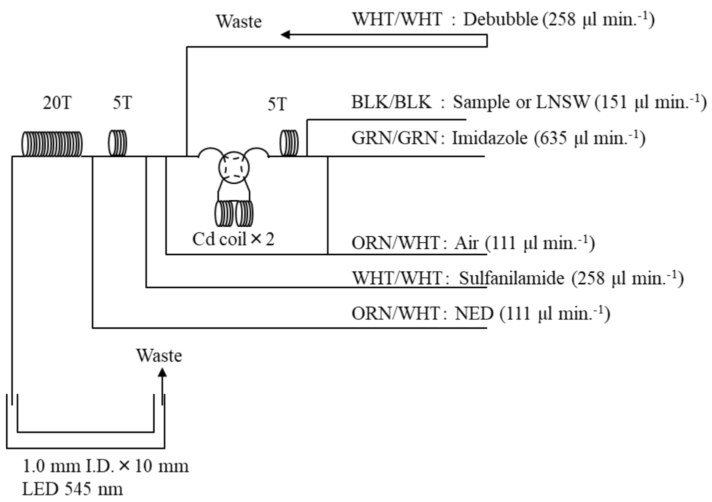

Figure 4.2-1 NO_3+NO_2 (1ch.) flow diagram.

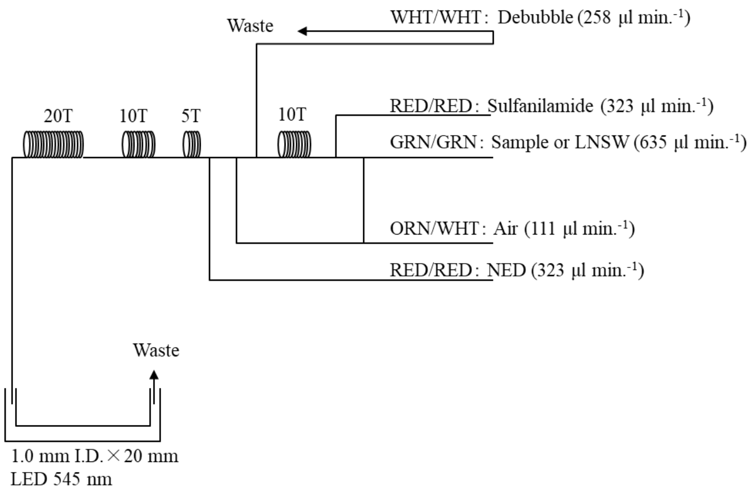

Figure 4.2-2 NO_2 (2ch.) flow diagram.

(4.2) Silicate

The method for silicate is analogous to that described for phosphate (4.3) and is essentially based on the method outlined by Grasshoff et al. (1999). The flow diagram is shown in Fig. 4.2-3. Silicomolybdic acid compound was first formed by mixing the silicate in the sample with the molybdic acid. This silicomolybdic acid was then reduced to silicomolybdous acid, known as "molybdenum blue," using L-ascorbic acid as the reductant. The signal was monitored at 630 nm.

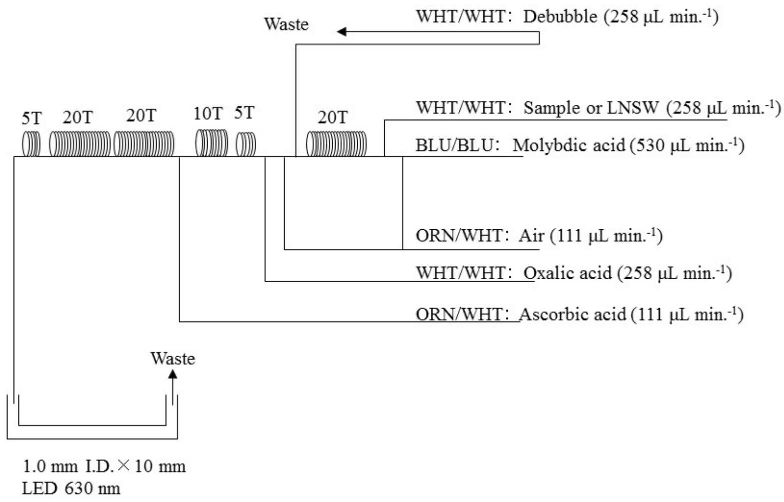

Figure 4.2-3 SiO_2 (3ch.) flow diagram.

Reagents

a) 15 % Sodium dodecyl sulfate solution: 75 g of sodium dodecyl sulfate (CAS No. 151-21-3) was mixed with 425 mL ultra-pure water.
b) Molybdic acid, 0.03 M (1 % w/v): Dissolved 7.5 g of sodium molybdate dihydrate (CAS No. 10102-40-6) in 980 mL ultra-pure water, and then added 12 mL of 4.5M sulfuric acid. After mixing, 20 mL of the 15 % sodium dodecyl sulfate solution was added. Note that the amount of sulfuric acid was reduced from the previous report (MR19-03C) since we have modified the method of Grasshoff et al. (1999).
c) Oxalic acid, 0.6 M (5 % w/v): Dissolved 50 g of oxalic acid (CAS No. 144-62-7) in 950 mL of ultra-pure water.
d) Ascorbic acid, 0.01 M (3 % w/v): Dissolved 2.5 g of L-ascorbic acid (CAS No. 50-81-7) in 100 mL of ultra-pure water. This reagent was freshly prepared every day.

(4.3) Phosphate

The methodology for the phosphate analysis is a modified procedure based on Murphy and Riley (1962). The flow diagram is shown in Fig. 4.2-4. Molybdic acid was added to the seawater sample to form the phosphomolybdic acid compound, which was then reduced to phosphomolybdous acid using L-ascorbic acid as the reductant. The signal was monitored at 880 nm.

Reagents

a) 15 % Sodium dodecyl sulfate solution: 75 g of sodium dodecyl sulfate (CAS No. 151-21-3) was mixed with 425 mL of ultra-pure water.
b) Stock molybdate solution, 0.03 M (0.8 % w/v): Dissolved 8 g of sodium molybdate dihydrate (CAS No. 10102-40-6) and 0.17 g of antimony potassium tartrate

trihydrate (CAS No. 28300-74-5) in 950 mL of ultra-pure water, and then added 50 mL of sulfuric acid (CAS No. 7664-93-9).

c) PO_4 color reagent: Dissolved 1.2 g of L-ascorbic acid (CAS No. 50-81-7) in 150 mL of the stock molybdate solution. After mixing, 3 mL of the 15 % sodium dodecyl sulfate solution was added. This reagent was freshly prepared before every measurement.

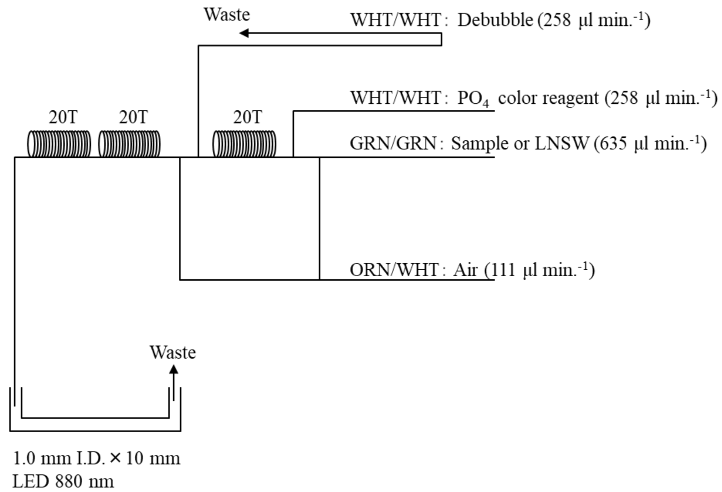

Figure 4.2-4 PO_4 (4ch.) flow diagram.

(4.4) Ammonia

The ammonia in seawater was determined using the flow diagrams shown in Fig. 4.2-5. The sample was mixed with an alkaline solution containing EDTA, which converted ammonia into its gaseous state. The ammonia gas was then absorbed in a sulfuric acid though a 0.5 μm pore-size membrane filter (ADVANTEC PTFE) at the dialyzer attached to the analytical system. The ammonia absorbed in sulfuric acid was subsequently determined by coupling it with phenol and hypochlorite to form indophenols blue, with the signal monitored at 630 nm.

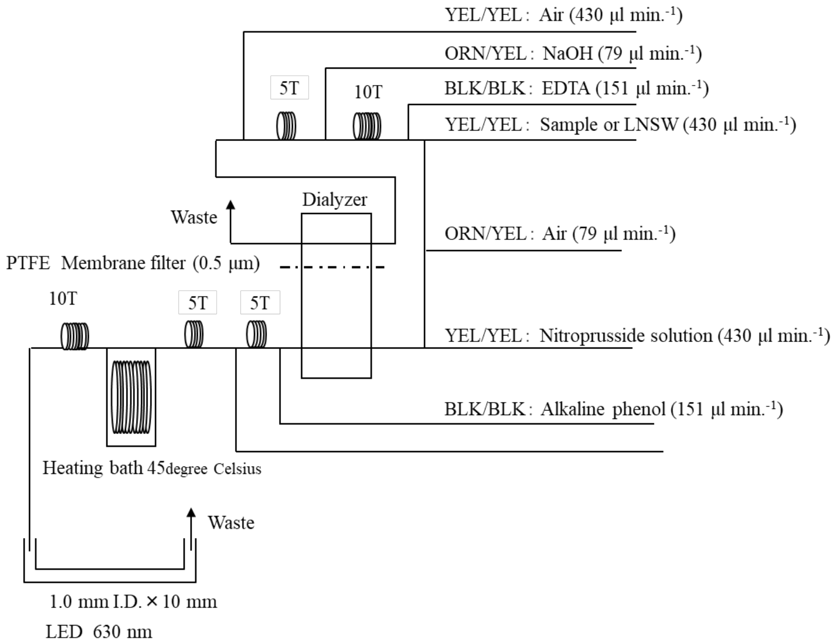

Figure 4.2-5 NH_4 (5ch.) flow diagram.

<u>Reagents</u>

a) 30 % Triton solution: 30 mL of the Triton® X-100 (CAS No. 9002-93-1) was mixed with 70 mL ultra-pure water.

b) EDTA: Dissolved 41 g of tetrasodium;2-[2-[bis(carboxylatomethyl)amino]ethyl-(carboxylatemethyl)amino]acetate;tetrahydrate (CAS No. 13235-36-4) and 2 g of boric acid (CAS No. 10043-35-3) in 200 mL of ultra-pure water. After mixing, 1 mL of the 30 % triton solution was added. This reagent is prepared every week.

c) NaOH liquid: Dissolved 1.5 g of sodium hydroxide (CAS No. 1310-73-2) and 16 g of tetrasodium;2-[2-[bis(carboxylatomethyl)amino]ethyl-(carboxylatemethyl)amino]acetate;tetrahydrate (CAS No. 13235-36-4) in 100 mL of ultra-pure water. This reagent was prepared every week. Note that we reduced the amount of sodium hydroxide from 5 g to 1.5 g because pH of C standard solutions has been lowered 1 pH unit due to the change of recipe of B standards solution (the details of those standard solutions, see (6.4)).

d) Stock nitroprusside: Dissolved 0.25 g of sodium nitroferricyanide dihydrate (CAS No. 13755-38-9) in 100 mL of ultra-pure water, and then added 0.2 mL of 1M sulfuric acid. Stored in a dark bottle and prepared every month.

e) Nitroprusside solution: Added 4 mL of the stock nitroprusside and 4 mL of 1M sulfuric acid in 500 mL of ultra-pure water. After mixing, 2 mL of the 30 % triton solution was added. This reagent was stored in a dark bottle and prepared every 2 or 3 days.

f) Alkaline phenol: Dissolved 10 g of phenol (CAS No. 108-95-2), 5 g of sodium hydroxide

(CAS No. 1310-73-2) and 2 g of sodium citrate dihydrate (CAS No. 6132-04-3) in 200 mL of ultra-pure water. Stored in a dark bottle and prepared every week.

g) NaClO solution: Mixed 3 mL of sodium hypochlorite (CAS No. 7681-52-9) in 47 mL of ultra-pure water. Stored in a dark bottle and fleshly prepared before every measurement. This reagent needs to be 0.3 % available chlorine.

(4.5) Sampling procedures

Sampling for the nutrient samples was conducted after collecting samples for other gas parameters. Seawater samples were collected in two new 10 mL polyacrylate vials without using the sample drawing tube typically used for the oxygen samples. Each vial was rinsed three times before filling and sealed immediately without any head space. The vials were then placed in a water bath at 20.6 ± 0.3 degree Celsius for over 30 minutes before measurement. When the transmissometer signal (Xmiss) of a sample was less than 95 % or if particles were observed in the vial, the sample was centrifuged using a CN-820 centrifuge (Hsiang Tai) at approximately 3400 rpm for 2.5 minute. Note that the sample in the original vial was placed directly on an autosampler (AIM 4000, BL TEC K.K.) tray for analysis. The seawater samples were analyzed within 24 hours of collection.

(4.6) Data processing

Raw data from QuAAtro 39-J were processed as follows:

a) Checked if there were any baseline shifts.
b) Checked the shape of each peak and positions of peak values. If necessary, a change was made for the positions of peak values.
c) Conducted carry-over correction and baseline drift correction followed by sensitivity correction to apply to the peak height of each sample.
d) Conducted baseline correction and sensitivity correction using linear regression. Conducted baseline correction and sensitivity correction using linear regression.
e) Using the salinity (from CTD data* or determined on the ship) and the laboratory room temperature (20 degree Celsius), the density of each sample was calculated. The obtained density was used to calculate the final nutrient concentration with the unit of $\mu mol\ kg^{-1}$.
f) Calibration curves to obtain the nutrient concentrations were assumed second-order equations.

* Raw CTD pre-calibrated data have been used.

(5) Certified Reference Material of nutrients in seawater

Certified reference materials (CRMs) produced by KANSO Co., Ltd. were used to ensure the comparability and traceability of nutrient measurements during this cruise.

The KANSO CRMs cover inorganic nutrients (nitrate, nitrite, silicate, phosphate, and ammonia) in seawater and are produced using autoclaved natural seawater, following a quality control system based on ISO Guide 34 (JIS Q 0034). KANSO Co., Ltd. has been accredited as a CRM producer under the National Institute of Technology and Evaluation (ASNITE) System since 2011. (ASNITE 0052 R)

Certified values for the CRMs were calculated as the arithmetic means of measurements from 30 bottles per batch (measured in duplicates), performed by both KANSO Co., Ltd. and Japan Agency for Marine-Earth Science and Technology (JAMSTEC) using the colorimetric method (continuous flow analysis, CFA). The salinity of the calibration standards solution for each calibration curve was adjusted to match the CRM salinity within ± 0.5.

Each certified value of nitrate, nitrite, and phosphate in KANSO CRMs was calibrated using Japan Calibration Service System (JCSS) standard solutions for the respective ions. The JCSS standard solutions were in turn calibrated using JCSS secondary solutions, which was calibrated with primary solutions produced by the Chemicals Evaluation and Research Institute (CERI), Japan. CERI primary solutions were further calibrated with the National Metrology Institute of Japan (NMIJ) primary standards solution of nitrate, nitrite, and phosphate ions, respectively. The certified value of silicate of KANSO CRM was calibrated using a newly developed silicon standards solution ("exp32" and "exp64" produced by JAMSTEC and KANSO and Lot. AA produced by KANSO), produced via an alkaline dissolution technique. The mass fraction of silicon in this solution was calibrated based on NMIJ CRM 3645-a Si standard solution through the technology consulting system of the National Institute of Advanced Industrial Science and Technology (AIST), providing traceability to the International System of Units (SI).

During this cruise, 15 sets of CRM lots CQ, CR, CO, CP were used (Table 4.2-1), with serial numbers selected randomly. The CRM bottles were stored in the ship's "BIOCHEMICAL LABORATORY" at a maintained temperature of approximately 18.43 degree Celsius – 22.19 degree Celsius.

Table 4.2-1 Certified concentration and the uncertainty (k=2) of CRMs (μmol kg^{-1}).

Lot	Nitrate	Nitrite*	Silicate	Phosphate	Ammonia**
CQ	0.06 ± 0.03	0.074 ± 0.07	2.20 ± 0.07	0.030 ± 0.009	1.76 ± 0.07
CR	5.46 ± 0.16	0.975 ± 0.07	14.0 ± 0.3	0.394 ± 0.014	0.95 ± 0.15
CO	15.86 ± 0.15	0.056 ± 0.04	34.72 ± 0.16	1.177 ± 0.014	0.54
CP	24.8 ± 0.3	0.318 ± 0.07	61.1 ± 0.3	1.753 ± 0.018	0.87

* For Nitrite concentration, there is a trend that the value has been increased 0.004 ± 0.002 μmol kg^{-1} per year. Nitrite concentration values were determined by

JAMSTEC in June 2023.

** Ammonia values are all reference value. The value of CQ and CR were reported by KANSO. The other values were determined by JAMSTEC.

(6) Standards

To obtain the calibration curves, we prepared in-house standard solutions because (1) the phosphate concentrations in CRM lot CP were lower than the maximum concentrations in sweater samples, (2) the concentration range for nitrite in the CRMs was insufficient for the calibration curves, and (3) the ammonia concentrations in the CRMs are not certified values.

(6.1) Volumetric laboratory-ware of in-house standards

All volumetric glassware and polymethylpentene (PMP) volumetric flasks were gravimetrically calibrated. Plastic volumetric flasks were calibrated gravimetrically at their water temperature, within 0.9 K of approximately 21.0 degree Celsius. “Class A” volumetric flasks were used for their nominal tolerances of 0.05 % or less across the size ranges relevant to this work. Since Class A flasks are made of borosilicate glass, standard solutions were transferred to plastic bottles immediately after being made up to volume and thoroughly mixed to prevent excessive silicate dissolution from the glass. PMP volumetric flasks were also gravimetrically calibrated and used only within 1.8 K of their calibration temperature. Volume adjustments for the glass flasks at temperatures other than the calibration temperatures were calculated using the linear expansion coefficient for borosilicate crown glass. The cubical expansion coefficients for each glass and PMP volumetric flask were determined through measurements in 2023. The cubical expansion coefficient of the glass volumetric flask (SHIBATA HARIO) ranged from 0.00000975 to 0.0000110 K^{-1}, and for the PMP volumetric flask (NALGEN PMP), from 0.00038 to 0.00042 K^{-1}. Calibration weights were corrected for the water density and air buoyancy. All glass pipettes, which have nominal calibration tolerances of 0.1 % or better, were gravimetrically calibrated to verify and, where possible, improve upon there nominal tolerances.

(6.2) Reagents

For nitrate standard, we used “potassium nitrate 99.995 suprapur®” provided by Merck, Batch B1983565, CAS No. 7757-79-1. For nitrite standard solution, nitrite ion standard solutions (NO_2^- 1000) from Wako Chemicals (Lot TPH2043, Code. No. 146-06453) was used, with the certified standard solutions from Wako Chemicals. The calibration result was 1004 mg L^{-1} at 20 degree Celsius, with an expanded uncertainty of 0.8 % (k=2). For the silicate standard solution, Si standard solutions Lot. AA produced by KANSO, was used. The silicon mass fraction in the Lot. AA solution was calibrated based on NMIJ CRM 3645-a Si standard solution. For the phosphate standard, “potassium dihydrogen phosphate anhydrous 99.995 suprapur®” provided by Merck (Batch B2024308, CAS No.: 7778-77-0), was used. For the ammonia standard, we used ammonium chloride (CRM 3011-a) from NMIJ, CAS No. 12125-02-9, with a reported purity of >99.9 % by the manufacturer. The expanded uncertainty of calibration (k=2) was 0.026 %.

(6.3) Low nutrients seawater (LNSW)

Surface water with low nutrient concentrations was taken and filtered using a 0.20 μm pore capsule cartridge filter near 13°N and 136°E during the MR21-03 cruise in June 2021. The filtered seawater was drained into multiple 20 L Cubitainer (flexible containers) and stored in cardboard boxes. This water has since been used as low-nutrients seawater (LNSW) for nutrients measurements. The concentrations in each LNSW container were measured in June 2022, yielding average values of 0.01, 0.003, 1.08, 0.075, and 0.01 μmol L^{-1} for nitrate, nitrite, silicate, phosphate, and ammonia, respectively. The concentrations of nitrate, nitrite, and ammonia were below the detection limit.

(6.4) Standard solutions and calibration curves

Concentrations of nutrients for standard solutions A, B, C, and D are shown in Table 4.2-2. The KANSO Si standard solution was used for the A standard of silicate, which doesn’t require neutralization with hydrochloric acid. The B standard was diluted from the A standard following the recipes shown in Table 4.2-3. To match the salinity and the density of the B standard solution to those of the LNSW, 15.00 g of sodium chloride powder was dissolved in the B standard solution, and then the final volume was adjusted to 500 mL. The C standard solution was prepared in the LNSW following the recipes shown in Table 4.2-4. The actual concentrations of nutrients in each standard solution were calculated based on the solution temperature and the calibrated factors of volumetric laboratory wares. Calibration curves for each run of nitrate, nitrite, silicate, and phosphate were obtained using five levels: C-2, C-3, C-4, C-6, C-7. For ammonia, calibration was achieved using three levels: C-1, C-5, C-7. C-1 was LNSW, C-2, C-3, C-4 and C-6 were the CRM of nutrients in seawater, and C-5 and C-7 were diluted using the B standard solution. The D standard solutions, used to calculate the reduction rate of the Cd coil, were diluted from the A standard solution with pure water (milli-Q). In-house standard solutions were remade according to the “renewal time” intervals listed in Table 4.2-5.

Table 4.2-2 Nominal concentrations of nutrients for A, D, B and C standards (µmol kg^{-1}).

	A	B	D	C-1	C-2	C-3	C-4	C-5	C-6	C-7*
NO_3	22500	670	900	-	CQ	CR	CO	-	CP	42.0
NO_2	21800	26	870	-	CQ	CR	CO	-	CP	1.6
SiO_2	35500	1420		-	CQ	CR	CO	-	CP	86.3
PO_4	6000	60		-	CQ	CR	CO	-	CP	3.7
NH_4	4000	160		LNSW	-	-	-	4.8	-	9.6

Table 4.2-3 B standard recipes. Final volume was 500 mL.

	A Std.
NO_3	15 mL
NO_2*	15 mL
SiO_2	20 mL
PO_4	5 mL
NH_4	20 mL

*NO_2 was D standard solution which was diluted from A standard.

Table 4.2-4 Working calibration standard recipes. Final volume was 500 mL.

C Std.	B Std.
C-5	15 mL
C-7	30 mL

Table 4.2-5 Renewal times of in-house standards.

Standard	Renewal time
A-1 Std. (NO_3)	maximum a month
A-2 Std. (NO_2)	commercial prepared solution
A-3 Std. (SiO_2)	commercial prepared solution
A-4 Std. (PO_4)	maximum a month
A-5 Std. (NH_4)	maximum a month
D-1 Std.	maximum 8 days
D-2 Std.	maximum 8 days
B Std. (mixture of A-1, D-2, A-3, A-4 and A-5 Std.)	maximum 8 days
C Std.	every 24 hours
36 µM NO_3	when C Std. renewed

(diluted D-1 Std. for reduction estimate) 35 µM NO_2 (diluted D-2 Std. for reduction estimate)	when C Std. renewed

(7) Data quality

During this cruise, a total of the 20 runs were conducted to measure samples collected by 38 casts across 38 stations. In total, 501 seawater samples were collected. The samples were collected into two vials and measured independently as replicate measurements.

(7.1) Precision

The highest-concentration standard solution (C-7) was repeatedly determined every 5 to 12 samples to assess the analytical precision of the nutrient analyses during this cruise. Each run, included 8 to 17 C-7 determinations, depending on the run. Analytical precision for each run was calculated from these C-7 results, and overall precision for this cruise were calculated from the combined precision across all runs (Table 4.2-6). The overall median precisions during this cruise were 0.12%, 0.21%, 0.13%, 0.16%, and 0.29% for nitrate, nitrite, silicate, phosphate, and ammonia, respectively. These values are comparable to those obtained during the previous cruises conducted from 2009 to 2023.

Table 4.2-6 Overall precisions based on the replicate analyses (k=1)

	Nitrate CV %	Nitrite CV %	Silicate CV %	Phosphate CV %	Ammonia CV %
Median	0.12	0.21	0.13	0.16	0.29
Mean	0.12	0.20	0.13	0.16	0.28
Maximum	0.16	0.33	0.20	0.20	0.40
Minimum	0.07	0.09	0.02	0.09	0.13
n	20	20	20	20	20

(7.2) Comparability

CRM lots CP was measured during each run to evaluate the comparability across the measurements during this cruise. All measured concentrations were within the uncertainty of certified values for nitrate, nitrite, silicate, and phosphate (Table 4.2-7).

Table 4.2-7 CRM lot CP measurements (μmol kg^{-1}).

	Nitrate	Nitrite	Silicate	Phosphate	Ammonia
Median	24.77	0.32	61.04	1.751	0.96
Mean	24.77	0.32	61.03	1.751	0.95
STDEV	0.06	0.00	0.10	0.008	0.08
n	20	20	20	20	20

(7.3) Carryover

We also summarized the magnitudes of carry over, which refers to sample-to-sample contamination during flow analysis. To evaluate carryover in each run, we measured the C-7 standard solution followed by two consecutive measurements of the LNSW solution. The difference from LNSW-1 to LNSW-2 was used to estimate the carryover (%) using the following equation (1) where [ ] denotes concentrations.

Carryover (%) = ([LNSW-1] – [LNSW-2]) / ([C-8] – [LNSW-2]) * 100 (1)

The carryover (%) are shown in Table 4.2-8. Overall, the results indicated low carryover percentages. These low percentages suggest that there was no significant issue during this cruise.

Table 4.2-8 Carryovers (%)

	Nitrate	Nitrite	Silicate	Phosphate	Ammonia
Median	0.27	0.18	0.27	0.17	1.10
Mean	0.26	0.17	0.26	0.16	1.10
Maximum	0.36	0.40	0.33	0.45	1.29
Minimum	0.20	0.03	0.17	0.04	0.94
n	20	20	20	20	20

(7.4) Uncertainty (Repeatability)

Empirical equations of (2), (3) and (4) were obtained based on 20 measurements of 15 sets of CRMs (Table 4.2-1) to estimate the uncertainty (repeatability) of measurements of nitrate, silicate, and phosphate, respectively (Figs. 4.2-6-8).

Uncertainty of measurement of nitrate (%) = 0.26873 + 0.67809 * (1 / C_{NO3}) (2)

Uncertainty of measurement of silicate (%) = 0.12042 + 3.0735 * (1 / C_{SiO2}) (3)

Uncertainty of measurement of phosphate (%) = 0.10219 + 0.51124 * (1 / C_{PO4}) (4)

where C_{NO3}, C_{SiO2}, and C_{PO4} are nitrate, silicate, and phosphate concentrations of sample (µmol kg^{-1}), respectively.

Empirical equations, eq. (5) and (6) were obtained based on duplicate measurements of the samples to estimate the uncertainty (repeatability) of measurements of nitrite and ammonia (Figs. 4.2-9-10).

Uncertainty of measurement of nitrite (%) =
0.21793 + 0.185 * (1 / C_{NO2}) + 0.000032095 * (1 / C_{NO2}) * (1 / C_{NO2}) (5)

Uncertainty of measurement of ammonia (%) = 1.4959 + 0.68806 * (1 / C_{NH4}) (6)

where C_{NO2} and C_{NH4} are nitrite and ammonia concentrations of sample (µmol kg^{-1}), respectively.

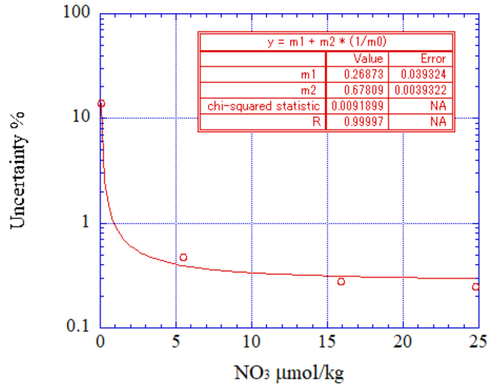

Figure 4.2.6 Uncertainty for NO_3.

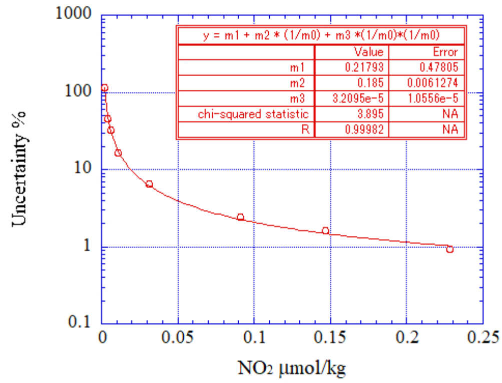

Figure 4.2.7 Uncertainty for NO_2.

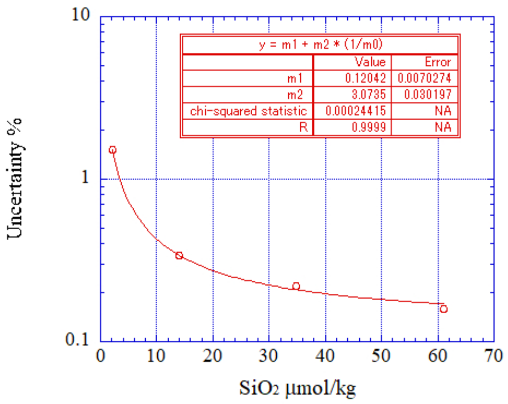

Figure 4.2.8 Uncertainty for SiO_2.

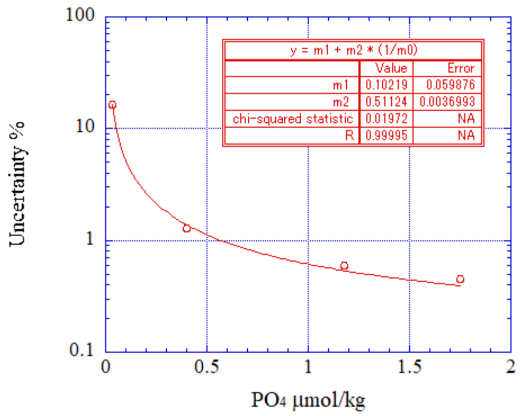

Figure 4.2.9 Uncertainty for PO_4.

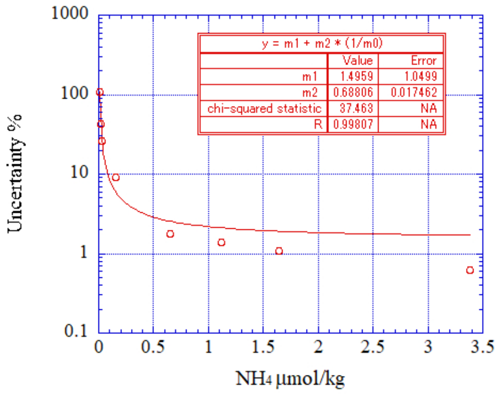

Figure 4.2.10 Uncertainty for NH_4.

(7.5) Detection limit and quantitative determination

The LNSW was measured every 5 to 12 samples to estimate the detection limit of nutrient analyses during this cruise. In each run, the total number of the LNSW determination ranged from 8 to 16, depending on the specific run. The detection limit was calculated based on the LNSW results from all runs using the following equation:

Detection limit = 3 * standard deviation of repeated measurement of LNSW (7)

The estimated detection limits are shown in Table 4.2-9. The quantitative determination of nutrient analyses reflects concentrations with an uncertainty of 33 % as indicated in the empirical equations, eq. (2) to (6). The estimated quantitative determinations are also shown in Table 4.2-9.

Table 4.2-9 Detection limit and quantitative determination.

	Nitrate $\mu mol\ kg^{-1}$	Nitrite $\mu mol\ kg^{-1}$	Silicate $\mu mol\ kg^{-1}$	Phosphate $\mu mol\ kg^{-1}$	Ammonia $\mu mol\ kg^{-1}$
Detection limit	0.01	0.004	0.09	0.006	0.02
Quantitative determination	0.02	0.01	0.09	0.016	0.02

Replicate samples were taken at most of the layers. The summary of average and standard deviation of the difference between each replicate pair of analysis was shown in Table 4.2-10.

Table 4.2-10 Average and standard deviation of the difference between each replicate pair of analysis.

	Nitrate $\mu mol\ kg^{-1}$	Nitrite $\mu mol\ kg^{-1}$	Silicate $\mu mol\ kg^{-1}$	Phosphate $\mu mol\ kg^{-1}$	Ammonia $\mu mol\ kg^{-1}$
Average	0.02	0.003	0.06	0.004	0.02
Standard deviation	0.02	0.002	0.05	0.004	0.02
n	499	501	500	501	500

(8) Problems

During the measurements of samples from stations 31, 33, a shift in the NO_3 base seawater value was observed. Therefore, we calculated the difference before and after the shift and subtracted it from the value after the shift occurred.

(9) List of reagents

List of reagents used in this cruise is shown in Table 4.2-11.

Table 4.2-11 List of reagents used in this cruise

IUPAC name	CAS Number	Formula	Compound Name	Manufacture	Grade
4-Aminobenzenesulfonamide	63-74-1	$C_6H_8N_2O_2S$	Sulfanilamide	FUJIFILM Wako Pure Chemical Corporation	JIS Special Grade
Ammonium chloride	12125-02-9	NH_4Cl	Ammonium Chloride	FUJIFILM Wako Pure Chemical Corporation	JIS Special Grade
Antimony potassium tartrate trihydrate	28300-74-5	$K_2(SbC_4H_2O_6)_2 \cdot 3H_2O$	Bis[(+)-tartrato]diantimonate(III) Dipotassium Trihydrate	FUJIFILM Wako Pure Chemical Corporation	JIS Special Grade
Boric acid	10043-35-3	H_3BO_3	Boric Acid	FUJIFILM Wako Pure Chemical Corporation	JIS Special Grade
Hydrogen chloride	7647-01-0	HCl	Hydrochloric Acid	FUJIFILM Wako Pure Chemical Corporation	JIS Special Grade
Imidazole	288-32-4	$C_3H_4N_2$	Imidazole	FUJIFILM Wako Pure Chemical Corporation	JIS Special Grade
L-Ascorbic acid	50-81-7	$C_6H_8O_6$	L-Ascorbic Acid	FUJIFILM Wako Pure Chemical Corporation	JIS Special Grade
N-(1-Naphthalenyl)-1,2-ethanediamine, dihydrochloride	1465-25-4	$C_{12}H_{16}Cl_2N_2$	N-1-Naphthylethylenediamine Dihydrochloride	FUJIFILM Wako Pure Chemical Corporation	for Nitrogen Oxides Analysis
Oxalic acid	144-62-7	$C_2H_2O_4$	Oxalic Acid	FUJIFILM Wako Pure Chemical Corporation	Wako Special Grade
Phenol	108-95-2	C_6H_6O	Phenol	FUJIFILM Wako Pure Chemical Corporation	JIS Special Grade
Potassium nitrate	7757-79-1	KNO_3	Potassium Nitrate	Merck KGaA	Suprapur®
Potassium dihydrogen phosphate	7778-77-0	KH_2PO_4	Potassium dihydrogen phosphate anhydrous	Merck KGaA	Suprapur®
Sodium chloride	7647-14-5	NaCl	Sodium Chloride	FUJIFILM Wako Pure Chemical Corporation	TraceSure®
Sodium citrate dihydrate	6132-04-3	$Na_3C_6H_5O_7 \cdot 2H_2O$	Trisodium Citrate Dihydrate	FUJIFILM Wako Pure Chemical Corporation	JIS Special Grade
Sodium dodecyl sulfate	151-21-3	$C_{12}H_{25}NaO_4S$	Sodium Dodecyl Sulfate	FUJIFILM Wako Pure Chemical Corporation	for Biochemistry
Sodium hydroxide	1310-73-2	NaOH	Sodium Hydroxide for Nitrogen Compounds Analysis	FUJIFILM Wako Pure Chemical Corporation	for Nitrogen Analysis
Sodium hypochlorite	7681-52-9	NaClO	Sodium Hypochlorite Solution	Kanto Chemical co., Inc.	Extra pure
Sodium molybdate dihydrate	10102-40-6	$Na_2MoO_4 \cdot 2H_2O$	Disodium Molybdate(VI) Dihydrate	FUJIFILM Wako Pure Chemical Corporation	JIS Special Grade
Sodium nitroferricyanide dihydrate	13755-38-9	$Na_2[Fe(CN)_5NO] \cdot 2H_2O$	Sodium Pentacyanonitrosylferrate(III) Dihydrate	FUJIFILM Wako Pure Chemical Corporation	JIS Special Grade
Sulfuric acid	7664-93-9	H_2SO_4	Sulfuric Acid	FUJIFILM Wako Pure Chemical Corporation	JIS Special Grade
tetrasodium;2-[2-[bis(carboxylatomethyl)amino]ethyl-(carboxylatomethyl)amino]acetate;tetrahydrate	13235-36-4	$C_{10}H_{12}N_2Na_4O_8 \cdot 4H_2O$	Ethylenediamine-N,N,N',N'-tetraacetic Acid Tetrasodium Salt Tetrahydrate (4NA)	Dojindo Molecular Technologies, Inc.	-
Synonyms: t-Octylphenoxypolyethoxyethanol 4-(1,1,3,3-Tetramethylbutyl)phenyl-polyethylene glycol Polyethylene glycol tert-octylphenyl ether	9002-93-1	$(C_2H_4O)_nC_{14}H_{22}O$	Triton®X-100	MP Biomedicals, Inc.	-

(10) Data archives

These data obtained in this cruise will be submitted to the Data Management Group of JAMSTEC, and will be opened to the public via "Data Research System for

Whole Cruise Information in JAMSTEC (DARWIN)" in JAMSTEC web site. <http://www.godac.jamstec.go.jp/darwin/e>

(11) References

Becker, S., Aoyama, M., Malcolm E., Woodward, S., Bakker, K., Coverly, S., Mahaffey, C., Tanhua, T., (2019) The precise and accurate determination of dissolved inorganic nutrients in seawater, using Continuous Flow Analysis methods, n: The GO-SHIP Repeat Hydrography Manual: A Collection of Expert Reports and Guidelines. Available online at: http://www.go-ship.org/HydroMan.html. DOI: http://dx.doi.org/10.25607/OBP-555

Grasshoff, K. (1976). Automated chemical analysis (Chapter 13) in Methods of Seawater Analysis. With contribution by Almgreen T., Dawson R., Ehrhardt M., Fonselius S. H., Josefsson B., Koroleff F., Kremling K. Weinheim, New York: Verlag Chemie.

Grasshoff, K., Kremling K., Ehrhardt, M. et al. (1999). Methods of Seawater Analysis. Third, Completely Revised and Extended Edition. WILEY-VCH Verlag GmbH, D-69469 Weinheim (Federal Republic of Germany).

Hydes, D.J., Aoyama, M., Aminot, A., Bakker, K., Becker, S., Coverly, S., Daniel, A., Dickson, A.G., Grosso, O., Kerouel, R., Ooijen, J. van, Sato, K., Tanhua, T., Woodward, E.M.S., Zhang, J.Z., (2010). Determination of Dissolved Nutrients (N, P, Si) in Seawater with High Precision and Inter-Comparability Using Gas-Segmented Continuous Flow Analysers, In: GO-SHIP Repeat Hydrography Manual: A Collection of Expert Reports and Guidelines. IOCCP Report No. 14, ICPO Publication Series No 134.

Kimura (2000). Determination of ammonia in seawater using a vaporization membrane permeability method. 7th auto analyzer Study Group, 39-41.

Murphy, J., and Riley, J.P. (1962). Analytica Chimica Acta 27, 31-36.

4.3. Dissolved Inorganic Carbon
4.3.1. Bottled-water analysis

(1) Personnel

Akihiko Murata	JAMSTEC	Principal Investigator
Yasuhiro Arii	MWJ	Operation Leader
Nagisa Fujiki	MWJ	

(2) Objective

To clarify vertical distributions of total dissolved inorganic carbon (DIC) in water columns.

(3) Parameter

Total dissolved Inorganic Carbon (DIC)

(4) Instruments and Methods

a. Seawater sampling

Seawater samples were collected by 12-liter sampling bottles mounted on the CTD/Carousel Water Sampling System and a bucket at 37 stations. Seawater was sampled in a 250 mL glass bottle (SHOTT DURAN) that was previously soaked in 5 % alkaline detergent solution at least 3 hours and was cleaned by fresh water for 5 times and Milli-Q ultrapure water for 3 times. A sampling silicone rubber tube with PFA tip was connected to the outlet of Niskin bottle for water sampling. The glass bottles were filled from its bottom gently, without rinsing, and were overflowed by about twice the bottle volume. They were sealed using the polyethylene inner lids with care not to leave any bubbles in the bottle. Immediately after the water sampling on the deck, the glass bottles were carried to the laboratory for the addition of saturated solution of mercury (II) chloride ($HgCl_2$). Small volume (3 mL) of the sample (1 % of the bottle volume) was removed from the bottle and 100 µL of $HgCl_2$ was added. Then the samples were sealed by the polyethylene inner lids tightly and stored in a refrigerator at approximately 5 °C. About one hour before the analysis, the samples were taken from refrigerator and put in the water bath kept ~20 °C.

b. Seawater analysis

Measurements of DIC were made with total CO_2 measuring system (Nihon ANS Inc.). The system comprises of seawater dispensing unit, a CO_2 extraction unit, and a coulometer (Model 3000, Nihon ANS Inc.) The seawater dispensing unit has an auto-sampler (10 ports), which dispenses the seawater from a glass bottle to a pipette of nominal 15 mL volume. The pipette was kept at 20.00 °C ± 0.05 °C by a water jacket, in which water circulated through a thermostatic water bath. The CO_2 dissolved in a seawater sample is extracted in a stripping chamber of the CO_2 extraction unit by adding

10 % phosphoric acid solution. The stripping chamber is made approx. 25 cm long and has a fine frit at the bottom. First, a constant volume of acid is added to the stripping chamber from its bottom by pressurizing an acid bottle with nitrogen gas (99.9999 %). Second, a seawater sample kept in a pipette is introduced to the stripping chamber by the same method. The seawater and phosphoric acid are stirred by the nitrogen bubbles through a fine frit at the bottom of the stripping chamber. The stripped CO_2 is carried to the coulometer through two electric dehumidifiers (kept at 2 °C) and a chemical desiccant (magnesium perchlorate) by the nitrogen gas (flow rate of 140 mL min^{-1}). Measurements of system blank (phosphoric acid blank), 1.5 % CO_2 standard gas in a nitrogen base, and seawater samples (6 samples) were programmed to repeat. The values of DIC were set to the certified values of CRM (batch 217) provided by Scripps Institution of Oceanography, Univ. of California.

(5) Observation log

Seawater samples were collected at 37 stations.

(6) Preliminary results

A few replicate samples were taken at most of the stations and difference between each pair of analyses was plotted on a range control chart (Fig. 4.3.1-1). The repeatability was estimated to be provisionally 0.7±0.6 μmol kg^{-1} (n = 58).

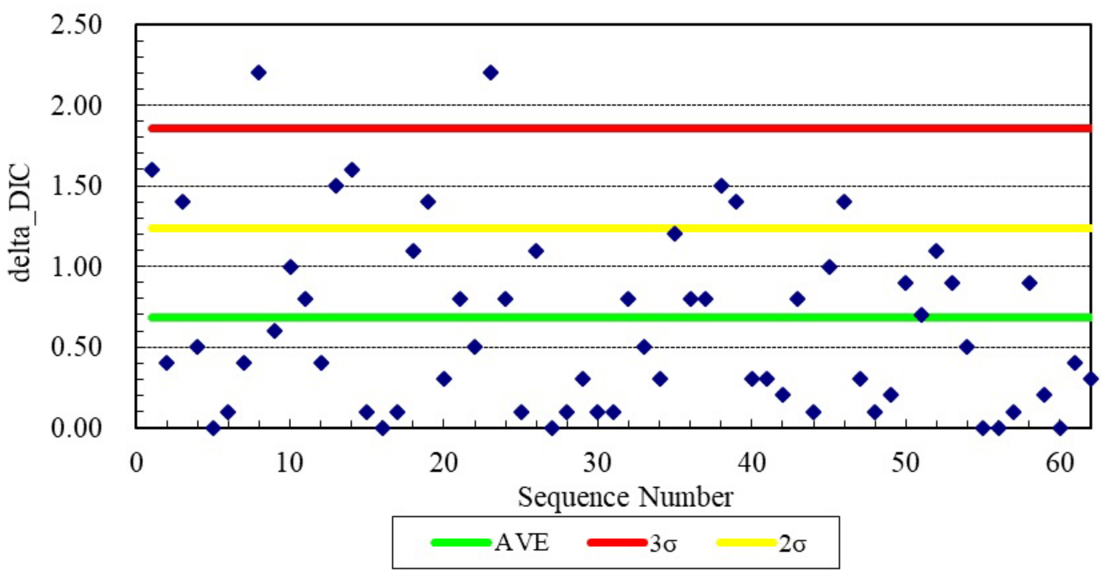

Fig. 4.3.1-1. Range control chart of the absolute differences of replicate measurements of DIC carried out during this cruise. The 2σ and 3σ indicate the upper control limits of standard deviation (σ) × 2 and σ × 3, respectively.

(7) Data archives

These data obtained in this cruise will be submitted to the Data Management Group of JAMSTEC, and will opened to the public via "Data Research System for Whole Cruise Information in JAMSTEC (DARWIN)" in JAMSTEC web site. http://www.godac.jamstec.go.jp/darwin/e.

4.3.2. Underway DIC

(1) Personnel

Akihiko Murata	JAMSTEC	Principal Investigator
Nagisa Fujiki	MWJ	Operation Leader
Yasuhiro Arii	MWJ	

(2) Objective

To elucidate spatial variations of total dissolved inorganic carbon (DIC) concentration in surface seawater.

(3) Parameter

Total Dissolved Inorganic Carbon (DIC)

(4) Instruments and Methods

Surface seawater samples for DIC measurement were continuously collected during this cruise. Surface seawater was taken from an intake placed at the approximately 4.5 m below the sea surface by a pump, and was filled in a 250 mL glass bottle (SCHOTT DURAN) from the bottom, without rinsing, and overflowed for more than 2 times the amount. Before the analysis, the samples were put in the water bath kept about 20°C for one hour. Measurements of DIC were made with total CO_2 measuring system (Nihon ANS Inc.). The system was comprised of seawater dispensing unit, a CO_2 extraction unit, and a coulometer (Model 3000A, Nihon ANS Inc.). The seawater dispensing unit has an auto-sampler (6 ports), which dispenses the seawater from a glass bottle to a pipette of nominal 15 mL volume. The pipette was kept at 25.00°C ± 0.05 °C by a water jacket, in which water circulated through a thermostatic water bath. The CO_2 dissolved in a seawater sample is extracted in a stripping chamber of the CO_2 extraction unit by adding 10 % phosphoric acid solution. The stripping chamber is made approx. 25 cm long and has a fine frit at the bottom. First, the certain amount of acid is taken to the constant volume tube from an acid bottle and transferred to the stripping chamber from its bottom by nitrogen gas (99.9999 %). Second, a seawater sample kept in a pipette is introduced to the stripping chamber by the same method as that for an acid. The seawater and phosphoric acid are mixed by the nitrogen bubbles through a fine frit at the bottom of the stripping chamber. The stripped CO_2 is carried to the coulometer through two electric dehumidifiers (kept at 2 °C) and a chemical desiccant (Magnesium perchlorate) by the nitrogen gas (flow rate of 140 mL min^{-1}). Measurements of approx.1.5 % CO_2 standard gas in a nitrogen base, system blank (phosphoric acid blank), and seawater samples (6 samples) were programmed to repeat. Both CO_2 standard gas and blank signals were used to correct the signal drift results from chemical alternation of coulometer solutions. The coulometer solutions were renewed every about 2 days, and JAMSTEC reference materials (batch Q43) and CRM (batch 217) were measured to correct systematic difference between measurements.

(5) Observation log

The cruise track during underway DIC observation is shown in Figure 4.3.2.

(6) Results

Spatial variations of DIC in surface sweater along the cruise track are shown in Figure 4.3.2.

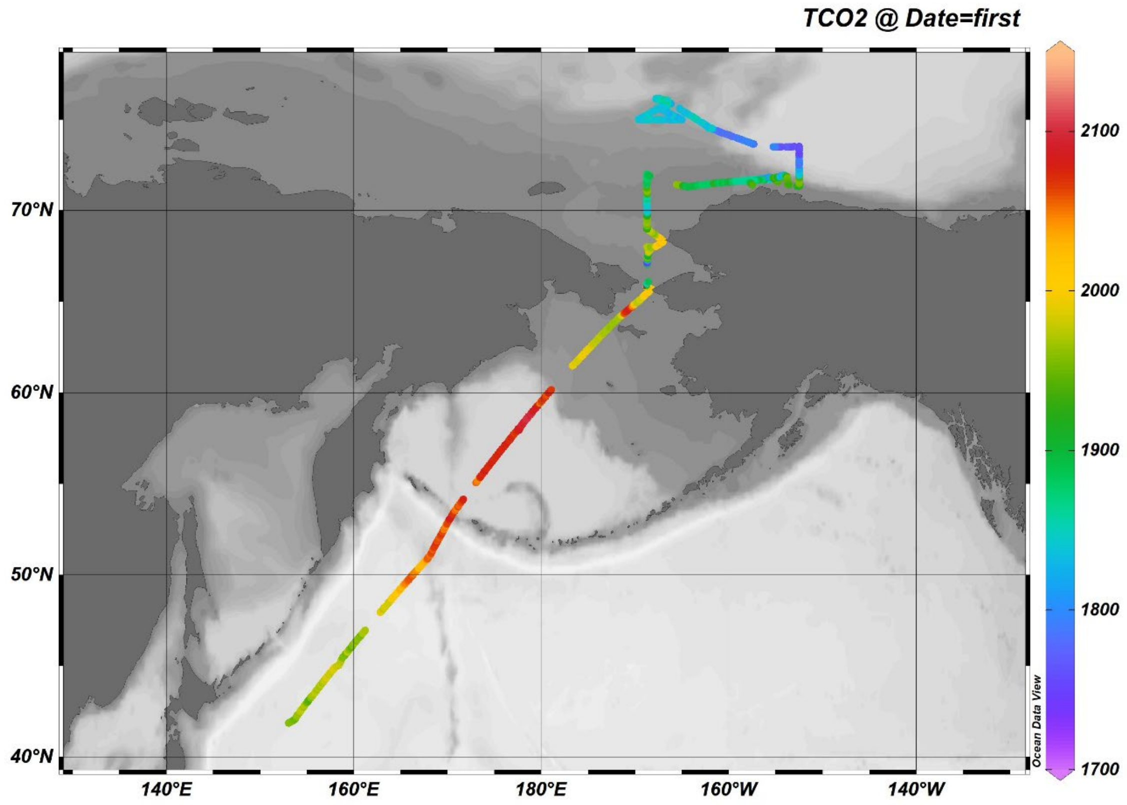

Figure 4.3.2. Distributions of surface seawater DIC along the cruise track.

(7) Date archives

These data obtained in this cruise will be submitted to the Data Management Group (DMG) of JAMSTEC, and will open to the public via "Data Research System for Whole Cruise Information in JAMSTEC (DARWIN)" in JAMSTEC web site. http://www.godac.jamstec.go.jp/darwin/e.

4.4. Total Alkalinity

(1) Personnel

Akihiko Murata	JAMSTEC	Principal Investigator
Nagisa Fujiki	MWJ	Operation Leader
Yasuhiro Arii	MWJ	

(2) Objective

To survey influences of sea ice melting water and river input on carbonate system properties.

(3) Parameters

Total alkalinity (TA)

(4) Instruments and Methods

a. Seawater sampling

Seawater samples were collected by 12 L Niskin bottles mounted on the CTD/Carousel Water Sampling System and a bucket at 37 stations. The seawater from the Niskin bottle was filled into 250 or 100 mL borosilicate glass bottles (SHOTT DURAN) using a sampling silicone rubber tube with PFA tip. The water was filled into the bottle from the bottom smoothly, without rinsing, and overflowed for 2 times bottle volume (20 or 10 seconds). These bottles were pre-washed in advance by soaking in 5 % alkaline detergent for more than 3 hours, and then rinsed 5 times with tap water and 3 times with Milli-Q deionized water. The samples were stored in a refrigerator at approximately 5 °C before the analysis, and were put in the water bath with its temperature of about 25 °C for one hour before analysis.

b. Seawater analysis

TA was measured using a spectrophotometric system (Nihon ANS, Inc.) using a scheme of Yao and Byrne (1998). The calibrated volume of sample seawater was transferred from a sample bottle into the titration cell with its light path length of 4 cm long via dispensing unit. The TA is calculated by measuring two sets of absorbance at three wavelengths (730, 616 and 444) nm with the spectrometer (TM-UV/VIS C10082CAH, HAMAMATSU). One is the absorbance of seawater sample before injecting an acid with indicator solution (bromocresol green sodium) and another is the one after the injection. To mix the acidified-indicator solution with seawater sufficiently, the mixed solution is circulated in a circulation line by a peristaltic pump for 5 minutes. Nitrogen bubble were introduced into the titration cell for degassing CO_2 from the mixed solution sufficiently. The TA is calculated based on the following equation:

$$\mathrm{TA} = (-[\mathrm{H}^+]_\mathrm{T}\mathrm{V}_\mathrm{SA} + \mathrm{M}_\mathrm{A}\mathrm{V}_\mathrm{A})/\mathrm{V}_\mathrm{S},$$

where M_A is the molarity of the acid titrant added to the seawater sample, $[H^+]_T$ is the total excess hydrogen ion concentration in the seawater, and V_S, V_A and V_{SA} are the initial seawater volume, the added acid titrant volume, and the combined seawater plus acid titrant volume, respectively. $[H^+]_T$ is calculated from the measured absorbances based on the following equation (Yao and Byrne, 1998):

$$pH_T = -\log[H^+]_T = 4.2699 + 0.002578(35 - S) + \log((R - 0.00131)/(2.3148 - 0.1299R)) \\ - \log(1 - 0.001005S),$$

where S is the sample salinity, and R is the absorbance ratio calculated as:

$$R = (A_{616} - A_{730})/(A_{444} - A_{730}),$$

where A_i is the absorbance at wavelength i nm.

(5) Observation log

Seawater samples were collected at 37 stations.

(6) Preliminary results

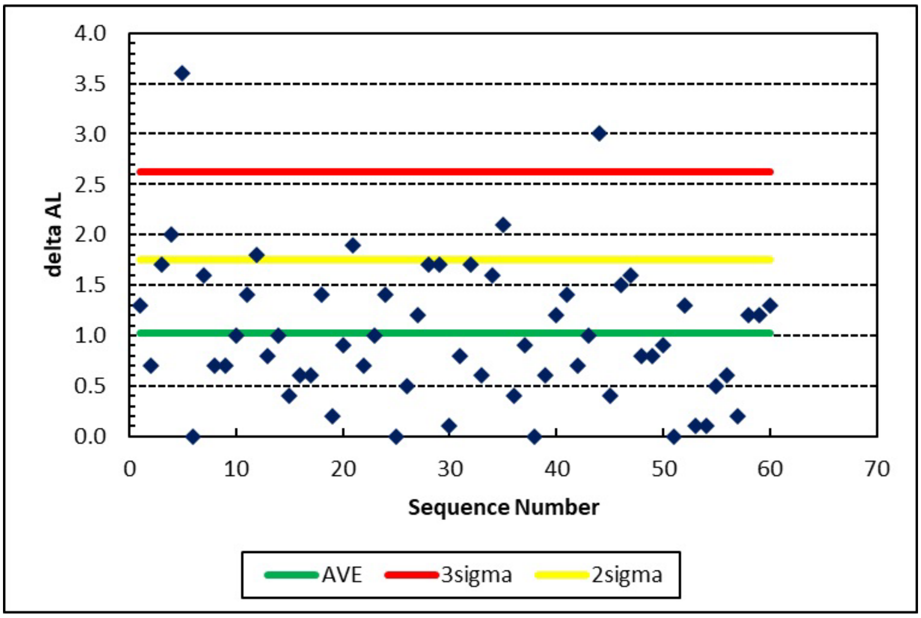

Figure 4.4-1. Range control chart of the absolute differences of replicate measurements of TA. The AVE indicates average. The 2 and 3 sigma indicate the upper control limits of sigma × 2 and that × 3, respectively.

The repeatability of this system was provisionally 0.9 ± 0.8 μmol kg^{-1} (n = 58), which was calculated from replicate samples. A range control chart of TA measurement is illustrated in Figure 4.4-1

We measured certified RM (CRM, batch 217) provided by Prof. Dickson of SIO to monitor data quality of TA during the cruise. We found a shift in the CRM values measured: 2218.1 ± 1.5 μmol kg^{-1} (n = 6) and 2208.3 ± 2.5 μmol kg^{-1} (n = 20). At present, we have no idea why this shift occurred.

(7) Date archives
These data obtained in this cruise will be submitted to the Data Management Group (DMG) of JAMSTEC, and will open to the public via "Data Research System for Whole Cruise Information in JAMSTEC (DARWIN)" in JAMSTEC web site.
http://www.godac.jamstec.go.jp/darwin/e.

4.5. Chlorophyll *a* and phytoplankton community structure

4.5.1. Chlorophyll *a*

(1) Personnel

Amane FUJIWARA	(JAMSTEC): Principal Investigator
Yuri FUKAI	(JAMSTEC)
Shota KUSAKABE	(JAMSTEC)
Ikkan KAMIYAMA	(JAMSTEC)
Kentaro UMEMURA	(JAMSTEC)
Masahiro ORUI	(Marine Works Japan Ltd.; MWJ)
Misato KUWAHARA	(MWJ): Operation leader
Takuya IZUTSU	(MWJ)

(2) Objective

Phytoplankton biomass in the ocean can be roughly expressed by photosynthetic pigment, chlorophyll-a concentration. The ecological function of phytoplankton can also be characterized by the cell size. To investigate the spatial distribution of phytoplankton biomass and size structure in the Arctic Ocean, we routinely measured the horizontal and vertical distribution of bulk and size-fractionated chl-a concentration.

(3) Parameters

Total chlorophyll *a*

Size-fractionated chlorophyll *a*

(4) Instruments and methods

We collected samples for total chlorophyll *a* (chl-*a*) concentration from 6 to 11 depths and size-fractionated chl-*a* from 2 to 5 depths between the surface and 75 m depth including a chl-*a* maximum layer. The chl-*a* maximum layer was determined by a fluorometer (Seapoint Sensors, Inc.) attached to the CTD system. Replicate water samples were taken at chl-*a* maximum depth from the same Niskin bottle in order to assess the precision of chl-*a* measurements.

Seawater samples for total chl-*a* were vacuum-filtrated (< 0.02 MPa) through the 25mm-diameter ADVANTEC GF-75 filter. Seawater samples for size-fractionated chl-*a* were passed through 20 μm pore-size nylon filter (47 mm in diameter), and 2μm pore-size polyester membrane filter (47 mm in diameter), and ADVANTEC GF-75 filter (25 mm in diameter) under gentle vacuum (< 0.02 MPa).

Each filter sample was immediately soaked in 7 ml of N,N-dimethylformamide (DMF, Wako Pure Chemical Industries Ltd.) in a polypropylene tube (Suzuki and Ishimaru, 1990). The tubes were stored at -20 °C under the dark condition to extract chl-*a* at least for 24 hours.

Chl-*a* concentrations were measured by a fluorometer (10-AU, TURNER DESIGNS) following to the method of Welschmeyer (1994). The 10-AU fluorometer was calibrated against a pure chl-*a* (Sigma-Aldrich Co., LLC) prior to the analysis.

(5) Preliminary results

At each station, water samples were taken in replicate for water of chlorophyll *a* maximum layer. Results of replicate samples were shown in table 4.5.1-1.

Table 4.5.1-1. Results of the replicate sample measurements.

	All samples
Number of replicate sample pairs	34
Standard deviation (μg L^{-1})	0.24

Table 4.5.1-2. Number of samples and casts.

	Number of samples	Number of casts
Total chlorophyll *a*	347	37
size-fractionated chlorophyll *a*	243	19

(6) Data archives

These data obtained in this cruise will be submitted to the Data Management Group of JAMSTEC, and will be opened to the public via "Data Research System for Whole Cruise Information in JAMSTEC (DARWIN)" in JAMSTEC web site.
<http://www.godac.jamstec.go.jp/darwin/e>

(7) Reference

Suzuki, R., & Ishimaru T. (1990). An improved method for the determination of phytoplankton chlorophyll using N, N-dimethylformamide. *J. Oceanogr. Soc. Japan*, 46, 190-194.

Welschmeyer, N. A. (1994). Fluorometric analysis of chlorophyll *a* in the presence of chlorophyll *b* and pheopigments. *Limnol. Oceanogr.* 39(8), 1985-1992.

4.5.2. Phytoplankton community structure

(1) Personnel
Amane Fujiwara (JAMSTEC) -Principal Investigator
Yuri Fukai (JAMSTEC)

(2) Objectives
Phytoplankton contain various pigments, such as chlorophylls, photosynthetic carotenoids, and photoprotective carotenoids. Since pigment composition varies among phytoplankton groups (e.g., diatoms, dinoflagellates, and cyanobacteria), these pigments are widely used to characterize phytoplankton community structure. Molecular approaches have also recently been increasingly used to identify phytoplankton at a species level. At the same time, microscopy is still commonly used to reveal their community structure, especially for large phytoplankton such as diatoms.
To investigate the spatial distribution of phytoplankton community structure in the Arctic Ocean, we collected data on the horizontal and vertical distribution of phytoplankton pigment concentrations, DNA, and microscopy.

(3) Parameters
Phytoplankton pigments
Phytoplankton DNA
Diatom cell concentration

(4) Instruments and methods

Seawater samples for phytoplankton pigments were collected using an underway surface water pump system and the Niskin-X bottles on the CTD/R. 1 – 2.5 L of water samples were filtered onto a glass fiber filter (GF-75 φ47 mm, Advantec) and stored in liquid nitrogen. Pigment concentrations will be analyzed on land using high-performance liquid chromatography (HPLC) (Agilent Technologies 1300 series) following the method of van Heukelem and Thomas (2001) after the cruise.

Phytoplankton samplings for DNA and microscopy were conducted using a bucket and Niskin-X bottles attached to the CTD/R. To collect phytoplankton for DNA analysis, 1.08 L seawater was filtered onto a PTFE membrane filter (pore size 0.2 μm, Merck) or a PES membrane filter (pore size 0.22 μm, Merck). Phytoplankton in the samples will be identified on land by DNA metabarcoding. Microscopy samples of 100 mL seawater were fixed using 20% formalin at a final concentration of ca.2%. The fixed samples will be used to reveal diatom communities under a light microscope.

(5) Station list and sampling location

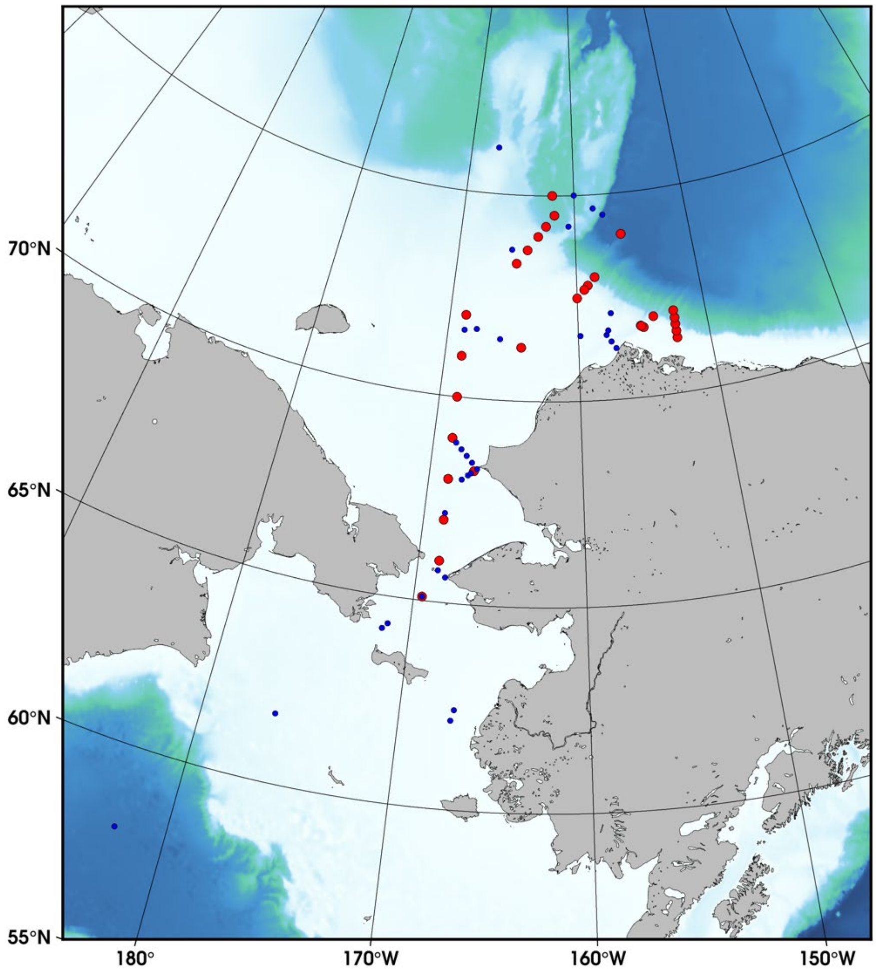

Figure 4.5.2-1. Sampling locations where HPLC phytoplankton pigment samples were collected. Blue and red dots indicate the sites where the samples were collected using an underway surface water pumping system and a CTD rosette sampler, respectively.

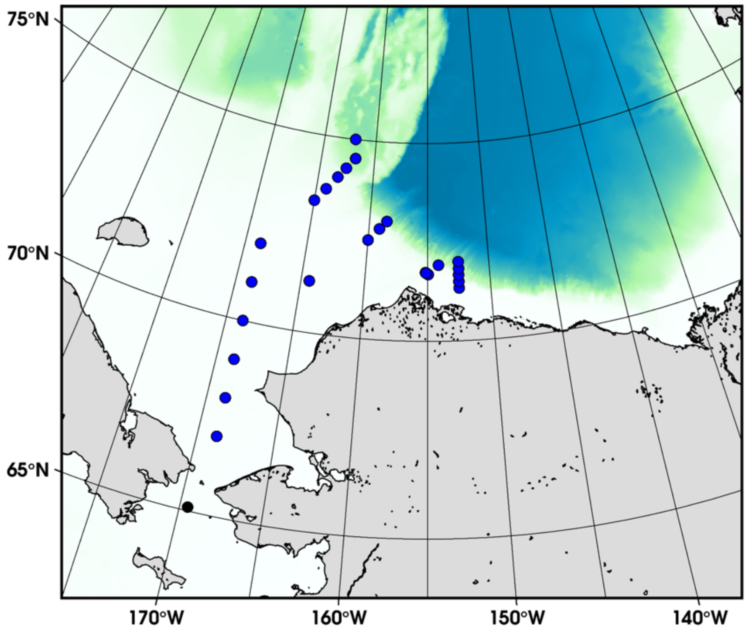

Figure 4.5.2-2. Sampling locations where samples for phytoplankton DNA and microscopy were collected. A black dot indicates the sites where we only took the DNA sample, while blue dots denote sites where we collected both samples.

(6) Data archives

These data obtained in this cruise will be submitted to the Data Management Group of JAMSTEC, and will be opened to the public via "Data Research System for Whole Cruise Information in JAMSTEC (DARWIN)" in JAMSTEC web site.
<http://www.godac.jamstec.go.jp/darwin/e>

(7) Reference cited

Van Heukelem, L, Thomas C. S. 2001. Computer-assisted high-performance liquid chromatography method development with applications to the isolation and analysis of phytoplankton pigments. *J Chromatogr A*, 910, 31–49.

4.6. δ^{18}O

(1) Personnel

Daiki Nomura (Hokkaido University, not on board) – Principal Investigator
Manami Tozawa (Hokkaido University)
Mariko Hatta (JAMSTEC)

(2) Objectives

Meltwater and river water flow into the Arctic Ocean, influencing its physical and biogeochemical environment in ways that vary depending on the origin of the freshwater. To calculate the fraction of seawater, sea ice meltwater, and meteoric water, we have collected 175 water samples from multiple depths to analyze the oxygen isotopic ratio (δ^{18}O). Combined with salinity values, this analysis will allow us to determine the fractions of each fresh water source.

(3) Parameters

●Oxygen isotopic ratio (δ^{18}O)

(4) Instruments and methods

Water samples were collected in 15-mL glass vials with minimal air space, and stored at +4˚C in the dark until analysis.

(5) Station list or Observation log

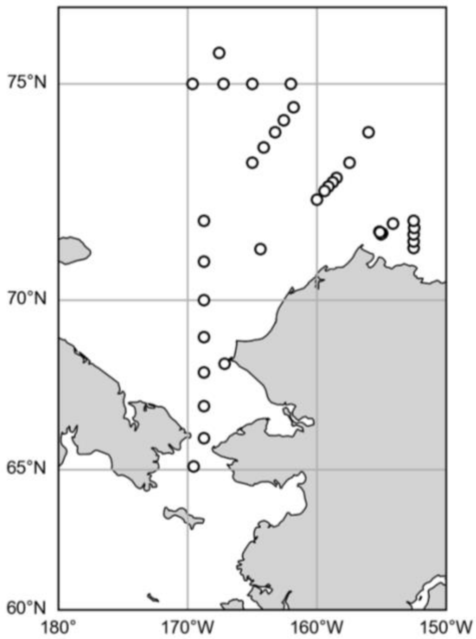

Figure 4.6-1: Map of Stations

Table 4.6-1: Station list

Station	Date	Latitude (˚N)	Longitude (˚E)
2	2024/9/5	65.094	–169.519
3	2024/9/5	66.005	–168.751
4	2024/9/5	67.002	–168.749
5	2024/9/6	68.000	–168.750
6	2024/9/6	68.243	–167.127
7	2024/9/6	68.999	–168.756
8	2024/9/6	70.000	–168.750
9	2024/9/7	71.000	–168.753
10	2024/9/7	72.000	–168.750
11	2024/9/7	71.300	–164.350
12	2024/9/8	71.736	–155.159
13	2024/9/9	71.688	–154.942
14	2024/9/10	71.924	–154.108
15	2024/9/12	71.334	–152.499
16	2024/9/12	71.500	–152.503
17	2024/9/13	71.667	–152.500
18	2024/9/13	71.823	–152.480
19	2024/9/13	72.000	–152.499
22	2024/9/15	74.519	–161.808
23	2024/9/18	75.606	–167.544
24	2024/9/19	75.002	–169.631
25	2024/9/19	75.001	–167.234
26	2024/9/20	75.000	–165.000
27	2024/9/21	73.333	–165.000
28	2024/9/21	73.667	–164.123
31	2024/9/22	74.000	–163.232
33	2024/9/22	74.250	–162.561
34	2024/9/22	74.999	–162.007
35	2024/9/23	74.000	–155.996
37	2024/9/23	73.333	–157.467
38	2024/9/24	73.000	–158.500
39	2024/9/24	72.901	–158.800
40	2024/9/24	72.802	–159.100
41	2024/9/24	72.700	–159.400
43	2024/9/24	72.500	–160.000
45	2024/9/25	71.666	–155.051
46	2024/9/25	71.725	–155.120
47	2024/9/26	68.000	–168.750

(6) Data archives

Data obtained during this cruise will be submitted to the Data Management Group at JAMSTEC, and made publicly available through the "Data Research System for Whole Cruise Information in JAMSTEC (DARWIN)" on the JAMSTEC website.
<http://www.godac.jamstec.go.jp/darwin/e>

4.7. CDOM

(1) Personnel

Daiki Nomura (Hokkaido University, not on board) – Principal Investigator
Manami Tozawa (Hokkaido University)
Amane Fujiwara (JAMSTEC)

(2) Objectives

The Arctic major rivers drain large volumes of freshwater, contributing to the freshening of the ocean surface and supplying terrestrial materials that influence hydrographic circulation and biogeochemical cycles. Additionally, river discharge has increased over the past decades. Concentrations of CDOM (Colored Dissolved Organic Matter) can serve as indicators of mixing of the water masses, as riverine waters are a primary source of high CDOM concentrations. To understand the spread of riverine water and its impact on the oceanic environment, we collected 81 CDOM samples extensively throughout the cruise.

(3) Parameters

- Colored Dissolved Organic Matter (CDOM)

(4) Instruments and methods

Water samples were filtered through 0.2 μm PTFE Membrane filters (Merck Millipore Corporation, 47 mm) and collected into 40-mL glass vials that had been acid-washed and combusted (450°C, 4 h) before samplings. The filtered water samples were stored at +4˚C in the dark until analysis on land. We will measure the absorption coefficient of CDOM (a_{CDOM}) using a long-path spectrophotometer (Ultrapath, World Precision Instruments, Inc.) and Fluorescent DOM (FDOM) using a fluorometer (FluoroMax-4, HORIBA Instruments Inc.).

(5) Station list or Observation log

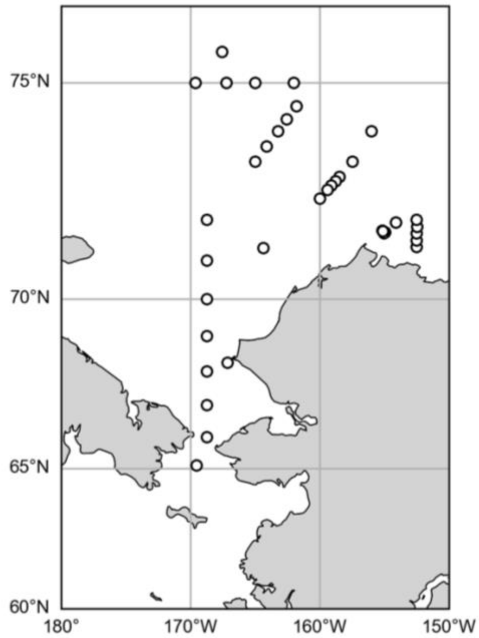

Figure 4.7-1: Map of Stations

Table 4.7-1: Station list

Station	Date	Latitude (˚N)	Longitude (˚E)
2	2024/9/5	65.094	–169.519
3	2024/9/5	66.005	–168.751
4	2024/9/5	67.002	–168.749
5	2024/9/6	68.000	–168.750
6	2024/9/6	68.243	–167.127
7	2024/9/6	68.999	–168.756
8	2024/9/6	70.000	–168.750
9	2024/9/7	71.000	–168.753
10	2024/9/7	72.000	–168.750
11	2024/9/7	71.300	–164.350
12	2024/9/8	71.736	–155.159
13	2024/9/9	71.688	–154.942
14	2024/9/10	71.924	–154.108
15	2024/9/12	71.334	–152.499
16	2024/9/12	71.500	–152.503
17	2024/9/13	71.667	–152.500
18	2024/9/13	71.823	–152.480
19	2024/9/13	72.000	–152.499
22	2024/9/15	74.519	–161.808
23	2024/9/18	75.606	–167.544
24	2024/9/19	75.002	–169.631
25	2024/9/19	75.001	–167.234
26	2024/9/20	75.000	–165.000

27	2024/9/21	73.333	–165.000
28	2024/9/21	73.667	–164.123
31	2024/9/22	74.000	–163.232
33	2024/9/22	74.250	–162.561
34	2024/9/22	74.999	–162.007
35	2024/9/23	74.000	–155.996
37	2024/9/23	73.333	–157.467
38	2024/9/24	73.000	–158.500
39	2024/9/24	72.901	–158.800
40	2024/9/24	72.802	–159.100
41	2024/9/24	72.700	–159.400
43	2024/9/24	72.500	–160.000
45	2024/9/25	71.666	–155.051
46	2024/9/25	71.725	–155.120
47	2024/9/26	68.000	–168.750

(6) Data archives

These data obtained in this cruise will be submitted to the Data Management Group of JAMSTEC, and will be opened to the public via "Data Research System for Whole Cruise Information in JAMSTEC (DARWIN)" in JAMSTEC web site.
<http://www.godac.jamstec.go.jp/darwin/e>

4.8. I-129 and U-236

(1) Personnel

Yuichiro Kumamoto (Principal Investigator)
Japan Agency for Marine-Earth Science and Technology (not on board)

(2) Objectives

In order to investigate the water circulation and ventilation process in the Bering Sea and Arctic Ocean, seawater samples were collected for measurements of iodine-129 (I-129) and uranium-236 (U-236).

(3) Parameters

I-129 and U-236

(4) Instruments and methods

Surface seawater samples were collected from continuous pumped-up water from about 4-m depth at 11 stations. We also collected seawater samples vertically at three stations (Stns. 22, 23, and 38) from the sea surface to near the bottom layer. The seawater samples were collected into a 1-L plastic bottle for I-129 and a 5-L plastic container for U-236 after a two-time rinsing. The total numbers of the seawater samples for I-129 and U-236 are 30 and 30, respectively. I-129 in the seawater sample is extracted using solvent extraction with carrier iodine added. The sample is precipitated as silver iodide and I-129/I-127 is measured using accelerator mass spectrometry at the MALT (Micro Analysis Laboratory, Tandem accelerator), The University of Tokyo. 5mL aliquot of the sample is measured for I-127 by ICP-MS. U-236 in the seawater sample is co-precipitated with Fe hydroxide and purified by UTEVA® resin. The purified sample is co-precipitated as uranium oxide with 1.5 mg Fe hydroxide and U-236/U-238 is also measured using accelerator mass spectrometry at MALT. 5mL aliquot of the sample is measured for U-238 by ICP-MS.

(5) Station list

Table 4.8.-1: Sampling stations.

No.	Station		Date (UTC)	Time (UTC)	Latitude	Longitude
1	P-14 (9)	start	2024/9/6	23:27	70-59.98945N	168-45.03097W
		end	2024/9/6	23:37	70-59.97867N	168-45.11321W
2	P-15 (15)	start	2024/9/12	15:48	71-20.01044N	152-30.05910W

		end	2024/9/12	15:52	71-20.01047N	152-30.08837W
3	P-16 (21)	start	2024/9/13	21:00	72-34.87665N	152-29.99081W
		end	2024/9/13	21:22	72-35.24192N	152-30.15729W
4	P-17 (22)	start	2024/9/15	20:04	74-31.13779N	161-48.43818W
		end	2024/9/15	20:30	74-31.13302N	161-48.31739W
5	P-18 (23)	start	2024/9/18	21:25	75-36.36983N	167-32.60207W
		end	2024/9/18	21:30	75-36.36851N	167-32.53114W
6	P-19 (24)	start	2024/9/19	13:59	75-00.07626N	169-37.86021W
		end	2024/9/19	14:20	75-00.07606N	169-37.93850W
7	P-20 (34)	start	2024/9/22	19:50	74-59.92999N	162-00.34771W
		end	2024/9/22	19:55	74-59.92879N	162-00.33807W
8	P-21 (36)	start	2024/9/23	14:07	73-29.97671N	157-00.12668W
		end	2024/9/23	14:11	73-29.98290N	157-00.14309W
9	P-22 (38)	start	2024/9/24	00:56	72-59.94227N	158-29.85471W
		end	2024/9/24	01:15	72-59.90719N	158-29.84056W
10	P-23	start	2024/9/27	23:44	62-59.07198N	167-25.25556W
		end	2024/9/27	23:55	62-57.52574N	167-24.41451W
11	P-24	start	2024/9/28	23:24	59-39.03205N	168-03.00000W
		end	2024/9/28	23:30	59-38.26348N	168-02.51169W
12	22	end	2024/9/15	19:37	74-31.13N	161-48.46W
13	23	end	2024/9/18	21:22	75-36.38N	167-32.62W
14	38	end	2024/9/24	02:42	72-59.97N	158-29.99W

(6) Data archives

These data obtained in this cruise will be submitted to the Data Management Group of JAMSTEC, and will be opened to the public via “Data Research System for Whole Cruise Information in JAMSTEC (DARWIN)” in JAMSTEC web site.

<http://www.godac.jamstec.go.jp/darwin/e>

4.9. Polycyclic Aromatic Hydrocarbons (PAHs)

(1) Personnel

Yuichiro Kumamoto (Principal Investigator)

Japan Agency for Marine-Earth Science and Technology (not on board)

(2) Objectives

Determination of polycyclic aromatic hydrocarbons (PAHs) concentration in surface seawater in the Arctic Ocean and Bering Sea.

(3) Parameters

PAHs

(4) Instruments and methods

Surface seawater samples were collected from continuous pumped-up water from about 4-m depth at 7 stations. The seawater sample was collected into a 10-L stainless container after two time washing. Just after the water sampling, 300 ml of methanol was added. Particulate and dissolved phases of 10 L seawater sample are separated by filtration through 0.5 μm glass-fiber filters. Dissolved organic compounds, including PAHs, are concentrated using C18 solid-phase extraction disks. Particulate and dissolved PAHs are respectively extracted from the glass-fiber filters using an ultrasonic method and eluted from the C18 disks with dichloromethane. Dimethyl sulfoxide is added to both extracted solutions, the dichloromethane is evaporated to dryness, and the residue of dimethyl sulfoxide is dissolved in acetonitrile. PAHs in the samples were quantified using the HPLC system with a fluorescence detector.

(5) Station list

Table 4.9.-1: Sampling stations.

No.	Station		Date (UTC)	Time (UTC)	Latitude	Longitude
1	P-2	start	2024/8/30	00:32	44-33.35625N	157-22.84841E
		end	2024/8/30	00:43	44-34.90731N	157-25.27673E
2	P-10	start	2024/9/2	18:17	58-02.12250N	177-33.09972E
		end	2024/9/2	18:22	58-02.80614N	177-34.23858E
4	P-16 (21)	start	2024/9/13	21:00	72-34.87665N	152-29.99081W
		end	2024/9/13	21:22	72-35.24192N	152-30.15729W
5	P-17 (22)	start	2024/9/15	20:04	74-31.13779N	161-48.43818W
		end	2024/9/15	20:30	74-31.13302N	161-48.31739W

3	P-19 (24)	start	2024/9/19	13:59	75-00.07626N	169-37.86021W
		end	2024/9/19	14:20	75-00.07606N	169-37.93850W
6	P-22 (38)	start	2024/9/24	00:56	72-59.94227N	158-29.85471W
		end	2024/9/24	01:15	72-59.90719N	158-29.84056W
7	P-24	start	2024/9/28	23:24	59-39.03205N	168-03.00000W
		end	2024/9/28	23:30	59-38.26348N	168-02.51169W

(6) Data archives

These data obtained in this cruise will be submitted to the Data Management Group of JAMSTEC, and will be opened to the public via "Data Research System for Whole Cruise Information in JAMSTEC (DARWIN)" in JAMSTEC web site.

<http://www.godac.jamstec.go.jp/darwin/e>

4.10. Cs-137, Ra-226, and Ra-228

(1) Personnel

Yuichiro Kumamoto (Principal Investigator)
Japan Agency for Marine-Earth Science and Technology (not on board)

(2) Objectives

In order to investigate the water circulation process in the Bering Sea and Arctic Ocean, seawater samples were collected for measurements of radiocesium (Cs-137) and radium isotopes (Ra-226 and Ra-228).

(3) Parameters

Cs-137, Ra-226, and Ra-228

(4) Instruments and methods

Surface seawater samples were collected from continuous pumped-up water from about 4-m depth at 20 stations. The seawater sample was collected into a 20-L plastic container after two time washing. The seawater sample was not filtered and acidified by adding nitric acid. Cs-137 in the seawater sample is concentrated using ammonium phosphomolybdate (AMP) that forms an insoluble compound with cesium. Cs-137 in the compound is measured using Ge detectors. Ra-free barium carrier and SO_4^{2-} are added to the supernatant seawater for Cs-137 to coprecipitate Ra-226 and Ra-228 with $BaSO_4$. After evaporating to dryness, the $BaSO_4$ fractions are compressed to disc as a mixture of $Fe(OH)_3$ and NaCl for gamma-spectrometry.

(5) Station list

Table 4.10.-1: Sampling stations.

No.	Station		Date (UTC)	Time (UTC)	Latitude	Longitude
1	P-1	start	2024/8/29	07:42	42-11.77761N	153-51.56385E
		end	2024/8/29	07:44	42-12.09488N	153-51.94994E
2	P-2	start	2024/8/30	00:32	44-33.35625N	157-22.84841E
		end	2024/8/30	00:43	44-34.90731N	157-25.27673E
3	P-3	start	2024/8/30	08:42	45-40.01676N	159-07.29319E
		end	2024/8/30	08:44	45-40.27555N	159-07.71449E
4	P-4	start	2024/8/30	20:36	47-20.33869N	161-49.43519E
		end	2024/8/30	20:40	47-20.88578N	161-50.36828E
5	P-5	start	2024/8/31	07:43	48-53.39117N	164-22.66950E

		end	2024/8/31	07:46	48-53.76578N	164-23.33346E
6	P-6	start	2024/8/31	20:38	50-36.03970N	167-19.29153E
		end	2024/8/31	20:40	50-36.29025N	167-19.72485E
7	P-7	start	2024/9/1	07:18	52-16.76948N	169-22.04224E
		end	2024/9/1	07:22	52-17.48250N	169-22.80894E
8	P-8	start	2024/9/1	19:40	54-23.73361N	172-01.08607E
		end	2024/9/1	19:42	54-24.05909N	172-01.54638E
9	P-9	start	2024/9/2	06:39	56-09.14024N	174-37.92664E
		end	2024/9/2	06:42	56-09.61328N	174-38.63276E
10	P-10	start	2024/9/2	18:17	58-02.12250N	177-33.09972E
		end	2024/9/2	18:22	58-02.80614N	177-34.23858E
11	P-11	start	2024/9/3	17:38	60-14.87835N	178-47.87451W
		end	2024/9/3	17:42	60-15.55709N	178-46.75912W
12	P-12	start	2024/9/4	04:54	62-02.99896N	175-38.18296W
		end	2024/9/4	04:58	62-03.65686N	175-37.03067W
13	P-13	start	2024/9/4	17:35	64-05.78707N	171-46.07527W
		end	2024/9/4	17:38	64-06.28098N	171-44.97647W
14	P-14 (9)	start	2024/9/6	23:27	70-59.98945N	168-45.03097W
		end	2024/9/6	23:37	70-59.97867N	168-45.11321W
15	P-16 (21)	start	2024/9/13	21:00	72-34.87665N	152-29.99081W
		end	2024/9/13	21:22	72-35.24192N	152-30.15729W
16	P-17 (22)	start	2024/9/15	20:04	74-31.13779N	161-48.43818W
		end	2024/9/15	20:30	74-31.13302N	161-48.31739W
17	P-19 (24)	start	2024/9/19	13:59	75-00.07626N	169-37.86021W
		end	2024/9/19	14:20	75-00.07606N	169-37.93850W
18	P-22 (38)	start	2024/9/24	00:56	72-59.94227N	158-29.85471W
		end	2024/9/24	01:15	72-59.90719N	158-29.84056W
19	P-23	start	2024/9/27	23:44	62-59.07198N	167-25.25556W
		end	2024/9/27	23:55	62-57.52574N	167-24.41451W
20	P-24	start	2024/9/28	23:24	59-39.03205N	168-03.00000W
		end	2024/9/28	23:30	59-38.26348N	168-02.51169W

(6) Data archives

These data obtained in this cruise will be submitted to the Data Management Group of JAMSTEC, and will be opened to the public via "Data Research System for Whole Cruise Information in JAMSTEC (DARWIN)" in JAMSTEC web site.

<http://www.godac.jamstec.go.jp/darwin/e>

4.11. Nitrate isotopes

(1) Personnel

Aymeric P. M. Servettaz	(JAMSTEC, RIGC) - Principal investigator
Akiko Makabe	(JAMSTEC, X-STAR) - not on board
Chisato Yoshikawa	(JAMSTEC, MRU) - not on board

(2) Objectives

Surface water in the Chukchi sea is nitrate depleted during summer. The phytoplankton activity depends on vertical transport of regenerated nitrate or horizontal transport through the Bering strait. Isotopic analysis of Nitrogen in nutrients may inform on the rate of utilization in case of partial surface depletion: due to the preferential uptake of light isotopologues by biology, the remaining nutrients are enriched in ^{15}N and ^{18}O. In the case of Chukchi shelf, complete depletion in the surface usually occurs, so that regeneration in the bottom waters or the sediment plays an important role in the N-cycle (Brown et al., 2015). Regeneration of nitrate (nitrification) in anoxic sediments may be followed by denitrification that partially removes ^{15}N depleted nitrate, while ^{15}N rich ammonia can diffuse back in the oxygenated water and be nitrified or used by phytoplankton (Granger et al., 2011). The coupled nitrification-denitrification occurring in the sediment may have a gradually increasing signature with utilization-regeneration cycles, which we expect to be more pronounced further away from fresh nutrient source in Pacific Water.

(3) Parameters

Nitrate $\delta^{15}N$ and $\delta^{18}O$ isotope ratios.

(4) Instruments and methods

Water samples were collected into single-use 60 mL syringes with attached 0.45 µm pore size filters. Samples were immediately filtered to remove particulate organic matter, and water was collected into two 25 mL centrifuge tubes rinsed with the filtrate, and frozen at -20°C to stop biological activity without chemical additives. Samples will be transported frozen until isotopic analysis on land.

We briefly describe here the planned analytical methods for isotopic measurement (Isaji et al., 2022). Samples for isotopic analysis are prepared by culturing a strain of denitrifying bacteria that lack N_2O-reductase activity into the sampled water, following the method described by Sigman et al. (2001). Nitrate is transformed to N_2O but not assimilated for producing biogenic compounds as the growth medium is saturated with additional ammonium. The produced N_2O is collected, and its nitrogen and oxygen isotopic composition is determined by coupled Gas Chromatography-Mass Spectrometry.

(5) Station list

The main target for this study is the South to North transect on the Chukchi shelf, with aging Pacific Water (Stations 2-13, Figure 4.11-1). Sampling was conducted at regular depths of 10 m, 20 m, 30 m, and shelf bottom, although the upper layers might be depleted in nitrate, some cases of vertical mixing were reported to replete nitrate in upper layers even in summer. Secondary target sampling was performed to follow the Shelf Water inflow into the Canadian Basin (stations 15, 17, 19), potential contribution of sea ice meltwater to surface nutrients (stations 22, 23), and repeat of one shelf location (station 47). Based on nutrient concentrations, we expect to be able to measure isotopes of nitrate in the S-N transect at depth of 30 m or more; waters shallower than this have too low concentrations of nutrients. A total of 17 CTD/R stations were sampled, with 93 water samples taken, of which 16 stations and 53 water samples contain sufficient nitrate for isotopic analysis. In addition, 38 ammonium-rich samples may be considered for exploration of ammonium isotopic analysis, although the method requires development.

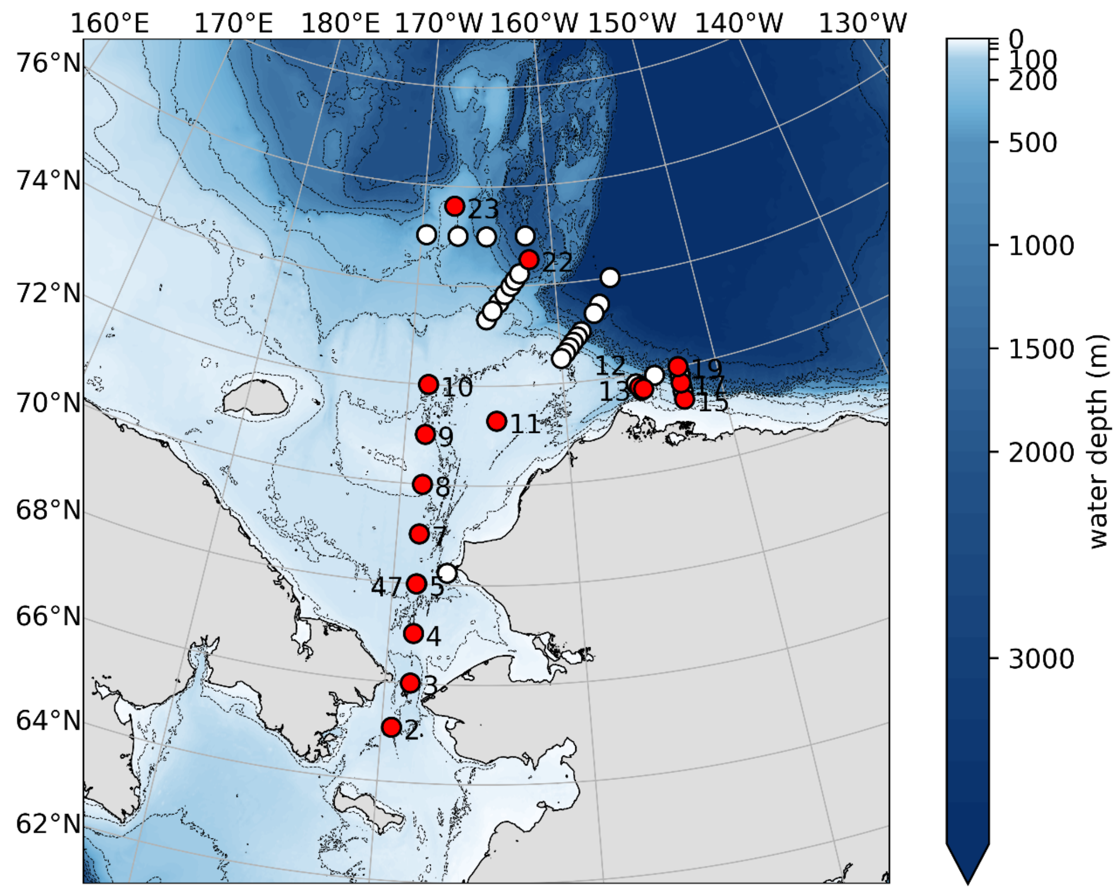

Figure 4.11-1. Location of CTD/R stations sampled for nitrate isotope analysis (red dots with station number). For reference, CTD stations that have not been sampled for nitrate isotopic analysis are indicated with white dots. Blue color contours indicate water depth, emerged land is colored in light grey.

(6) Data archives

The data obtained in this cruise will be submitted to the Data Management Group of JAMSTEC, and will be opened to the public via “Data Research System for Whole Cruise Information in JAMSTEC (DARWIN)” in JAMSTEC web site.
<http://www.godac.jamstec.go.jp/darwin/e>

(7) References

Brown, Z. W., Casciotti, K. L., Pickart, R. S., Swift, J. H., and Arrigo, K. R.: Aspects of the marine nitrogen cycle of the Chukchi Sea shelf and Canada Basin, Deep Sea Research Part II: Topical Studies in Oceanography, 118, 73–87, https://doi.org/10.1016/j.dsr2.2015.02.009, 2015.

Granger, J., Prokopenko, M. G., Sigman, D. M., Mordy, C. W., Morse, Z. M., Morales, L. V., Sambrotto, R. N., and Plessen, B.: Coupled nitrification-denitrification in sediment of the eastern Bering Sea shelf leads to 15N enrichment of fixed N in shelf waters, Journal of Geophysical Research: Oceans, 116, https://doi.org/10.1029/2010JC006751, 2011.

Isaji, Y., Yoshikawa, C., Ogawa, N. O., Matsumoto, K., Makabe, A., Toyoda, S., Ishikawa, N. F., Ogawa, H., Saito, H., Honda, M. C., and Ohkouchi, N.: Nitrogen Sources for Phytoplankton in the Eastern Indian Ocean Determined From $\delta^{15}N$ of Chlorophyll a and Divinylchlorophyll a, Geochem Geophys Geosyst, 23, https://doi.org/10.1029/2021GC010057, 2022.

Sigman, D. M., Casciotti, K. L., Andreani, M., Barford, C., Galanter, M., and Böhlke, J. K.: A Bacterial Method for the Nitrogen Isotopic Analysis of Nitrate in Seawater and Freshwater, Anal. Chem., 73, 4145–4153, https://doi.org/10.1021/ac010088e, 2001.

4.12. Beryllium

(1) Personnel

Yusuke Suganuma, National Institute of Polar Research
Masanobu Yamamoto, Hokakido University
Shinya Iwasaki, Hokkaido University
Kenta Suzuki, Chiba Institute of Technology
Masanori Arai, Hokkaido University

(2) Objectives

Beryllium isotope ratio ($^{10}Be/^{9}Be$) is a strong tool identifying sediment provenance. They are used for sediments retrieved during the MR22-06C cruise and will be used for sediments retrieved during the MR24-06C. However, the spatial distribution of beryllium isotopes are still unclear in the western Arctic Ocean because of lack of previous studies' results. Thus, we sampled water samples in the Chukchi and Bering Seas at different depths corresponding to water masses.

(3) Parameters

Beryllium isotope concentrations

(4) Instruments and methods

The water was sampled basically using a Niskin sampler, except for 6 m deep samples which was sampled using a vessel pump.

(5) Station list

The sampling dates and locations are summarized in Table 4.12-1.

Table 4.12-1. Sampling dates and locations

Site name	Year	Month	Day	Time (UTC)	Latitude (degree N)	Longitude (degree W)	Sample depth (m)	Volume	Water mass
St. 02	2024	09	05	0:13	65.0938	169.5183	10	20	PSW
St. 02	2024	09	05	0:13	65.0938	169.5183	46	20	PWW
St. 06	2024	09	06	4:30	68.2432	167.1294	5	20	PSW
St. 14	2024	09	10	16:49	71.9244	154.1084	50	20	PSW
St. 14	2024	09	10	16:49	71.9244	154.1084	125	20	PWW
St. 14	2024	09	10	16:49	71.9244	154.1084	250	20	Atlantic water
St. 18	2024	09	13	5:43	71.8231	152.4802	20	20	PSW
St. 18	2024	09	13	5:43	71.8231	152.4802	150	20	PWW
St. 18	2024	09	13	5:43	71.8231	152.4802	600	20	Atlantic water
St 23	2024	09	18	21:27	75.6061	167.5427	75	20	PWW
St. 26	2024	09	20	0:11	75.0000	165.0000	100	20	PWW
St. 26	2024	09	20	0:11	75.0000	165.0000	300	20	Atlantic water
St. 34	2024	09	22	18:00	74.9983	162.0056	51	20	PSW
Bering Sea#1	2024	09	27	16:10	64.5848	168.2050	488	20	PSW (Yukon) 27.0 psu
Bering Sea#2	2024	9	28	0:49	62.8317	167.3476	6	20	PSW (Yukon) 27.0 psu
Bering Sea#3	2024	9	28	1:34	62.7255	167.2989	6	20	PSW (Yukon) 25.9 psu
Bering Sea#4	2024	9	28	16:03	60.6521	168.1623	6	20	PSW (Yukon) 31.5 psu

(7) Data archives

These data obtained in this cruise will be submitted to the Data Management Group of JAMSTEC, and will be opened to the public via "Data Research System for Whole Cruise Information in JAMSTEC (DARWIN)" in JAMSTEC web site.
<http://www.godac.jamstec.go.jp/darwin/e>

4.13. Trace Metals

(1) Responsible personnel

Mariko Hatta JAMSTEC

(2) Purpose, background

The three purposes involved in this project related to this shipboard activity and analysis of seawater samples, specifically focusing on aluminum concentration in the Arctic Ocean. Here's a breakdown of each purpose:

1. Establish the shipboard Aluminum system using a programmable flow injection system and identify potential trouble and establish the troubleshooting protocol:

- Purpose: The primary objective here is to set up a shipboard system for monitoring aluminum concentrations in the Arctic Ocean, which is known for its complexity and the challenges it poses for instrumentation. The goal is to create an analytical system that is user-friendly and suitable for shipboard use, eliminating the need for labor-intensive and complicated processes. This system should also avoid the pre-concentration step, which can be challenging in oceanographic conditions due to the low level of the concentrations (~nM). Additionally, it aims to anticipate potential technical issues and establish troubleshooting procedures to ensure the reliability of data collection. The simplified system using a programmable flow injection system can streamline the analysis of aluminum concentrations in seawater, making it more accessible and efficient for research purposes in the challenging Arctic environment. It addresses the need for a more practical and user-friendly approach to studying aluminum concentrations in this unique and sensitive ecosystem.
- Background: Aluminum is an important element in oceanography studies as it can serve as a tracer for various ocean processes. In contrast of the most of the ocean, the value of the Aluminum concentrations were higher and different profiles in the Arctic, and it is still unknown why. Thus, the specific objective is to monitor aluminum concentrations in the Arctic Ocean and to understand how to control its distribution in this region and also understand the geochemical cycles using the element. However, historical instrumentation on board is labor-intensive and complicated to handle at sea, and shore-based determination by

ICPMS also requires special instrumentation together with the significant background value issue. Thus, this project, the newly development methodology using programmable flow injection technique is adapted as a shipboard analytical platform to determine the Aluminum at sea. Last year it was a first time to deploy the system to determine some samples and this year the modified methodology to enhanced the sensitivity and also further testing potential improvement of the chemical assay. Since the newly introduced analytical system on board is still under developing phase, and thus shore-based determination also requires to evaluate the capability of this methodology.

2. Collect seawater samples via Niskin-X bottles attached with a Kevlar cable and with a regular rosette system, to identify any specific contamination:

- Purpose: This purpose involves the collection of seawater samples using specialized Niskin-X bottles attached with Kevlar cables, as well as a regular rosette system. The goal is to examine these samples for any potential contamination from the sampling units.
- Background: Collecting "trace-metal clean" seawater samples is a fundamental but critical activity in the trace metal chemistry in the ocean. The use of Niskin-X bottles and Kevlar cables ensures that samples can be collected at specific depths without contamination. The regular rosette system has potential contamination from its metal cable or settings but likely collects samples from various depths more efficiently. The objective here is to ensure the integrity of the collected samples and assess whether any contamination may affect the analysis of aluminum concentrations from the regular rosette sampling system. Collect seawater samples via Niskin-X bottles attached with a Kevlar cable and with a regular rosette system, to identify any specific contamination.

3. Characterize the water masses with dissolved Aluminum concentration and expand the database in the Arctic Ocean:

- Purpose: This purpose focuses on characterizing different water masses in the Arctic Ocean by analyzing their dissolved aluminum concentrations. Additionally, there's a goal to contribute to and expand the existing database of aluminum concentration data.

- Background: The Arctic Ocean's water masses can vary in their chemical composition, and dissolved aluminum concentration is one parameter used to characterize these variations. Expanding the database of aluminum concentration data in this region contributes to a better understanding of the Arctic Ocean's dynamics and can aid in research related to ocean circulation, biogeochemistry, and environmental changes.

In summary, these purposes represent a comprehensive effort to establish an analytical system, collect seawater samples with minimal contamination, and expand the data base, and then contribute to the understanding of the Arctic Ocean's water masses through the analysis of dissolved aluminum concentrations. These activities are essential for oceanography research and environmental monitoring in the Arctic region.

(3) Activities (observation, sampling, development)

Seawater samples were collected from the following stations, shown in the map (Figure 4.13-1):

Regular rosette system: Stations 2, 3, 4, 5, 6, 7, 8, 9, 10, 11, 12 (BCC), 13 (BCE), 14 (BC2-2), 15, 16, 17, 18, 19, 22 (NAP), 23, 24, 25, 26, 27, 28, 31, 33, 34, 35, 36, 37, 38, 40, 41, 43, 46, Total 36 stations.

Clean-sampling system: Stations 18, 21 (XCTD32), 34, 38, total 4 stations.

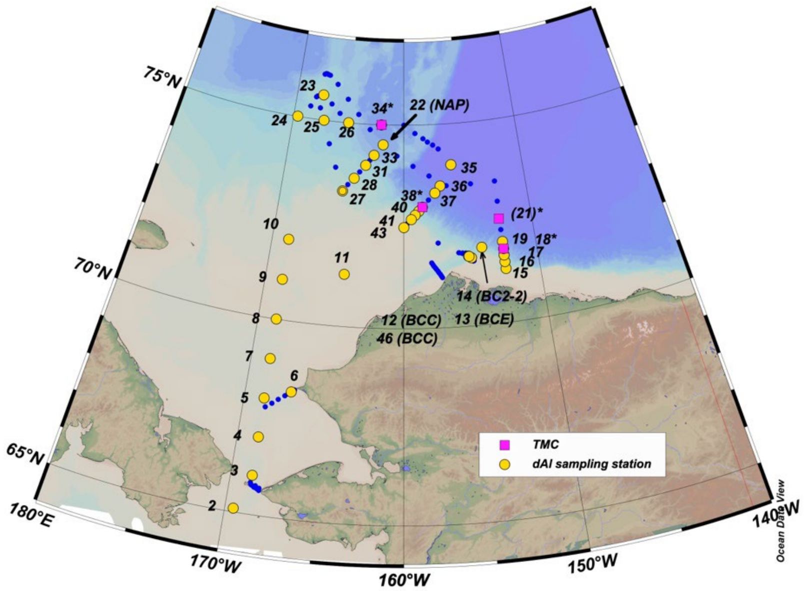

Figure 4.13-1. Sampling location during MR24-06C. Blue dots are all of the X-CTD stations, and yellow circles are the stations to collect dissolved Aluminum samples.

Pink squares are the station to collect samples using trace metal sampling system.

Targeting Parameters

- Conductivity, Temperature, Depth, Turbidity, Chlorophyll, DO from a portable RINKO-Profiler
- Depth from a portable depth sensor
- Salinity
- Nutrients (NH_4, NO_3, NO_2, PO_4, SiO_2)
- Dissolved trace metals (Fe, Al etc.)

The ranges and accuracies of parameters measured by the RINKO-Profiler (ASTD152, S/N:0659) are as follows:

Parameter	Range	Accuracy
Conductivity	0.5 ~ 70 [mS/cm]	+/- 0.01 [mS/cm]
Temperature	-3 ~ 45 [deg-C]	+/- 0.01 [deg-C]
Depth	0 ~ 600 [m]	+/- 0.3 [%] FS
Turbidity	0 ~ 1000 [FTU]	+/- 0.3 [FTU] or +/- 2 [%]
Chlorophyll	0 ~ 400 [ppb]	+/- 1 [%] FS
DO	0 ~ 200 [%]	+/- 2 [%] FS

The calibration data sheet (Date: 2020-07-10):

Parameter.	Actual.	Measured.	Deff.	Accuracy
Temp.[deg-C]	12.655	12.654.	-0.001	+/- 0.008 [deg-C]
Cond. [ms/cm]	40.607	40.607	0.000	+/- 0.008 [mS/cm]
TURB. [FTU]	172.68	172.61	-0.07	+/- 3.11 [FTU]
Chl. [ppb].	75.22.	77.22.	2.00	+/- 4.00 [ppb]
Depth [MPa].	4.500=447.68 (m)	447.67	-0.01	+/- 2.50 [m]
DO [%].	99.04	98.92.	-0.12.	+/- 1.00 [%]

The collected seawater samples were subjected to acidification using 500 µL of 20% trace metal clean hydrochloric acid (6M HCl) spiked into a 100 mL sample. Subsequently, the determination of dissolved aluminum content was carried out using the newly established protocol, employing the programmable flow injection technique in conjunction with a PMT detector.

(4) Methods, instruments

(4.1) Trace metal clean sampling system

The sampling process was executed with the use of individual Niskin-X bottles directly attached to a Kevlar cable. To ensure secure attachment, vinyl tape was wrapped around the Kevlar cable, and each Niskin sampling bottle was affixed using stainless pins designed to fit the cable. This meticulous attachment method was employed to minimize any potential damage to the Kevlar cable during the mounting of Niskin bottles.

At the lowermost part of the cable, a weight system consisting of two sets of 20 kg weights, combined by a rope, was attached, along with a portable RINKO profiler, using a shackle. These weights served the crucial purpose of providing negative buoyancy for the Kevlar line. To mitigate the risk of equipment-induced contamination, the deepest Niskin bottle was positioned at least 1 meter away from the profiler and weights.

The shallower sampling depths were located at points exceeding 20 meters. The standard approach of manually suspending individual Teflon-coated Niskin bottles on the Kevlar cable was employed. This time-tested method, in use for over three decades (as outlined by Bruland et al., 1979), proved effective.

Each Niskin bottle was equipped with an internally recording depth sensor (JFA Advantech) to accurately capture the sampling depth. The techniques and data used for verifying depth should be comprehensively documented in the cruise metadata.

The cable was lowered and rolled up at a controlled speed of less than 0.5 meters per second during the sampling process. Samples were collected at specific locations as follow:

Station	Target Depth (m)	Sample	RINKO
18	20,50,100,300,400	Y	Y
21	20,50,100,300,400	Y	Y
34	20,50,100,300,400	Y	Y
38	20,50,100,300,400	Y	Y

(4.2) Niskin-X bottle

In this cruise, the Niskin-X bottles were meticulously prepared to maintain the integrity of the samples. Here's a step-by-step summary of the preparation and handling process:

1. Before the cruise commenced, the Niskin-X bottles were coated with Teflon, and all the O-rings were replaced with Viton ones that had been pre-acid washed. No acid made contact with the external surfaces of the bottles, especially the nylon components.
2. At the start of this cruise, each bottle was cleaned according to the GEOTRACES cookbook protocol, ensuring thorough decontamination. The cleaning process involved the following steps:
   a. Each bottle was filled with a 5% detergent solution and left for one day.
   b. Bottles were rinsed ten times with deionized ultra-high purity water (Milli-Q water) until there were no traces of detergent.
   c. Bottles were filled with 0.1M HCl (analytical grade) for two days and then emptied through the spigot to rinse.
   d. Bottles were rinsed five times with deionized ultra-high purity water (Milli-Q water).
   e. Bottles were filled with ultra-high purity water (Milli-Q water) for two days.
   f. After discarding the Milli-Q water, bottles were filled with ultra-high purity water (Milli-Q water) until ready for use.
3. Following the cleaning process, the Niskin bottles were transferred to a clean booth (located in WET2 lab), where they were prepared for sampling. Each bottle was covered with big plastic bags, and a Teflon-coated messenger was added when required. These preparations were completed in a WET 2 lab.
4. The Niskin bottles, equipped with depth sensors (JFA Advantech), were arranged inside the clean sampling booth. The plastic bags covering the bottles were removed right before attaching them to the Kevlar cable.
5. During the deployment, two different sizes of Niskin bottles were used based on the specific cast requirements.
6. Once the Kevlar cable reached the target depth, a Teflon-coated messenger was released, and a brief waiting period of approximately 1 minute (or 3 mins, depending on the depth) allowed the last bottle to be tripped.
7. After completing the cast, each Niskin bottle was transferred to the clean booth for the sampling process. A custom-built Niskin bottle cart (an updated version) was used to carefully transport the sampling bottles, which were then hung on

the sampling rack located in a clean sampling booth. This process was facilitated by personnel, typically a helper, who received the bottles through a door in the WET2 lab.

8. The sampling rack itself was specifically constructed for this activity, ensuring secure handling and storage of the Niskin bottles during the entire sampling operation. This meticulous approach in bottle preparation and handling was crucial for maintaining the integrity of the collected samples and ensuring the reliability of the data obtained during the cruise.

(4.3) Sub-sampling in the clean booth

The following samples were collected within a HEPA filtered temporal clean booth.

Parameter	Filtered[y/n]	Analysis on the board[y/n]	Stored samples[y/n]
Salinity	n	y	n
Nutrients	y	y	n
Dissolved Al	y	y	n
Dissolved Fe	y	n	y

The handling and preparation of samples for various analyses, including salinity, nutrients, and dissolved metals (Aluminum and Iron) involved several meticulous steps:

Salinity/nutrient Samples:

- Salinity samples were transferred directly from the Niskin bottles to individual subsampling bottles.
- Nutrient samples were filtered through 0.2 µm Acropak filters directly from the Niskin bottles to individual subsampling bottles.

Dissolved Aluminum and Iron Samples:

- Samples dissolved metal analysis, including Aluminum, were filtered through 0.2 µm Acropak filters.
- Dissolved Aluminum samples were directly collected in acid-clean PMP (perfluoropolymer) bottles. Prior to the cruise, these bottles were pre-cleaned with 1M HCl.
- Dissolved Iron samples were stored in pre-cleaned 100 mL PFA (perfluoroalkoxy) bottles. These bottles were cleaned using the GEOTRACES

cookbook protocols in a shore-based laboratory.

The cleaning process for both types of bottles was as follows:

1. Bottles were soaked for one day in an alkaline detergent.
2. Rinsed ten times with ultra-high purity water (Milli-Q water) until no traces of detergent remained.
3. Soaked in a 6 M reagent-grade HCl bath for more than one day.
4. Rinsed five times with ultra-high purity water (Milli-Q water).
5. Filled with 1M nitric acid (analytical grade) and heated to 80°C for 5 hours in a heated oven. Each bottle was packed with a plastic bag containing Milli-Q water in case of any spills.
6. Rinsed five times with ultra-high purity water (Milli-Q water) inside an ISO Class-5 laminar flow hood.
7. Filled the bottles with ultra-high purity water (Milli-Q water) and heated them at 80°C for 5 hours in a heated oven. Each bottle was again packed with a plastic bag containing Milli-Q water as a precaution.
8. Rinsed five times with ultra-high purity water (Milli-Q water) inside an ISO Class-5 laminar flow hood.
9. The cleaned bottles were packed in sets of six within double bags until they were ready for use.

These rigorous cleaning and preparation procedures were essential to ensure the integrity of the collected samples and to prevent any contamination during subsequent analysis. The specific steps were designed to meet the high purity standards required for accurate dissolved metal measurements in the samples.

(4.4) Shipboard dissolved Al measurement

(4.4.1) Instrumentation

The instrument, miniSIA-2 (Global FIA, Fox Island, WA, USA), comprises two high precision, synchronously refilling milliGAT pumps, two thermostated holding coils, a 6-port LOV (model COV-MANI-6, constructed from polymethyl methacrylate, Perspex®) furnished with a module for an fluoroecence flow cell (Figure 4.13-2). All tubing connections, downstream from the milliGAT pumps including the holding coils (volume 1000 µL), were made with 0.8 mm I.D. polytetrafluoroethylene (PTFE). The holding coils were thermostated at 50C for all aluminium analysis. The tubing between the carrier stream reservoirs and the milliGAT pump was made from 1.6 mm I.D. PTFE tubing to minimize degassing under reduced pressure at higher aspiration flow rates. Photon counter for fluorescence measurement with filter holder mounted for easy access (Global FIA, Fox Island, WA, USA) with a high intensity LED with filter holder mounted encased in 0.8 mm I.D. black tubing. The end of each fiber exposed to the liquid was cemented with epoxy, cut square, and polished. All assay steps were computer-controlled using commercially available software (FloZF, GlobalFIA, Fox island, WA, USA). The outlet of the flow cell was fitted with a 40-psi flow restrictor (GlobalFIA, Fox Island, WA, USA), which, by elevating the pressure within the flow path, efficiently prevented the formation of microbubbles from spontaneous outgassing.

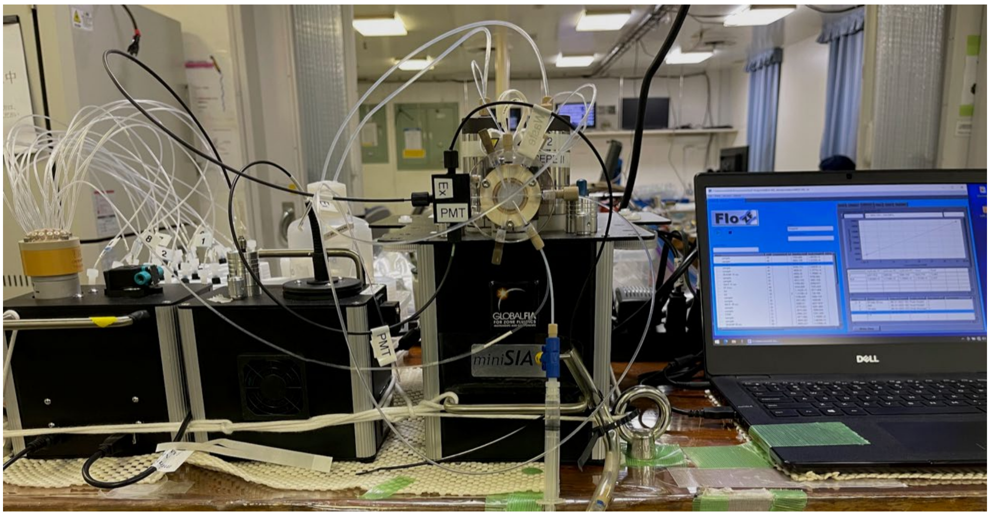

Figure 4.13-2. Shipboard analytical system for dissolved Aluminium determination using the programmable flow injection technique (photo from MR23-06C).

(4.4.2) Analytical methodology

Methodology (pFI-Al) using Programmable Flow Injection Technique:

1. Carrier Solution:

The carrier solution used in the analysis is MilliQ water, which is known for its high purity and suitability for analytical purposes.

2. Stock Aluminum Standard Solution:

A stock Aluminum standard solution with a concentration of 100.1 mg/L was purchased. This stock solution was then diluted with acidified MilliQ water (pH 1) to create a primary stock solution with a concentration of 3.7 μM.

3. Working Standards:
Working standards with different concentrations were prepared using the primary stock solution and filtered seawater solution or with MilliQ water. The working standards created include:
0 nM (control or blank), 3.7nM, 11.08 nM, 22.09 nM, 43.92nM, 72.62nM.

4. Reaction Reagent:
Dissolve 0.05g of Lumogalion in 30 mL of MilliQ water to create Lumogalion stock solution.
Combine 1 mL of the Lumogalion solution with 100 mL of a 2M ammonium acetate buffer solution at a pH of 6.

5. Brij Solution:
The Brij solution was stored in a 40°C oven to maintain a liquid form.
To create the 5% Brij solution, dissolve 17.5 mL of Brij solution and scale it up to a total volume of 200 mL with MilliQ water.

(5) Results, Future Plans, Lists (samples, observation equipment, deployment & recovery), Local field map (dive tracks, sampling points, survey lines), etc

Results:

- During the cruise, a total of 476 seawater samples were collected and analyzed using the developed method.
- The detection limit of this method was approximately 1-2 nM, indicating its sensitivity to low concentrations of Aluminum in seawater.
- The excellent agreement of the values obtained from the regular rosette system and from the trace metal cast at Station 18 indicated that there are not significant contaminations on dissolved Al values based on the different sampling technique (Figure 4.13-3).
- Preliminary vertical profiles of dissolved Aluminum (dAl) were generated, and a subset of these profiles is shown in Figure 4.13-4.
- The dAl values increased with depth, and a significant dAl difference at the deep waters were observed in the regions, suggesting a potential input into the deep waters.
- Subsurface waters exhibited lower dAl values and were characterized as

"winter water" based on Danielson et al.'s classification (2020).

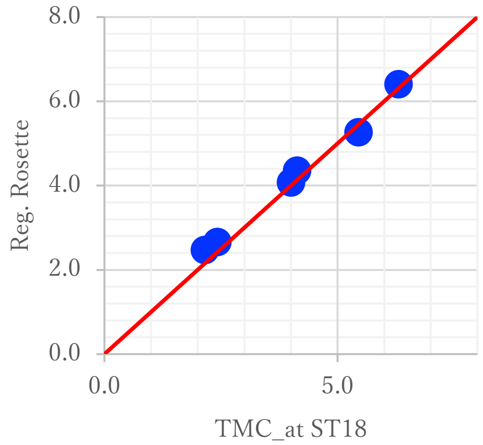

Figure 4.13-3. The comparison between two different sampling techinique. X-axis is by X-Niskin bottles dirfreretly attached on Kevlar cable. Y-axis is by X-Niskin attached on a regular rosette system.

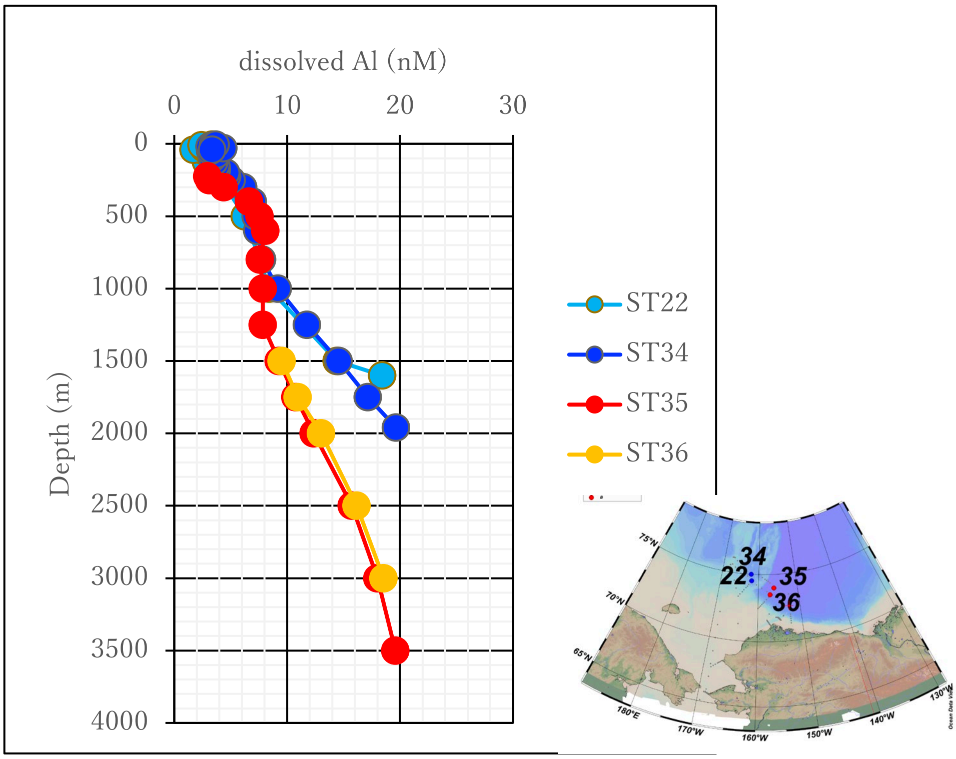

Figure 4.13-4. Vertical profiles of dissolved Al during MR24-06C.

Future Plans:

- Further analysis and interpretation of the entire dataset to provide a comprehensive view of dissolved Aluminum concentrations in the study area.

- Investigation of the factors influencing the observed dAl anomalies, such as riverine inputs and water mass dynamics.
- Comparisons and validations with other data sources and cruises to refine the understanding of the spatiotemporal distribution of dAl in the region.
- Refining the analytical methodology and enhancing the detection limits for more precise measurements in future research.
- Continued monitoring and data collection to build on the insights gained during this cruise and contribute to a better understanding of oceanographic processes in the Arctic Ocean.

(6) References

Danielson, S. L., Ahkinga, O., Ashjian, C., Basyuk, E., Cooper, L. W., Eisner, L., et al. (2020). Manifestation and consequences of Arctic amplification in the Bering and Chukchi Seas. Deep Sea Res.

Resing and Measures (1994). Fluorometric Determination of AI in Seawater by Flow Injection Analysis with In-line Preconcentration, Anal. Chem., 66, 4105-4111.

4.14. Exploring microplankton interactions and their functional roles in a changing Arctic

1) Personnel:

Eva Lopes (Faculty of Sciences of University of Porto – FCUP; Interdisciplinary Centre of Marine and Environmental Research – CIIMAR) – onboard

2) Background/Purpose

The immense variety of prokaryotes and protists plays a crucial role in marine ecosystems through distinctive metabolic processes, yet the impact of global warming on their interactions remains unclear. Global warming is driving significant changes in the Pacific side of the Arctic Ocean, leading to accelerated ice retreat and ecological shifts. Analyzing the redistribution of plankton microbial communities and their functions in this changing environment is highly relevant, as these diverse species and their rapid responses dictate shifts in ocean primary production and ecosystem sustainability. This campaign and the previous campaign (MR23-06C) will represent a step forward in generating new knowledge regarding microplankton responses to already demonstrated climate change driving forces in one of the most difficult regions to sample. Additionally, it will enable the analysis of a temporal pattern by having two years' worth of data. During this campaign, the Arctic Ocean prokaryotic and unicellular eukaryotic communities will be analysed from a community dynamics and ecological perspective. First by understanding how planktonic prokaryotic and unicellular eukaryotic communities interplay and secondly by investigating the dynamics between viruses and their microplankton hosts. The main goals of this campaign are:

1. Discover the key interconnections (taxonomical and functional) between prokaryotic and unicellular eukaryotic communities in the Arctic Ocean, by studying its dynamic interaction in field surveys.
2. Understand the influence of viruses in controlling the taxonomic and functional (N cycle pathways) interactions between the prokaryotes and unicellular eukaryotic communities.
3. Evaluate the environmental differences between the Pacific and Arctic water masses (focusing mainly on temperature and nitrogen availability) and their influence on the interactive dynamics between planktonic prokaryotes and unicellular eukaryotes.

3) Parameters

Genomics (microbial DNA)

4) Instruments and Methods

In order to analyse the marine microbial communities, seawater samples were collected across the Pacific-Arctic Ocean, with some specific locations. Such as the Bering Strait, Chucki Sea, Barrow Canyon, and Canada Basin (Table 1). Two different depth layers were used on board: Surface Chlorophyll Maximum (SCM; n = 64) and Bottom (n = 64). The Bottom layer was defined as 5 m (B-5) or 10 m (B-10) above the sea floor, depending on the station depth. Similar to the MR23-06C sampling campaign, seawater samples from the sediment of the Chucki Sea line were collected (n=6). Furthermore, water samples from ice were also collected (n=4).

Table 4.14-1: Geospatial description of samples collected onboard R/V Mirai (SCM: Surface Chlorophyll Maximum) (following page)

Station	Sample ID	Sample Type	Collection Instrument	Date	Latitude	Longitude	Depth
S02	S2_040924_B1/B2	Seawater	Niskin	04/09/2024	65.1	-169.522222	Bottom
S02	S2_040924_SCM1/SCM2	Seawater	Niskin	04/09/2024	65.1	-169.522222	SCM
S03	S3_040923_B1/B2	Seawater	Niskin	04/09/2024	66	-168.75	Bottom
S03	S3_040923_SCM1/SCM2	Seawater	Niskin	04/09/2024	66	-168.75	SCM
S04	S4_050924_B1/B2	Seawater	Niskin	05/09/2024	67	-168.75	Bottom
S04	S4_050924_SCM1/SCM2	Seawater	Niskin	05/09/2024	67	-168.75	SCM
S04	S4_SeDia_050924_1/2	Sediment Water	Ashura	05/09/2024	67	-168.75	Bottom
S05	S5_050924_B1/B2	Seawater	Niskin	05/09/2024	68	-168.75	Bottom
S05	S5_050924_SCM1/SCM2	Seawater	Niskin	05/09/2024	68	-168.75	SCM
S07	S7_060924_B1/B2	Seawater	Niskin	06/09/2024	69	-168.75	Bottom
S07	S7_060924_SCM1/SCM2	Seawater	Niskin	06/09/2024	69	-168.75	SCM
S07	S7_SeDia_060924_1/2	Sediment Water	Ashura	06/09/2024	69	-168.75	Bottom
S09	S9_060921_B1/B2	Seawater	Niskin	06/09/2024	71	-168.75	Bottom
S09	S9_060921_SCM1/SCM2	Sediment Water	Niskin	06/09/2024	71	-168.75	SCM
S10	S10_060921_B1/B2	Seawater	Niskin	06/09/2024	72	-168.75	Bottom
S10	S10_060921_SCM1/SCM2	Sediment Water	Niskin	06/09/2024	72	-168.75	SCM
S10	S10_SeDia_060924_1/2	Seawater	Ashura	06/09/2024	72	-168.75	Bottom
S11	S11_070924_B1/B2	Seawater	Niskin	07/09/2024	71.3	-164.35	Bottom
S11	S11_070924_SCM1/SCM2	Seawater	Niskin	07/09/2024	71.3	-164.35	SCM
S12	S12_080924_B1/B2	Seawater	Niskin	08/09/2024	71.735	-155.164	Bottom
S12	S12_080924_SCM1/SCM2	Seawater	Niskin	08/09/2024	71.735	-155.164	SCM
S13	S13_090924_B1/B2	Seawater	Niskin	09/09/2024	71.677	-154.983333	Bottom
S13	S13_090924_SCM1/SCM2	Seawater	Niskin	09/09/2024	71.677	-154.983333	SCM
S14	S14_100924_B1/B2	Seawater	Niskin	10/09/2024	71.929	-154.119722	Bottom
S14	S14_100924_SCM1/SCM2	Seawater	Niskin	10/09/2024	71.929	-154.119722	SCM
S15	S15_120924_B1/B2	Seawater	Niskin	12/09/2024	71.333	-152.5	Bottom
S15	S15_120924_SCM1/SCM2	Seawater	Niskin	12/09/2024	71.333	-152.5	SCM
S16	S16_120924_B1/B2	Seawater	Niskin	12/09/2024	71.5	-152.5	Bottom
S16	S16_120924_SCM1/SCM2	Seawater	Niskin	12/09/2024	71.5	-152.5	SCM
S17	S17_120924_B1/B2	Seawater	Niskin	12/09/2024	71.667	-152.5	Bottom
S17	S17_120924_SCM1/SCM2	Seawater	Niskin	12/09/2024	71.667	-152.5	SCM
S18	S18_120924_B1/B2	Seawater	Niskin	12/09/2024	71.833	-152.5	Bottom
S18	S18_120924_SCM1/SCM2	Seawater	Niskin	12/09/2024	71.833	-152.5	SCM
S19	S19_130924_B1/B2	Seawater	Niskin	13/09/2024	72	-152.5	Bottom
S19	S19_130924_SCM1/SCM2	Seawater	Niskin	13/09/2024	72	-152.5	SCM
S20	S20_130924_B1/B2	Seawater	Niskin	13/09/2024	72.583	-152.5	Bottom
S20	S20_130924_SCM1/SCM2	Seawater	Niskin	13/09/2024	72.583	-152.5	SCM
S22	S22_150924_B1/B2	Seawater	Niskin	15/09/2024	74.527	-161.948333	Bottom
S22	S22_150924_SCM1/SCM2	Seawater	Niskin	15/09/2024	74.527	-161.948333	SCM
S23	S23_180924_B1/B2	Seawater	Niskin	18/09/2024	75.617	-167.516667	Bottom
S23	S23_180924_SCM1/SCM2	Seawater	Niskin	18/09/2024	75.617	-167.516667	SCM
S24	S24_190924_B1/B2	Seawater	Niskin	19/09/2024	75	-169.633333	Bottom
S24	S24_190924_SCM1/SCM2	Seawater	Niskin	19/09/2024	75	-169.633333	SCM
S26	S26_190924_B1/B2	Seawater	Niskin	19/09/2024	75	-165	Bottom
S26	S26_190924_SCM1/SCM2	Seawater	Niskin	19/09/2024	75	-165	SCM
S28	S28_210924_B1/B2	Seawater	Niskin	21/09/2024	73.333	-165	Bottom
S28	S28_210924_SCM1/SCM2	Seawater	Niskin	21/09/2024	73.333	-165	SCM
S31	S31_210924_B1/B2	Seawater	Niskin	21/09/2024	74	-163.233333	Bottom
S31	S31_210924_SCM1/SCM2	Seawater	Niskin	21/09/2024	74	-163.233333	SCM
S33	S33_220924_B1/B2	Seawater	Niskin	22/09/2024	74.25	-162.566667	Bottom

S33	S33_220924_SCM1/SCM2	Seawater	Niskin	22/09/2024	74.25	-162.566667	SCM
S34	S34_220924_B1/B2	Seawater	Niskin	22/09/2024	75	-162.016667	Bottom
S34	S34_220924_SCM1/SCM2	Seawater	Niskin	22/09/2024	75	-162.016667	SCM
S35	S35_220924_B1/B2	Seawater	Niskin	22/09/2024	74	-156	Bottom
S35	S35_220924_SCM1/SCM2	Seawater	Niskin	22/09/2024	74	-156	SCM
S37	S37_230924_B1/B2	Seawater	Niskin	23/09/2024	73.333	−157.4667	Bottom
S37	S37_230924_SCM1/SCM2	Seawater	Niskin	23/09/2024	73.333	−157.4667	SCM
S38	S38_230924_B1/B2	Seawater	Niskin	23/09/2024	73	−158.5000	Bottom
S38	S38_230924_SCM1/SCM2	Seawater	Niskin	23/09/2024	73	−158.5000	SCM
ICE 1	Ice1_230924_1/2	Melted Ice Water	Ice Catch	17/09/2024	76.152	−167.7693	Surface
ICE 4	Ice4_230924_1/2	Melted Ice Water	Ice Catch	17/09/2024	76.152	−167.7693	Surface
S40	S40_240924_B1/B2	Seawater	Niskin	24/09/2024	72.8	-152.1	Bottom
S40	S40_240924_SCM1/SCM2	Seawater	Niskin	24/09/2024	72.8	-152.1	SCM
S43	S43_240924_B1/B2	Seawater	Niskin	24/09/2024	72.5	-160	Bottom
S43	S43_240924_SCM1/SCM2	Seawater	Niskin	24/09/2024	72.5	-160	SCM
S46	S46_250924_B1/B2	Seawater	Niskin	25/09/2024	71.741	−155.1105	Bottom
S46	S46_250924_SCM1/SCM2	Seawater	Niskin	25/09/2024	71.741	−155.1105	SCM
S47	S47_260924_B1/B2	Seawater	Niskin	26/09/2024	68	−168.7500	Bottom
S47	S47_260924_SCM1/SCM2	Seawater	Niskin	26/09/2024	68	−168.7500	SCM

Along the cruise, seawater samples were collected using 12 L Niskin bottles on a CTD/Rosette multi-sampler, between the 4th and 26th of September 2024. Every water sample was collected on a 10 L plastic and foldable container and rinsed three times. Regarding filtration, a peristaltic pump (JIHUMP; BT-100CA) was used. To prevent contamination, the filtration tubes were cleaned with 2 L of sample water. The seawater samples, were then, filtered through a 0.22 µm pore size Sterivex filter (SVGV010RS, Merck Millipore, Portugal). Each station and each depth had duplicated samples. Filtration was stopped when the water volume was finished or when the Sterivex filters were strongly clogged. Once the filtration was complete, the filters were stored on board at -80 °C, until further genomic (16S and 18S) and metagenomic analysis. These samples were collected to observe the dynamics of the microbial communities across the water column in the Arctic Ocean.

Across the Chucki Sea line, sediment samples were collected from a multiple core sampler, Ashura, and the joint water was filtered through a 0.22 µm pore size Sterivex filter (SVGV010RS, Merck Millipore, Portugal). A total of eight samples were collected and stored on board at -80 °C, until further genomic and metagenomic analysis. These samples were collected to compare the microbial communities' differences between the sediments and water, with a special focus on diatoms.

During the Ice Catch sampling, an opportunistic sampling occurred. From two different ice blocks, seawater was collected. This is, for three days the block ices were put to defrost in the climate room of R/V Mirai. After the ice was completed, the water was filtered through a 0.22 µm pore size Sterivex filter (SVGV010RS, Merck Millipore, Portugal).). A total of four samples were collected and stored on board at -80 °C, for further genomic and metagenomic analysis. These samples were collected to compare the microbial communities' differences between the ice and water column.

(6) Preliminary results

During this cruise, genomics samples were collected from a total of thirty-four stations (Fig. 4.14-1). These samples will be the subject of genomic (16S and 18S) and metagenomic analyses, to understand how prokaryotes and unicellular eukaryotes interact with each other, and eventually, how virus influences these communities.

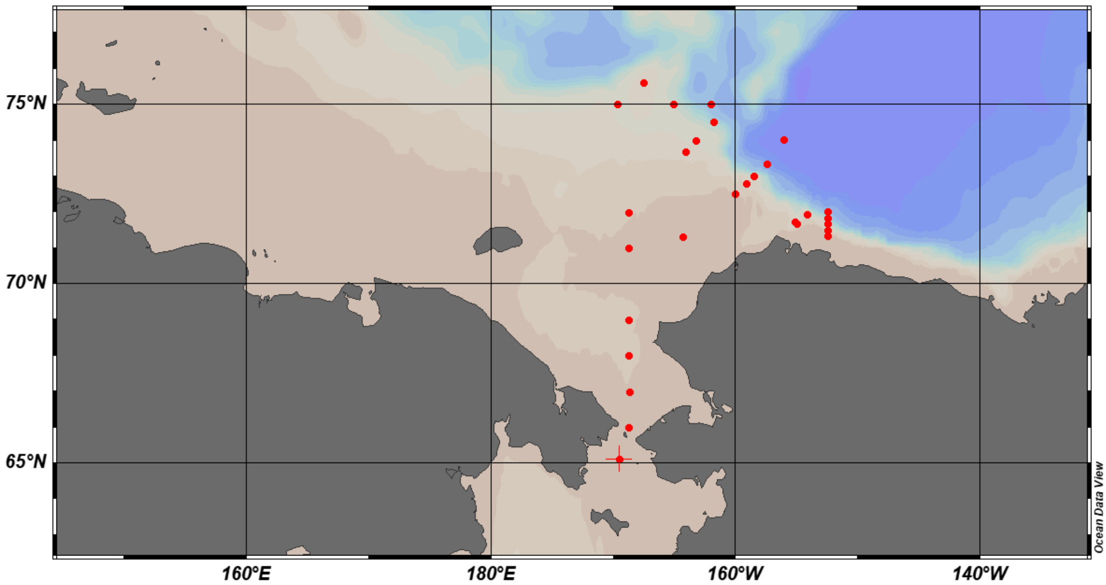

Figure 4.14-1: Map of the sampling area and sampling sites.

(7) Data archives

The data obtained in this cruise will be submitted to the Data Management Group of JAMSTEC and will be opened to the public via the “Data Research System for Whole Cruise Information in JAMSTEC (DARWIN)” on the JAMSTEC website.

4.15. Underway surface water monitoring
4.15.1. TSG, Density and FDOM

(1) Personnel

Mariko Hatta (JAMSTEC): Principal Investiator
Masahiro Orui (MWJ)
Misato Kuwahara (MWJ)
Takuya Izutsu (MWJ)

(2) Objective

Our purpose is to obtain temperature, salinity, dissolved oxygen, and fluorescence data continuously in near-sea surface water.

(3) Parameters

Temperature
Salinity
Dissolved oxygen
Fluorescence
Turbidity

(4) Instruments and Methods

The Continuous Sea Surface Water Monitoring System (Marine Works Japan Co. Ltd.) has four sensors and automatically measures temperature, salinity, dissolved oxygen, fluorescence, and turbidity in near-sea surface water every one minute. This system is located in the “sea surface monitoring laboratory” and connected to shipboard LAN-system. Measured data, time, and location of the ship were stored in a data management PC. Sea water was continuously pumped up to the laboratory from an intake placed at the approximately 4.5 m below the sea surface and flowed into the system through a vinyl-chloride pipe. The flow rate of the surface seawater was adjusted to 10 dm^3 min^{-1}.

a. Instruments

Software

Seamoni Ver.1.2.0.0

Sensors

Specifications of the each sensor in this system are listed below.

Temperature and Conductivity sensor

Model: SBE-45, SEA-BIRD ELECTRONICS, INC.

Serial number: 4552788-0264

Measurement range: Temperature -5 ^{o}C - +35 ^{o}C

Conductivity 0 S m^{-1} - 7 S m^{-1}

Initial accuracy: Temperature 0.002 ^{o}C

Conductivity 0.0003 S m^{-1}

Typical stability (per month): Temperature 0.0002 ^{o}C

Conductivity 0.0003 S m^{-1}

Resolution: Temperature 0.0001 ^{o}C

Conductivity 0.00001 S m^{-1}

Bottom of ship thermometer

Model: SBE 38, SEA-BIRD ELECTRONICS, INC.

Serial number: 38-1299

Measurement range: -5 ^{o}C - +35 ^{o}C

Initial accuracy: ±0.001 ^{o}C

Typical stability (per 6 month): 0.001 ^{o}C

Resolution: 0.00025 ^{o}C

Dissolved oxygen sensor

Model: RINKO II, JFE ADVANTECH CO. LTD.

Serial number: 0035

Measuring range: 0 mg L^{-1} - 20 mg L^{-1}

Resolution: 0.001 mg L^{-1} - 0.004 mg L^{-1} (25 ^{o}C)

Accuracy: Saturation ± 2 % F.S. (non-linear) (1 atm, 25 ^{o}C)

Fluorescence & Turbidity sensor

Model: C3, TURNER DESIGNS

Serial number: 2300707

Measuring range: Chlorophyll in vivo 0 μg L^{-1} – 500 μg L^{-1}

Minimum Detection Limit: Chlorophyll in vivo 0.03 μg L^{-1}

Measuring range: Turbidity 0 NTU - 1500 NTU

Minimum Detection Limit: Turbidity 0.05 NTU

Refractive index density

Model: Prototype1, JAMSTEC, Kanagawa, JAPAN (Uchida et al.2019)

Ultraviolet fluorometer

Model: Seapoint Sensors, Inc.

Serial number: 6262

(5) Observation log

Periods of measurement, maintenance, and problems during this cruise are listed in Table 4.15.

Table 4.15 Events list of the Sea surface water monitoring during MR24-06C

System Date [UTC]	System Time [UTC]	Events
2024/08/27	09:21:00	All the measurements started and data was available.
2024/09/02	19:15:00 to 19:20:00	Filter Cleaning.
2024/09/10	21:35:00 to 21:40:00	Filter Cleaning.
2024/09/24	13:31:00 to 13:35:00	Filter Cleaning.
2024/09/28	23:56:00	All the measurements stopped.

We took the surface water samples from this system once a day to compare sensor data with bottle data of dissolved oxygen, and chlorophyll a. The results are shown in fig. 4.15.1-2. All the dissolve oxygen samples were analyzed by Winkler method (see 4.1), chlorophyll a were analyzed by 10-AU manufactured by Turner Designs. (see 4.5).

(a)

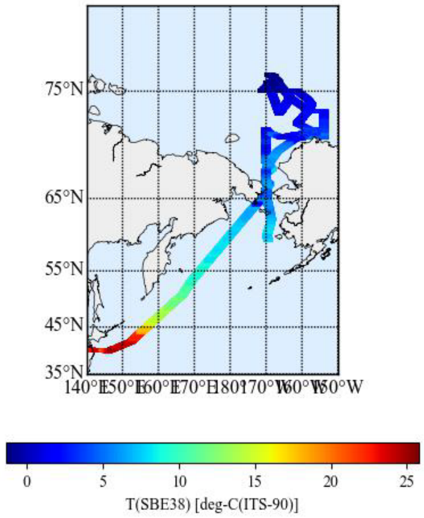
75°N
65°N
55°N
45°N
35°N
140°E 150°E 160°E 170°E 180° 170°W 160°W 150°W
0
5
10
15
20
25
T(SBE38) [deg-C(ITS-90)]

(b)

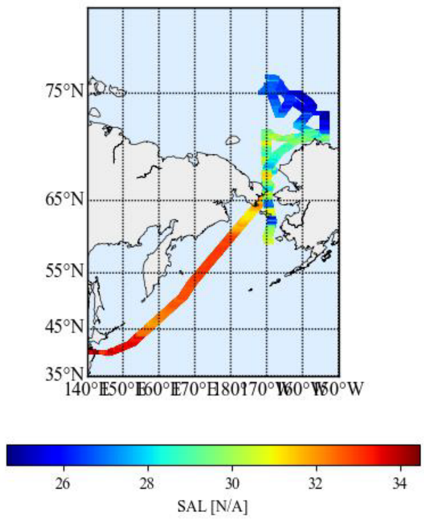
75°N
65°N
55°N
45°N
35°N
140°E 150°E 160°E 170°E 180° 170°W 160°W 150°W
26
28
30
32
34
SAL [N/A]

(c)

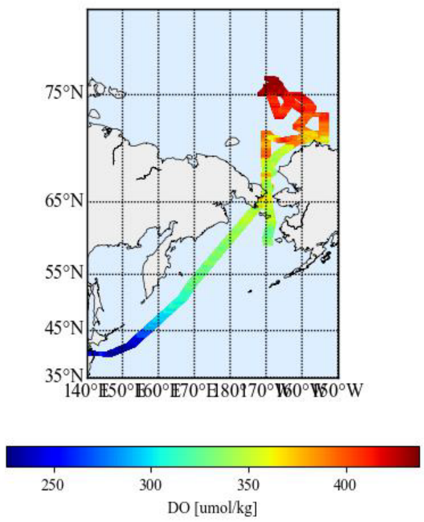

(d)

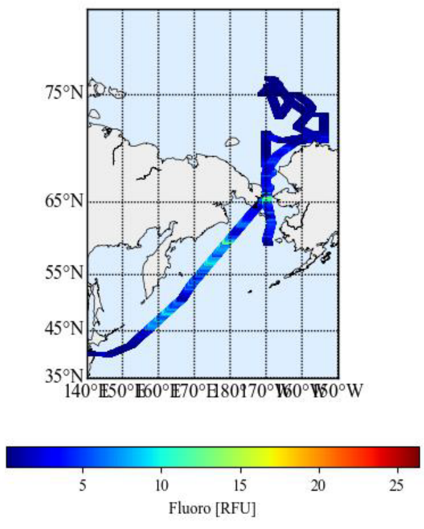

Figure 4.15.1-1 Spatial and temporal distribution of (a) temperature, (b) salinity, (c) dissolved oxygen, and (d) fluorescence in MR24-06C cruise.

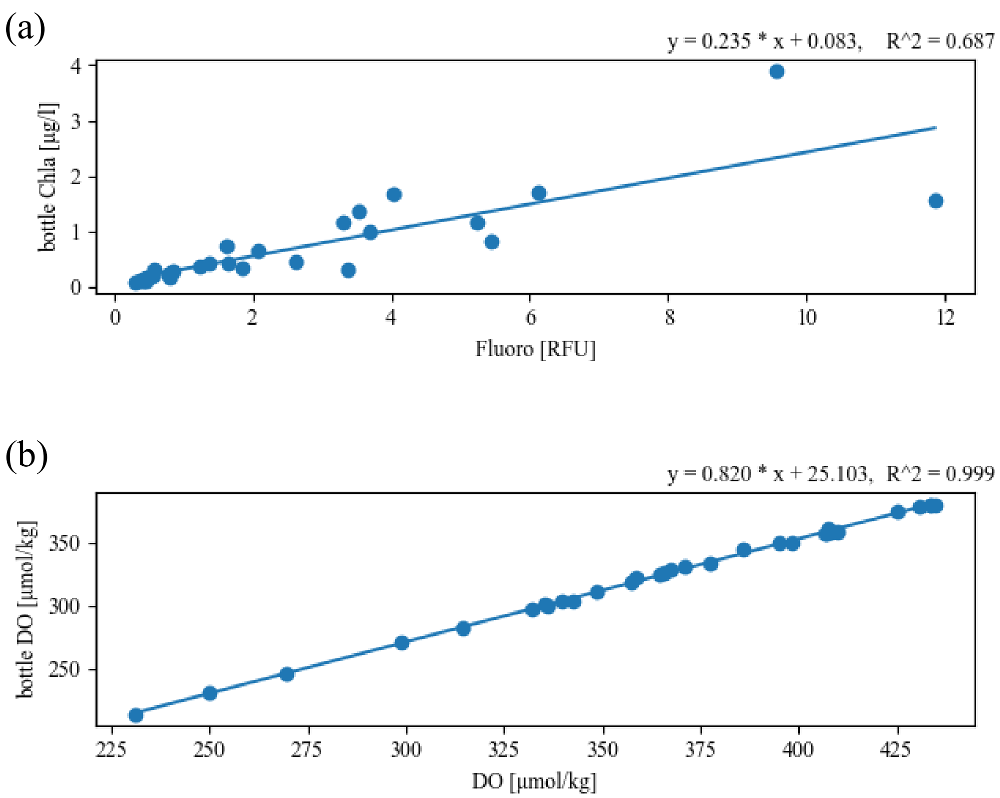

Figure 4.15.1-2 (a) Correlation of between fluorescence sensor data and bottle chlorophyll-a concentration, and (b) dissolved oxygen between the sensor and bottle measured data.

(7) Data archives

These data obtained in this cruise will be submitted to the Data Management Group of JAMSTEC, and will be opened to the public via "Data Research System for Whole Cruise Information in JAMSTEC (DARWIN)" in JAMSTEC web site.
<http://www.godac.jamstec.go.jp/darwin/e>

4.15.2. Discrete samplings

(1) Personnel

Daiki Nomura (Hokkaido University, not on board)
Manami Tozawa (Hokkaido University)
Amane Fujiwara (JAMSTEC)
Mariko Hatta (JAMSTEC)

(2) Objectives

A primary goal of this project is to understand how biogeochemical exchanges and primary production occur at the surface water of the Arctic Ocean. Freshwater inflow from various sources, including sea ice meltwater, snow meltwater, and river water, plays a significant role in the interactions between surface and atmospheric boundaries. By studying the biogeochemical environment, we aim to clarify how these processes influence on another. To achieve this, we are evaluating freshwater distribution by collecting water samples for oxygen isotopic ratio ($\delta^{18}O$) and Colored Dissolved Organic Matter (CDOM). Additional samples for nutrients and high-performance liquid chromatography (HPLC) will help us examine primary production, further supporting our understanding of the Arctic's surface water dynamics and their broader impacts.

(3) Parameters

- Oxygen isotopic ratio ($\delta^{18}O$)
- Colored Dissolved Organic Matter (CDOM)
- Nutrients
- HPLC

(4) Instruments and methods

Surface water samples for $\delta^{18}O$ and CDOM were collected into acid-washed syringes and filtered through a 0.22 μm PVDF Membrane filter (Merck Millipore Corporation, 33 mm). Samples for $\delta^{18}O$ were placed into 15-mL glass vials with minimal air space, while samples for CDOM were collected in 40-mL glass vials that had been acid-washed and combusted at 450°C for 4 hours. The samples were stored at +4˚C in the dark until analysis.

See Sections 4.2 and 4.5 for the further details of the sampling and analysis methods for nutrients and HPLC, respectively.

(5) Station list or Observation log

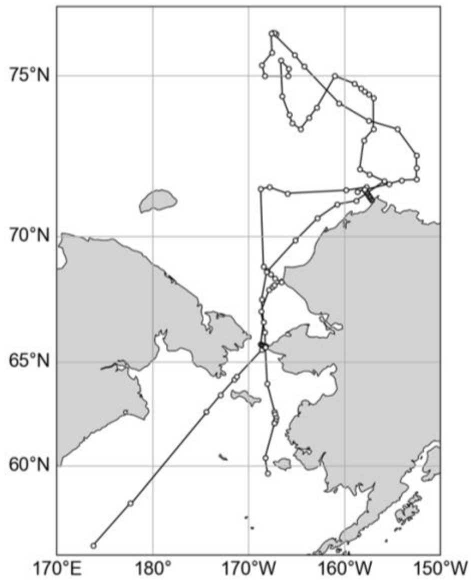

Figure 4.15.2-1: Map of Stations

Table 4.15.2-1: Station list

Station	Date Time	Latitude (˚N)	Longitude (˚E)
1	2024/9/2 2:57	55.578	173.765
2	2024/9/3 3:42	58.002	177.650
3	2024/9/4 2:40	61.690	–176.278
4	2024/9/4 9:00	62.713	–174.418
5	2024/9/4 14:00	63.508	–172.937
6	2024/9/4 18:15	64.210	–171.527
7	2024/9/9 19:01	64.343	–171.243
8	2024/9/5 4:30	65.533	–168.627
9	2024/9/5 5:32	65.690	–168.273
10	2024/9/5 11:00	66.272	–168.307
11	2024/9/5 18:30	67.140	–168.720
12	2024/9/6 2:30	68.001	–167.867
13	2024/9/6 3:15	68.128	–167.495
14	2024/9/6 3:42	68.185	–167.308
15	2024/9/6 5:48	68.300	–166.602
16	2024/9/6 6:45	68.442	–167.290
17	2024/9/6 7:45	68.593	–167.682
18	2024/9/6 8:45	68.740	–168.072
19	2024/9/6 9:45	68.890	–168.465
20	2024/9/7 3:33	71.632	–168.745
21	2024/9/7 8:55	71.683	–167.817
22	2024/9/7 12:22	71.482	–165.985

23	2024/9/8 2:00	71.585	–159.850
24	2024/9/8 7:00	71.687	–157.698
25	2024/9/9 4:55	71.247	–157.165
26	2024/9/9 5:18	71.288	–157.248
27	2024/9/9 5:33	71.330	–157.332
28	2024/9/9 5:49	71.372	–157.415
29	2024/9/9 6:04	71.413	–157.498
30	2024/9/9 6:20	71.455	–157.583
31	2024/9/9 6:31	71.497	–157.668
32	2024/9/9 6:51	71.537	–157.753
33	2024/9/9 7:06	71.578	–157.838
34	2024/9/9 7:23	71.620	–157.925
35	2024/9/9 9:00	71.540	–158.632
36	2024/9/10 3:52	71.797	–155.355
37	2024/9/10 9:12	71.912	–154.018
38	2024/9/13 8:25	71.938	–152.507
39	2024/9/13 16:30	72.300	–152.500
40	2024/9/14 0:15	72.693	–152.497
41	2024/9/14 6:55	73.500	–154.500
42	2024/9/14 23:52	73.750	–157.500
43	2024/9/15 5:11	74.250	–160.575
44	2024/9/16 5:28	75.258	–164.228
45	2024/9/16 7:19	75.565	–165.217
46	2024/9/16 16:48	76.122	–167.487
47	2024/9/16 23:21	76.097	–167.162
48	2024/9/17 4:40	76.122	–167.338
49	2024/9/17 16:36	76.107	–167.663
50	2024/9/18 5:53	75.617	–167.572
51	2024/9/19 1:31	75.300	–168.608
52	2024/9/19 17:40	75.000	–168.338
53	2024/9/19 22:37	75.000	–165.885
54	2024/9/20 3:16	75.202	–165.810
55	2024/9/20 4:40	75.412	–166.667
56	2024/9/21 5:07	74.443	–166.492
57	2024/9/21 7:53	73.915	–165.768
58	2024/9/21 11:00	73.668	–165.445
59	2024/9/21 23:08	73.500	–164.605
60	2024/9/22 1:35	73.832	–163.700
61	2024/9/22 7:53	74.125	–162.900
62	2024/9/22 23:35	75.000	–161.000
63	2024/9/23 1:18	74.800	–159.000
64	2024/9/23 2:28	74.667	–158.308
65	2024/9/23 3:09	74.583	–157.917
66	2024/9/23 3:53	74.500	–157.467
67	2024/9/23 4:42	74.400	–157.000
68	2024/9/23 14:07	73.500	–157.000
69	2024/9/23 23:20	73.167	–158.000

70	2024/9/25 2:35	72.262	–158.432
71	2024/9/25 4:15	72.100	–157.383
72	2024/9/25 6:40	71.883	–155.865
73	2024/9/25 20:55	71.235	–158.803
74	2024/9/26 0:33	71.117	–160.750
75	2024/9/26 4:30	70.642	–162.823
76	2024/9/26 10:30	69.857	–165.117
77	2024/9/26 17:04	68.683	–168.128
78	2024/9/27 0:35	67.617	–168.663
79	2024/9/27 4:52	66.702	–168.455
80	2024/9/27 9:33	65.764	–168.747
81	2024/9/27 9:59	65.742	–168.633
82	2024/9/27 10:20	65.716	–168.550
83	2024/9/27 10:40	65.696	–168.460
84	2024/9/27 11:01	65.677	–168.355
85	2024/9/27 11:23	65.646	–168.270
86	2024/9/27 19:13	64.023	–168.065
87	2024/9/28 1:35	62.725	–167.300
88	2024/9/28 2:30	62.597	–167.237
89	2024/9/28 3:40	62.425	–167.158
90	2024/9/28 4:40	62.288	–167.233
91	2024/9/28 5:30	62.170	–167.300
92	2024/9/28 5:41	62.167	–167.300
93	2024/9/28 17:40	60.427	–168.290
94	2024/9/28 23:38	59.625	–168.033

(6) Data archives

These data obtained in this cruise will be submitted to the Data Management Group of JAMSTEC, and will be opened to the public via "Data Research System for Whole Cruise Information in JAMSTEC (DARWIN)" in JAMSTEC web site.
<http://www.godac.jamstec.go.jp/darwin/e>

4.15.3. Silicate

(1) Responsible personnel

Mariko Hatta JAMSTEC

(2) Purpose, background

1. Establish the shipboard system using a programmable flow injection system and identify potential trouble and establish the troubleshooting protocol:

- Purpose: The primary purpose of this study is to develop a compact and automated microfluidic analyzer for nutrient analysis. This innovative system is designed to meet specific criteria for efficient, unsupervised operation, including durability, minimal reagent consumption, and computer-controlled manipulations. In essence, it aims to create a state-of-the-art tool for analyzing nutrients in ocean samples with a focus on practicality and precision.
- Background: The background provides essential context for the study:. ***Current Knowledge Gap:*** It is established that there's a significant gap in our understanding of ocean biogeochemical data. This knowledge gap is attributed to the complexity and intricacy of the analytical procedures involved in both at-sea and on-land sample analysis.

2. Identify the water mass characteristics with shipboard silicate and phosphate data with the other physical parameters (i.e. Temperature, salinity, oxygen) obtained from the underway surface water monitoring system:

- Purpose: This goal aims to collect and analyze data related to water mass characteristics. It mentions specific parameters such as silicate and phosphate concentrations along with temperature, salinity, and oxygen levels. The purpose is to understand the composition and characteristics of the water masses the ship encounters during its journey.
- Background: ***Arctic Ocean Significance***: The study highlights the significance of the Arctic Ocean, which experiences dynamic changes in freshwater influx due to factors such as sea ice melt and river inputs. These changes have substantial effects on the surface ocean. ***Continental Shelves:*** The Arctic Ocean's unique geographical characteristics, notably its extensive continental shelves, play a

vital role in the transport of geochemical substances from the continental boundary to the Arctic interior. These processes are influenced by climate change, making it increasingly important to understand the Arctic's geochemical cycles.

In summary, the study aims to address the existing knowledge gap by developing an advanced microfluidic analyzer that facilitates nutrient analysis in ocean samples and expands the database. This innovation is particularly important given the intricate nature of existing analytical procedures and the unique environmental changes occurring in the Arctic Ocean. Understanding the geochemical cycles in the Arctic region has broad implications, making this research significant in the context of oceanography and environmental science.

(3) Activities (observation, sampling, development)

The activities described in this section involve the process of collecting and analyzing seawater samples for real-time determination of Silicate (SiO_2) using a programmable flow injection technique. Here's a breakdown of the activities:

1. **Seawater Sample Collection:** Samples were aspirated into the analysis system using an underway water sampling pump system, waters were collected approximately at 4.5m depth.
2. **Real-Time Analysis:** The collected seawater samples are then subjected to real-time analysis. The analysis focuses on two key parameters: Silicate (SiO_2).
3. **Programmable Flow Injection Technique:** The analysis technique being employed is the programmable flow injection technique. This technique involves the controlled injection of samples and reagents into a flowing stream. It allows for precise and automated measurements and is valuable for continuous monitoring.

(4) Methods, instruments

4.1. Instrumentation

The instrument, miniSIA-2 (Global FIA, Fox Island, WA, USA), comprises two high precision, synchronously refilling milliGAT pumps, two thermostated holding coils, a 6-port LOV (model COV-MANI-6, constructed from polymethyl methacrylate, Perspex®) furnished with a module for an external flow cell (Figure 4.15.3). All tubing connections, downstream from the milliGAT pumps including the holding coils (volume

1000 µL), were made with 0.8 mm I.D. polytetrafluoroethylene (PTFE). The holding coils were thermostated at 40C temperature for all silicate and phosphate analysis. The tubing between the carrier stream reservoirs and the milliGAT pump was made from 1.6 mm I.D. PTFE tubing to minimize degassing under reduced pressure at higher aspiration flow rates. A spectrophotometer (Flame, Ocean Insight, Orlando, FL, USA) and a light source were connected to the flow cells by using optical fibers with 500-µm silica cores encased in 0.8 mm I.D. green PEEK tubing. The end of each fiber exposed to the liquid was cemented with epoxy, cut square, and polished. An Ocean Optics Tungsten Halogen (HL-2000, Ocean Insight, Orlando, FL, USA) light source was used. All assay steps were computer-controlled using commercially available software (FloZF, GlobalFIA, Fox island, WA, USA). The Linear Light Path (LLP) flow cell was purchased from Global FIA. The outlet of the LLP flow cell, was fitted with a 40-psi flow restrictor (GlobalFIA, Fox Island, WA, USA), which, by elevating the pressure within the flow path, efficiently prevented the formation of microbubbles from spontaneous outgassing.

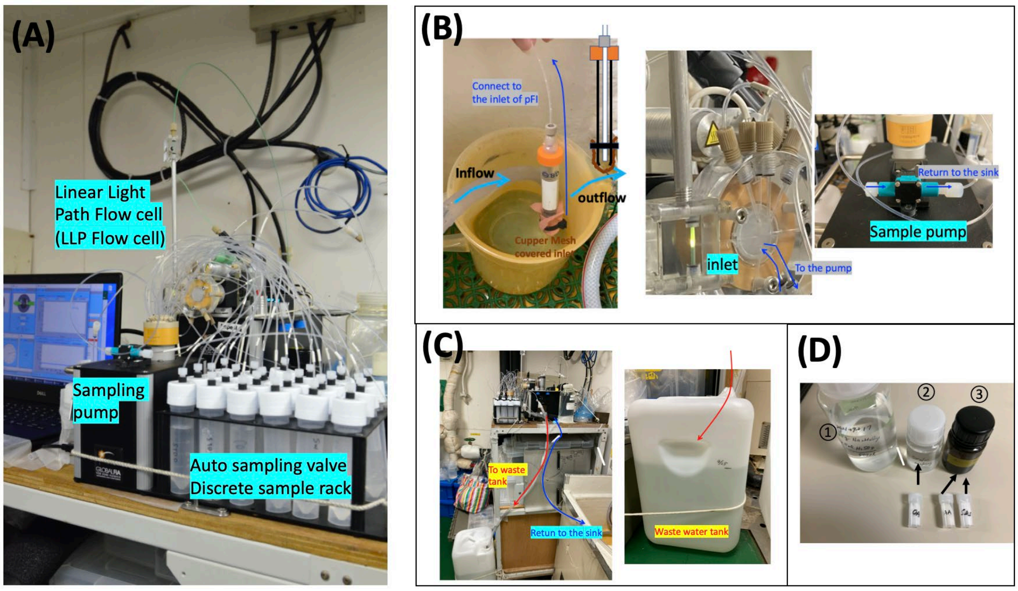

Figure 4.15.3. Shipboard analytical system for continuous silicate determination using the programmable flow injection technique. (A) the mini-SIA2 system and the autosampler. (B) Newly established sampling inlet. (C) The waste water drains system (D) Preparation for the reagents for the Silicate analysis during the cruise.

Remarks:

- **Flow Cell Length:** This year, a flow cell with a length of 10 centimeters was utilized. The flow cell is a key component of the analysis system and is used to pass the seawater samples through for analysis.

- **Sample Collection Frequency:** Surface water samples were collected approximately every 5 minutes. This frequent sampling interval allows for more detailed temporal resolution in the data.
- **Sample Aspiration:** Samples were aspirated into the analysis system using a sample pump for a duration of 10 or 20 seconds. Aspiration is the process of drawing the seawater samples into the system for analysis.
- **Temperature Adjustment:** After aspiration, the samples were homogenized to adjust their temperature to room temperature, which is about 25 degrees Celsius. Maintaining a consistent temperature is important for accurate and reproducible analysis, but the room temperature changes significantly during the analysis time or date. Thus, the heating coil has been adjusted to 40 degrees C during this cruise to meet the constant determination throughout the cruise.
- **Return of Flushed Surface Samples:** Samples that weren't analyzed, which are referred to as "flushed surface samples". Since they were not mixed with any reagent, these samples were directly returned to the sink, indicating that they were not retained after analysis.
- **Waste Handling:** Any waste samples and reagents generated during the analysis process were drained into a waste tank. These waste materials were stored in the waste tank until the end of the cruise. Proper waste management is crucial for environmental and safety reasons.

(4.2) Analytical methodology

The detailed the methodology using programmable flow injection technique was published in Hatta et al., 2021. The detailed of each reagent and standards were made as follow:

Carrier solution: MilliQ water.
Certified reference materials (KANSO) have been analyzed as a standard solution for this cruise (see Table 4.15.3).

Table. The certified reference materials

CRMs	Reported silicate value
CQ	2.20±0.07

CR	14.0±0.3
CS	34.0±0.3
CP	61.1±0.3

Silicate analysis:

The acidified molybdate reagent was prepared by dissolving 2 g of ammonium molybdate tetrahydrate crystalline in 500 mL of acidified MilliQ water (2.5 mL of conc. sulfuric acid was added). This solution was stable for 2 months. The mixed solution of ascorbic acid and SDS solution was prepared by dissolving 4 g of L (+)-ascorbic acid in 200 mL of MilliQ water, and then 4 g of solid of ultrapure sodium dodecyl sulfate was added into this ascorbic acid solution, and then 4 g of solid of oxalic acid was added into this mixture.

(5) Results, Future Plans, Lists (samples, observation equipment, deployment & recovery), Local field map (dive tracks, sampling points, survey lines), etc

Results:

- During the cruise, the surface samples for continuous determination were collected every 5 minutes. Over 2200 samples were determined during this cruise.
- The significant air bubble issue was detected while the low temperature seawater were introduced into the sampling line, modified the sampling line and slightly improved the frequency of the air bubble injection, but still need to be improved.

Future Plans:

- Further analysis and interpretation of the entire dataset to provide a comprehensive view of silicate in the study area.
- Investigation of the factors influencing the observed silicate anomalies, such as riverine inputs and water mass dynamics.
- Comparisons and validations with other data sources and cruises to refine the understanding of the spatiotemporal distribution of silicate in the region.
- Refining the analytical methodology, especially sample introducing system.
- Continued monitoring and data collection to build on the insights gained during this cruise and contribute to a better understanding of oceanographic processes in the Arctic Ocean.

(6) References

Hatta et al., 2021. Programmable flow injection in batch mode: Determination of nutrients in seawater by using a single, salinity-independent calibration line, obtained with standards prepared in distilled water, Talanta. https://doi.org/10.1016/j.talanta.2021.122354.

4.16. Continuous measurement of pCO_2 and pCH_4

(1) Personnel

Akihiko Murata	JAMSTEC	Principal Investigator
Yasuhiro Arii	MWJ	Operation Leader
Nagisa Fujiki	MWJ	

(2) Objective

Our purpose is in-situ measurement of concentrations of carbon dioxide (CO_2) and methane (CH_4) in surface seawater.

(3) Parameters

Partial pressures of CO_2 (pCO_2) and CH_4 (pCH_4)

(4) Methods, Apparatus and Performance

Atmospheric and surface seawater CO_2 and CH_4 were measured using an automated system equipped with Off-Axis Integrated-Cavity output Spectroscopy gas analyzer (Off-Axis ICOS; 911-0011, Los Gatos Research) developed on the basis of Cavity Ring-Down Spectroscopy. Standard gases and atmospheric air taken from the bow of the ship (approx.13 m above the sea level) were also measured. Seawater was taken from an intake placed at the approximately 4.5 m below the sea surface and introduced into the equilibrator at the flow rate of (4 - 5) L min^{-1} by a pump. The equilibrated air was circulated in a closed loop by a pump at flow rate of (0.6 - 0.7) L min^{-1} through two electric cooling units, a starling cooler, and the Off-Axis ICOS.

(5) Preliminary result

Distributions of atmospheric and surface seawater CO_2 are shown in Figure 4.16-1, along with those of sea surface temperature (SST). As shown in Figure 4.16-1, the atmospheric CO_2 concentration shows anomalous temporal variations. This is due to the malfunction of the pump used to introduce air from outside the ship. It is possible that air was also introduced inside the laboratory. Therefore, it is recommended not to use the atmospheric CO_2 data. Those of CH_4 are shown in Figure 4.16-2. The atmospheric CH_4 concentrations do not show the anomalous variations found in atmospheric CO_2. This is probably because there is no obvious source of CH_4 in the laboratory. However, because the air is sampled with the same pump used for CO_2, the data for atmospheric CH_4 should be treated with caution.

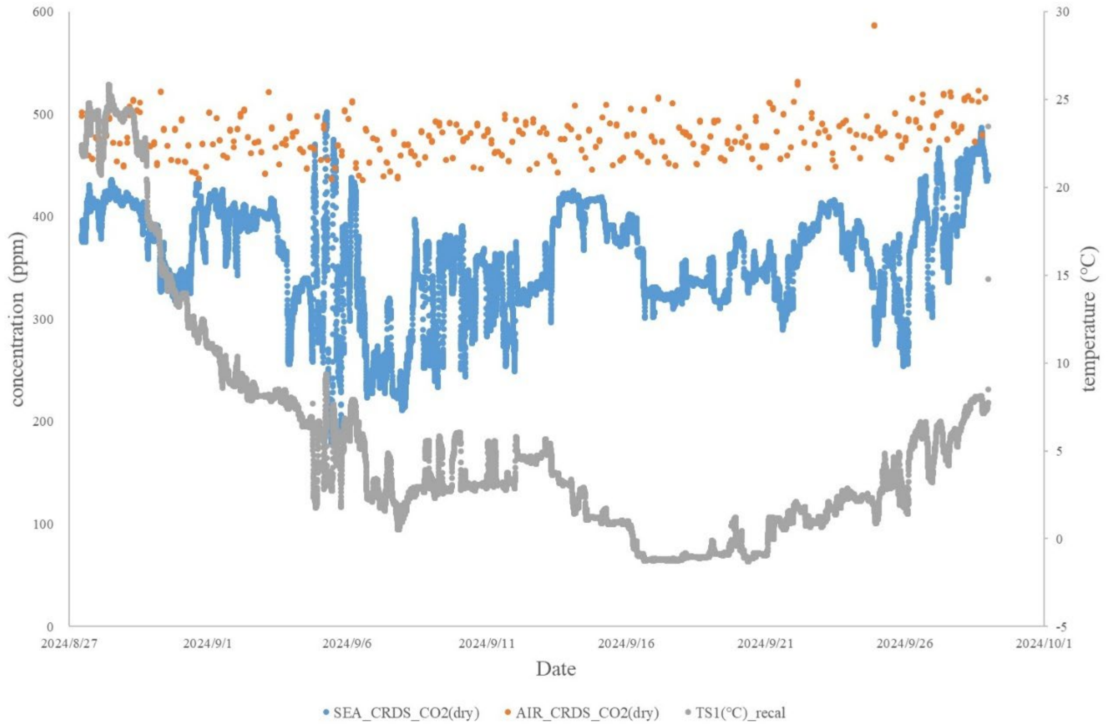

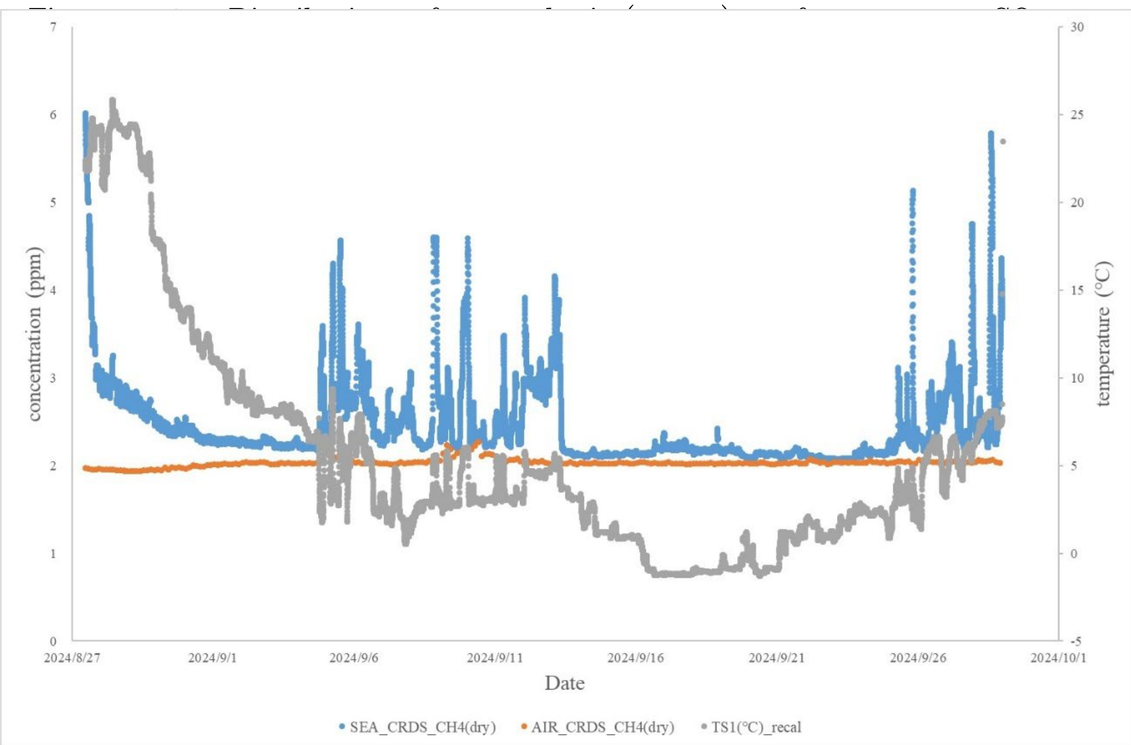

Figure 4.16-2. Distributions of atmospheric (orange), surface seawater CH_4 (blue) and SST (grew) as a function of observation time.

(6) Date archives

These data obtained in this cruise will be submitted to the Data Management Group (DMG) of JAMSTEC, and will open to the public via "Data Research System for Whole Cruise Information in JAMSTEC (DARWIN)" in JAMSTEC web site.
http://www.godac.jamstec.go.jp/darwin/e.

4.17. Plankton
4.17.1. Zooplankton

(1) Personnel

Kohei Matsuno (Hokkaido University) - Principal Investigator, Not on board
Shino Kumagai (Hokkaido University)

(2) Objectives

The goals of this study are the following:

1) Clarifying spatial distribution of mesozooplankton communities derived by plankton net and *in-situ* imaging instrument

(3) Parameters

Mesozooplankton abundance
Mesozooplankton wet weight

(4) Sampling and treatment

(4-1) Plankton net sampling

Zooplankton samples were collected by vertical hauls of a Quad-NORPAC net at 37 stations in the Pacific Arctic Ocean. Quad-NORPAC net (mesh sizes: 335, 150, 100 and 63 µm with large cod-end, mouth diameter: 45 cm) was towed between surface and 150 m depth or bottom -7 m (stations where the bottom shallower than 150 m) at all stations (Fig. 4.17.1-1 and Table 4.17.1-1). The volume of water filtered through the net was estimated from the reading of a flow-meter mounted in the mouth ring. The zooplankton samples collected by the NORPAC net with 335, 150 and 100 µm mesh were immediately fixed with 5% buffered formalin for zooplankton community structure analysis. Samples collected with 63 µm mesh were fixed with 99.5% ethanol as backup samples for haplotype analysis of zooplankton. The 63-µm mesh samples collected at five stations located in the Chukchi Sea (cf. red circle in Fig. 4.17.1-1) were used for genetical analysis of copepods by Dr. Junya Hirai (The University of Tokyo) and Dr. Grace Wyngaard (James Madison University).

(4-2) On-board treatment

At five stations located in the Chukchi Sea (cf. red circle in Fig. 4.17.1-1), We immediately added with 10% soda water (CO_2 water) into samples collected by 63 µm NORPAC after net sampling. We sorted with *C. glacialis/marshallae*, and moved into a microplate filled with filtered seawater. After 2-3 hours incubation in a refrigerator, active-swimming individuals were moved into cryovials and fixed with 95% ethanol or RNA later. The samples were preserved in a refrigerator for one day, then preserved in a freezer (-20°C). The samples will be used for obtaining whole genome of *C. glacialis/marshallae* will be read by Dr. Junya Hirai (The University of Tokyo). Seawater in the remaining samples were removed as much as possible by 30-µm mesh, then remaining specimens were moved into a plastic bottle filled with 95% ethanol. The samples were preserved in a freezer (-20°C). The samples will be used for measuring genome size of *Pseudocalanus* spp. by Dr. Grace Wyngaard (James Madison University).

(4-3) Continuous Particle Imaging and Classification System (CPICS) observation

At all stations where plankton net sampling was made, vertical tows of CPICS were performed (Table 4.17.1-2, Fig. 4.17.1-1). The vertical owing speed was 0.3 m s^{-1}.

(5) Station list

Table 4.17.1-1: Data on plankton samples collected by vertical hauls with a Quad-NORPAC net.

Station no.	Position Lat. (N)		Position Lon.		S.M.T. Date	S.M.T. Hour		Length of wire (m)	Angle of wire (°)	Depth estimated by wire angle (m)	Mesh size (μm)	Flowmeter No.	Flowmeter Reading	Estimated volume of water filtered (m^3)	Remark
002	65	05.6	169	31.1 W	4 Sep.	15:43 -	15:46	44	9	43	335	3994	438	6.78	
											150	3996	481	7.08	
											100	3993	458	6.70	
											63				1)
003	65	59.75	168	45.09 W	5 Sep.	0:00 -	0:03	50	19	47	335	3994	442	6.84	
											150	3996	345	5.08	
											100	3993	250	3.65	
											63				
004	67	00.23	168	44.81 W	5 Sep.	8:55 -	8:58	38	8	38	335	3994	335	5.18	
											150	3996	331	4.87	
											100	3993	321	4.69	
											63				1)
006	68	14.54	167	7.63 W	5 Sep.	20:46 -	20:49	37	9	37	335	3994	362	5.60	
											150	3996	390	5.74	
											100	3993	390	5.70	
											63				
007	68	59.94	168	44.88 W	6 Sep.	2:34 -	2:38	47	9	46	335	3994	418	6.47	
											150	3996	395	5.82	
											100	3993	398	5.82	
											63				1)
008	69	59.98	168	44.95 W	6 Sep.	9:46 -	9:48	34	8	34	335	3994	351	5.43	
											150	3996	310	4.57	
											100	3993	265	3.87	
											63				
009	70	59.96	168	44.99 W	6 Sep.	15:21 -	15:24	38	11	37	335	3994	356	5.51	
											150	3996	321	4.73	
											100	3993	274	4.01	
											63				
010	71	59.98	168	44.98 W	6 Sep.	22:03 -	22:05	45	3	45	335	3994	406	6.28	
											150	3996	370	5.45	
											100	3993	328	4.79	
											63				
011	71	18.00	164	20.98 W	7 Sep.	8:03 -	8:05	38	0	38	335	3994	320	4.95	
											150	3996	238	3.50	
											100	3993	220	3.22	
											63				
012	71	44.25	155	9.61 W	8 Sep.	15:38 -	15:45	150	0	150	335	3994	1258	19.46	
											150	3996	1291	19.01	
											100	3993	1200	17.54	
											63				
013	71	41.83	154	53.42 W	9 Sep.	15:25 -	15:30	100	8	99	335	3994	880	13.61	
											150	3996	929	13.68	
											100	3993	800	11.69	
											63				
014	71	55.46	154	7.07 W	10 Sep.	8:03 -	8:09	150	4	150	335	3994	1269	19.63	
											150	3996	1271	18.72	
											100	3993	1290	18.86	
											63				
015	71	19.99	152	29.98 W	12 Sep.	8:43 -	8:47	56	8	55	335	3994	533	8.25	
											150	3996	588	8.66	
											100	3993	521	7.62	
											63				
016	71	30.70	152	29.92 W	12 Sep.	12:00 -	12:06	102	7	101	335	3994	928	14.36	
											150	3996	1961	28.88	
											100	3993	665	9.72	
											63				
017	71	39.99	152	29.98 W	12 Sep.	17:15 -	17:22	152	11	149	335	3994	1324	20.48	
											150	3996	1402	20.65	
											100	3993	1216	17.78	
											63				
018	71	49.76	152	29.29 W	12 Sep.	20:32 -	20:40	153	12	150	335	3994	1492	23.08	
											150	3996	1640	24.15	
											100	3993	1432	20.93	
											63				
019	72	00.05	152	30.07 W	13 Sep.	4:02 -	4:09	153	12	150	335	3994	1384	21.41	
											150	3996	2439	35.92	
											100	3993	1350	19.73	
											63				

S.M.T. is UTC-8h

1) Samples for genetic analysis by Dr. Junya Hirai (The University of Tokyo) and Dr. Grace Wyngaard (James Madison University).

Table 4.17.1-1: (Continued).

Station no.	Position Lat. (N)		Lon.		S.M.T. Date	Hour			Length of wire (m)	Angle of wire (°)	Depth estimated by wire angle (m)	Mesh size (μm)	Flowmeter No.	Reading	Estimated volume of water filtered (m^3)	Remark
020	72	18.02	152	30.07 W	13 Sep.	7:01	-	7:08	150	4	150	335	3994	1331	20.59	
												150	3996	2395	35.27	
												100	3993	1339	19.57	
												63				
021	72	35.04	152	29.94 W	13 Sep.	10:20	-	10:26	150	4	150	335	3994	1300	20.11	
												150	3996	1367	20.13	
												100	3993	1320	19.30	
												63				
023	75	36.52	167	32.52 W	18 Sep.	14:08	-	14:15	150	0	150	335	3994	1319	20.41	
												150	3996	1399	20.60	
												100	3993	1280	18.71	
												63				
024	75	00.07	169	38.14 W	19 Sep.	7:04	-	7:12	150	0	150	335	3994	1311	20.28	
												150	3996	1350	19.88	
												100	3993	1259	18.40	
												63				
025	75	00.00	167	14.08 W	19.Sep	11:05	-	11:11	150	0	150	335	3994	1278	19.77	
												150	3996	1330	19.59	
												100	3993	1227	17.94	
												63				
026	75	00.05	165	0.03 W	19 Sep.	17:15	-	17:21	150	2	150	335	3994	1281	19.82	
												150	3996	1351	19.90	
												100	3993	1269	18.55	
												63				
027	73	20.01	165	0.1 W	20 Sep.	8:41	-	8:44	150	4	150	335	3994	616	9.53	
												150	3996	605	8.91	
												100	3993	531	7.76	
												63				
028	73	39.93	164	6.97 W	21 Sep.	11:18	-	11:24	150	2	150	335	3994	1349	20.87	
												150	3996	1419	20.90	
												100	3993	1240	18.13	
												63				
031	74	00.04	163	14.1 W	21 Sep.	21:04	-	21:11	151	6	150	335	3994	1289	19.94	
												150	3996	1342	19.76	
												100	3993	1230	17.98	
												63				
033	74	15.05	162	33.92 W	22 Sep.	4:41	-	4:48	150	4	150	335	3994	1395	21.58	
												150	3996	1371	20.19	
												100	3993	1290	18.86	
												63				
034	74	59.90	162	0.33 W	22 Sep.	10:11	-	10:19	151	6	150	335	3994	1392	21.54	
												150	3996	1361	20.04	
												100	3993	1272	18.59	
												63				
035	73	59.90	155	59.7 W	23 Sep.	2:29	-	2:36	156	16	150	335	3994	1490	23.05	
												150	3996	1452	21.38	
												100	3993	1381	20.19	
												63				
037	73	20.00	157	27.99 W	23 Sep.	13:43	-	13:49	152	10	150	335	3994	1288	19.93	
												150	3996	1355	19.95	
												100	3993	1281	18.73	
												63				
038	72	39.92	158	29.84 W	23 Sep.	17:36	-	17:43	150	4	150	335	3994	1330	20.58	
												150	3996	1416	20.85	
												100	3993	1320	19.30	
												63				
039	72	54.06	158	47.81 W	24 Sep.	1:06	-	1:14	150	4	150	335	3994	1412	21.85	
												150	3996	1494	22.00	
												100	3993	1335	19.51	
												63				
040	72	48.07	159	6.07 W	24 Sep.	4:01	-	4:07	153	12	150	335	3994	1329	20.56	
												150	3996	1412	20.79	
												100	3993	1381	20.19	
												63				

S.M.T. is UTC-8h

1) Samples for genetic analysis by Dr. Junya Hirai (The University of Tokyo) and Dr. Grace Wyngaard (James Madison University).

Table 4.17.1-1: (Continued).

Station no.	Position Lat. (N)	Position Lon.	S.M.T. Date	S.M.T. Hour	Length of wire (m)	Angle of wire (°)	Depth estimated by wire angle (m)	Mesh size (μm)	Flowmeter No.	Flowmeter Reading	Estimated volume of water filtered (m^3)	Remark
041	72 41.98	159 24.04 W	24 Sep.	8:58 - 9:02	76	4	76	335	3994	762	11.79	
								150	3996	862	12.69	
								100	3993	809	11.83	
								63				
043	72 30.00	159 59.95 W	24 Sep.	15:37 - 15:39	42	0	42	335	3994	545	8.43	
								150	3996	421	6.20	
								100	3993	390	5.70	
								63				
046	71 43.69	155 6.46 W	25 Sep	2:25 - 2:33	153	12	150	335	3994	1351	20.90	
								150	3996	1479	21.78	
								100	3993	1369	20.01	
								63				1)
047	68 00.00	168 44.98 W	26 Sep.	13:45 - 13:47	52	2	52	335	3994	598	9.25	
								150	3996	531	7.82	
								100	3993	494	7.22	
								63				1)

S.M.T. is UTC-8h

1) Samples for genetic analysis by Dr. Junya Hirai (The University of Tokyo) and Dr. Grace Wyngaard (James Madison University).

Table 4.17.1-2: Data on zooplankton in-situ imaging by vertical tows of CPICS.

Station no.	Position Lat. (N)	Position Lon. (W)	Start (UTC) Date	Start (UTC) Hour	End (UTC) date	End (UTC) hour	Length of wire (m)	Angle of wire (°)	Depth estimated by wire angle (m)	Data name	Remark
002	65.093	169.518	2024/9/5	0:53	2024/9/5	0:59	43m	9	43m	MR2406C_st002	0.3 m/s
003	65.996	168.752	2024/9/5	8:14	2024/9/5	8:19	48m	5	48m	MR2406C_st003	0.3 m/s
004	67.004	168.747	2024/9/5	17:06	2024/9/5	17:11	38m	0	38m	MR2406C_st004	0.3 m/s
006	68.242	167.127	2024/9/6	4:55	2024/9/6	5:00	37m	0	37m	MR2406C_st006	0.3 m/s
007	68.999	168.748	2024/9/6	8:45	2024/9/6	8:50	47m	0	47m	MR2406C_st007	0.3 m/s
008	70.000	168.749	2024/9/6	17:55	2024/9/6	18:00	34m	0	34m	MR2406C_st008	0.3 m/s, No images were recorded
009	70.999	168.750	2024/9/6	23:29	2024/9/6	23:34	37m	0	37m	MR2406C_st009	0.3 m/s
010	72.000	168.750	2024/9/7	6:12	2024/9/7	6:18	45m	0	45m	MR2406C_st010	0.3 m/s
011	71.300	164.350	2024/9/7	16:14	2024/9/7	16:19	38m	3	38m	MR2406C_st011	0.3 m/s
012	71.738	155.160	2024/9/8	23:52	2024/9/9	0:11	150m	3	150m	MR2406C_st012	0.3 m/s, Images only downcast
013	71.697	154.890	2024/9/9	23:36	2024/9/9	23:48	99m	2	99m	MR2406C_st013	0.3 m/s
014	71.924	154.118	2024/9/10	16:16	2024/9/10	16:35	150m	0	150m	MR2406C_st014	0.3 m/s
015	71.333	152.500	2024/9/12	16:52	2024/9/12	16:59	55m	0	55m	MR2406C_st015	0.3 m/s
016	71.512	152.499	2024/9/12	20:13	2024/9/10	20:25	101m	0	101m	MR2406C_st016	0.3 m/s
017	71.667	152.500	2024/9/13	1:31	2024/9/13	1:51	150m	0	150m	MR2406C_st017	0.3 m/s
018	71.829	152.488	2024/9/13	4:48	2024/9/13	5:07	150m	3	150m	MR2406C_st018	0.3 m/s
019	72.001	152.501	2024/9/13	12:15	2024/9/13	12:35	150m	0	150m	MR2406C_st019	0.3 m/s
020	72.300	152.501	2024/9/13	15:13	2024/9/13	15:33	150m	0	150m	MR2406C_st020	0.3 m/s
021	72.584	152.499	2024/9/13	18:32	2024/9/13	18:50	150m	0	150m	MR2406C_st021	0.3 m/s
023	75.609	167.542	2024/9/18	23:26	2024/9/18	23:44	150m	0	150m	MR2406C_st023	0.3 m/s
024	75.001	169.636	2024/9/19	15:18	2024/9/19	15:37	150m	0	150m	MR2406C_st024	0.3 m/s
025	75.000	167.235	2024/9/19	19:17	2024/9/19	19:35	150m	3	150m	MR2406C_st025	0.3 m/s
026	75.001	165.001	2024/9/20	1:27	2024/9/20	1:16	150m	3	150m	MR2406C_st026	0.3 m/s
027	73.334	165.002	2024/9/20	16:50	2024/9/20	16:58	65m	0	65m	MR2406C_st027	0.3 m/s, A part of images were lost
028	73.666	164.116	2024/9/21	19:30	2024/9/21	19:48	150m	0	150m	MR2406C_st028	0.3 m/s
031	74.001	163.235	2024/9/22	5:17	2024/9/22	5:34	150m	0	150m	MR2406C_st031	0.3 m/s
033	74.251	162.565	2024/9/22	12:54	2024/9/22	13:12	150m	2	150m	MR2406C_st033	0.3 m/s
034	74.998	162.006	2024/9/22	18:23	2024/9/22	18:39	150m	0	150m	MR2406C_st034	0.3 m/s
035	73.998	155.995	2024/9/23	10:41	2024/9/23	11:00	151m	6	150m	MR2406C_st035	0.3 m/s
037	73.333	157.467	2024/9/23	21:56	2024/9/23	22:12	150m	0	150m	MR2406C_st037	0.3 m/s
038	72.665	158.497	2024/9/24	1:48	2024/9/24	2:06	150m	0	150m	MR2406C_st038	0.3 m/s
039	72.901	158.797	2024/9/24	1:19	2024/9/24	1:38	151m	5	150m	MR2406C_st039	0.3 m/s
040	72.801	159.101	2024/9/24	12:12	2024/9/24	12:31	150m	2	150m	MR2406C_st040	0.3 m/s
041	72.700	159.401	2024/9/24	17:08	2024/9/24	17:17	77m	0	77m	MR2406C_st041	0.3 m/s
043	72.500	159.999	2024/9/24	23:44	2024/9/24	23:49	42m	0	42m	MR2406C_st043	0.3 m/s
046	71.728	155.108	2024/9/25	10:38	2024/9/25	10:58	150m	2	150m	MR2406C_st046	0.3 m/s

(6) Preliminary results

As a preliminary results, we present the following items.

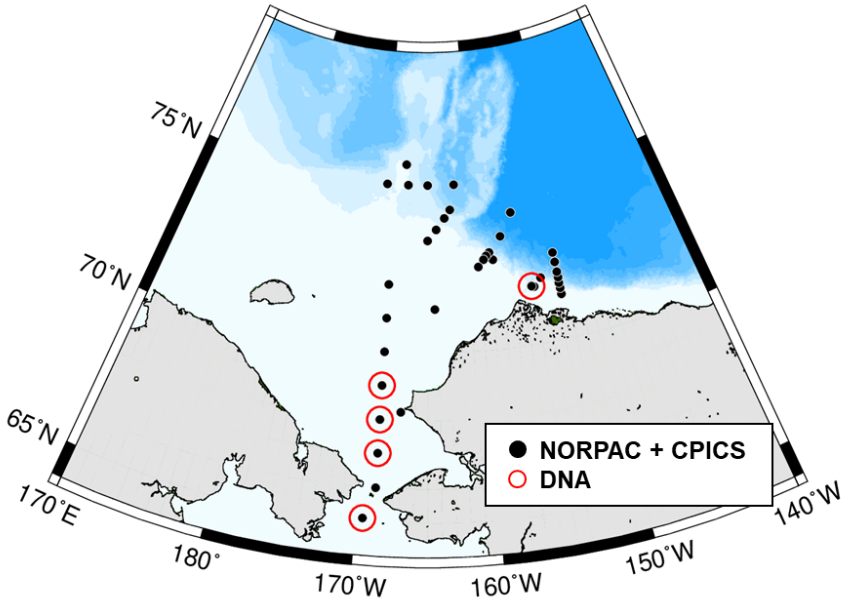

Fig. 4.17.1-1. Location of the sampling stations in the Pacific Arctic Ocean from 4 to 26 September in 2024.

(7) Data archives

These data obtained in this cruise will be submitted to the Data Management Group of JAMSTEC, and will be opened to the public via "Data Research System for Whole Cruise Information in JAMSTEC (DARWIN)" in JAMSTEC web site.
<http://www.godac.jamstec.go.jp/darwin/e>

4.17.2. Phytoplankton

(1) Personnel

Kohei Matsuno (Hokkaido University) - Principal Investigator, Not on board

Shino Kumagai (Hokkaido University)

(2) Objective

The goals of this study are the following:

1) Clarifying spatial distribution of phytoplankton and microprotist assemblages by a microscopy
2) Evaluating photosynthetic activity by a pulse-amplitude modulated fluorometer

(3) Parameters

Phytoplankton community in cell number

Fv/Fm

alpha

ETRm

(4) Sampling and treatment

(4-1) Surface monitoring

We took surface water samples (2L) from the underway system twice a day to examine cell density and photosynthetic activity from the North Pacific Ocean to the Bering Sea (Fig. 4.17.2-1). The water sample was filtered with 200 μm mesh, then filtered with reverse filtration using 20 μm mesh to concentrate the sample. Using the concentrated samples, maximum photochemical efficiency (Fv/Fm) was measured with a pulse-amplitude modulated fluorometer (Water-PAM; Walz, Effeltrich, Germany) in the sediment preservation room (3-5°C). After light-acclimatation in the dark bottle for over 15 minutes, samples (4 mL) were placed in a quartz cuvette. Fv/Fm of each sample was determined by a red LED with a peak illumination at 650 nm. The initial fluorescence (Fv) was measured by applying a weak measuring light, and a saturating pulse was applied to determine the maximum fluorescence (Fm). Then, the samples in the measuring cuvette were light-acclimated for 15 minutes by turning off the internal actinic light source of the PAM fluorometer. After the acclimation, rapid light curve was obtained by illuminating the samples for 10 s before each ΔF/Fm measurement at each of a series of eight irradiances that increased in steps from 136 to 2122 μmol photons m^{-2} s^{-1}. The remaining samples were fixed by glutaraldehyde (1% final concentration), and kept in a dark glass bin in a refrigerator. Subsequent to the phytoplankton sampling, seawater was collected in a plastic tube and frozen for measuring macronutrients by MWJ.

(4-2) Niskin sampler and bucket

Sea water samples (2 L) were collected from surface and chlorophyll *a* maximum layer (SCM) by a bucket and Niskin water sampler at 39 stations (Fig. 4.17.2-1, Table 4.17.2-1). The sample analysis procedure was the same as mentioned above.

(5) Station list

Table 4.17.2-1: Data on water samples collected by Niskin water sampler and bucket.

Station	Date (UTC)	Latitude (°N)		Longitude		E or W	Sampling depth (m)
	2024/8/28 22:42	41	23.8	151	31.3	E	0
	2024/8/29 6:17	42	1.3	153	32.4	E	0
	2024/8/29 21:54	44	15.2	156	54.1	E	0
	2024/8/30 5:08	45	6.8	158	27	E	0
	2024/8/30 20:54	47	22.8	161	53.8	E	0
	2024/8/31 14:03	48	23.2	163	32.5	E	0
	2024/8/31 21:06	50	39.6	167	25.6	E	0
	2024/9/1 4:03	51	43	168	45.9	E	0
	2024/9/1 20:12	54	29	172	8.6	E	0
	2024/9/2 3:57	55	34.5	173	45.6	E	0
	2024/9/2 19:10	58	3.4	177	36	E	0
	2024/9/3 3:42	58	0.1	177	39	E	0
	2024/9/3 18:08	60	20.08	178	39.4	W	0
	2024/9/4 2:40	61	41.4	176	16.7	W	0
	2024/9/4 18:15	64	12.6	171	31.6	W	0
	2024/9/4 19:56	64	29.1	170	54.6	W	0
2	2024/9/5 0:13	65	5.6	169	31.1	W	0, 15
3	2024/9/5 8:49	65	59.8	168	45.9	W	0, 15
4	2024/9/5 16:12	67	0.2	168	44.8	W	0, 10
6	2024/9/6 4:11	68	14.5	167	7.6	W	0, 10
7	2024/9/6 11:32	68	59.9	168	44.9	W	0, 15
8	2024/9/6 17:06	69	59.98	168	44.95	W	0, 20
9	2024/9/7 0:00	70	59.96	168	44.99	W	0, 15
10	2024/9/7 5:22	71	59.98	168	44.98	W	0, 25
11	2024/9/7 16:40	71	17.99	164	20.91	W	0, 25
	2024/9/8 1:58	71	35.1	159	51.3	W	0
12	2024/9/8 22:38	71	44.1	155	9.5	W	0, 15
13	2024/9/9 22:14	71	40.46	154	59.7	W	0, 15
14	2024/9/10 16:44	71	55.46	154	7.07	W	0, 25
15	2024/9/12 16:06	71	19.95	152	99.78	W	0, 17
16	2024/9/12 20:48	71	30.7	152	29.92	W	0, 7
17	2024/9/12 23:57	71	39.99	152	29.98	W	0, 25
18	2024/9/13 5:14	71	49.76	152	29.29	W	0, 17
19	2024/9/13 9:59	72	0.06	152	30.08	W	0, 28
20	2024/9/13 16:29	72	18.01	152	30.08	W	0
21	2024/9/13 21:05	72	35.94	152	29.94	W	20
22	2024/9/15 18:10	74	31.13	161	48.34	W	0, 40
23	2024/9/18 21:12	75	36.38	167	32.68	W	0, 45
24	2024/9/19 13:59	75	0.05	169	38.07	W	0, 40
25	2024/9/19 20:00	75	0.06	167	13.98	W	0, 45
26	2024/9/19 23:36	74	59.84	165	4.26	W	0, 44
27	2024/9/21 16:00	73	19.97	165	0.01	W	0, 25
28	2024/9/21 19:53	73	39.96	164	7.24	W	0, 30
31	2024/9/22 3:58	74	0.02	163	14.05	W	0, 40
33	2024/9/22 10:59	74	15.03	162	33.53	W	0, 40
34	2024/9/22 18:48	72	59.88	162	0.39	W	0, 40
35	2024/9/23 7:20	74	1.05	156	2.62	W	0, 45
37	2024/9/23 18:57	73	20.05	157	28.02	W	0, 25
38	2024/9/24 2:12	72	59.95	158	29.86	W	0, 25
39	2024/9/24 7:58	72	54	158	48.07	W	0, 25
40	2024/9/24 12:58	72	48.16	159	6.05	W	0, 30
41	2024/9/24 17:39	72	41.99	159	24.14	W	0, 28
43	2024/9/24 23:01	72	30.01	159	59.96	W	0, 16
46	2024/9/25 11:04	71	43.57	155	7.11	W	0, 15
47	2024/9/26 21:08	68	0	168	44.96	W	0, 15

(6) Preliminary results

As a preliminary results, we present the following items.

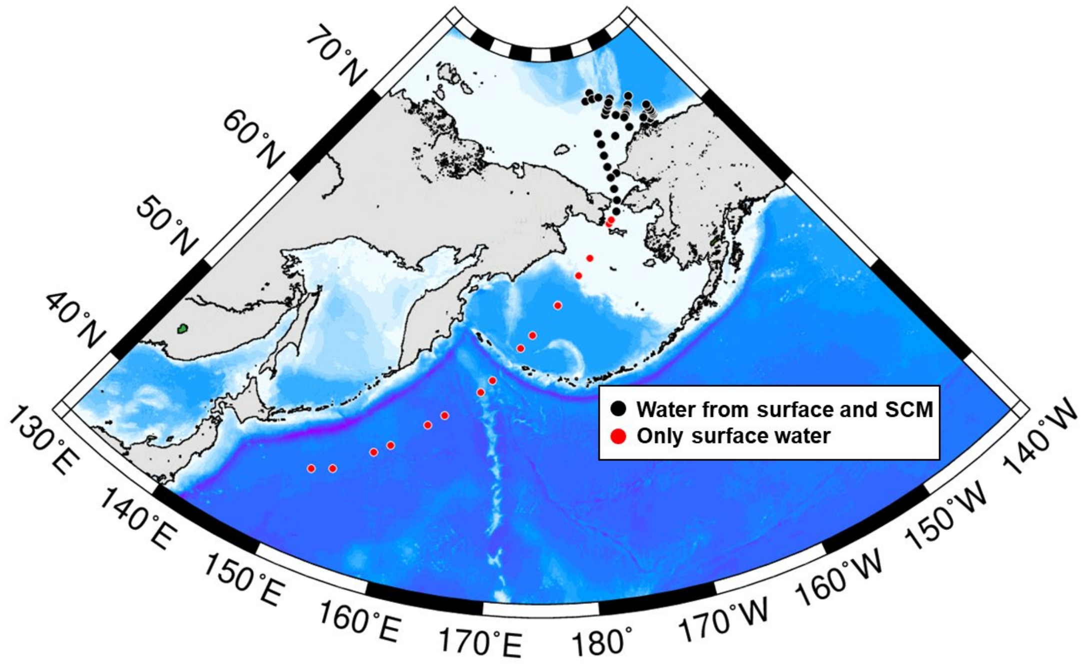

Fig. 4.17.2-1. Location of water (surface and sub-surface chlorophyll maximum) and sediment sampling stations in the Pacific Arctic Ocean.

(7) Data archives

These data obtained in this cruise will be submitted to the Data Management Group of JAMSTEC, and will be opened to the public via "Data Research System for Whole Cruise Information in JAMSTEC (DARWIN)" in JAMSTEC web site.
<http://www.godac.jamstec.go.jp/darwin/e>

4.18. Surface Sediment
4.18.1. Microalgae

(1) Personnel
Yuri Fukai (JMASTEC) – Principal Investigator
Amane Fujiwara (JAMSTEC)
Satoshi Kimura (JAMSTEC)
Kohei Matsuno (Hokkaido University)

(2) Objectives
The accumulated microalgae in the sediments would reflect microalgal bloom history in the water column, which is susceptible to environmental changes. We conducted sediment sampling to reveal the spatial distribution of microalgae relating to spring blooms by investigating pigment, diatom cell number, and ice-algae biomarkers in sediments.

(3) Parameters
Chlorophyll-a concentration
Diatom cell number
IP^{25}

(4) Instruments and methods

Multiple corer system (Ashura) used in this cruise consists of the main body (60 kg weight) and three acryl corer attachments. The core barrel is 60 cm long and has a 7.4 cm inner diameter. At the beginning of the multiple corer system going down, the speed of wire out was set to be 1.0 m s^{-1}. Wire out was stopped at a depth of about 5–10 m above the seafloor, and the core system was left to stand for 30 seconds to reduce any pendulum motion of the system. After stabilizing the multiple corer system, the wire was stored at a speed of 0.3 m s^{-1} while carefully watching a tension meter. After confirmation of the multiple corer system touching the bottom, the wire continued until bowing. The rewinding of the wire was started at a dead slow speed (0.3 m s^{-1}), and then the winch wire was wound up at 1.0 m s^{-1}.

Sediment sampling by the multiple corer system was conducted at five stations in the Chukchi shelf (Table 4.18.1-1). Surface sediment subsamples for chlorophyll-a and diatom cell analyses were collected from the sediment cores using a spatula. A part of the sediment (1 cm^3) was soaked immediately in 7 mL of *N,N*-dimethylformamide (DMF, Wako Pure Chemical Industries Ltd.) and stored at -20°C in the dark for at least 24 hours to extract chlorophyll-a. Chlorophyll-a concentrations were measured by a fluorometer (10-AU, TURNER DESIGNS) following the method of Welschmeyer (1994). Before the analysis, the 10-AU fluorometer was calibrated against pure chlorophyll-a (Sigma-

Aldrich Co., LLC). The rest of the sediment has been stored in a refrigerator until further analysis on land for the ice-algae biomarker (by Dr. Takuto Ando at Akita University) and diatom communities.

(5) Station list

Table 4.18.1-1: Sediment sampling location

Station No.	Date (UTC)	Latitude (°N)	Longitude (°W)	Bottom depth (m)
2	2024/9/5	65.09	190.48	51
4	2024/9/5	67.00	191.25	46
7	2024/9/6	69.00	191.24	53
9	2024/9/7	71.00	191.25	45
10	2024/9/7	72.00	191.25	51

(6) Preliminary results

Figure 4.18.1-1 shows chlorophyll-a concentrations in sediments as preliminary results.

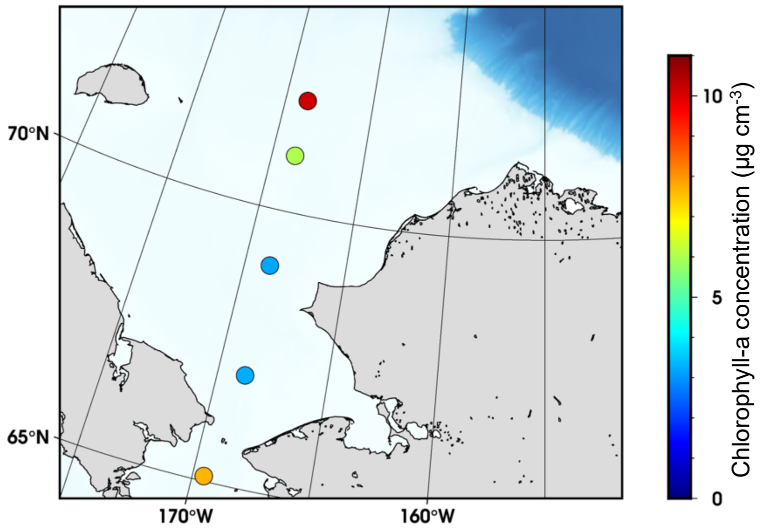

(7) Data archives

These data obtained in this cruise will be submitted to the Data Management Group of JAMSTEC, and will be opened to the public via "Data Research System for Whole Cruise Information in JAMSTEC (DARWIN)" in JAMSTEC web site.
<http://www.godac.jamstec.go.jp/darwin/e>

(8) References

Welschmeyer, N. A. (1994), Fluorometric analysis of chlorophyll a in the presence of chlorophyll b and pheopigments. *Limnol. Oceanogr.* 39, 1985–1992.

4.18.2. Microplastic

(1) Personnel
Takahito Ikenoue (JAMSTEC): Principal investigator (not on board)
Yuri Fukai (JAMSTEC) Acting principal investigator (on board)
Amane Fujiwara (JAMSTEC) (on board)

(2) Objectives

The distribution of microplastics in the open ocean of the Arctic Ocean is largely undocumented. Substantial numbers of studies on microplastics have been reported in the Pacific and Atlantic Oceans, yet very few data are available in the polar oceans. In the present study, we conducted microplastic surveys along the cruise track to fill gaps in the Arctic Ocean.

(3) Parameters

Microplastics

(4) Instruments and methods

(4-1) *Sea floor sediment sampling for microplastic analysis*

A multiple corer system (Asyura) equipped with three acrylic tubes was used to collect microplastics in the sea floor sediment. The acrylic tube is 60 cm length and 7.4 cm inner diameter. At the beginning of multiple corer system going down, the speed of wire out was set to be 0.5 m s^{-1}. Wire out was stopped at a depth about 10 m above the seafloor and the corer system was left stand for 1 minute to reduce any pendulum motion of the system. After the multiple corer system was stabilized, the wire was stored out at a speed of 0.5 m s^{-1} with carefully watching a tension meter. After confirmation of the multiple corer system touching the bottom, the wire continued out till bowing. The rewinding of the wire was started at a dead slow speed (0.3 m s^{-1}), and then winch wire was wound up at 0.5 m s^{-1}. One of the three cores was used for microplastic analysis. Sediment core samples were stored in a refrigerator until analysis. Time and position of the sea floor sediment sampling are shown in Table 4.18.2-1.

Microplastic samples will be subjected to enumeration and identification of plastic types using a microscope and FT-IR. The distribution and concentration of microplastics in this study will be compared with the previous reports in the Arctic Ocean.

(5) Station list

Table 4.18.2-1: Time and position of the sea floor sediment sampling.

(6) Data archives

These data obtained in this cruise will be submitted to the Data Management Group of JAMSTEC, and will be opened to the public via "Data Research System for Whole Cruise Information in JAMSTEC (DARWIN)" in JAMSTEC web site.
<http://www.godac.jamstec.go.jp/darwin/e>

Table 4.18.2-1. Time and position of the sea floor sediment sampling.

Station No.	Date (UTC)	Time (UTC)	Latitude	Longitude	Sea floor depth (m)
2	2024/9/5	1:23	65-5.63N	169-31.11W	51
10	2024/9/7	6:26	72-0.01N	168-45.02W	51

4.19. Sea ice biogeochemistry

(1) Personnel

Amane Fujiwara (JAMSTEC) – Principal investigator
Manami Tozawa (Hokkaido University)
Yuri Fukai (JAMSTEC)
Mariko Hatta (JAMSTEC)
Aymeric Servettaz (JAMSTEC)
Eva Lopes (CIIMAR)
Daiki Nomura (Hokkaido University), not onboard
Masato Ito (National Institute of Polar Research), not onboard

(2) Objective

Arctic sea ice is undergoing significant alterations, characterized by rapid reductions in summer sea ice extent and a transition toward a predominance of younger, thinner first-year ice instead of thick multi-year ice. While the influence of sea ice formation and melting on biogeochemical cycles in the ocean has been previously explored, the specific impacts of sea ice melt processes on the biogeochemistry of the surface waters remain inadequately understood. Consequently, this study involved the collection of sea ice samples of the melt season.

(3) Parameters

- Ice temperature
- Ice salinity
- carbonate chemistry (DIC and TA)
- Oxygen isotopic ratio
- Dissolved nitrogen isotopic ratio
- Nutrient concentration
- Chl-a concentration
- Organic/Inorganic Particle weight
- Bacterial DNA
- Particulate organic carbon/nitrogen
- CDOM/FDOM
- Turbidity
- Particle Organic Carbon (POC)
- Suspended Particulate Matter (SPM)
- Scanning Electron Microscope (SEM)
- Transparent Expolymer Particle (TEP)
- Thick/Thin section

(4) Instruments and methods

Floating sea ice samples were collected at an ice-edge site (Table 4.19-1 and Figures 4.19-1) utilizing a wire mesh pallet cage (1.2 x 1.0 x 0.9 m) deployed via the ship's crane. The temperatures of the ice samples were measured immediately post-collection using a needle-type temperature sensor (ASF-270T, AsONE, Japan). Vertical profiles of ocean temperature, salinity, dissolved oxygen concentration, turbidity, and chlorophyll-a fluorescence in the surface layer of the sampling site were obtained using a RINKO profiler.

The collected sea ice samples were sectioned into smaller pieces, with some allocated for the measurement of vertical profiles of biogeochemical properties on board, taken at approximately 5 cm increments from the top. These samples were melted under dark and cool conditions (temperature < 4 °C), and subsequent analyses were conducted on the melted water for salinity, nutrient concentrations, chlorophyll-a, and particulate weight. Remaining samples were stored frozen for later analysis of the aforementioned biogeochemical parameters on land.

(5) Observation log and the sampling site

Table 4.19-1 List of ice sampled location and time

Ice ID	Sampled date & time [UTC]	Sampled location	Ice Size (W x L x H [cm])
T-1	2024.9.17 21:35	76-08.992N/167-47.706W	133 x 96 x 39
T-2	2024.9.17 21:55	76-09.069N/167-47.255W	65 x 65 x 45
T-3	2024.9.17 22:10	76-09.142N/167-46.766W	40 x 38 x 30
T-4	2024.9.17 22:25	76-09.149N/167-46.414W	122 x 72 x 34
T-5	2024.9.17 22:30	76-09.137N/167-46.342W	110 x 75 x 30

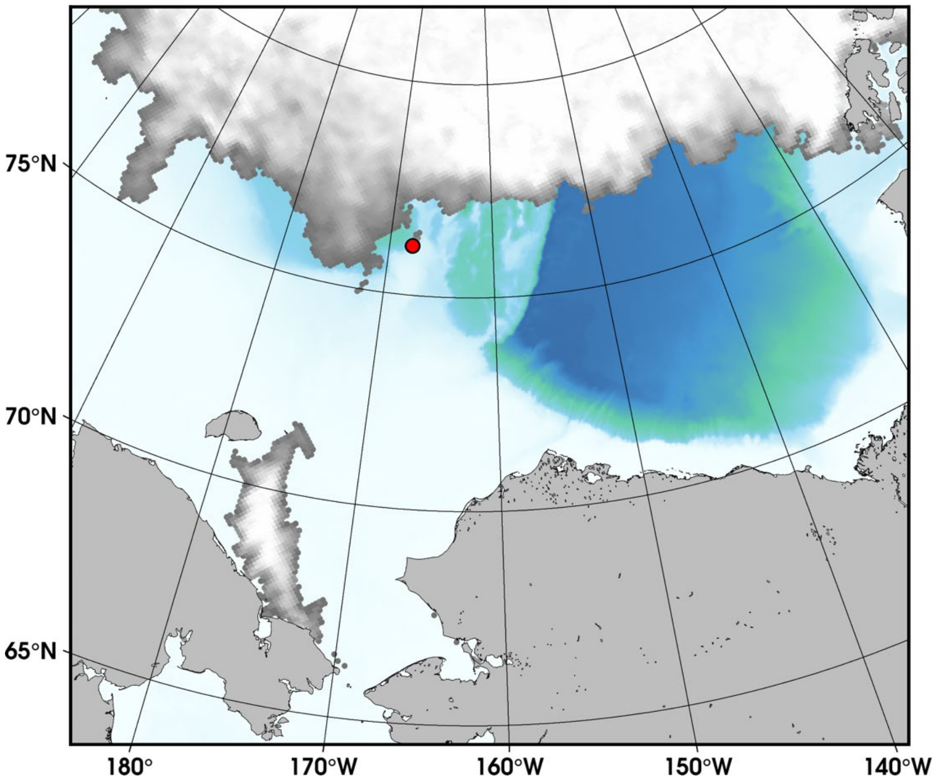

Figure 4.19-1 Location where the floating ice samplings were conducted. AMSR-2 sea ice concentration on Sep 17 is plotted with gray scale.

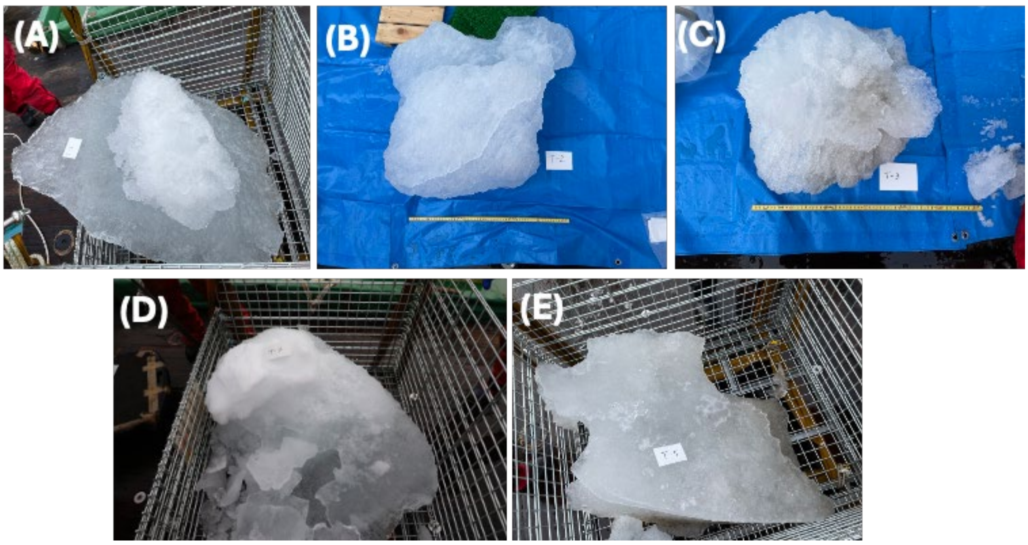

Figure 4.19-2. Photos of the collected sea ice samples. A; T-1, B; T-2, C; T-3, D; T-4, E; T-5.

(6) Data archives

These data obtained in this cruise will be submitted to the Data Management Group of JAMSTEC, and will be opened to the public via "Data Research System for Whole Cruise Information in JAMSTEC (DARWIN)" in JAMSTEC web site <http://www.godac.jamstec.go.jp/darwin/e>.

5. Under Ice Drone Trials

(1) Science Party

Shojiro Ishibashi (JAMSTEC) – COMAI System Integrator (Not on board)
Kiyotaka Tanaka (JAMSTEC) – Operation Leader and System Engineer
Makoto Sugesawa (JAMSTEC) – System Engineer and Operator
Hiroshi Yoshida (JAMSTEC) – System adviser and Operator
Asahi Hasegawa (University of Tokyo) – Operator
Satomi Ogawa (Nippon Marine Enterprises, Ltd.; NME) – Operator
Haruna Yamanaka (Nippon Marine Enterprises, Ltd.; NME) – Operator
Satoshi Kimura (JAMSTEC) – Operation supporter
Mariko Hatta (JAMTEC) – Operation supporter
Amane Fujiwara (JAMSTEC) – Operation supporter
Yosaku Maeda (JAMSTEC) – Engineer (Not on board)
Hiroshi Matsumoto (JAMSTEC) – Engineer (Not on board)

(2) Objective

The under-ice drone named COMAI (Fig. 5.1) is a middle size autonomous underwater vehicle (AUV) for observations under ice in the Arctic. The drone will autonomously cruise and observe environment under ice in coverage area planed of 15 km. A completion of fully autonomous operation under ice is more complex than operation in open sea because of two big breakthrough items: positioning and emergency recovery. At high latitudes, performance of magnetic compasses or inertial navigation systems (INS) degrades and navigation errors increase. In this cruise, we evaluate the performance of navigation and autonomous cruise, and attempt observations under sea ice, after addressing problems that arose during the previous year's cruise.

Figure 5.1.　A recovery scene of COMAI.

The test items are followings:

1) evaluation of the navigation system in high latitude area,
2) cruising tests using the autonomous control mode, and
3) observation under the ice.

All tests were carried out with a thin tether including optical fiber cable because the recovery functions are not yet evaluated in this season's trial

(3) Instruments and Methods

The drone is a platform of observation sensors under sea-ice. It will autonomously cruises and surveys under sea- ice without a tether cable (At this time a tether cable is used in all trials). Specifications of the drone is listed in Table 5.1. The maximum cruising range designed is about 30 km or endurance is about 16 hours (at cruising speed of 1 kt). The drone utilizes a hybrid navigation system consisting of a MEMS inertial measurement unit, a magnetic compass and a Doppler velocity log (DVL) as shown in Fig. 5.2. The drone has four operation modes: 1) an untethered, which means that the connection is made with a thin optical fiber instead of a thick cable, remotely operated vehicle mode (UROV) , 2) an acoustical ROV mode (AROV), 3) a radio wave ROV mode (RROV), and 4) an autonomous underwater vehicle (AUV) mode. In the AUV mode, three cruising patterns (heading-depth control, way-point control, and way-line control) are selectable. It has a special cruising mode named "escape mode" (the ability to exit the sea ice zone in the event of a system anomaly under sea ice). in addition to them. If one of the navigation devices is down, the drone automatically changes the control mode to the heading-depth control with an acoustical super short baseline navigation toward an acoustic light house pre-deployed as shown in Fig. 5.3.

Table 5.1: Specifications of COMAI.

Items	Specifications	Remarks
Size	2.3 x 0.6 x 0.7 m	
Weight	330 kg	in air
Depth rating	300 m	
Cruising speed	2 kt	3 kt max.
Cruising range	30 km	
Power	Li-ion battery (5.7 kWh)	

Actuators	Horizontal thrusters (100 W) x 2 Vertical thruster (100 W) x 1 Rudders	
Scientific payloads	CTD (conductivity, temperature, depth) sensor Turbidity and chlorophyll meter Snap shot camera Multi beam sonar	 installed on top side installed on top side

COMAI is equipped with scientifical sensors: a CTD sensor (miniCTD, Valeport), a turbidity and chlorophyll meter (ECO FLUNTU, WET Labs), a snap shot camera (2592 x 1944 pixels, F2.2) with LED strobe lights, and a 260 kHz multi beam sonar (837B Delta T, IMAGENEX). The camera and the multi beam sonar are mounted on top side of the body because of ice bottom observations. All data obtained are automatically logged in a drone internal memory and a hard disk of the personal computer of the ship-side console (if each ROV mode).

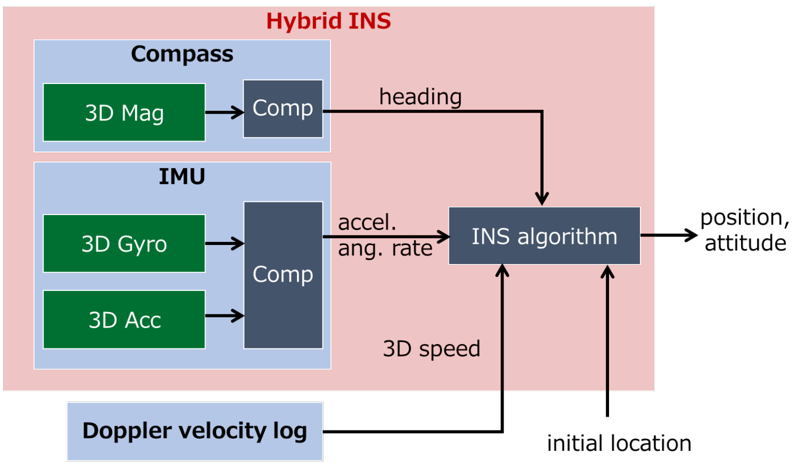

Figure 5.2 Block diagram of the hybrid navigation system.

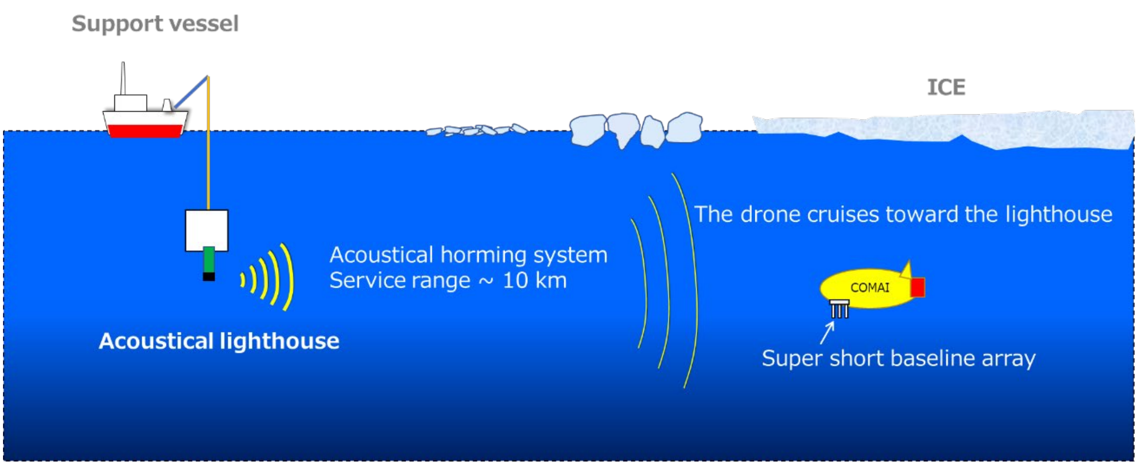

Figure 5.3. A working image of the heading-depth control with the acoustical super short baseline navigation in the escape mode.

(4) Test log

Table 5.2 and Figure 5.4 show the dive points of COMAI.

Table 5.2: The Dive list of COMAI.

Dive No.	Test No.	Date UTC	SMT (UTC-8)	JST (UTC+9)	Area	Lat.	Lon.	Depth (m)	Hoist Up (SMT)	Launch (SMT)	Hoist Up (SMT)	On Deck (SMT)
Dive1	Test1	9/14/24	9/14/24	9/15/24	Barrow	73-45.04N	157-51.48W	3491	9:47	9:50	11:37	11:39
Dive2	Test1	9/14/24	9/14/24	9/15/24	Barrow	73-45.00N	157-51.36W	3492	13:38	13:40	15:04	15:06
Dive3	Test2	9/17/24	9/17/24	9/18/24	Chukchi Shelf	76-06.87N	167-41.53W	398	9:34	9:38	11:23	11:25
Dive4	Test2	9/18/24	9/18/24	9/19/24	Chukchi Shelf	75-36.44N	167-34.60W	190	9:25	9:27	11:03	11:06
Dive5	Test2	9/20/24	9/20/24	9/21/24	Chukchi Shelf	75-33.50N	168-05.80W	174	9:29	9:34	10:49	10:51
Dive6	Test2	9/20/24	9/20/24	9/21/24	Chukchi Shelf	75-32.04N	168-11.69W	175	13:59	14:02	15:08	15:10

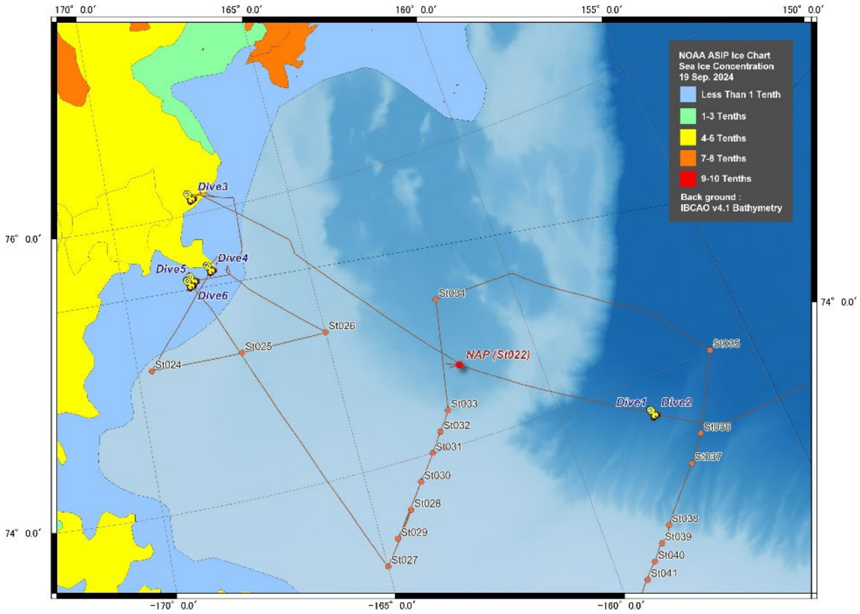

Figure 5.4. Map of the dive points.

(5) Preliminary results

1) Navigation performance

Dive 1 and 2 were conducted in the open sea without ice. Fig. 5.5 shows tracks of the drone (blue crosses: acoustic positioning, black dots: DVL-INS hybrid system) measured and the support ship (green open circles) in the dive #2. Because COMAI was cruising at a depth of about 50 meters in 3,000-meter-deep waters, the DVL-INS hybrid system was used to measure the water-speed. In this test, the DVL-INS measurement values were not updated by acoustic positioning values. In this Dive, COMAI came close to the mother vessel due to the current immediately after the COMAI was launched, so the mother vessel's thrusters were used to keep COMAI away. Therefore, COMAI was in a cone-firm state for a few minutes immediately after landing on the water. This may have greatly increased the error in the position measurement by the DVL-IND hybrid system.

The actual position of COMAI measured by the acoustic positioning system will be compared with the position measured by the Hybrid system.

① The initial position of COMAI, which was updated by COMAI's GPS, and the position of the mother ship were off by about 50 m to the east at the launch.

② COMAI's heading measured by the hybrid system is off by about -100° from the true heading.

③ The position comparison at 06:55, 06:58, and 07:04 (JST) shows that the position error was about 100 m at point A, and increased to about 200 m at point B after 9 minutes.

④ The COMAI and the mother ship are drifting westward, but the Hybrid is not able to detect them. (DVL cannot measure the water movement because it measures the velocity against the water.)

Fig. 5.10 shows the wake map in the sea ice area, where the heading of COMAI does not deviate significantly from the actual heading. However, the position error increased from 20 m to 45 m in the 7 minutes from 02:45 to 02:52, indicating that the acoustic position correction algorithm is necessary for the DVL-INS hybrid with water velocity measurements.

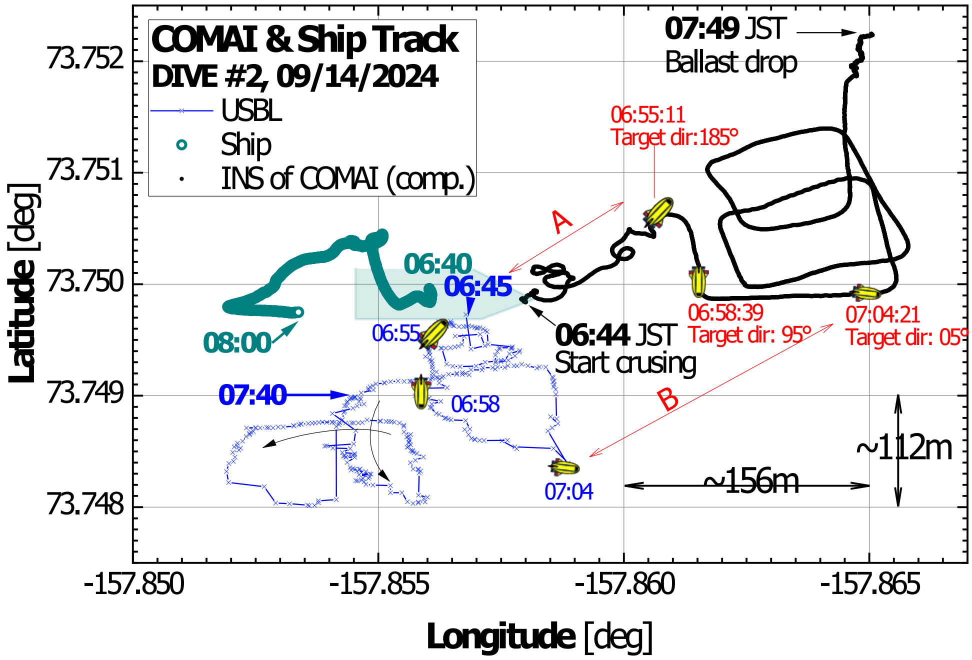

Figure 5.5. The drone track in the Dive 2. Blue cross, green circle, and black circle denote COMAI track measured by acoustic localization, support ship track, and COMAI track measured by INS, respectively.

Note the heading of COMAI from 06:44, when COMAI was launched, to 06:55, when the heading stabilized in Fig. 5.6. At 06:51, the heading and depth control (AUV mode) is commanded, but it is not stable because it is just after the cone firings. At 06:52, the drone descended manually, and at 06:55, heading and depth control was applied, finally stabilizing the drone. Since then, both heading and depth have been controlled stably until surfacing. In this test, the craft was navigated in a square counter-clockwise direction at depths of 50 m, 20 m, and 10 m. The depth was changed after a 360-degree turn, but the heading instability was observed when changing from autonomous control to UROV control. At 10m depth, the cruise was terminated at 270 degrees. The heading appears to change violently from 7:35 to 7:45, but the graph only looks that way because the heading is moving back and forth between 360° and 0° on the compass.

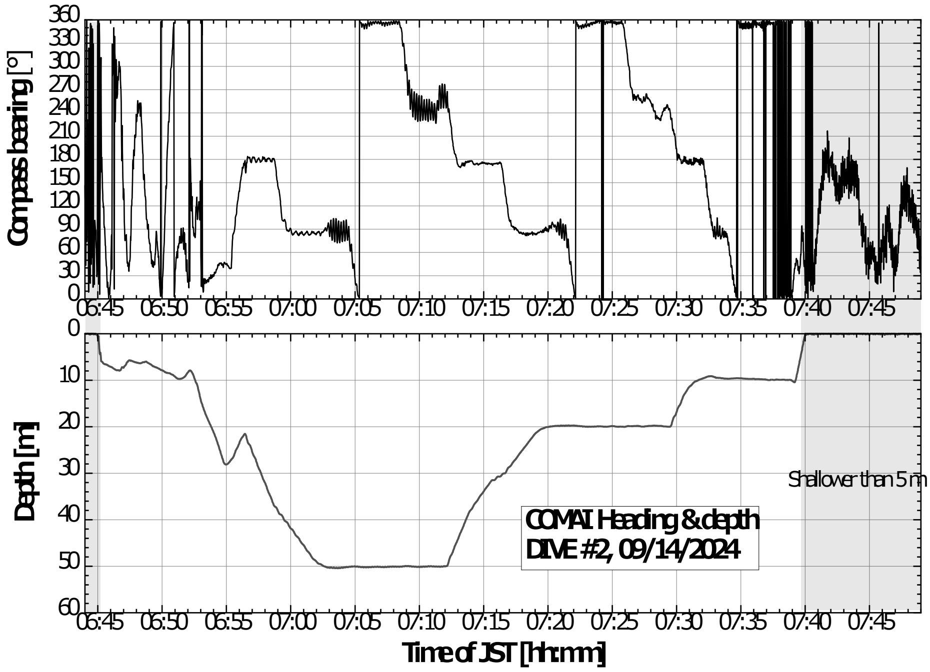

Figure 5.6. Time-series data of compass bearing (upper) and depth of COMAI (lower) in Dive 2 .

2) Observation performance

The depth dependence of Dive 2 fluorescence and turbidity is shown in Figure 5.7, where a region of chlorophyll dominance was observed at depths greater than 40 m. At this depth, the camera captured a large number of plankton. Figure 5.8 shows the plankton taken for reference.

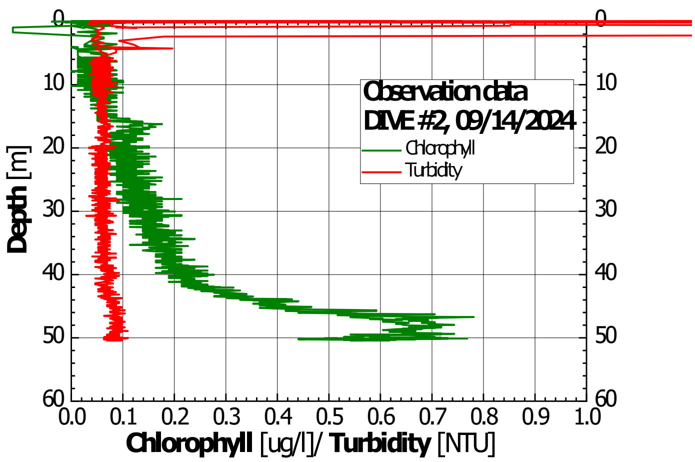

Figure 5.7. The depth dependence of Dive 2 fluorescence and turbidity.

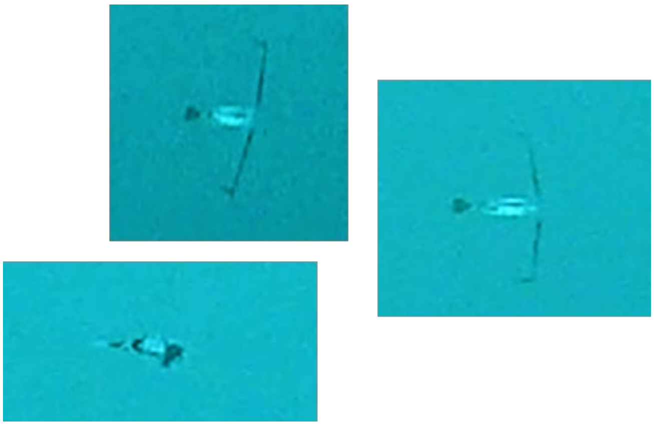

Figure 5.8.　Snap shot images taken at depths greater than 40 m.

Dive 3 to 6 were conducted in the sea ice area. In Dive 3, COMAI attempted to observe the bottom of the large 30-meter class sea ice, but unexpectedly, an ice dish spread out below the sea surface, preventing COMAI from diving close to the ice. Of course, COMAI tried again, but the tether became entangled in the surrounding ice, and as the ice moved, COMAI was pulled by the ice and became uncontrollable, so it gave up further diving.

Images of the ice were obtained in Dive 4 and Dive 5. Figure 5.9 shows the ice in Dive 4. The drone's track and the location where the ice was photographed and snap shot of a sea-ice bottom in Dive 5 are shown in Figure 5.10.

Although the drone was able to photograph the ice this time, it was closer to the ice than on the 2022 cruise, and the relative velocity between the ice and COMAI was higher this time, so it was not possible to obtain clear photographs and multibeam images. Improvement is needed in taking ice images.

Figure 5.9.　Snap shot image of sea-ice bottom in dive 4

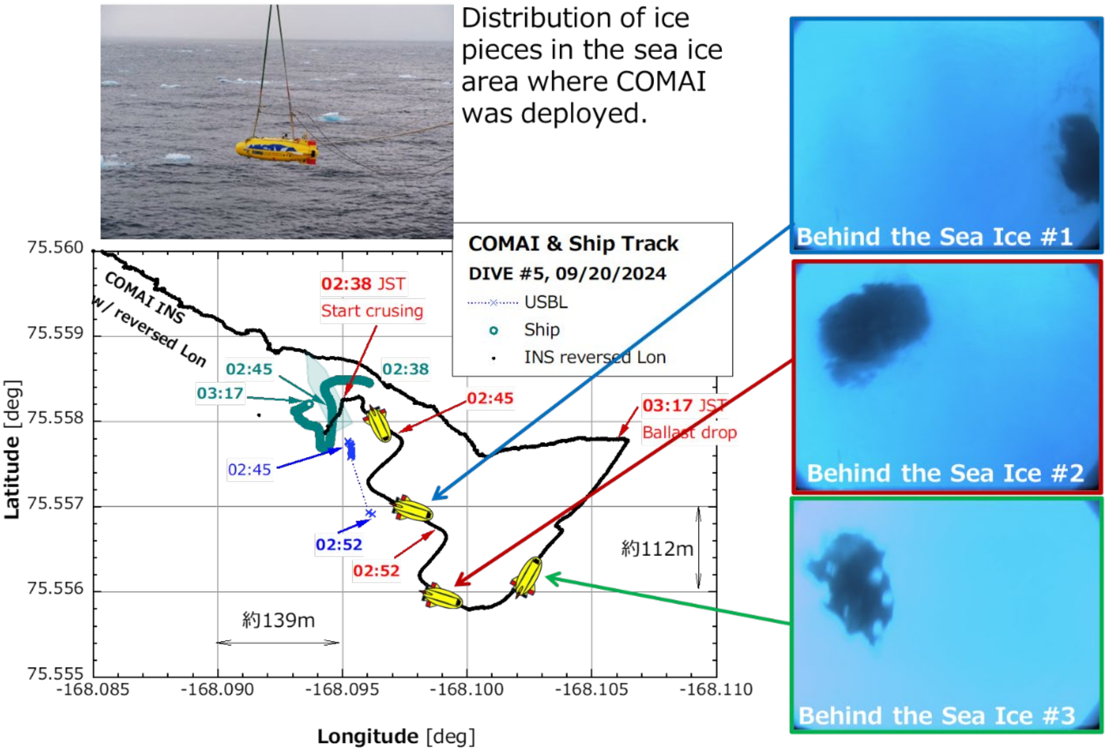

Figure 5.10 Photographs of ice in the COMAI deployment area, track maps, and the underside of sea ice taken in passing in the dive #5

3) Summary of Diving Tests

In the fourth year of this cruise, the drone was able to navigate freely with autonomous control, and acoustic positioning and communication became possible by shutting down the vessel's acoustic equipment (MBE, ADCP). On the other hand, problems that had not been identified before became apparent:

- When entering a sea ice group, the tethers become entangled in the ice and take the COMAI with them, and
- The scenario with fixed way point (WP) coordinates makes it impossible to observe moving ice.

The latter is a very difficult problem that overturns conventional AUV operations. We hope to conduct tether-less diving in FY2025, but there are many challenges.

During this year's cruise, the captain and the ice navigator gave us a lot of advice on testing in icy waters. We also thank the Chief Scientist for the precise opportunity to dive the COMAI. Furthermore, during the operation, they did a great job involving the entire ship. We would like to express my sincere appreciation. However, since the AUV was originally designed to be used by a small number of people, we are determined to bring it to a state of full-scale operation as soon as possible.

(6) Data archives

These data obtained in this cruise will be submitted to the Data Management Group (DMG) of JAMSTEC, and will be opened to the public via "Data Research System for Whole Cruise Information in JAMSTEC (DARWIN)" in JAMSTEC web site.

<http://www.godac.jamstec.go.jp/darwin/e>

6. Geology

6.1. Sediment core sampling

(1) Personnel

Masanobu Yamamoto (Hokkaido University): Principal Investigator
Shinya Iwasaki (Hokkaido University)
Kenta Suzuki (Chiba Institute of Technology)
Masanori Arai (Hokkaido University)
Satomi Ogawa (NME)
Souichiro Sueyoshi (NME)
Shinya Okumura (NME)
Haruna Yamanaka (NME)
Yuta Shinomiya (MWJ)
Ritsuko Sawada (MWJ)
Ko Arihara (MWJ)
Jonaotaro Onodera (JAMSTEC)

(2) Objectives

The Arctic Ocean and terrestrial environment have recently been reported to be changing drastically, but it is unclear whether these changes are similar to natural variations in the past or how sudden and large the changes are compared to natural variations. In this study, we plan to generate a detailed record of environmental change since the preindustrial period. High-resolution records of the ocean and terrestrial environments that can be compared with observation records will enable us to reinterpret observation data accumulated by the Arctic research communities.

(3) Parameters

Site Survey

Geophysical seafloor surveys were performed in the area selected for coring, the Barrow Canyon (BC) area (Figure 6.1-1). Survey was performed by the NME team and Masanobu Yamamoto on September 10 and 11 (UTC). The survey included the Multi-Beam Echo-Sounder (MBES) seafloor mapping, and attendant high-resolution Sub-Bottom Profiling (SBP) performed at a slow cruising speed of ~3 knots for better quality results. The survey strategy capitalized on the comparable MBES and SBP data and sediment cores collected from the R/V Araon in 2013 (ARA04-B&C) and R/V Mirai in 2022 (MR22-06C).

A SeaBeam 3012 MBES collected swath bathymetry with wide beam angles ranging from 120 (60° to -60°) to 140 (70° to -70°) degrees. The MBES data were processed onboard using the Caris HIPS software. The resolution of the processed images has 50-m grid, depending on the water depth of survey areas. The mapped swath bathymetry was superimposed on the International Bathymetric Chart of the Arctic Ocean (IBCAO v. 4; Jakobsson et al., 2020) with QGIS software. High-resolution CHIRP Sub-Bottom Profiling (SBP) data were obtained by Bathy 2010 Sub-bottom profiler with the frequency set to 3.5 kHz with the ping rates of 1.33 to 2.08 Hz.

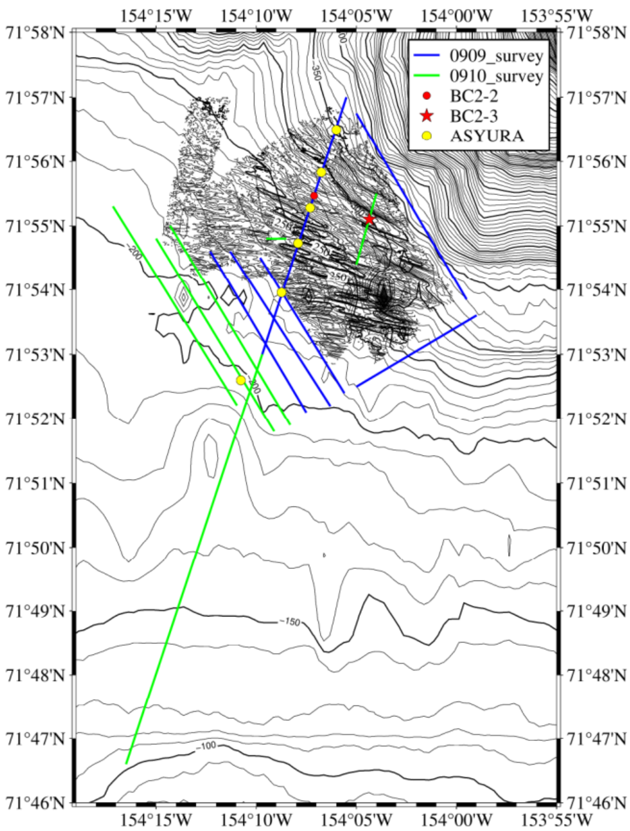

測線名	緯度	経度	備考
Line1	71-53.00 N	154-09.70 W	SBP Line1
	71-57.00 N	154-05.50 W	
Line2	71-56.75 N	154-05.00 W	
	71-53.85 N	153-59.50 W	
Line3	71-53.60N	153-59.00 W	
	71-52.50N	154-05.00 W	
Line4	71-52.40N	154-05.60 W	
	71-54.50N	154-09.80 W	
Line5	71-54.60N	154-11.30 W	
	71-52.20N	154-06.30 W	
Line6	71-52.10N	154-07.50 W	
	71-54.60N	154-12.30 W	
Line7	71-55.00 N	154-14.30 W	
	71-51.90 N	154-08.30 W	
Line8	71-54.80 N	154-15.00 W	
	71-51.80 N	154-09.10 W	
Line9	71-54.80 N	154-09.50 W	
	71-54.80 N	154-08.50 W	
Line10	71-55.50 N	154-04.00 W	SBP Line2
	71-54.40 N	154-05.00 W	
Line11	71-53.00 N	154-09.70 W	
	71-46.60 N	154-16.50 W	
Line12	71-52.21 N	154-10.96 W	
	71-55.30 N	154-17.15 W	

Fig. 6.1-1: Information on geophysical survey data acquisition.

The survey objectives included:

- Selecting sites for coring
- Collecting background information for the study areas
- Addressing attendant scientific problems, where applicable

Gravity Corer (GC)

The gravity corer system consists of a weight, a 7 m-long stainless steel barrel with an acryl liner tube, and a pilot core sampler. The Inner Diameter (I.D.) of the steel barrel is 127 mm; the acryl liner tube is 114 mm, respectively. We used a small multiple corer ("Asyura") of approximately 100 kg weight for a pilot core sampler. The total weight of the system is about 750 kg.

Multiple Corer (MC)

A multiple-core sampler was used for retrieving the surface sediment. This core sampler consists of a main body of 620 kg-weight and eight sub-core samplers (I.D. 74mm and length of 60cm) equipped with a set of transparent polycarbonate liners and acryl liner tube.

Asyura corer

An Asyura corer sampler was used for retrieving the surface sediment. This core sampler consists of a main body and three sub-core samplers (I.D. 74 mm and length 60cm) equipped with two transparent acryl liner tubes and a polycarbonate liner tube.

(4) Instruments and methods

CCR measurements

After splitting each section of cores into working and archive halves, and the Core Color Reflectance (CCR), the value calculated for the spectral reflectance from 400 to 700 nm in wavelengths using the Konica Minolta CM-700d, was measured from the archive halves.

Calibrations include zero calibration and white calibration before the measurement of core samples. Zero calibration is carried out in the air. White calibration is carried out using the white calibration piece (CM-700d standard accessories) without clear polyethylene wrap. The color of the split sediment (archive half core) was measured every 1 cm or 0.5 cm through transparent polyethylene film.

We used the LAB system that is visualized as a cylindrical coordinate system in which the cylinder's axis is the lightness variable L*, ranging from 0% to 100%, and the radii are the chromaticity variables a* and b*. Variable a* is the green (negative) to the red (positive) axis, and variable b* is the blue (negative) to the yellow (positive) axis.

Core Photographs

After splitting each section of cores into working and archive halves, sectional photographs of the archive half were taken using a digital camera.

(5) Station list

We retrieved two gravity, two pilot Asyura, six Asyura and one multiple cores at geologically targeted BC2-2 and BC2-3 sites. In addition, we retrieved 33 Asyura cores in the Chukchi and Beaufort Seas. The locations of cores are summarized in Figure 6.1-2 and Table

6.1-1.

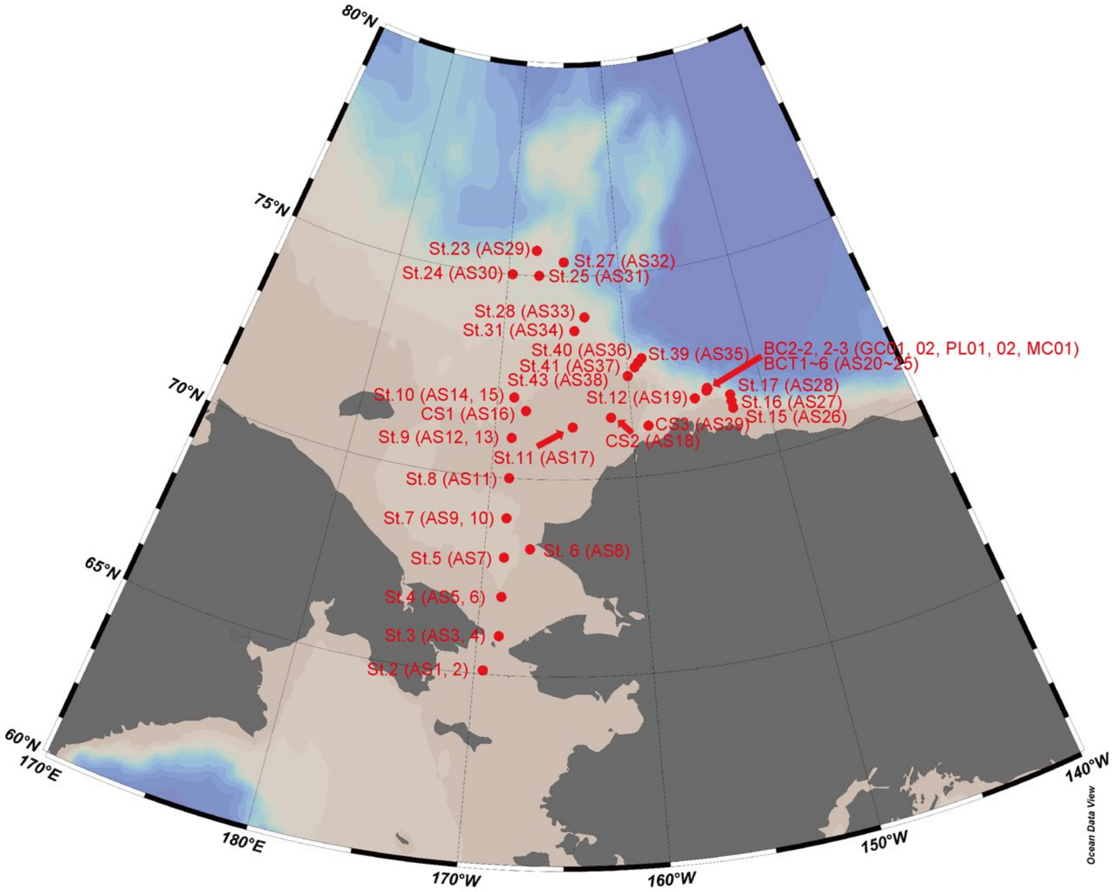

Figure 6.1-2: Location of coring sites.

Table 6.1-1: Core information

Shipboard ID (core name)	Site name	Year	Month	Day	Time (UTC)	Latitude (degree)	Longitude (degree)	Water depth (m)	Core length (cm)	Section or hand
MR24-06C AS01	St. 02	2024	09	05	1:23	65.0938	169.5022	50.7	17	3
MR24-06C AS02	St. 02	2024	09	05	1:37	65.0938	169.5022	50.7	21	3
MR24-06C AS03	St. 03	2024	09	05	8:29	66.0019	168.7498	53.6	0.1	3
MR24-06C AS04	St. 03	2024	09	05	8:38	66.0031	168.7500	53.5	9.5	1
MR24-06C AS05	St. 04	2024	09	05	17:25	67.0054	168.7451	45.8	5	3
MR24-06C AS06	St. 04	2024	09	05	17:33	67.0048	168.7442	45.7	9	3
MR24-06C AS07	St. 05	2024	09	05	23:53	67.9997	168.7514	59.2	25	3
MR24-06C AS08	St. 06	2024	09	06	1:23	68.2450	167.1358	43.8	11	3
MR24-06C AS09	St. 07	2024	09	06	11:10	68.9984	168.7531	53.2	26	3
MR24-06C AS10	St. 07	2024	09	06	11:17	68.9981	168.7525	52.9	25.5	3
MR24-06C AS11	St. 08	2024	09	06	18:08	69.9998	168.7491	41	15	3
MR24-06C AS12	St. 09	2024	09	06	23:41	70.9996	168.7517	44.6	16	3
MR24-06C AS13	St. 09	2024	09	06	23:48	70.9998	168.7521	44.8	21	3
MR24-06C AS14	St. 10	2024	09	07	6:26	72.0023	168.7463	50.7	25	3
MR24-06C AS15	St. 10	2024	09	07	6:35	72.0017	168.7473	50.8	24	3
MR24-06C AS16	CS-1	2024	09	07	9:01	71.6836	167.8134	50.3	24.5	3
MR24-06C AS17	St. 11	2024	09	07	16:28	71.3000	164.3489	45.9	21	3
MR24-06C AS18	CS-2	2024	09	07	22:02	71.5086	161.4987	47.8	26	3
MR24-06C AS19	St. 12	2024	09	09	0:27	71.7433	155.1511	302	50.5	3
MR24-06C GC01	BC2-2	2024	09	10	19:20	71.9245	154.1209	264	488	6
MR24-06C PL01	BC2-2	2024	09	10	19:20	71.9245	154.1209	264	26.5	3
MR24-06C AS20	BCT-1	2024	09	10	21:33	71.9419	154.1004	346	39	3
MR24-06C AS21	BCT-2	2024	09	10	22:10	71.9312	154.1110	289	28	3
MR24-06C AS22	BCT-3	2024	09	10	22:44	71.9218	154.1207	260	25.5	3
MR24-06C AS23	BCT-4	2024	09	10	23:15	71.9127	154.1316	244	29	3
MR24-06C AS24	BCT-5	2024	09	10	23:52	71.8995	154.1465	242	32	3
MR24-06C AS25	BCT-6	2024	09	10	0:37	71.8769	154.1782	196	27.5	3
MR24-06C GC02	BC2-3	2024	09	11	16:54	71.9191	154.0757	279	473	6
MR24-06C PL02	BC2-3	2024	09	11	16:54	71.9191	154.0757	279	31	3
MR24-06C MC01	BC2-3	2024	09	11	17:56	71.9191	154.0757	279	26	8
MR24-06C AS26	St. 15	2024	09	12	17:09	71.3335	152.4988	62.8	11.5	2
MR24-06C AS27	St. 16	2024	09	12	20:35	71.5000	152.5019	108	28	3
MR24-06C AS28	St. 17	2024	09	13	2:04	71.6678	152.4933	323	32	3
MR24-06C AS29	St. 23	2024	09	18	22:56	75.6059	167.5358	194	11	3
MR24-06C AS30	St. 24	2024	09	19	15:47	75.0033	169.6367	238	37	3
MR24-06C AS31	St. 25	2024	09	19	19:45	75.0011	167.2332	259	1	3
MR24-06C AS32	St. 27	2024	09	21	17:07	75.3336	165.0014	72.4	28.5	3
MR24-06C AS33	St. 28	2024	09	21	19:59	73.6663	164.1215	169	39.5	3
MR24-06C AS34	St. 31	2024	09	22	5:46	73.9983	163.2470	297	34	3
MR24-06C AS35	St. 39	2024	09	24	9:55	72.9028	158.7978	411	29	3
MR24-06C AS36	St. 40	2024	09	24	12:44	72.8026	159.1012	200	40	3
MR24-06C AS37	St. 41	2024	09	24	17:26	72.6999	159.4023	84.6	34	3
MR24-06C AS38	St. 43	2024	09	24	23:57	72.5002	160.0000	48.8	34	3
MR24-06C AS39	CS-3	2024	09	25	21:07	71.2345	158.8032	109	31	3

(6) Preliminary results

Lithologic descriptions are summarized in Table 6.1-2. The photographs of cores are shown in Fig. 6.1-3. The color indices are shown in Fig. 6.1-4.

Table 6.1-2: Brief description of cores

Shipboard ID (core name)	Hand	Length (cm)	Description
MR24-06C AS01	1	6.2	0-6.2 cm brownish black well sorted m.g. sand
MR24-06C AS01	2	14	0-14 cm grayish well sorted olive m.g. sand
MR24-06C AS04	1	8	0-8 cm homogenous olive gray m.g.sand
MR24-06C AS06	3	3.5	0-3.5 cm massive muddy f-m.gsand
MR24-06C AS07	1	18	0-3 cm graish olive sandy mud, 3-5 cm soft black sandy mud, 5-7 cm olive black sandy mud, 7-9 cm black sandy mud, 9-18 cm olive black sandy mud
MR24-06C AS08	1	7	0-7 cm olive black unsorted m-c.g.sand
MR24-06C AS09	1	26	0-4 cm graish olive sandy mud, 4-6 cm black sand mud, 6-26 cm olive black sandy mud and mud (upward coasening)
MR24-06C AS11	1	13	0-2 cm olive black mud and pebbles, 2-13 cm pebbles and granules
MR24-06C AS12	1	11.7	0-3 cm gray sandy mud, 3-11.7 cm olive gray sandy mud
MR24-06C AS14	1	24	0-3 cm grayish oive mud, 3-24 cm olive black mud
MR24-06C AS16	1	23.7	0-3 cm gray f.g-sand-containing mud, 3-23.7 cm olive back f.g.-sand-containing mud
MR24-06C AS17	1	15.5	0-3 cm gray f.g.sand-containing mud, 3-15.5 cm olive gray f.g.-sand-containing sandy mud
MR24-06C AS18	1	14.2	0-2 cm grayish olive sand-containing mud, 8-14.2 cm Cm-scale alternated beds of black and olive black sand-containing mud
MR24-06C AS19	1	43	0-7 cm gray f.g-sand-containing mud, 7-10.5 cm olive black f.g.sand-containing mud, 10.5-24 cm gray sand-containing mud, 24-29 cm olive black mud, 29-43 cm black and olive black muds
MR24-06C GC01		488	0-488 Biotubated alterenated beds of gray and black muds. Black bands changes denser downward.
MR24-06C PL01	1	24.5	0-21cm Gray mud, 21-24 cm black mud
MR24-06C AS20	1	32.5	0-16 cm gray sandy mud, 16-20 cm, black-spots concentrated mud, 20-32.5 cm gray mud
MR24-06C AS21	1	25	0-20 cm
MR24-06C AS22	1	22.3	0-8 cm gray sand-containing mud, 8-20 cm gray mud, 20-21 cm black mud
MR24-06C AS23	1	22.5	0-8 cm gray sand-containing mud, 8-22.5 cm gray sand-containing mud
MR24-06C AS24	1	19.5	0-11 cm gray sand-containing mud, 11-19.5 cm gray sand-containing mud
MR24-06C AS25	1	26	0-14 cm gray sand-containing mud, 14-26 cm gray mud
MR24-06C GC02		473	0-488 Biotubated alterenated beds of gray and black sandy muds. Black bands changes denser downward.
MR24-06C PL02	1	29.5	0-23 cm Gray mud, 23-27 cm black mud, 27-29.5 cm gray mud
MR24-06C MC01	1	24.5	0-22 cm gray mud, 22-24.5 alternated beds of black and gray muds
MR24-06C AS26	2	10.5	0-1 cm brownish gray sandy mud, 1-8 cm gray sandy mud
MR24-06C AS27	1	15	0-6.5 cm graish olive sandy mud, 6.5-15 cm bioturbated mixture of black and gray sandy muds
MR24-06C AS28	1	29.5	0-6 cm homogenous grayish olive sand-containig mud, 6-7 cm black mud, 7-12 cm gray mud, 12-15.5 cm black mud, 15.5-29.5 cm gray mud
MR24-06C AS29	2	10	0-4 cm dark olive brwon clay, 4-10 cm gray clay
MR24-06C AS30	2	36	0-4 cm brownish black clay, 4-10 cm dark reddish brown clay, 10-29 cm dark greenish gray clay, 29-36 cm bluish gray clay
MR24-06C AS32	1	22	0-7 cm gray clay, 7-11 cm black clay, 11-16 cm gray clay, 16-22 cm black clay
MR24-06C AS33	1	39	0-1 cm brownish black clay, 1-39 cm dark greenish gray clay
MR24-06C AS34	3	33.5	0-6 cm dark olive brown silty clay, 6-33.5 cm dark greenish gray clay
MR24-06C AS35	3	30.7	0-2.5 cm Brownish black sand-containing mud, 2.5-16 cm gray (7.5Y 4/1) mud, 16-23 cm gray (N 4/1) mud, 23-30 cm gray (N 4/1) mud
MR24-06C AS36	1	39	0-2 cm Brownish gray clay, 2-39 cm gray clay
MR24-06C AS37	2	25	0-2 cm Yellowish gray (2.5Y 4/1) sand-containing mud, 2-25 cm yellowish to gray muds
MR24-06C AS38	1	25	0-1 cm grayish olive sand-cotaning mud, 1-25 cm gray sand-containing mud
MR24-06C AS39	3	29.5	0-2.5 cm gray sandu mud, 2.5-24.5 cm black mud, 24.5-29.5 cm gray granule-containing mud

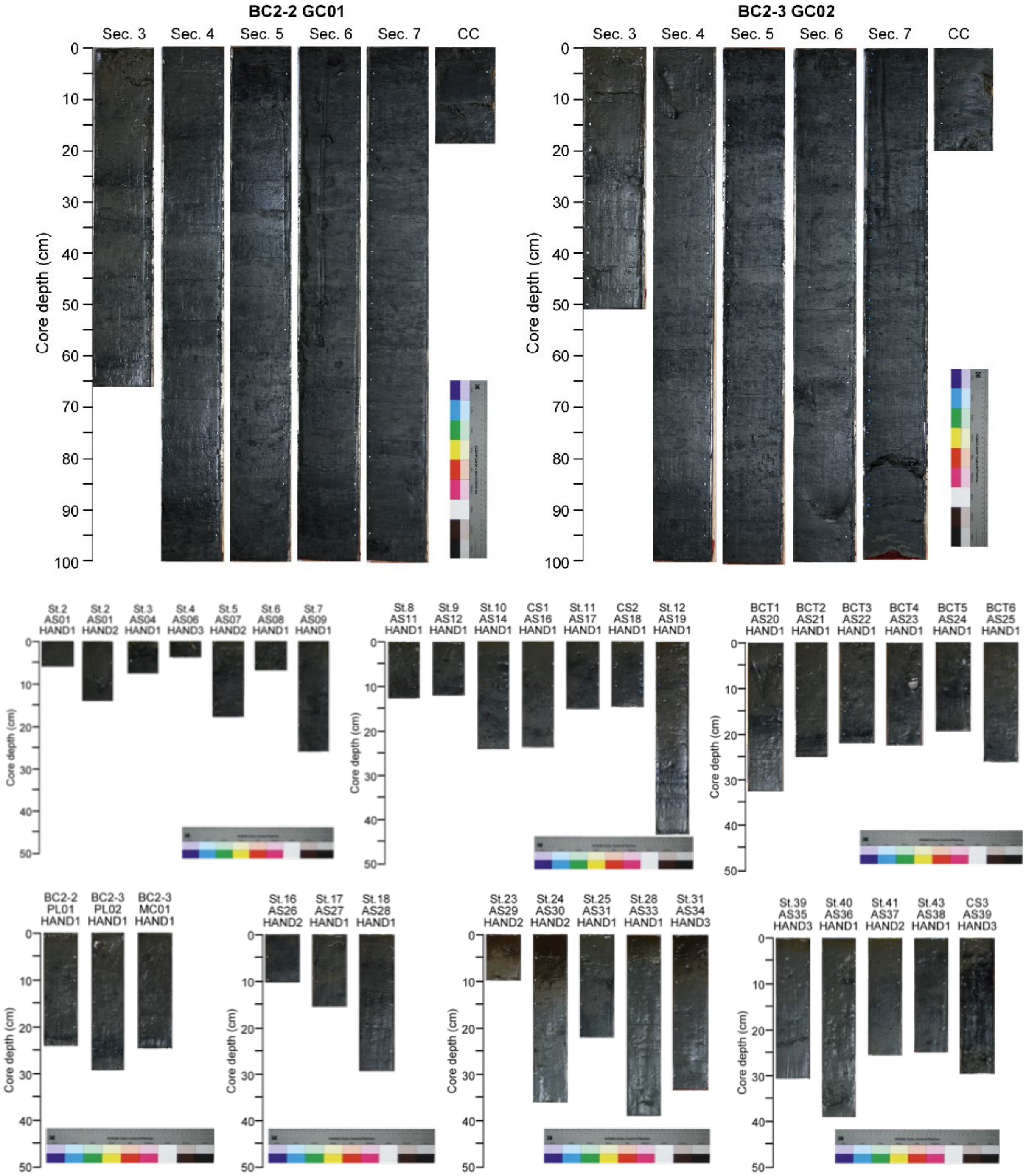

Fig. 6.1-3: Photographs of cores.

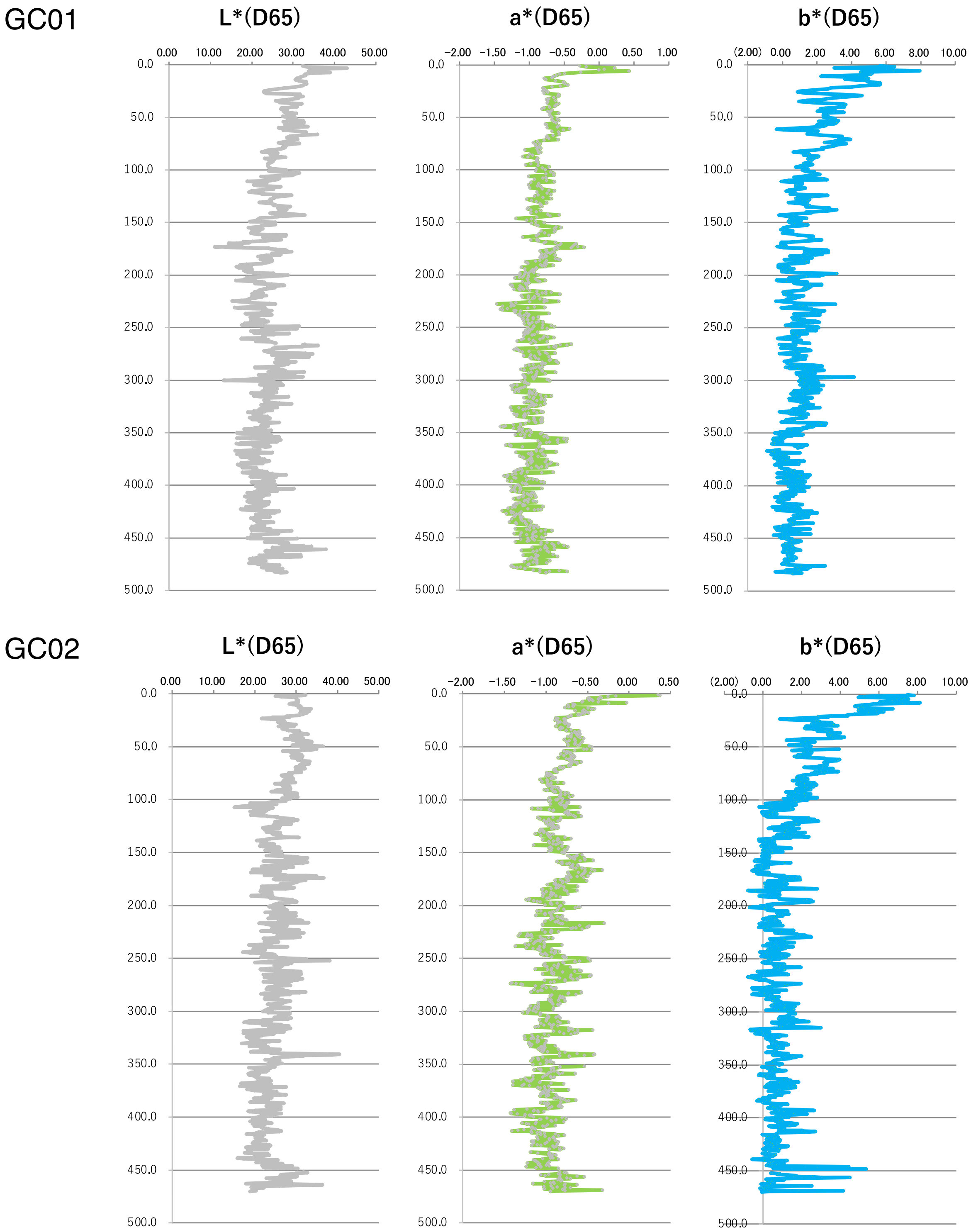

Fig. 6.1-4 (1): The color indices of GC01 and GC02 cores. The vertical axis indicates the sediment depth (cm).

PL01

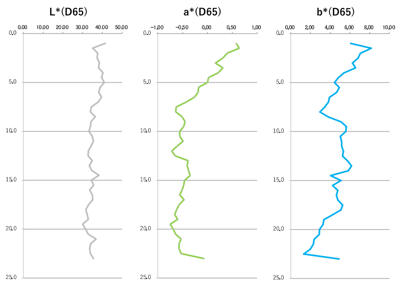

PL02

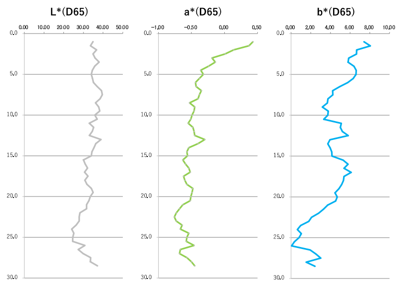

MC01

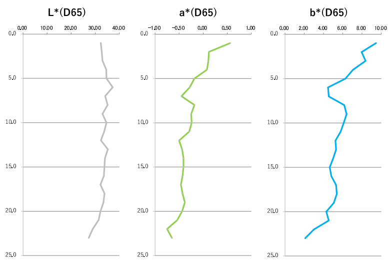

AS01

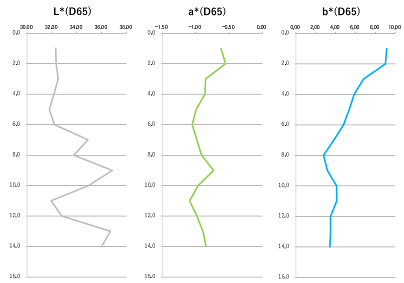

AS04

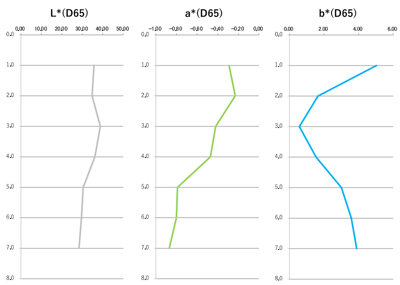

AS06

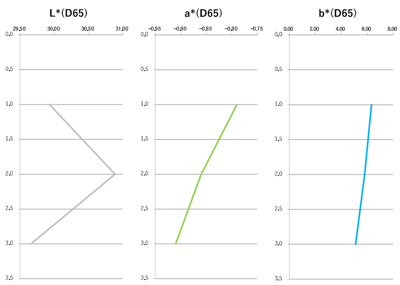

AS07

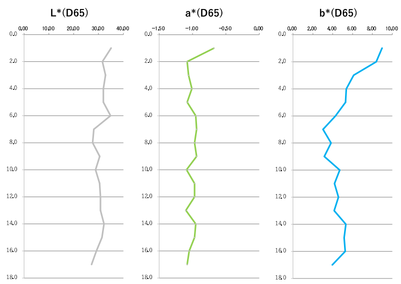

AS08

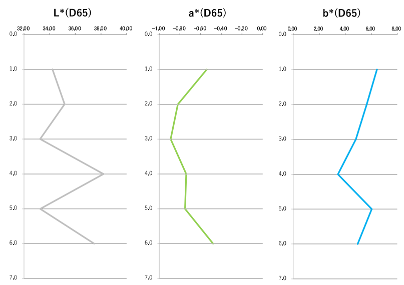

AS09

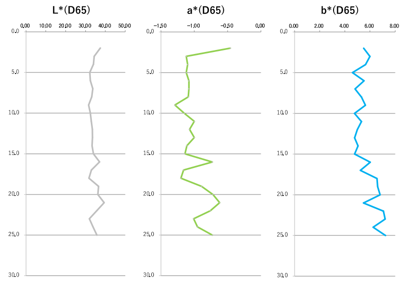

AS11

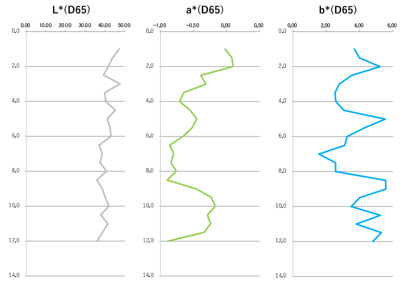

AS12

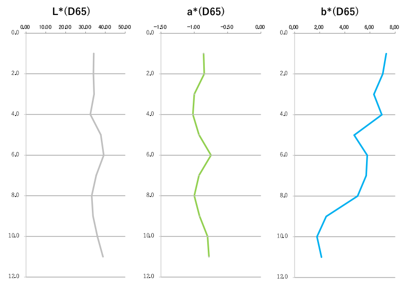

AS14

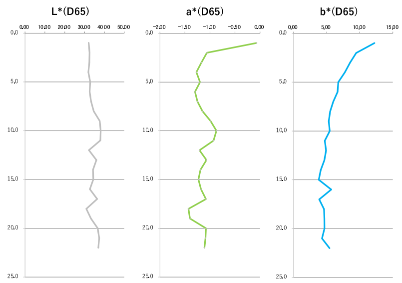

AS16

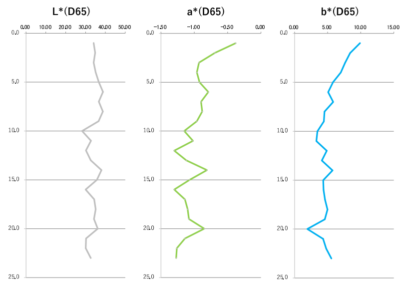

AS17

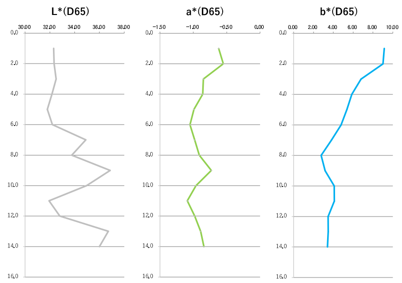

AS18

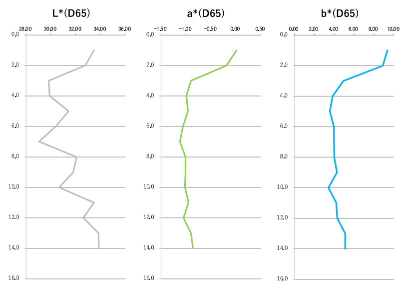

AS19

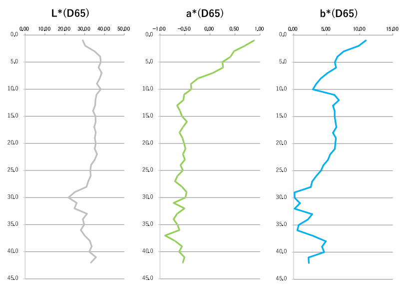

AS20

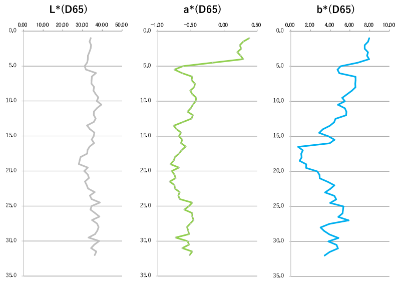

AS21

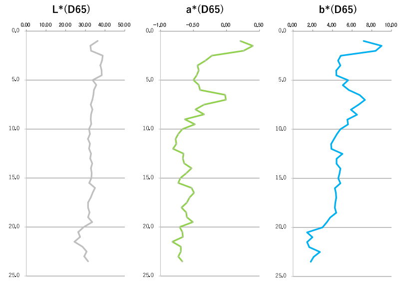

AS22

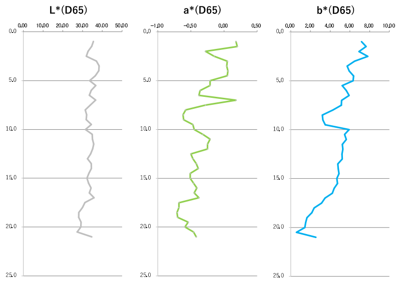

AS23

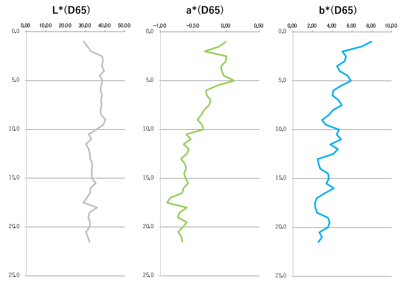

AS24

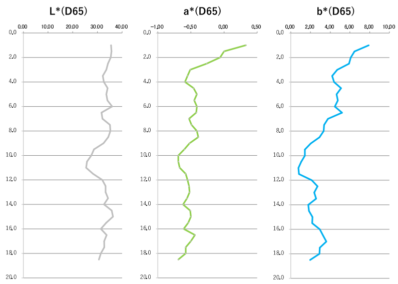

AS25

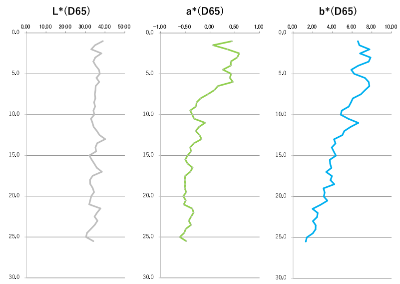

AS26

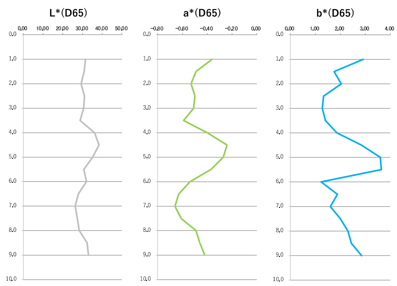

AS27

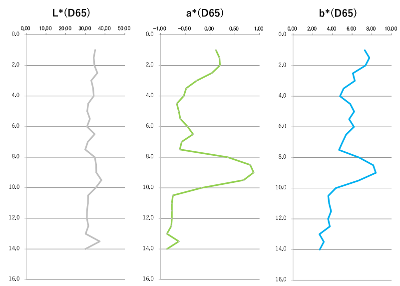

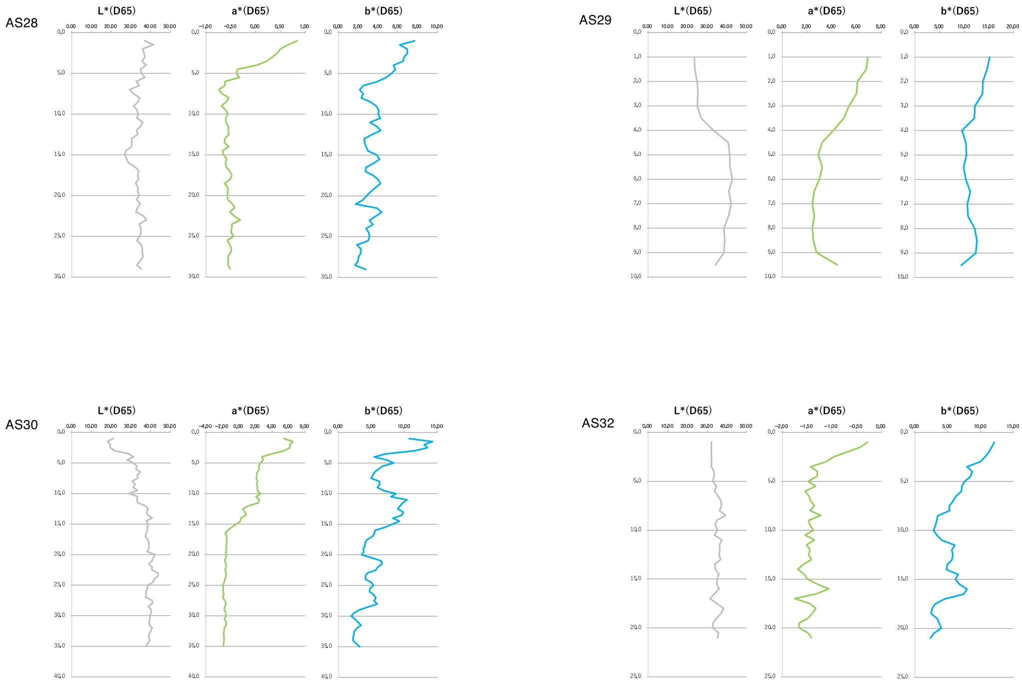

Fig. 6.1-4 (2): The color indices of pilot, multiple and Asyura cores. The vertical axis indicates the sediment depth (cm).

(7) Data archive

These data obtained in this cruise will be submitted to the Data Management Group of JAMSTEC. They will be opened to the public via “Data Research System for Whole Cruise Information in JAMSTEC (DARWIN)” on the JAMSTEC website.
<http://www.godac.jamstec.go.jp/darwin/e>

6.2. Sea bottom topography measurements

(1) Personnel

Masanobu Yamamoto	Hokkaido University	-PI
Satomi Ogawa	NME (Nippon Marine Enterprises, Ltd.)	
Souichiro Sueyoshi	NME	
Shinya Okumura	NME	
Haruna Yamanaka	NME	
Masanori Murakami	MIRAI Crew	

(2) Objectives

R/V MIRAI is equipped with the Multi Beam Echo Sounding system (MBES; SEABEAM 3012 (L3 Communications ELAC Nautik, Germany)) and Sub-Bottom Profiler (SBP), Bathy 2010 (SyQwest). The objective of MBES and SBP is to collect continuous bathymetric data and sub-bottom profiling data along ship track especially for geological and geophysical studies.

(3) Parameters

MBES: Depth [m]

SBP: Sub-bottom profiling [m]

(4) Instruments and Methods

The “SEABEAM 3012” on R/V MIRAI was used for bathymetry mapping during this cruise. To get accurate sound velocity of water column for ray-path correction of acoustic beams, we determined sound velocities at the depth of 6.62m, the bottom of the ship, by the surface sound velocimeter. We made sound velocity profiles based on the observations of CTD, XCTD and Argo float conducted in this cruise by the equation in Del Grosso (1974).

The “Bathy 2010” system was used for determining physical properties of the sea floor and for imaging and characterizing geological information several tens of meters below the sea floor. Its sound velocity was fixed 1,500m/s during operations. In the site surveys of MT1, MT2 and BC2, Bathy 2010 and SEABEAM 3012 were operated in 3kt vessel speed over ground. In the geophysical wide area survey around Barrow Canyon, these instruments were operated in 8kt over ground. During operations, settings of these instruments were changed according to the water depth, bottom type and condition of the bottom and sediment layers detection.

Table 6.2-1 and 6.2-2 show system configuration and performance of SEABEAM 3012 and Bathy2010 system.

Table 6.2-1: SEABEAM 3012 System configuration and performance

Frequency:	12 kHz
Transmit beam width:	2.0 degree
Transmit power:	4 kW
Transmit pulse length:	2 to 20 msec.
Receive beam width:	1.6 degree
Depth range:	50 to 11,000 m
Number of beams:	301 beams (Spacing mode: Equi-angle)
Beam spacing:	1.5 % of water depth (Spacing mode: Equi-distance)
Swath width:	60 to 150 degrees
Depth accuracy:	< 1 % of water depth (average across the swath)

Table 6.2-2: Bathy2010 System configuration and performance

Frequency:	3.5 kHz (FM sweep)
Transmit beam width:	30 degree
Transmit pulse length:	0.5 to 50 msec
Strata resolution:	Up to 8 cm with 300 m of bottom penetration according to bottom type
Depth resolution:	0.1 feet, 0.1 m
Depth accuracy:	±10 cm to 100 m, ± 0.3% to 6,000 m
Sound velocity:	1,500 m/s (fix)

(5) Observation log

MBES: 27 Aug. 2024 - 25 Sep. 2024

SBP: 10 Sep. 2024 - 11 Sep.2024

(6) Preliminary Results

The results will be published after primary processing.

(7) Data archives

These data obtained in this cruise will be submitted to the Data Management Group of JAMSTEC, and will be opened to the public via "Data Research System for Whole Cruise Information in JAMSTEC (DARWIN)" in JAMSTEC web site.
< https://www.godac.jamstec.go.jp/darwin/en/ >

(8) Remarks

i) The following periods, MBES data acquisition was suspended due to sending acoustic commands of ANS.

19:31UTC 02 Sep. 2024 - 20:44UTC 02 Sep. 2024
14:40UTC 08 Sep. 2024 - 14:50UTC 08 Sep. 2024
16:09UTC 08 Sep. 2024 - 16:19UTC 08 Sep. 2024
17:39UTC 08 Sep. 2024 - 17:49UTC 03 Sep. 2024
19:51UTC 09 Sep. 2024 - 19:55UTC 08 Sep. 2024
21:49UTC 09 Sep. 2024 - 21:51UTC 08 Sep. 2024
00:16UTC 16 Sep. 2024 - 00:45UTC 16 Sep. 2024

ii) The following periods, MBES data acquisition was suspended due to the shallow water area.
20:00UTC 03 Sep. 2024 - 13:47UTC 08 Sep. 2024
07:20UTC 09 Sep. 2024 - 07:35UTC 09 Sep. 2024
00:01UTC 10 Sep. 2024 - 01:02UTC 10 Sep. 2024
01:02UTC 12 Sep. 2024 - 20:59UTC 12 Sep. 2024
13:46UTC 21 Sep. 2024 - 18:05UTC 21 Sep. 2024
12:29UTC 24 Sep. 2024 - 06:35UTC 25 Sep. 2024

iii) The following periods, MBES data acquisition was suspended due to operating of the AUV "COMAI".
16:45UTC 14 Sep. 2024 - 19:58UTC 14 Sep. 2024
20:46UTC 14 Sep. 2024 - 22:48UTC 14 Sep. 2024
17:24UTC 17 Sep. 2024 - 18:30UTC 17 Sep. 2024
17:17UTC 18 Sep. 2024 - 18:45UTC 18 Sep. 2024
17:13UTC 20 Sep. 2024 - 18:25UTC 20 Sep. 2024
21:54UTC 20 Sep. 2024 - 22:54UTC 20 Sep. 2024

iv) The following periods, MBES data acquisition was stopped due to system trouble.
13:30UTC 15 Sep. 2024 - 13:55UTC 15 Sep. 2024
17:31UTC 23 Sep. 2024 - 17:50UTC 23 Sep. 2024

v) The following periods, MBES data acquisition was stopped due to system maintenance.
13:07UTC 03 Sep. 2024 - 13:08UTC 03 Sep. 2024
04:05UTC 10 Sep. 2024 - 04:32UTC 10 Sep. 2024
01:35UTC 13 Sep. 2024 - 01:36UTC 13 Sep. 2024

vi) The following periods, the SBP observation was carried out.
06:47UTC 10 Sep. 2024 - 14:29UTC 10 Sep. 2024
01:11UTC 11 Sep. 2024 - 08:46UTC 11 Sep. 2024

6.3. Sea surface gravity measurements

(1) Personnel

Motoyo Itoh	JAMSTEC	-PI
Satomi Ogawa	NME (Nippon Marine Enterprises, Ltd.)	
Souichiro Sueyoshi	NME	
Shinya Okumura	NME	
Haruna Yamanaka	NME	
Masanori Murakami	MIRAI Crew	

(2) Objective

The local gravity is an important parameter in geophysics and geodesy. The gravity data were collected during this cruise.

(3) Parameters

Relative Gravity [CU: Counter Unit]

[mGal] = (coefl: 0.9946) * [CU]

(4) Instruments and Methods

The relative gravity using LaCoste and Romberg air-sea gravity meter S-116 (Micro-g LaCoste, LLC) was measured during the cruise. To convert the relative gravity to absolute one, we measured gravity, using the portable gravity meter (Scintrex gravity meter CG-5), at Sekinehama and Shimizu port as the reference points.

(5) Observation log

26 Aug. 2024 - 30 Sep. 2024

(6) Preliminary Results

Absolute gravity table is shown in Table 6.3-1

Table 6.3-1: Absolute gravity table of the MR24-06C cruise

No.	Date m/d	UTC	Port	Absolute Gravity [mGal]	Sea Level [cm]	Ship Draft [cm]	Gravity at Sensor *1 [mGal]	S-116 Gravity [mGal]
#1	8/25	03:20	Sekinehama	980371.89	280	647	980373.01	12647.52
#2*2	10/**	**:**	Shimizu (******)	******.**	***	***	******.**	*****.**

*1: Gravity at Sensor = Absolute Gravity + Sea Level*0.3086/100 + (Draft-530)/100*0.2222

*2: The scheduled date and port of the end of the next cruise.

(7) Data archives

These data obtained in this cruise will be submitted to the Data Management Group of JAMSTEC, and will be opened to the public via "Data Research System for Whole Cruise Information in JAMSTEC (DARWIN)" in JAMSTEC web site.

< https://www.godac.jamstec.go.jp/darwin/en/ >

(8) Remarks

i) The following periods, navigation data (speed over ground, gyro, longitude, latitude and sea depth) were invalid.

07:44:38UTC 06 Sep. 2024 - 07:44:41UTC 06 Sep. 2024

6.4. Surface magnetic field measurements

(1) Personnel

Motoyo Itoh	JAMSTEC	-PI
Satomi Ogawa	NME (Nippon Marine Enterprises, Ltd.)	
Souichiro Sueyoshi	NME	
Shinya Okumura	NME	
Haruna Yamanaka	NME	
Masanori Murakami	MIRAI Crew	

(2) Objective

Measurement of magnetic force on the sea is required for the geophysical investigations of marine magnetic anomaly caused by magnetization in upper crustal structure. We measured geomagnetic field using a three-component magnetometer during this cruise.

(3) Parameters

Three components of a magnetic field vector on-board, Hx, Hy, Hz [nT]

Hx : A magnetic field component in the bow/stern direction on the vessel horizontal plane. "To bow" is positive.

Hy : A magnetic field component in the port/starboard direction on the vessel horizontal plane. "To starboard" is positive.

Hz : A perpendicular magnetic field component to the vessel horizontal plane. "upward" is positive.

(4) Instruments and Methods

A shipboard three-components magnetometer system (SFG2018, Tierra Tecnica) is equipped on-board R/V MIRAI. Three-axes flux-gate sensors with ring-cored coils are fixed on the fore mast. Outputs from the sensors are digitized by a 20-bit A/D converter (1 nT/LSB) and sampled at 8 times per second. Yaw (heading), Pitch and Roll are measured by the Inertial Navigation Unit (INU) for controlling attitude of a Doppler radar. Ship's position, speed over ground (Differential GNSS) and gyro data are taken from LAN every second.

The relation between a magnetic-field vector observed on-board, $\mathbf{H}_{\mathrm{ob}}$, (in the ship's fixed coordinate system) and the geomagnetic field vector, $\mathbf{F}$, (in the Earth's fixed coordinate system) is expressed as:

$$\mathbf{H}_{\mathrm{ob}} = \widetilde{\mathbf{A}}\ \widetilde{\mathbf{R}}\ \widetilde{\mathbf{P}}\ \widetilde{\mathbf{Y}}\ \mathbf{F} + \mathbf{H}_{\mathrm{p}} \qquad \text{(a)}$$

where $\widetilde{\mathbf{R}}$, $\widetilde{\mathbf{P}}$ and $\widetilde{\mathbf{Y}}$ are the matrices of rotation due to roll, pitch and heading of a ship, respectively. $\widetilde{\mathbf{A}}$ is a 3 x 3 matrix which represents magnetic susceptibility of the ship, and $\mathbf{H}_\mathrm{p}$ is a magnetic field vector produced by a permanent magnetic moment of the ship's body. Rearrangement of Eq. (a) makes

$$\widetilde{\mathbf{B}}\,\mathbf{H}_{\mathrm{ob}} + \mathbf{H}_{bp} = \widetilde{\mathbf{R}}\ \widetilde{\mathbf{P}}\ \widetilde{\mathbf{Y}}\ \mathbf{F} \quad \text{(b)}$$

where $\widetilde{\mathbf{B}} = \widetilde{\mathbf{A}}^{-1}$, and $\mathbf{H}_{bp} = -\widetilde{\mathbf{B}}\,\mathbf{H}_\mathrm{p}$. The magnetic field, $\mathbf{F}$, can be obtained by measuring, $\widetilde{\mathbf{R}}$, $\widetilde{\mathbf{P}}$, $\widetilde{\mathbf{Y}}$ and $\mathbf{H_{ob}}$, if $\widetilde{\mathbf{B}}$ and $\mathbf{H}_{bp}$ are known. Twelve constants in $\widetilde{\mathbf{B}}$ and $\mathbf{H_{bp}}$ can be determined by measuring variation of $\mathbf{H_{ob}}$ with, $\widetilde{\mathbf{R}}$, $\widetilde{\mathbf{P}}$, and, $\widetilde{\mathbf{Y}}$ at a place where the geomagnetic field, $\mathbf{F}$, is known.

(5) Observation log

26 Aug. 2024 - 30 Sep. 2024

(6) Preliminary Results

The results will be published after the primary processing.

(7) Data archives

These data obtained in this cruise will be submitted to the Data Management Group of JAMSTEC, and will be opened to the public via "Data Research System for Whole Cruise Information in JAMSTEC (DARWIN)" in JAMSTEC web site.
< https://www.godac.jamstec.go.jp/darwin/en/ >

(8) Remarks

i) For calibration of the ship's magnetic effect, "figure-eight" turns (a pair of clockwise and anti-clockwise rotation) were held at the following periods and positions.

03:02UTC 03 Sep. 2024 - 03:24UTC 03 Sep. 2024 (57-57N, 177-36E)
19:19UTC 13 Sep. 2024 - 19:39UTC 13 Sep. 2024 (72-35N, 152-30W)
00:40UTC 18 Sep. 2024 - 01:01UTC 18 Sep. 2024 (76-03N, 166-32W)

ii) The following periods, navigation data (speed over ground, gyro, longitude, latitude and sea depth) were invalid.

04:58:31UTC 30 Aug. 2024 - 05:49:28UTC 30 Aug. 2024
06:45:11UTC 31 Aug. 2024 - 09:43:18UTC 31 Aug. 2024
07:44:28UTC 06 Sep. 2024 - 07:44:35UTC 06 Sep. 2024

7. Notice on using

This cruise report is a preliminary documentation as of the end of cruise.
This report is not necessarily corrected even if there is any inaccurate description (i.e. taxonomic classifications). This report is subject to be revised without notice. Some data on this report may be raw or unprocessed. If you are going to use or refer the data on this report, it is recommended to ask the Chief Scientist for latest status.
Users of information on this report are requested to submit Publication Report to JAMSTEC.

https://www.godac.jamstec.go.jp/darwin/en/note.html#report
E-mail: submit-rv-cruise@jamstec.go.jp